

**Evaluating Synthetic Lethal Interactions in DNA Damage Signaling for Breast Cancer
Therapy**

by

Amirali Bukhari

A thesis submitted in partial fulfillment of the requirements for the degree of

Doctor of Philosophy

in

Cancer Sciences

Department of Oncology
University of Alberta

© Amirali Bukhari, 2021

Abstract

Breast cancer is the most common cancer amongst women in Canada. The current treatment regime for early stage breast cancers is breast-conserving surgery with radiation therapy. However, 10-20% of patients develop local recurrence, and some exhibit metastatic spread, which is associated with a high mortality rate. Treatment resistance is commonly seen in such patients. In this regard, therapies combining two or more therapeutic agents/drugs has become a cornerstone of cancer therapy. Oncogene-induced DNA damage is a common feature of cancer cells, which leads to high levels of replication stress in cancer cells compared to normal proliferating cells.

To achieve the necessary therapeutic window for a wide range of tumors, in view of tumor heterogeneity, we tested whether increasing genotoxic stress and simultaneously inhibiting an important rescue pathway would lead to cancer cell-selective death by evaluating the efficacy of combined inhibition of the kinases ATR and Wee1. ATR is essential in the DNA damage checkpoint in response to replication stress, whereas Wee1 is an effector kinase required to maintain the G2/M and intra S-phase checkpoints. Our findings suggest that inhibition of Wee1 kinase leads to ATR activation, and combined inhibition of the two kinases promotes synergistic cell killing in a panel of cancer cells, but not in non-tumorigenic epithelial cell lines *in vitro*. Live cell microscopy experiments monitoring the fate of individual cells showed that combined treatment with ATR and Wee1 inhibitors leads to a significant increase in the number of cancer cells undergoing centromere fragmentation and mitotic catastrophe, eventually resulting in cell death in mitosis. Cell cycle synchronization experiments indicate that combined ATR and Wee1 inhibition leads to a significant delay of S and G2/M phases. Furthermore, 4-day cell survival assays using reversible inhibition of ATR and/or Wee1 for short periods during the cell cycle show that not only do the two drugs act synergistically, but suppression of checkpoint activation and

DNA repair in the two cell cycle phases, S and G2, also cooperate to kill cancer cells. In an orthotopic breast cancer model, tumor-selective synergistic lethality between ATR and Wee1 inhibitors led to tumor remission and inhibited metastasis with minimal side effects.

Furthermore, early identification of non-responders in the clinic could help identify patients that should be put on alternative therapies to minimize unnecessary toxicities. In this regard, we show that [¹⁸F]-FLT uptake, measured by positron emission tomography, can be employed as a predictive biomarker to evaluate *early* response to combined ATR and Wee1 inhibitor treatment. Lastly, we assess the impact of combined ATR and Wee1 inhibitors as adjuvant to radiotherapy or surgery. Our preliminary data suggests that combined ATR and Wee1 inhibitor treatment results in radiosensitization of 4T1 tumors. Furthermore, when combined ATR and Wee1 inhibitors were used adjuvant to surgery for advanced tumors, we observed tumor “cure” in a few cases, despite the aggressive nature of the cancer model.

As these inhibitors of ATR and Wee1 are currently undergoing phase I/II clinical trials, this knowledge could soon be translated into the clinic, especially because we showed that the combination treatment targets a wide range of tumor cells. Particularly the anti-metastatic effect of combined ATR and Wee1 inhibition and the low toxicity of ATR inhibitors compared to Chk1 inhibitors show great clinical potential.

Preface

This thesis is an original work by Amirali Bukhari. Portions of this thesis have been previously published as indicated below:

Chapter 2: Published as Bukhari AB, Lewis CW, Pearce JJ, Luong D, Chan GK, and Gamper AM, “Inhibiting Wee1 and ATR kinases produces tumor-selective synthetic lethality and suppresses metastasis” *The Journal of Clinical Investigations*, vol. 129, issue 3, 1329-1344 (2019). Bukhari AB, Lewis CW, Chan GK, and Gamper AM designed the experiments. The published research article has been cleared for use in this thesis by the Copyright Clearance Center of the American Society for Clinical Investigation (Order number: 1119632). Bukhari AB, Lewis CW, Pearce JJ, and Luong D performed crystal violet assays. Bukhari AB, Lewis CW, and Gamper AM performed *in vitro* experiments and analyzed the data. Bukhari AB performed *in vivo* experiments and analyzed the data. Bukhari AB performed statistical analysis. Chan GK and Gamper AM conceived the data. Bukhari AB and Gamper AM wrote the manuscript. All figures and tables have been re-numbered and supplementary figures and materials have been incorporated as main figures and text. All animal experiments were approved by the Animal Care Committee at the Cross Cancer Institute under protocol AC16225.

Acknowledgements

I would like to thank my supervisor, Dr. Armin Gamper, for his continued support and guidance throughout my time in his laboratory. Armin has always made himself available to discuss experimental data, troubleshoot problems, and help with experimental planning. I am truly grateful to him for all the freedom he provided when it came to planning and executing new experimental ideas. Despite his commitments to teaching and grant writing, he was always available to review scholarship applications, written proposals, or go over upcoming presentations.

I would like to thank my PhD supervisory committee members, Drs. Lynne-Marie Postovit and David Murray, for their helpful feedback and suggestions throughout my graduate studies. I am grateful for all the time they spared out of their busy schedules to meet with me and go over suggestions on grant writing or making experimental outlines. I am thankful to our collaborators: Drs. Gordon Chan, Frank Wuest, and Melinda Wuest for their support and guidance in various aspects of my PhD research. I am grateful to Dr. John Lewis for their allowing me to use their *in vivo* optical imager. I am also thankful to Dr. Kristi Baker for providing us with the C57BL/6 mice and all those helpful discussions on the cancer immunology aspects of my research. Special thanks to Drs. Roseline Godbout and Mary Hitt for providing us with the breast cancer cell lines and their continuous support, guidance, and encouragement.

I am thankful to my fellow (former) lab members, Michelle, and Leila, for their help during the animal experiments especially over the last two years of my PhD. The long hours spent irradiating mice on the SARRP would have been gruesome without them around. I would like to extend my thanks to my students, Jo, and Deandra for their help with the crystal violet assays and mice dissections during the early years of my PhD. Their hard work, dexterity, and dedication has been truly appreciated.

I am grateful to Dr. Xuejun Sun and Geraldine Barron for their assistance in the cell imaging facility. I am thankful to Dr. Anne Galloway, Dr. Aja Rieger, and Sabina Baghirova for their assistance with flow cytometry and letting me use the cell sorter after hours, and during university holidays. I am thankful to Dan McGinn, Cheryl Santos, Daming Li, and Liping Jiang for their assistance in the vivarium. I am also thankful to April Scott and Jolanta Paul for their technical assistance.

I am grateful to Allison, Cody, Ted, Daniel (Choi), Faisal, Kevin, Cindy, Joanne, and Andrew for their friendship, support, and encouragement. I am immensely thankful to my partner, Steph, for her continued love, support, encouragement, and patience especially during those long hours and all-nighters in the lab. You made the difficult times easier and the good times unforgettable. Finally, I thank my parents for always believing in me. Without them, I would be nothing.

Lastly, this work was supported by a Canadian Institute of Health Research (CIHR) and University of Alberta start-up grant. I am thankful to the Alberta Cancer Foundation and the Cancer Research Institute of Northern Alberta (CRINA) for awarding me the Dr. Cyril M. Kay Graduate Studentship to support my stipend. Additional stipend support provided by John & Rose McAllister Graduate Scholarship, Friends of the Faculty of Graduate Studies and Research Scholarship, Andrew Stewart Memorial Graduate Prize, Med Star Graduate Student Award, Joan and Bob Turner Oncology Graduate Achievement Award, and Marie Arnold Cancer Research Scholarship is greatly acknowledged.

Table of Contents

Abstract	ii
Table of Contents	vii
List of Tables	xii
List of Figures	xiii
Abbreviations	xv
Chapter 1: Introduction	1
1.1 Breast cancer	2
1.1.1 Epidemiology.....	3
1.1.2 Screening	7
1.1.3 Diagnosis	8
1.1.4 Pathology	8
1.1.5 Prognosis.....	10
1.2 Triple Negative Breast Cancer (TNBC)	11
1.3 Management of breast cancer	12
1.3.1 Early (non-metastatic) breast cancer	13
1.3.2 Advanced (metastatic) breast cancer	14
1.3.3 Management of TNBCs.....	16
1.4 Radiation therapy for breast cancer	17
1.5 The mammalian cell cycle	19
1.5.1 Regulation of cell cycle progression <i>via</i> CDK/cyclin complexes	20
1.5.2 CDK1 is an essential CDK required for cell cycle progression	21
1.6 Wee1	22
1.6.1 Wee1 kinase regulates the cell cycle checkpoint.....	23
1.7 The DNA damage response	23
1.8 Ataxia Telangiectasia and Rad3-related (ATR)	25
1.8.1 ATR signaling is a multi-step process resulting in cell cycle arrest.....	26
1.8.2 ATR is an essential kinase.....	27
1.9 Targeting the DNA damage response for cancer therapy	28

1.10 ATR and Wee1 as targets of cancer therapy.....	29
1.10.1 ATR inhibitors for cancer therapy.....	29
1.10.2 Wee1 inhibitors for cancer therapy.....	33
Chapter 2: Inhibiting Wee1 and ATR Kinases Produces Tumor-Selective Synthetic Lethality and Suppresses Metastasis	37
2.1 Introduction.....	38
2.2 Materials and Methods.....	41
2.2.1 Cell lines and plasmids	41
2.2.2 Antibodies and reagents.....	41
2.2.3 Crystal violet assay	41
2.2.4 Cell synchronization and cell cycle analysis	42
2.2.5 Side population assay	43
2.2.6 Mammosphere assay.....	43
2.2.7 Immunofluorescence.....	44
2.2.8 Live cell imaging	44
2.2.9 High-content screening microscopy	45
2.2.10 Assessment of mouse hematopoietic progenitor cells	45
2.2.11 Orthotopic breast cancer xenografts and drug treatments	46
2.2.12 Bioluminescence imaging.....	46
2.2.13 Immunohistochemistry	47
2.2.14 TUNEL assay.....	48
2.2.15 Statistical analysis.....	48
2.3 Results	49
2.3.1 Synergistic cell killing of cancer cells by ATR and Wee1 inhibition <i>in vitro</i>	49
2.3.2 Combination treatment of cancer cells with ATR and Wee1 inhibitors leads to centromere fragmentation and mitotic catastrophe.....	54
2.3.3 Events in S phase and G2/M phase contribute to the synergistic cancer cell killing by the combination treatment of cancer cells with ATR and Wee1 inhibitors	58
2.3.4 Combined inhibition of ATR and Wee1 leads to increased DNA damage in tumors <i>in vivo</i>	61
2.3.5 Combined ATR and Wee1 inhibition is well tolerated	64

2.3.6 Combined inhibition of ATR and Wee1 leads to tumor remission, increased survival and inhibition of metastasis.....	70
2.3.7 ATR and Wee1 activity are critical for breast cancer stem cell survival	74
2.4 Discussion	78
2.4.1 A model for the synergistic cell killing by ATR and Wee1 inhibition.....	79
2.4.2 Cancer-selective synthetic lethality, tumor remission and inhibition of metastasis	80
2.4.3 Potential strategies for patient selection	82
2.5 Acknowledgements	83
2.6 Conflict of interest	83
2.7 References.....	84
2.8 Supplementary information.....	89
Chapter 3: [¹⁸F]-FLT-PET as a Predictive Biomarker for Combined ATR and Wee1 Inhibitor Treatment	107
3.1 Introduction.....	108
3.2 Materials and Methods.....	112
3.2.1 Antibodies and chemicals	112
3.2.2 Cell lines	112
3.2.3 Crystal violet assay	112
3.2.4 Orthotopic breast cancer syngeneic mouse models and drug treatment.....	112
3.2.5 Immunohistochemistry	113
3.2.6 Radiosynthesis	114
3.2.7 PET imaging	114
3.2.8 Statistical analysis.....	115
3.3 Results	116
3.3.1 Combined ATR and Wee1 inhibitor treatment leads to synergistic cell killing in 4T1 but not in the EMT6 murine breast cancer cell line.....	116
3.3.2 [¹⁸ F]-FLT-PET imaging can be used as a biomarker to assess combined ATR and Wee1 inhibitor therapy response in breast tumors <i>in vivo</i>	119
3.3.3 Early changes in [¹⁸ F]-FLT uptake translate to tumor volume response.....	124
3.3.4 [¹⁸ F]-FLT uptake correlates with Ki-67 immunohistochemical staining	126

3.3.5 Early changes in [¹⁸ F]-FLT uptake correlate with tumor growth delay and longer overall survival of mice treated with combined ATR and Wee1 inhibitors	128
3.4 Discussion	130
3.4.1 EMT6 as model cell line for cancers refractory to ATR and Wee1 inhibitor treatment	130
3.4.2 Changes in FLT uptake during early treatment stage as biomarker for tumor response.....	131
3.4.3 [¹⁸ F]-FLT uptake correlates with Ki-67 immunohistochemical staining	134
Chapter 4: Combined ATR and Wee1 Inhibition as Adjuvant to Breast Cancer Radiotherapy or Surgery	136
4.1 Introduction.....	137
4.2 Materials and Methods.....	141
4.2.1 Antibodies and chemicals	141
4.2.2 Cell lines	141
4.2.3 Orthotopic mouse model, drug, and radiation treatments.....	141
4.2.4 Tumor infiltrating lymphocytes isolation and staining.....	142
4.2.5 Primary tumor removal surgeries	144
4.2.6 Statistical analysis.....	144
4.3 Results	145
4.3.1 Combined inhibition of ATR and Wee1 radiosensitizes 4T1 tumors, leads to growth delay and prolongs survival	145
4.3.2 Combined inhibition of ATR and Wee1 attenuates expression of CD8 ⁺ T cell exhaustion markers following radiation.....	147
4.3.3 IR but not combined inhibition of ATR and Wee1 alone, temporarily reduces the ratio of Tregs in the tumors.....	150
4.3.4 Combined inhibition of ATR and Wee1 concomitant with radiation diminishes CD8 ⁺ T cell effector function in 4T1 tumors in a time dependent manner	153
4.3.5 Combined inhibition of ATR and Wee1 as an adjuvant to surgery prolongs overall survival of BALB/c mice	155
4.4 Discussion	158
4.4.1 ATR and Wee1 inhibitors as radiosensitizers.....	158
4.4.2 ATR and Wee1 inhibitors as activators of the immune response.....	159

4.4.3 A model for pre-clinical evaluation of ATR and Wee1 inhibitors as adjuvant therapy	162
Chapter 5: General Discussion and Future Directions	164
5.1 ATR and Wee1 inhibition as a promising approach for breast cancer treatment	165
5.2 Identification of potential biomarkers to predict sensitivity to ATR and Wee1 inhibitor treatment	167
5.3 ATR and Wee1 inhibitor treatment in combination with other DDR targets	169
5.4 ATR and Wee1 inhibitors in combination with radiotherapy and immune checkpoint blockade inhibitors	171
5.5 Conclusions.....	173
Bibliography	174

List of Tables

Table 2.1. Synergistic cancer cell killing by ATR and Wee1 inhibition.	53
Table 2.2. Metastases in animals treated with ATR and Wee1 inhibitors.	73
Table 2.3. Mammosphere-forming capabilities of SP and NSP cells.	77
Table 3.1. Synergistic murine breast cancer cell killing by ATR and Wee1 inhibition.	117
Table 3.2. Mutation status in 4T1 and EMT6 murine breast cancer cell lines of genes with potential impact on ATR inhibitor sensitivity.	121
Supplementary Table 2.1. Complete blood count (CBC) analysis of mice treated with ATR and/or Wee1 inhibitors.	105
Supplementary Table 2.2. Manual differential analysis of mice treated with ATR and/or Wee1 inhibitors.	106

List of Figures

Figure 1.1. Distribution of cancer incidence and mortality in 2020.	4
Figure 1.2. Histological subtypes of invasive breast cancer.	9
Figure 2.1. Wee1 inhibition activates ATR and shows synergistic cancer cell killing with ATR inhibition.	52
Figure 2.2. Combined ATR and Wee1 inhibition leads to mitotic defects and cancer cell death.	56
Figure 2.3. Contribution of cell cycle phases, during which ATR and/or Wee1 was inhibited, to overall cell killing.	60
Figure 2.4. AZD6738 and AZD1775 inhibit ATR and Wee1, respectively, <i>in vivo</i>	63
Figure 2.5. Combination treatment with ATR and Wee1 inhibitors and normal tissue toxicity. .	66
Figure 2.6. Evaluation of normal tissue DNA damage.	69
Figure 2.7. Combination treatment with ATR and Wee1 inhibitors and tumor control.	72
Figure 2.8. Synergistic killing of breast cancer stem cells by ATR and Wee1 inhibitors.	76
Figure 3.1. ATR and Wee1 inhibition leads to synergistic cell killing in 4T1, but not in EMT6.	118
Figure 3.2. Combination treatment with ATR and Wee1 inhibitors and non-invasive monitoring of treatment response with [¹⁸ F]-FLT-PET imaging.	122
Figure 3.3. Effect of ATR and Wee1 inhibitors on tumor volume response.	125
Figure 3.4. Histological evaluation of cell proliferation status.	127
Figure 3.5. Combined treatment with ATR and Wee1 inhibitors and tumor response.	129
Figure 3.6. Changes in SUV _{mean} correlates with changes in tumor volume.	132
Figure 4.1. Combined inhibition of ATR and Wee1 kinases radiosensitizes 4T1 tumors and prolongs survival.	146
Figure 4.2. Combined inhibition of ATR and Wee1 attenuates expression of T cell exhaustion markers.	149
Figure 4.3. Radiation reduces the proportion of Tregs among TILs.	152
Figure 4.4. Impact of combined ATR, Wee1, and radiation treatment on CD8 ⁺ T cell effector function.	154
Figure 4.5. Combined inhibition of ATR and Wee1 as adjuvant therapy to surgery.	157

Supplementary Figure 2.1. Wee1 inhibition activates ATR.	89
Supplementary Figure 2.2. Wee1 and ATR inhibition synergistically kills cancer cells.	90
Supplementary Figure 2.3. Wee1 and ATR inhibition synergistically kills cancer cells.	91
Supplementary Figure 2.4. The Chk1 inhibitor UCN-01 is highly toxic in MCF10A and hTERT-HME1, alone and in combination with AZD1775.	92
Supplementary Figure 2.5. Combined ATR and Wee1 inhibition leads to mitotic defects and cancer cell death.	94
Supplementary Figure 2.6. Quantification of photon flux for MDA-MB-231-fluc2-tdTomato cells <i>in vitro</i>	95
Supplementary Figure 2.7. ATR phosphorylation at T1989 is a marker of ATR activation.	96
Supplementary Figure 2.8. Hair growth changes in mice treated with ATR and/or Wee1 inhibitors.	97
Supplementary Figure 2.9. Immunohistochemistry evaluation of ATR pThr1989 levels in normal tissues of NSG mice.	98
Supplementary Figure 2.10. Evaluation of apoptotic cells by TUNEL assay in ileum.	99
Supplementary Figure 2.11. Immunohistochemistry evaluation of CDK1 pTyr15 levels.	100
Supplementary Figure 2.12. Immunohistochemistry evaluation of CDK1 pTyr15 in other normal tissues.	101
Supplementary Figure 2.13. Immunohistochemistry evaluation of γ H2AX staining in normal tissue.	102
Supplementary Figure 2.14. Longitudinal studies of tumor-bearing mice treated with ATR and Wee1 inhibitors.	103
Supplementary Figure 2.15. G2/M and S phase checkpoint regulation by ATR and Wee1.	104

Abbreviations

[¹⁸ F]-FDG	[¹⁸ F]2'-fluoro-2'-deoxyglucose
[¹⁸ F]-FLT	[¹⁸ F]3'-deoxy-3'-fluorothymidine
ABCG2	ATP-binding cassette super-family G member 2
APC	Antigen presenting cell
ARID1A	AT-rich interaction domain 1A
AT	Ataxia telangiectasia
ATM	Ataxia telangiectasia mutated
ATR	Ataxia telangiectasia and Rad3-related
ATRi	ATR inhibitor
ATRIP	ATR-interacting protein
BER	Base excision repair
bhFGF	Basic human fibroblast growth factor
BL1	Basal-like 1
BL2	Basal-like 2
BLIA	Basal-like immune activated
BLIS	Basal-like immunosuppressed
BMI	Body mass index
BSA	Bovine serum albumin
CBCT	Cone-beam computed tomography
CBCT	Cone beam computed tomography
CCD	Charged coupled device
Cdc25	Cell division cycle 25
CDK1	Cyclin dependent kinase 1
CDK2	Cyclin dependent kinase 2
CDK4/6	Cyclin dependent kinase 4/6
CENP-B	Centromere protein-B
CENP-F	Centromere protein-F
Chk1	Checkpoint kinase 1
CI	Combination indices
CR	Complete response
CTL	Cytotoxic T lymphocytes
DAB	3,3'-diaminobenzidine
DAMPs	Danger associated molecular patterns
DAPI	4',6-diamino-2-phenylindole
DC	Dendritic cells
DCV	DyeCycle Violet
DDK	DBF4-Dependent cdc7 kinase
DDR	DNA damage response

DMEM	Dulbecco's Modified Eagle's Medium
DMSO	Dimethyl sulfoxide
DNA	Deoxyribonucleic acid
DNA-PKcs	DNA-dependent protein kinase catalytic subunit
DSB	Double-strand break
DVH	Dose volume histogram
EDTA	Ethylenediaminetetraacetic acid
EGF	Epidermal growth factor
ENT1	Equilibrative nucleoside transporters 1
ER	Oestrogen receptor
ETAA1	Ewing's tumor-associated antigen 1
FACS	Fluorescence activated cell sorting
FBS	Fetal bovine serum
FBXW7	F-box/WD repeat-containing protein 7
FFPE	Formalin fixed paraffin embedded
FITC	Fluorescein isothiocyanate
FNAC	Fine needle aspiration cytology
FoxP3	Forkhead box P3
GFP	Green fluorescent protein
h	Hours
H2B	Histone H2B
HEAT	Huntington-elongation factor 3-protein phosphatase 2A-TOR1
HER2	Human epidermal growth factor receptor 2
HR	Homologous recombination
HRP	Horse radish peroxidase
ICD	Immunogenic cell death
IFN- γ	Interferon- γ
IGRT	Image-guided radiation therapy
IHC	Immunohistochemistry
IL-10	Interleukin-10
IL-2	Interleukin-2
IM	Immunomodulatory
IMRT	Intensity-modulated radiation therapy
IR	Irradiation
LAG-3	Lymphocyte-activation gene 3
LAR	Luminal androgen receptor
LD ₅₀	Limited dilution 50
LSM	Laser scanning microscope
mCherry	Monomeric Cherry fluorescent protein
MHC I	Major histocompatibility complex class I molecules

mins	Minutes
MIP	Maximum intensity projection
MMR	Mismatch repair
MRI	Magnetic resonance imaging
MSL	Mesenchymal stem-like
MUG	Mitotic cells with under-replicated genome
n	Number of samples
NEBD	Nuclear envelope break down
NHEJ	Nonhomologous end-joining
NK	Natural killer
NSCLC	Non-small cell lung cancers
NSP	Non-side population
OD	Optical density
PARP	Poly(ADP-ribose) polymerase
PBI	Partial breast irradiation
PBS	Phosphate buffered saline
PCNA	Proliferating cell nuclear antigen
PD	Progressive disease
PD-1	Programmed cell death-1
PD-L1	Programmed death-ligand 1
PET	Positron emission tomography
PI	Propidium iodide
PIKKs	Phosphatidylinositol 3-kinase-like protein kinases
PKMYT1	Protein kinase membrane-associated tyrosine/threonine 1
PLK1	Polo-like kinase 1
PMA	Phorbol myristate acetate
PR	Progesterone receptor
PR	Partial response
PRD	PIKK regulatory domain
RECIST	Response evaluation criteria in solid tumors
ROI	Region of interest
RPA	Replication protein A
RPMI	Roswell park memorial institute
RT	Radiation therapy
SARRP	Small animal radiation research platform
SD	Stable disease
siRNA	Small interference ribonucleic acid
SP	Side population
SSBR	Single-strand break repair
SUV	Standardized uptake values

TBI	Total breast irradiation
TCR	T cell receptor
TIM-3	T cell immunoglobulin and mucin-domain containing-3
TK1	Thymidine kinase 1
TNBC	Triple negative breast cancer
TopBP1	DNA topoisomerase II binding protein
Tregs	Regulatory T cells
TUNEL	Terminal deoxynucleotidyl transferase dUTP nick end labeling
UV	Ultraviolet
Wee1i	Wee1 inhibitor

Chapter 1: Introduction

1.1 Breast cancer

Breast cancer is the most diagnosed cancer amongst women around the world. Due to the heterogenous nature of the disease, over the last two decades, treatment options have increasingly taken into account biological parameters (gene signatures, protein expression levels) to tailor treatment plans to individual patients. However, locoregional tumor burden or presence of metastatic lesions remain the most important factors in deciding between therapeutic approaches. The confinement of cancer to the breast tissue or its spread just to the axillary lymph nodes is termed early breast cancer and is deemed curable in about 80-90% patients with existing treatment options (Harbeck *et al.* 2019). On the contrary, advanced, or metastatic breast cancer – that is, spread of cancer from the breast tissue to other parts of the body (most commonly to liver, lung, bone, and/or brain) – is not considered curable, but it is a treatable disease, for which the goal of therapy is to prolong survival keeping in mind treatment associated toxicities to improve the adjusted “quality” of life.

The histological and molecular characteristics of breast cancer are determining factors on the choice of treatment options – which include locoregional treatment (such as surgery or radiation therapy) and/or systemic therapy (such as chemotherapy or hormone therapy). Early pathological classification of breast cancer categorized it into four different subtypes: luminal A and B (hormone receptor - oestrogen receptor (ER) and progesterone receptor (PR) - positive), human epidermal growth factor receptor 2 (HER2) enriched, and basal-like (ER, PR, and HER2 negative) (Perou *et al.* 2000). The current practice in the clinical management of breast cancer classifies it into five subtypes: **luminal A-like** (high expression of ER and PR; HER2 negative), **luminal B-like HER2+** (ER+, HER2+, but lower ER and PR expression than luminal A-like), **luminal B-like HER2-** (ER+, HER2-, but lower ER and PR expression than luminal A-like),

HER2-enriched (ER-, PR-, HER2+), and **Triple negative breast cancer** (TNBC; ER-, PR-, HER2-).

1.1.1 Epidemiology

In 2020, more than 2.2 million women were newly diagnosed with breast cancer (24.51% of all newly diagnosed cancer cases in females) surpassing the global incidence of newly diagnosed colorectal and lung cancer cases in women by ~15% (**Fig. 1A**) (Sung *et al.* 2021). Additionally, approximately 685,000 (~ 15.5%) women died due to breast cancer making it the leading cause of cancer related deaths in women (**Fig. 1B**) (Sung *et al.* 2021). In Canada, it is estimated that about 28,000 women will be diagnosed with breast cancer representing ~ 21% of all new cancer cases in women in 2020 (**Fig. 1C**). Despite the rate of mortality in Canada dropping at ~ 0.2% between 1991 and 2015, likely due to increased mammographic screening programs resulting in early detection and better disease prognosis, about 5,700 women will still die of breast cancer accounting for 14% of all cancer related deaths – making breast cancer the second leading cause of death in women (Committee 2019) (**Fig. 1D**). In 2020, approximately 75 Canadian women will be diagnosed with breast cancer and approximately 13 will die due to it on average daily (Committee 2019). Nearly 40% of breast cancer cases are expected to be diagnosed in females aged 30 to 59.

Data collected by the National Cancer Institute between 2013 and 2017 indicates that luminal A (hormone receptor positive / HER2 negative) is the most diagnosed subtype of breast cancer with incidence of 87 new cases per 100,000 women. This was significantly higher than any other subtype [TNBC (hormone receptor negative / HER2 negative) incidence was 13 new cases per 100,000 women; luminal B (hormone receptor positive / HER2 positive) incidence was 13.3 new cases per 100,000 women; and HER2-enriched (hormone receptor negative / HER2 positive)

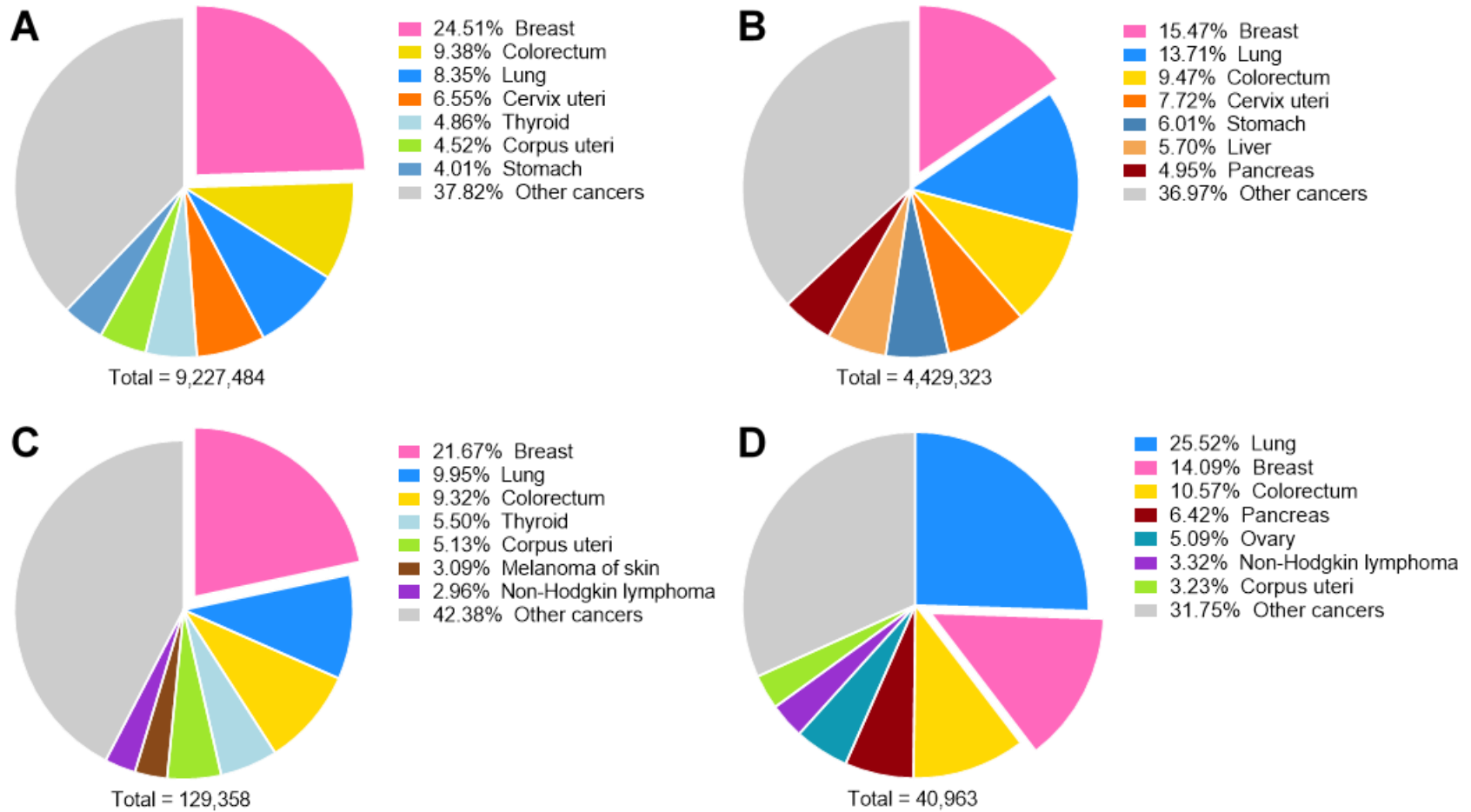


Figure 1.1. Distribution of cancer incidence and mortality in 2020.

Chart shows that breast cancer is the most diagnosed cancer (A) and the leading cause of cancer-related deaths amongst women globally (B). In Canada, breast cancer remains the most diagnosed cancer (C) and the second leading cause of cancer-related deaths amongst women (D). Data was accessed from GLOBOCAN 2020 (Sung *et al.* 2021).

incidence was 5.5 new cases per 100,000 women] (NCI). A recent study compared the change in incidence rates of breast cancer subtypes across various age and race/ethnic groups in the United States and found that out of the 320,124 women diagnosed with breast cancer between 2012 and 2016, the incidence of luminal A breast cancer increased from 2.3% to 4.2% in non-Hispanic White, and from 2.5% to 4.5% in non-Hispanic Asian/Pacific Islander women aged 40 to 54 years (Acheampong *et al.* 2020). The same study also noted an increase in the incidence of luminal B and HER2+ breast cancers across different racial/ethnic backgrounds in all age groups (Acheampong *et al.* 2020). Interestingly, a decline in the incidence of TNBCs was observed (Acheampong *et al.* 2020). These changes in the annual incidence of breast cancer with differing molecular subtypes may indicate changes in the prevalence of breast cancer risk factors by race, ethnicity, and age. The underlying reasons remain unknown but may include changes in lifestyle or screening. The absence of a national cancer registry in Canada limits the accessibility of similar epidemiological data for the different breast cancer subtypes. A recent population based analysis on the incidence of breast cancer in Canadian women found that the annual incidence in Ontario during 2012-2015 for TNBC was 15 new cases per 100,000, 21-23 new cases per 100,000 for the HER2-enriched group, and 97-105 new cases per 100,000 for luminal (hormone receptor positive/HER2 negative) breast cancers (Seung *et al.* 2020). Regarding outcome, women with stage IV TNBC have the lowest overall median survival of 8.9 months followed by advanced stage/metastatic HER2-enriched (median overall survival of 37.3 months) and luminal (median overall survival of 35.2 months) breast cancers (Seung *et al.* 2020).

Familial breast cancer accounts for about 5-10% of breast cancers (Shiovitz and Korde 2015). Carriers of germline mutations in two high penetrance genes – *BRCA1* and *BRCA2* – have about a 72% and 69% mean risk of developing breast cancer by the age of 80 years

(Kuchenbaecker *et al.* 2017). These mutations account for about 20-30% of all familial breast cancers (Yiannakopoulou 2014), and it is estimated that they are responsible for more than 90% of early-onset cancers in families with both breast and ovarian cancers. Over 2200 pathogenic mutant variants of *BRCA1* and *BRCA2* have been identified (Cline *et al.* 2018). However, only a few founder mutations were more common in certain populations, like Ashkenazi Jewish families with higher frequency (approx. 1 in 40) of the *BRCA1* 187delAG and 5385insC, and *BRCA2* 6174delT mutants (Foulkes 2008, Metcalfe *et al.* 2010, Walsh *et al.* 2017), or the Icelandic (*BRCA2* 999del5), and the French Canadian populations (*BRCA1* C4446T and *BRCA2* 8765delAG) (Tonin *et al.* 1998, Mikaelsdottir *et al.* 2004). The clinical availability of poly(ADP-ribose) polymerase (PARP) inhibitors has led to significant improvements by prolonging progression-free survival of breast cancer patients with BRCA defects through an interaction described as “synthetic lethality” (Fong *et al.* 2009). In addition to BRCA mutations, two rare hereditary cancer syndromes linked to germline mutation of *TP53* or *CHEK2* (Li-Fraumeni syndrome; affecting 1 in 5,000 to 1 in 20,000) and *PTEN* (Cowden syndrome; affecting 1 in 250,000) have also shown an increased risk of breast cancer (Malkin *et al.* 1990, Liaw *et al.* 1997). As a result, with the availability of next generation sequencing data, screening panels evaluating the risk of hereditary breast cancers have gone beyond *BRCA1* and *BRCA2* to include additional genes like *TP53*, *CDH1*, *PTEN*, *ATM*, *CHEK2*, *PALB2*, *STK11*, *RAD51C*, *BRIPI*, and *NBN* (Tung *et al.* 2015).

The pattern of breast cancer incidence differs among countries based on lifestyle, and the popularity of national awareness campaigns. An estimated 20% of breast cancers are attributed to obesity, physical inactivity, and alcohol consumption. Studies have shown an increased probability of developing breast cancer in postmenopausal women from Asia-Pacific, with higher body mass

index ($\text{BMI} \geq 5$) associated with an approximate 12% increase in overall risk (reviewed in (Renehan *et al.* 2008)). Additionally, this risk increases further by 20 to 40% in obese postmenopausal women compared to those with normal weight (Munsell *et al.* 2014). Data from epidemiological studies have also found a consistent link between increased risk of breast cancer and alcohol consumption with light drinkers (1-3 drinks per week) having a slightly increased risk (1.04-fold higher), and moderate (1 drink per day; 1.23-fold higher risk) and heavy drinkers (4 or more drinks per day; 1.6-fold higher risk) having a greater risk of breast cancer compared to non-drinkers (Chen *et al.* 2011, Bagnardi *et al.* 2015, LoConte *et al.* 2018). Interestingly, this association is observed in both premenopausal and postmenopausal women (Singletary and Gapstur 2001).

1.1.2 Screening

Population screening programs for breast cancer use non-invasive mammographs for early identification of breast cancers to enable effective treatments at an early stage. Meta-analysis of randomized controlled clinical trials suggests that the relative risk of breast cancer mortality in women aged 50 years and older was reduced by almost 20% if they were subject to breast cancer screens every 3 years compared to unscreened controls (Independent 2012, Nelson *et al.* 2016).

Women with mutations in genes implicated in breast cancer incidence are often advised to undergo risk-tailored screening where mammography (or digital breast tomosynthesis also referred to as near-3D mammography) is often combined with magnetic resonance imaging (MRI) or ultrasonography. While these technologies have helped increase breast cancer detection (Melnikow *et al.* 2016), they have not been assessed for mortality outcomes (Lauby-Secretan *et al.* 2015). Unfortunately, as this technology is relatively new there are no long-term efficacy data

available, which limits our understanding of actual benefits for patient outcomes (Marinovich *et al.* 2018).

1.1.3 Diagnosis

Women experiencing breast symptoms such as lump(s), pain, or nipple discharge, typically undergo the triple test as part of their diagnostic evaluation which comprises a physical examination, mammography or ultrasonography, and fine needle aspiration cytology (FNAC) (Irwig *et al.* 2002). The high accuracy of the triple test allows to accurately discriminate breast cancer *versus* benign or normal breast conditions avoiding unnecessary surgical interventions.

Breast ultrasonography is a frequent practice in guiding fine needle breast biopsies, and to evaluate localized symptoms, especially in young women with dense breasts where the results of a mammogram are negative or difficult to interpret (Hooley *et al.* 2013). Besides ultrasonography, MRI of the breast is also advised in select cases where the conventional imaging examinations have been either contradictory or inconclusive. Unlike in the case of mammography, the results from MRI are not affected by breast density and the technique has higher sensitivity for cancer detection. Interestingly, breast MRI is particularly useful in identification of axillary lymph node metastases with occult breast tumor (Morrow *et al.* 2011).

1.1.4 Pathology

Based on the WHO classification, breast cancer is divided into 19 different subtypes comprising invasive carcinomas of no special type (previously known as invasive ductal carcinomas), invasive lobular carcinoma, and carcinomas of special type which include 17 rare histological subtypes and their subclassifications (**Fig. 1.2**) (Lakhani *et al.* 2012, Tan *et al.* 2020). Among the special types, tubular, cribriform, and mucinous with no mixed histology (i.e., at least 90% pure) have excellent prognosis (Lakhani *et al.* 2012). On the other hand, pleiomorphic lobular

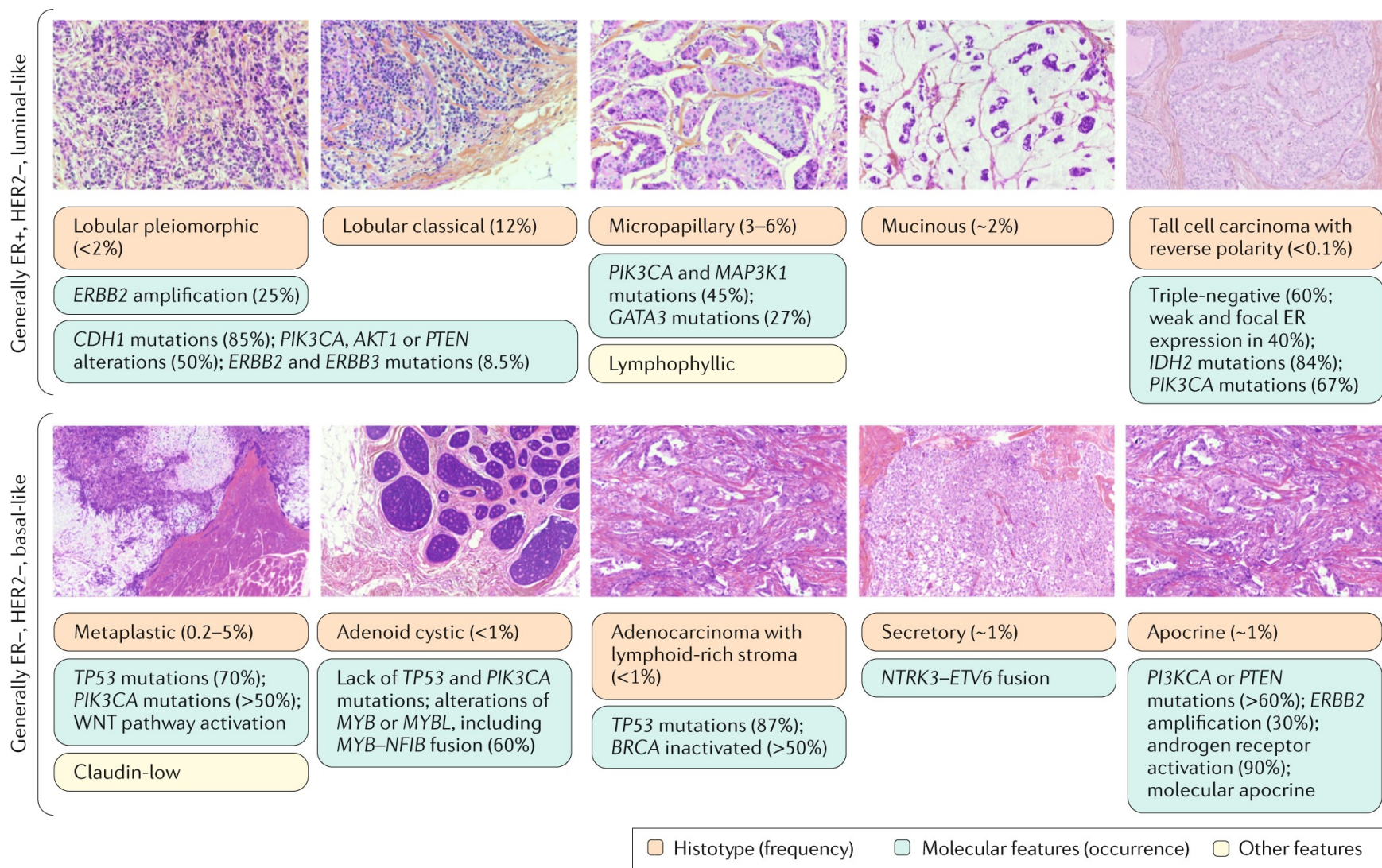


Figure 1.2. Histological subtypes of invasive breast cancer.

Figure represents the WHO classification of the various subtypes of invasive breast cancer, their prevalence, and frequently observed mutations. This figure was used with permission and without modification from Harbeck *et al.* (Harbeck *et al.* 2019).

carcinoma, high-grade metaplastic carcinoma, and micropapillary carcinoma special subtypes were associated with the poorest clinical outcome (Lakhani *et al.* 2012).

Histological evaluations take into consideration the proportion of cancer cells that are in tubule formation, the degree of nuclear pleomorphism, and the number of mitotic cells (Elston and Ellis 1991). A grade is assigned based on the Elston- and Ellis-modified Scarff-Bloom-Richardson system where each feature is scored with three-tier system, and the final grade (grade I, grade II, or grade III) is determined by adding individual scores to determine aggressiveness of the breast tumor (Elston and Ellis 1991). Based on the recommendations from international guidelines, determination of hormone receptor (ER/PR) and HER2 status is required for all patients with invasive breast cancer (Wolff *et al.* 2013, Senkus *et al.* 2015, NCCN 2021). The American Society of Clinical Oncology recently revised their guidelines to define HER2 positivity (3+) as more than 10% cells showing complete membrane staining by immunohistochemistry (IHC) or by an amplification of HER2 gene (≥ 6 gene copies or the ratio of HER2/chromosome 17 is ≥ 2) detected by *in situ* hybridization (Wolff *et al.* 2013).

1.1.5 Prognosis

The traditional prognostic markers (i.e., factors predicting risk of recurrence or death) for breast cancer include age, tumor size, histologic and nuclear grade, number of positive axillary lymph nodes, tumor angiogenesis, and subtype (Donegan 1997). Patients over the age of 75 typically experience 17% higher cancer related mortality than younger patients (Tao *et al.* 2019). While breast cancer in young women (< 35 years of age) is rare (< 5% of patients), it is frequently associated with a familial history and often has an aggressive phenotype.

The intrinsic molecular subtypes of breast cancers are an important criteria in treatment decisions. Breast cancer patients with luminal A-like tumors have good prognosis, and the relapse

rate is significantly lower than any other subtypes. These tumors frequently present with low histological grade, low proliferation, low Ki-67/PCNA immunohistochemistry staining, high ER and PR expression, and include special histological subtypes (tubular, invasive cribriform, mucinous, and lobular) (Carey *et al.* 2006, Yersal and Barutca 2014). On the contrary, patients with luminal B-like tumors are associated with an aggressive phenotype, have high ER but no (or to a lesser extent) PR expression, display a high histologic grade and a high proliferation index, and have a poor prognosis (Creighton 2012). HER2+ tumors are aggressive, have high proliferation, high grade (G2 or G3), low or absent ER and PR expression, and nearly 40% are p53 mutant (Tsutsui *et al.* 2003). TNBCs are highly aggressive, associated with high grade (G3), exceptionally high proliferation index, no expression of ER, PR, and HER2, and most of these tumors are infiltrating ductal tumors with high rate of metastasis to the lungs and brain (Heitz *et al.* 2009).

1.2 Triple Negative Breast Cancer (TNBC)

The research presented in this thesis uses TNBC cell lines to generate orthotopic mouse models and is focussed on improving therapeutic outcomes for early and advanced stage tumors. TNBCs account for 15-20% of all breast cancers and is more prevalent in younger women, particularly those with a familial history [48]. About two-third of TNBC patients present with grade III disease and have larger tumors compared to the other breast cancer subtypes [49]. Additionally, TNBC patients are also linked to significantly higher mortality (~42% of 5 year) where the median overall survival is about 4.2 years as compared to 6 years with other subtypes [49]. Patients with TNBC have an increased likelihood of recurrence (usually in the first 3 years after diagnosis), and many experience an early onset of distant metastasis [49].

To gain insights into the biology of TNBCs, Lehmann *et al.* used gene expression analysis and identified six distinct TNBC subtypes which include: two basal-like (BL1 and BL2), an immunomodulatory (IM), a mesenchymal (M), a mesenchymal stem-like (MSL), and luminal androgen receptor (LAR) subtype [50]. More recently, Burstein *et al.* revisited this initial classification by using RNA and DNA profiling analysis and classified TNBCs into four subtypes that is LAR, mesenchymal (MES), basal-like immunosuppressed (BLIS), and basal-like immune activated (BLIA) [51]. Among these, prognosis for both disease free survival and disease specific survival was worst for BLIS and best for BLIA [51].

1.3 Management of breast cancer

For early (non-metastatic) breast cancer, the main goals of therapy are eradicating tumor from the breast and regional lymph nodes and preventing metastatic recurrence. For this, treatment usually consists of surgical removal of primary tumor and axillary lymph nodes, with consideration of postoperative radiation therapy to eradicate any remaining microscopic disease. Systemic therapy may be given in either a neoadjuvant (before surgery; especially in women with larger tumors) or an adjuvant (after surgery) setting, or both. On that note, the molecular subtypes of breast cancer typically determine the type of standard systemic therapy administered usually comprising of endocrine therapy for all hormone receptor positive tumors and additional chemotherapy for some high risk patients with hormone receptor positive tumors, trastuzumab in combination with other chemotherapeutic drugs for HER2+ tumors, and chemotherapy alone for TNBCs.

As advanced (metastatic) breast cancer is considered not curable, the main goals of therapy are to prolong life and symptom palliation. Systemic therapies are similar to early breast cancers, and locoregional therapies (surgery and radiation therapy) are usually aimed at palliation.

1.3.1 *Early (non-metastatic) breast cancer*

Treatment of early breast cancers with surgery to remove the primary tumor and staging or excision of the affected axillary lymph nodes is the foundation of curative treatment. Over the past decade or so, more women have been open to breast-conserving surgery thus substituting mastectomy for lumpectomy to a great extent (McLaughlin 2013). For early breast cancers, primary tumor resection is usually the first step of treatment. However, in some cases, it may be preceded by neoadjuvant chemotherapy depending on tumor size, tumor to naïve breast size ratio, and patient choice (Margenthaler and Ollila 2016).

Postoperative treatments in the form of whole breast radiation and/or systemic therapy are governed by the initial tumor burden and the tumor subtype. Indeed, postoperative radiation therapy following breast-conserving surgery has improved disease-free and overall survival for patients with early breast cancer either by eliminating residual cancer cells (Ebtctg *et al.* 2014, Heil *et al.* 2020) and/or inducing an abscopal effect (where treatment of the primary tumor results in tumor shrinkage at a distant site) (Jatoi *et al.* 2018). Radiation biology models suggest a hypofractionated daily dose (approximately 42.5 Gy over 16 fractions) given over a shorter time (~3 weeks) may be just as effective (Fowler 1989), and most importantly more convenient for patients and less resource intensive than the historical standard (50 Gy over 25 fractions over a period of 5 weeks) (Whelan *et al.* 2010).

Systemic therapies for early breast cancer are very effective, but may vary based on tumor molecular subtype, initial tumor burden, and absolute risk of recurrence from one individual to another (Pan *et al.* 2017). For hormone receptor positive breast cancers, the standard duration of adjuvant endocrine therapy with tamoxifen is at least 5 years after surgery. This has helped reduce tumor recurrence rate and mortality (Early Breast Cancer Trialists' Collaborative *et al.* 2011).

Patients with a >10% risk of recurrence over 10 years are advised to receive chemotherapy in addition to endocrine therapy (Harbeck *et al.* 2019). Chemotherapy regimens commonly include docetaxel and cyclophosphamide, or doxorubicin given concurrently to manage long term toxicity (Mackey *et al.* 2016). The discovery of trastuzumab (Herceptin, an anti-HER2 monoclonal antibody) has been an important development in breast cancer treatment for HER2+ breast cancers. The use of trastuzumab with standard chemotherapy in an adjuvant or neoadjuvant setting was demonstrated to markedly improve disease-free survival and overall survival in randomized clinical trials, making it the standard of care for patients with HER2+ tumors (Romond *et al.* 2005, Slamon *et al.* 2011, Gianni *et al.* 2016). Like HER2+ breast cancers, TNBC patients undergo neoadjuvant chemotherapy which typically contains a taxane and an anthracycline, although docetaxel and cyclophosphamide combination is as effective at an early stage (Nitz *et al.* 2019). Additionally, PARP inhibitors and platinum compound-based chemotherapies have gained interest for the treatments of TNBC due to defects in DNA double strand break repair mechanisms arising because of mutations in *BRCA1/2* and other DNA repair genes (Denkert *et al.* 2017).

1.3.2 Advanced (metastatic) breast cancer

Advanced breast cancer is the spread of cancer beyond the breast tissue to the other sites – mainly bone, lungs, liver, and brain. Currently, it remains a virtually incurable disease with metastasis being the cause of death in almost all patients. Median survival ranges from 10-13 months for the highly metastatic TNBC subtype to 4-5 years for metastatic hormone receptor positive and HER2+ tumors. Breast cancer patients with metastatic disease receive treatment with the aim of symptom palliation and prolongation of adjusted “quality of life”. Although surgery is not a mainstay for patients with metastatic disease, it may be an option for a few patients showing

excellent response to systemic therapy and lower burden of distant disease, or for patients with resectable brain metastasis (Cardoso *et al.* 2020).

Radiation therapy is often recommended to patients with metastasis to bone and brain for symptom mitigation. Indeed, the prescription is individualized with dose and fractionation schedules being determined based on the severity of the lesion and remaining life expectancy. For instance in patients with painful bone metastasis, a single dose of 8 Gy may be sufficient and less toxic than a dose of 20 Gy given in multiple fractions (Chow *et al.* 2014). On the other hand, for metastatic lesions to the brain, stereotactic radiosurgery may be prescribed for patients with lesions up to 3 cm, and larger or multiple lesions may undergo treatment with whole-brain radiotherapy (Phillips *et al.* 2017).

As in the case of early breast cancers, systemic therapy for advanced metastatic breast cancers is guided based on the molecular subtype. Multigene panels have not been useful in the clinic for patients with metastatic disease. So the choice of systemic therapy, to a great extent, relies on biopsy and assessment of receptor status (ER and HER2) at the first metastasis (if possible), as it can help verify histology and assess potential changes in tumor biology at the lesion (Cardoso *et al.* 2020). For hormone receptor positive metastatic breast cancers, serial endocrine-based therapies are recommended until the patient stops responding (endocrine therapy resistance), and then treatment is transitioned to single-agent chemotherapy (Waks and Winer 2019). Premenopausal patients with hormone receptor positive tumors are advised to undergo treatment to achieve medical or surgical menopause in addition to treatment with an endocrine agent (aromatase inhibitor plus CDK4/6 inhibitor, tamoxifen, or fulvestrant) (Rugo *et al.* 2016, Cardoso *et al.* 2020). For postmenopausal patients with hormone receptor positive tumor, the first line of therapy is usually an aromatase inhibitor followed by treatments with fulvestrant, tamoxifen, or

Olaparib (for *BRCA1/2* mutation) as the later line resorts (Waks and Winer 2019). HER2+ metastatic breast cancers are treated with anti-HER2 targeting agents, and patients previously untreated with trastuzumab preferentially undergo dual HER2 blockade with trastuzumab and pertuzumab plus taxane based chemotherapy (Cardoso *et al.* 2020). Here, the later line therapy options usually include trastuzumab in combination with another chemotherapy drug like capecitabine or vinorelbine (Cardoso *et al.* 2020).

1.3.3 Management of TNBCs

For TNBC patients with metastatic disease, single-agent chemotherapy is recommended with the initial line of therapy being taxane-based, platinum-based, or anthracycline compounds (Waks and Winer 2019).

Studies found TNBCs to be particularly responsive to platinum compound-based chemotherapies if they had inherent deficiencies in DNA repair mechanisms (Silver *et al.* 2010, Vollebergh *et al.* 2011, Isakoff *et al.* 2015). As an example, findings from the phase 3 TNT trial found that metastatic TNBC patients with germline *BRCA* mutation had a significantly better response to carboplatin treatment as compared to docetaxel (Tutt *et al.* 2018). In another randomized phase 3 trial, metastatic TNBC patients (not selected for *BRCA* status) treated with cisplatin plus gemcitabine had better progression free survival (7.73 months; 95% CI 6.16-9.30) as compared to patients receiving paclitaxel plus gemcitabine (6.47 months; 95% CI 5.76-7.18) as first-line treatment (Hu *et al.* 2015).

Several PARP inhibitors have paved their way into the clinic for treatments of various cancers including TNBCs with germline *BRCA* mutations (deficient in homologous recombination). PARP inhibitors induce cytotoxicity in tumor cells by increasing reliance on homologous recombination which is often dysregulated in cancers with *BRCA* mutations. In *BRCA*

mutant TNBC patients, treatment with olaparib (median survival of 7 months) or talazoparib (median survival of 8.4 months) (PARP inhibitors) has shown improved progression free survival in comparison to standard single-agent chemotherapies (median survival of 4.2-5.6 months) (Robson *et al.* 2017, Litton *et al.* 2018).

Higher levels of tumor infiltrating lymphocytes have been positively correlated with improved patient outcomes particularly in the BLIA subtype of TNBCs suggesting these patients may benefit from immunotherapy (Denkert *et al.* 2010, Liu *et al.* 2012). Furthermore, recent reports have identified that the programmed cell death-1 (PD-1) receptor and its ligand PD-L1, an immune regulatory molecule that limits antitumor activity, is expressed in nearly 20-30% TNBCs thus making it an exciting therapeutic target (Mittendorf *et al.* 2014, Wimberly *et al.* 2015). As a result, several clinical trials are currently evaluating PD-1/PD-L1-based therapeutics for the treatment of metastatic TNBCs (reviewed in (Planes-Laine *et al.* 2019)).

The research presented in this thesis aims at assessing the impact of a novel combination of DNA damage response (ATR) and cell cycle checkpoint (Wee1) inhibitors for the treatment of early and metastatic TNBCs.

1.4 Radiation therapy for breast cancer

Radiation therapy is a mainstay in the multidisciplinary management of breast cancer, with the goal of the treatment modality being eradication of tumor cells. Recent advances in radiation therapy allow for image-based planning and directed delivery of the radiation dose to the tumor tissue, thereby minimizing damage to the surrounding tissue. However, the delivery of high-dose conformal radiation therapy can be difficult due to ambiguities in the accuracy of imaging, treatment planning and delivery, and changes in the tumor size during the treatment period.

Additionally, accurate identification of the tumor, its local extension, and the exact location of the surrounding organs at risk is of utmost importance. Planning errors can ultimately result in reduced tumor control and increased toxicity to the surrounding tissue due to higher dose delivery. These problems were overcome to a great extent with the integration of imaging technology into modern radiation therapy machines – referred to as image-guided radiation therapy (IGRT) – leading to increased precision and accuracy of dose delivery (Jaffray 2012).

The introduction of intensity-modulated radiation therapy (IMRT) allows for radiation dose delivery to irregularly shaped tumors. While the conventional radiotherapy methods were limited to the delivery of consistent dose across the treatment area, IMRT, together with advanced computation and planning, enables using multiple beams with varying intensity across each beam to maximize dose delivery to the tumor target and minimize damage to surrounding normal tissue (Taylor and Powell 2004, Alonzi 2015). Indeed, the use of IMRT for dose escalation (achieving higher total treatment dose) and hypofractionation (shorter therapy course with larger daily radiation fractions) studies have shown improved clinical outcomes without any added toxicity (Chao *et al.* 2001, Zelefsky *et al.* 2001, Kupelian *et al.* 2005, Mukesh *et al.* 2013).

With regards to breast cancers, accelerated partial breast irradiation (PBI) or total breast irradiation (TBI) following breast-conserving surgery is the standard of care. A meta-analysis of randomized control trials estimated that patients treated with breast-conserving surgery alone had local recurrence rates of 29.2% for node-negative and 46.5% for node-positive breast cancers (Clarke *et al.* 2005). This risk is reduced to 10% for node-negative and 13.1% for node-positive breast cancer patients by addition of PBI (Clarke *et al.* 2005). Moreover, radiotherapy to the breast after breast-conserving surgery can help eliminate microscopic minimal residual disease and significantly improves local disease control. In another meta-analysis of over 10,000 women

participating in 17 randomized clinical trials, radiotherapy to the breast after breast-conserving surgery reduced breast cancer mortality at 15-year follow-up by 3.3% for node-negative breast cancer patients and 8.5% for node-positive breast cancer patients (Early Breast Cancer Trialists' Collaborative *et al.* 2011).

Radiobiological mechanisms that ultimately determine tumor response to fractionated radiation therapy include radiosensitivity of the therapy-resistant tumor-initiating cells, tumor hypoxia and reoxygenation during treatment, DNA repair following cell cycle checkpoint blockade, repopulation between radiotherapy fractions, and cell cycle redistribution of the surviving cells. These factors are collectively referred to as the “5 Rs of radiobiology” (Steel *et al.* 1989). In this study, we provide preliminary indications for the use of drugs targeting the DNA damage response and show that fractionated radiotherapy in combination results in tumor growth delay *in vivo*.

1.5 The mammalian cell cycle

The mammalian cell cycle is a tightly regulated process that ensures precise duplication of the genome and proper cell division. Cell proliferation is dependent on the passage of cells through four distinct cyclin-dependent kinases (CDK)-cyclin complex-regulated phases of the cell cycle – G₀/G₁, S, G₂, and M. The S-phase ensures duplication of genetic material (DNA replication) and the M-phase ensures division of chromosomes (mitosis) and cytoplasm (cytokinesis). Mitosis comprises five phases – prophase, prometaphase, metaphase, anaphase, and telophase. Following cytokinesis, the daughter cells may either re-enter the cell cycle (G₁-phase) or enter the non-dividing phase (G₀ or quiescence).

1.5.1 Regulation of cell cycle progression via CDK/cyclin complexes

CDKs are a family of serine/threonine kinases that regulate cell cycle progression, and their activity can be inhibited by activation of cell cycle checkpoints in response to DNA damage. Activation of the cell cycle checkpoint (G1/S, intra-S, G2/M) results in cells halting progression through the cell cycle until the lesion is resolved (Hartwell and Weinert 1989). In humans, 20 CDKs have been identified, but only 4 have an active role during the cell cycle where CDK4, CDK6, and CDK2 are active during the G1, CDK2 is active in S, and CDK1 in G2 and M (Malumbres and Barbacid 2009). CDKs are activated by cyclins, and unlike cyclins, CDK protein levels remain stable during the cell cycle. Throughout the cell cycle, four different cyclins – cyclin D, cyclin E, cyclin A, and cyclin B – regulate cell cycle phase transition by limiting CDK activity to specific phases (Zerjatke *et al.* 2017). The binding of cyclin D to CDK4/6 to form the CDK4/6-cyclin D complex is a prerequisite for entry in S (Sherr 1994). Activation of the CDK4/6-cyclin D complexes results in partial inactivation of pocket proteins – Retinoblastoma (Rb) and Rb-related proteins (p107 and p130) – to allow expression of cyclin E, which binds CDK2 to form and activate the CDK2-cyclin E complex, which in turn results in complete inactivation of the pocket proteins by phosphorylation (Lundberg and Weinberg 1998, Harbour *et al.* 1999). The formation of this CDK2-cyclin E complex is essential to drive the G1/S transition (reviewed in (Hochegger *et al.* 2008)). Following the proteasomal degradation of cyclin E by the F-box/WD repeat-containing protein 7 (FBXW7) in the mid-S phase, CDK2 is subsequently activated by cyclin A2 to drive the transition from S to the G2 phase (Woo and Poon 2003). Lastly, cyclin A2 complexes with CDK1 (also known as cdc2) at the end of interphase and facilitates the onset of mitosis. Following nuclear envelope breakdown, cyclin A2 degrades and CDK1 forms a complex with cyclin B to induce mitosis (Malumbres and Barbacid 2005).

1.5.2 CDK1 is an essential CDK required for cell cycle progression

Studies from genetic mouse models have shown that CDK1 can interact with other cyclins to regulate cell cycle progression in the event that one or more interphase CDKs are lost (Santamaria *et al.* 2007, Satyanarayana *et al.* 2008), indicating that CDK1 is the only CDK essential for cell cycle progression (Santamaria *et al.* 2007). Loss of CDK1 results in early embryonic lethality (Satyanarayana *et al.* 2008). Additionally, CDK1 activity is absolutely required for mitotic entry and control of the initial steps of mitosis (Nurse 1990). Due to CDK1's essential function and defective G1 checkpoints in many cancers, cancer cells are often reliant on the CDK1-mediated G2/M checkpoint (Prevo *et al.* 2018).

CDK1 directly phosphorylates about 70 proteins in mammalian cells, although the list of putative targets may be much larger based on screens from yeast models (Ubersax *et al.* 2003). The CDK1/cyclin B complex enables the breakdown of the nuclear lamina by phosphorylating lamin A and C proteins, which promote intermediate filament disassembly (Peter *et al.* 1990). The CDK1/cyclin B complex is also involved in chromosomal condensation by phosphorylating histones (H1 and HMG-1) (Brizuela *et al.* 1989, Nissen *et al.* 1991) and condensin II subunits (Abe *et al.* 2011). The CDK1/cyclin B complex ensures fragmentation of the Golgi network proteins by phosphorylation of GM130, GRASP65, Nir2, and p47, and ensuring equal distribution of the fragmented vesicles and tubules between daughter cells during cell division (Lowe *et al.* 1998, Uchiyama *et al.* 2003, Wang *et al.* 2003, Litvak *et al.* 2004). Some of the other substrates regulated by the CDK1/cyclin B complex include microtubule-binding proteins (like dynein, MAP4, and MAP1B) and proteins implicated in replication (like MCM2, MCM4, and ribonucleotide reductase R2). Finally, mitotic exit is coordinated by CDK1 mediated

phosphorylation of the anaphase-promoting complex/cyclosome (APC/C, an E3 ubiquitin ligase), resulting in inactivation of the CDK1-cyclin B complex (Fujimitsu *et al.* 2016).

1.6 Wee1

The transition of cells into mitosis from the G2/M checkpoint is governed by the phosphorylation status of CDK1 and its association with cyclin B (Nurse 1990). To prevent premature entry into mitosis, CDK1 is maintained in an inactive state by Wee1-mediated CDK1 phosphorylation (Heald *et al.* 1993).

Wee1 is a tyrosine kinase originally discovered in *Schizosaccharomyces pombe* (Thuriaux *et al.* 1978). Human Wee1 was subsequently discovered as a crucial regulator of the G2/M checkpoint (Heald *et al.* 1993). The primary structure of Wee1 is composed of a N-terminal regulatory domain, a kinase domain, and a short C-terminal domain. The N-terminal domain coordinates signals to shuttle Wee1 into and out of the nucleus (Squire *et al.* 2005, Li *et al.* 2010). Wee1 consists of four cyclin binding motifs, RxL1, RxL2, RxL3, and RxL4, to facilitate interaction with CDK (Li *et al.* 2010).

The Wee kinase family comprises three serine/threonine kinases: *Wee1*, *PKMYT1*, and *Wee2*. In mammalian cells, Wee1 and PKMYT1 have a vital role in regulating the G2/M transition (Schmidt *et al.* 2017). Wee2 (or Wee1B) is only expressed in germ cells, where it prevents premature restart of oocyte meiosis prior to ovulation and permits metaphase II exit at fertilization (Oh *et al.* 2011). PKMYT1 (protein kinase membrane-associated tyrosine/threonine 1; also known as Myt1) functions as an essential component of an organelle-based cell cycle checkpoint to prevent CDK1-induced premature fragmentation of Golgi and the endoplasmic reticulum during

the G2 phase (Villeneuve *et al.* 2013). PKMYT1 negatively regulates CDK1 activity by phosphorylation on both threonine 14 and tyrosine 15 (Booher *et al.* 1997, Liu *et al.* 1997).

1.6.1 Wee1 kinase regulates the cell cycle checkpoint

The Wee1 kinase regulates CDK1 activity by inhibitory phosphorylation of CDK1 on tyrosine 15, which renders CDK1 inactive (McGowan and Russell 1995, Do *et al.* 2013). In the absence of DNA damage, CDK1 is dephosphorylated by the Cell division cycle 25 (Cdc25c) phosphatase resulting in CDK1/cyclin B activation and initiation of mitotic events (Donzelli and Draetta 2003). Polo-like kinase 1 (PLK1) phosphorylates Wee1 at the G2/M transition, which targets Wee1 for degradation *via* the ubiquitin ligase complex (Lindqvist *et al.* 2009). PLK1 also phosphorylates and activates the phosphatase cdc25 resulting in CDK1 activation (Lindqvist *et al.* 2009, Labib 2010). Wee1 also has a role in regulating replication dynamics during S phase. During S phase, initiation of replication results in the firing of many replication of origins triggered by the action of DBF4-Dependent cdc7 kinase (DDK) and CDK2, the S phase CDK (Labib 2010, Heller *et al.* 2011). Wee1 and cdc25 control CDK2 activity by regulating the phosphorylation status at tyrosine 15 (Beck *et al.* 2010). Additionally, Wee1 downregulation triggers a DNA damage response resulting in DNA replication stalling and reduced replication fork speed and causes cells to accumulate in S phase (Dominguez-Kelly *et al.* 2011). It was proposed that in unperturbed cells, Wee1 protects replication forks and prevents generation of DNA damage by inhibiting the Mus81 endonuclease (Dominguez-Kelly *et al.* 2011).

1.7 The DNA damage response

Genomic instability is a hallmark of cancer (Hanahan and Weinberg 2011). The genome is exposed to constant insults by several endogenous (reactive oxygen species, DNA replication errors) as well as exogenous (chemical mutagens, ionizing radiation, ultraviolet light) DNA

damaging factors. Ionizing radiation from cosmic radiations or medical treatments (X-ray scans or radiation therapy) can generate single and double-strand DNA breaks. Additionally, cancer chemotherapeutics can induce a variety of DNA lesions, including inter- and intra-strand cross-links arising from drugs like cisplatin or mitomycin C. To ensure safe passage of the genomic material to the next generation, all organisms have evolved mechanisms – collectively termed the DNA damage response (DDR) – to detect DNA damage and to activate a signaling cascade to promote repair, including *via* cell cycle checkpoint activation (Ciccia and Elledge 2010), or in the case of extensive DNA damage to trigger mechanisms to either permanently exit the cell cycle (senescence) or undergo programmed cell death (apoptosis), presumably preventing cells from accumulating mutations and resulting in the development of cancer.

Several DNA repair mechanisms have been identified to counteract DNA damage. For instance, mismatched DNA bases are replaced with correct bases *via* the mismatch repair (MMR) pathway (Jiricny 2006), base lesions that do not significantly alter the DNA are repaired by base excision repair (BER) pathway (Lindahl and Barnes 2000). Single-strand breaks are repaired by the single-strand break repair (SSBR) mechanism, whereas double-strand breaks (DSBs) are repaired by two main repair mechanisms: NHEJ (nonhomologous end-joining), which is more error prone, or HR (homologous recombination), which is error-free (West 2003, Caldecott 2008). The choice of DSB repair pathway is dependent on the cell cycle phase. NHEJ is prevalent in G1-phase cells, whereas HR is the preferred choice for S- and G2-phase cells (Shrivastav *et al.* 2008). By ligating broken DNA ends in an error prone process, NHEJ can result in loss of genetic information. In contrast, during the S- and G2-phases, repair by HR relies on the use of the homologous sequence of the sister chromatid as a template and ensures faithful repair.

The DDR is primarily mediated by proteins of the PIKKs (phosphatidylinositol 3-kinase-like protein kinases) family, namely ATM (Ataxia Telangiectasia Mutated), ATR (Ataxia Telangiectasia and Rad3-related), and DNA-PKcs (DNA-dependent Protein Kinase catalytic subunit). Indeed, defects in these kinases have been implicated in human disease. While somatic mutations in ATM are frequently found in many cancers, including those of the breast (Rodriguez *et al.* 2002, Lempiainen and Halazonetis 2009), germline mutation in ATM, ATR, and DNA-PKcs are linked to ataxia telangiectasia (AT), Seckel syndrome, and severe combined immunodeficiency, respectively (Savitsky *et al.* 1995, O'Driscoll *et al.* 2003, van der Burg *et al.* 2009). ATM and DNA-PKcs primarily get activated in response to DSBs and unlike ATR, neither are essential for cell survival (Brown and Baltimore 2000).

ATM and ATR are large kinases with significant sequence homology, mainly phosphorylate serine and threonine residues, and target an overlapping set of substrates including signaling proteins in pathways that arrest cell cycle to facilitate DNA repair.

1.8 Ataxia Telangiectasia and Rad3-related (ATR)

ATR is an important kinase in the DDR and is the primary sensor of replication stress which is elevated in cancer cells due to oncogene activation and/or an impaired G1 checkpoint. ATR, ATM, and DNA-PKcs – being members of the PIKK family – exhibit sequence homology. The ATR kinase domain is located near the carboxyl-terminal, which is flanked by the conserved FAT (FRAP-ATM-TRRAP) and FAT carboxy-terminal (FATC) domains (Fokas *et al.* 2014). Large amino-terminal and internal regions of ATR are composed of several α -helical HEAT (Huntington-elongation factor 3-protein phosphatase 2A-TOR1) repeats (Perry and Kleckner 2003). The HEAT region of ATR is crucial for mediating the ATR-ATRIP (ATR-Interacting Protein) interaction through its amino-terminal repeats (Ball *et al.* 2005). In response to DNA

damage, the FAT domain of ATR is phosphorylated at threonine 1989, which promotes the stimulation by its activator, TopBP1 (DNA Topoisomerase II Binding Protein 1) (Liu *et al.* 2011). The FATC domain of ATR is vital for its basal kinase activity. Additionally, a short region between the FATC and the kinase domain of ATR, the PIKK regulatory domain (PRD), was identified to interact with TopBP1 to activate ATR (Mordes *et al.* 2008).

ATR responds to a wide range of DNA damage, including DSBs, replication stress, base adducts, and inter-strand crosslinks. ATR is activated *via* ATRIP on sensing single-stranded DNA (ssDNA) structures, which can arise due to replication fork uncoupling or DSB resection.

1.8.1 ATR signaling is a multi-step process resulting in cell cycle arrest

The direct binding of ATRIP, the interacting partner of ATR, to replication protein A (RPA)-coated ssDNA triggers activation of the ATR pathway. ATR is then further activated by direct interaction with TopBP1 (Kumagai *et al.* 2006), which is recruited to RPA-coated ssDNA and dsDNA junctions by the Rad9 subunit (pSer387) of the Rad9-Rad1-Hus1 (9-1-1) complex (Delacroix *et al.* 2007, Lee *et al.* 2007). Like ATR, TopBP1 is essential, and loss of TopBP1 results in early embryonic lethality (Jeon *et al.* 2011). Besides TopBP1, ATR can also be activated by ETAA1 (Ewing's Tumor-Associated Antigen 1), which was found to contain a similar ATR activating domain as TopBP1 (Feng *et al.* 2016, Haahr *et al.* 2016). Once the active ATR complex is assembled at the site of DNA damage or stalled replication fork, signaling to coordinate cell cycle arrest and repair can initiate.

The adaptor protein Claspin interacts with the Checkpoint kinase 1 (Chk1), a downstream ATR effector, resulting in ATR mediated Chk1 phosphorylation at serines 317 and 345 (Liu *et al.* 2000). Chk1 phosphorylation results in reduced replication and cell cycle progression, thereby allowing time for repair. Active Chk1 kinase phosphorylates and targets the Cdc25 phosphatase

for degradation *via* the ubiquitin proteasomal system, causing activation of the G2/M cell cycle checkpoint (Liu *et al.* 2000, Dai and Grant 2010). During normal replication, ATR activation by ETAA1 blocks premature activation of the transcription factor FOXM1, preventing cells with under-replicated or damaged DNA from undergoing mitosis (Saldivar *et al.* 2018). Additionally, activation of ATR signaling can also lead to intra-S-phase checkpoint activation where ATR signaling inhibits the firing of replication origins *via* Chk1-mediated Cdc25 phosphorylation resulting in inactivation of Cdk2/cyclin A complex and S-phase arrest (Dai and Grant 2010). Besides having a role in the S- and G2-phase of the cell cycle, ATR can also be activated in G1 in response to IR damage and activate its downstream effector Chk1 (Gamper *et al.* 2013). More recently, it was found that inhibiting ATR activity in mitosis resulted in lagging anaphase chromosomes and aneuploidy, implying that ATR activity in mitosis is important for accurate chromosome segregation (Kabeche *et al.* 2018). In mitosis, ATR is recruited to the centromeres by Aurora A and CENP-F (Centromere Protein-F) and subsequently activated, where it promotes Chk1-mediated Aurora B activation to promote faithful chromosome segregation (Kabeche *et al.* 2018).

1.8.2 ATR is an essential kinase

ATR and its downstream effector Chk1 are essential for the survival of proliferating cells. *ATR*^{-/-} embryos die early during development, and at a cellular level, the blastocyst cells undergo severe chromosome fragmentation, implying that ATR is crucial in preventing premature mitotic entry (Brown and Baltimore 2000). A point mutation (W1147R) in the ATR-activating domain of TopBP1 preventing ATR activation also results in embryonic lethality, enforcing its role as an essential gene (Zhou *et al.* 2013). Patients with Seckel syndrome, a very rare genetic disorder, are a result of ATR hypomorphism (A2101G mutation) causing very low levels of ATR protein

(Alderton *et al.* 2004). These patients present with microcephaly, craniofacial abnormalities, and growth retardation (Mokrani-Benhelli *et al.* 2013).

1.9 Targeting the DNA damage response for cancer therapy

An early step in tumorigenesis is dysregulated cellular proliferation arising due to oncogene activation or overexpression. Most cancers have one or more DDR pathways dysregulated, increasing the reliance of those cancers on the remaining DDR pathways to ensure survival. Many traditional cancer therapeutics aim to kill cancer cells by increasing DNA damage in the rapidly proliferating cancer cells, yet cancer cells often develop therapeutic resistance. More importantly, a small subset of tumor-initiating cells (also known as “cancer stem cells”) have been shown to have an increased DDR and heightened repair capabilities suggesting them playing a role in therapy resistance (Debeb *et al.* 2009). This has made the discovery of new DDR drug targets an attractive avenue over the last decade or so.

Genomic instability, a hallmark of cancer, is associated with dysregulated DDR pathways, ultimately resulting in cancer (Hanahan and Weinberg 2011). However, defects in one DDR pathway often result in increased reliance on the remaining mechanisms causing their upregulation to ensure cancer cell survival. However, as conventional cancer therapies function by inducing DNA damage, cancer cells with upregulated DDR pathways allow circumvention of catastrophic DNA damage and resist cell death. This rationalized the use of drugs targeting the DDR to overcome therapy resistance if used in conjunction with chemo- and radiotherapy. Moreover, the loss of a DDR component may result in tumor-specific vulnerability if the compensatory DDR pathway can be targeted – an approach that has been described as synthetic lethality (Curtin 2012). Synthetic lethality occurs when defects in two or more genes cause cell death, while defects in one of the two genes alone are not lethal (O'Neil *et al.* 2017). With regards to DDR drug targets, one

event is frequently genetic and more specific to the tumor than the normal cells, and the second event is achieved through pharmacological inhibition of the DDR target. The clinical approval of PARP inhibitors (Olaparib, Talazoparib, Rucaparib, and Niraparib) for BRCA mutant (HR deficient) breast and ovarian cancers is one of the best-studied example of successful realization of synthetic lethality approaches (Robson *et al.* 2017, Litton *et al.* 2018, Moore *et al.* 2018).

1.10 ATR and Wee1 as targets of cancer therapy

The acknowledgment of the significance of DDR defects in promoting cancer growth has enabled the search for other therapeutically exploitable DDR targets to improve cancer therapy outcomes. Over the last decade, several drugs were identified targeting DDR kinases, like ATM, ATR, Chk1, and Wee1 amongst many others. At present, there are only two bioavailable ATM inhibitors (AZD0156 and KU60019), which are being evaluated for their safety and efficacy in phase I trials against advanced solid tumors (NCT02588105) and kidney cancer (NCT03571438), respectively. Furthermore, Chk1 inhibitor (AZD7762) clinical trials have been mainly discouraging due to excess cardio-toxicities associated with the compound (Seto *et al.* 2013, Sausville *et al.* 2014). Although most DDR inhibitors are confined to their use *in vitro*, several clinical trials are evaluating ATR and Wee1 inhibitors either as monotherapy agents or in combination with other genotoxic agents (Pilie *et al.* 2019). This reflects the importance of ATR and Wee1 kinases in cancers with increased DNA replication stress and a defective G1 checkpoint.

1.10.1 ATR inhibitors for cancer therapy

Rapidly proliferating cancer cells have high replication stress which results in the generation of SSBs and DSBs (Sanjiv *et al.* 2016). These cancer cells mostly rely on ATR to regulate the G2/M DNA damage checkpoint and resolve DNA damage before a cell can divide, making ATR an attractive target for cancer therapeutics. In this regard, several ATR inhibitors are

undergoing evaluation in pre-clinical (ETP-46464, VE-821, ATRN-119, and Compound 3) as well as Phase I/II clinical studies [AZD6738 (also known as Ceralasertib), M4344 (formerly VX-803), BAY-1895344, and M6620 (also known as Berzosertib; formerly VX-970)] (Forment and O'Connor 2018).

ETP-46464 was identified in a cell-based screen as the first highly potent and selective ATR inhibitor (Toledo *et al.* 2011) and was shown to sensitize cancer cells to IR (Gamper *et al.* 2013). However, its application was limited to cell-based studies due to poor *in vivo* pharmacokinetics (Toledo *et al.* 2011). VE-821 was found to be a selective ATR inhibitor in another high-throughput screen (Charrier *et al.* 2011). ATR inhibition by VE-821 increased cancer cell sensitivity to IR and various chemotherapeutics like platinum-compounds, gemcitabine, and etoposide (Prevo *et al.* 2012, Huntoon *et al.* 2013). Interestingly, cancer cell killing was increased by nearly 10-fold when VE-821 was combined with cisplatin in ATM deficient colon cancer cell lines (Reaper *et al.* 2011). These findings provided early evidence that cancers with defective ATM pathway are more reliant on ATR for survival following DNA damage (Cortez *et al.* 2001, Reaper *et al.* 2011). Furthermore, treatment with VE-821 showed increased cancer cell killing following IR by radiosensitization of the radioresistant hypoxic cancer cells (Pires *et al.* 2012). Most importantly, VE-821 monotherapy selectively induced killing of cancer cells, but not normal cells (Reaper *et al.* 2011). Besides ATM and p53, a promising study reported synthetic lethality when ATR is inhibited in *ARID1A* (AT-rich interaction domain 1A) mutant tumors (Williamson *et al.* 2016). Despite the early promise, VE-821 was associated with severe toxicities at higher concentrations, and so the compound was further optimized and its analogue M6620 (VX-970 or VE-822 or Berzosertib) was developed with increased potency and selectivity against ATR. M6620 was the first ATR inhibitor to enter clinical trials. M6620 has been reported to synergize

with platinum-based chemotherapies, with a trend toward greater sensitivity in p53-mutant tumors (Hall *et al.* 2014). Moreover, combined treatment with M6620 and cisplatin showed tumor regression in lung cancer PDX (patient derived xenografts) previously unresponsive to either monotherapies (Hall *et al.* 2014). When used in combination with oxaliplatin, ATR inhibition potentiated an increase in CD8⁺ T cells in colorectal cancer bearing syngeneic mice treated with combination compared to those treated with oxaliplatin monotherapy (Combes *et al.* 2019). Similarly, another highly potent and selective ATR inhibitor, AZD6738, was shown to synergize with cisplatin in tumors of various background (Vendetti *et al.* 2015, Min *et al.* 2017, Leonard *et al.* 2019). In a model of NSCLC (non-small cell lung cancers) xenografts, combined treatment with AZD6738 and cisplatin resulted in tumor growth inhibition of ~75% in ATM-proficient tumors and this further increased to nearly 85% in ATM-deficient tumors (Vendetti *et al.* 2015). In the context of radiation therapy, AZD6738 sensitizes cancer cells independent of p53 or BRCA2 status by abrogating the radiation-induced G2-checkpoint, blocking HR, and causing cells to enter mitosis with damaged DNA resulting in mitotic catastrophe (Dillon *et al.* 2017). AZD6738 was also reported to combine with IR to trigger a CD8⁺ T cell response by blocking radiation-induced PD-L1 upregulation on tumor cells and decreasing the number of tumor infiltrating regulatory T cells (Tregs) (Vendetti *et al.* 2018). More recently, another study reported that DNA damage following ATR inhibition and RT led to immunomodulatory effects in the tumor microenvironment by increasing innate immune cell infiltration (Dillon *et al.* 2019).

The abundance of promising preclinical studies formed the basis of several clinical trials (over 50 clinical trials listed on clinicaltrials.gov; accessed April 2021) evaluating the potential of ATR inhibitors for cancer treatment either as monotherapy or in combination with various other genotoxic agents (reviewed in (Barnieh *et al.* 2021)). M6620 was the first ATR inhibitor to enter

phase I clinical trials, where M6620 was evaluated as a monotherapy agent or in combination with carboplatin in advanced solid tumor patients (Yap *et al.* 2020). Out of the 17 patients receiving ATR inhibitor monotherapy, one patient with metastatic colorectal cancer (ATM loss and *ARID1A* mutant) achieved complete response with a progression-free survival of 29 months at the last assessment. M6620 monotherapy in general was safe and well tolerated with no dose limiting toxicities even at 480 mg/m². Amongst the 23 patients receiving M6620 with carboplatin, an advanced stage *BRCA1* mutant ovarian cancer patient showed partial response to the treatment despite being refractory to platinum treatment and resistant to PARP inhibitors. Additionally, 15 patients enrolled in the trial exhibited signs of stable disease as the best response. Unsurprisingly, dose limiting hematological toxicities were observed in patients that received the combination treatment requiring dose delays and reductions (the recommended phase 2 dose for M6620 in combination with carboplatin is 90 mg/m²) (Yap *et al.* 2020). An ongoing dose escalation trial evaluating M6620 in combination with gemcitabine for advanced solid tumors has so far reported partial response as the best response in four patients with two additional chemo-refractory patients showing indications of stable disease (Plummer *et al.* 2016). Overall, the results from phase I trials have been encouraging and phase II evaluation of M6620 with topotecan are currently underway for platinum refractory small cell lung cancers.

AZD6738 was the first oral ATR inhibitor to enter clinical trials and is being evaluated in patients with solid tumors as monotherapy and in combination with radiation therapy as part of the phase I PATRIOT trial (Dillon *et al.* 2018). Early indications from the dose escalation safety and efficacy study imply that AZD6738 is well tolerated as a monotherapy when given intermittently (2-week-on, 2-week-off) (Dillon *et al.* 2019). Three patients showed confirmed partial response, and one patient had unconfirmed partial response as the best response to monotherapy. To date,

the trial has not reported their findings on AZD6738 used in combination with radiation. In parallel, several clinical trials are also assessing AZD6738 in combination with the PARP inhibitor Olaparib, where early findings from a phase I trial reported 1 complete response, 5 partial responses, and 1 unconfirmed partial response in patients (n = 39) with advanced breast, ovarian, prostate, pancreatic and ampullary cancer and *BRCA1/2* mutation (Krebs *et al.* 2018). Lastly, preliminary results from the same trial also evaluating the combination of AZD6738 with durvalumab (anti-PD-L1 antibody) reported one complete response, two partial response, and one unconfirmed partial response out of the 21 NSCLC patients participating in the trial (Krebs *et al.* 2018). Interestingly, initial reports on trials using AZD6738 in combination with other chemotherapies report similar toxicity concerns as observed in M6620 trials.

Taken together, early findings from these clinical trials highlight that ATR inhibitors when used in combination with traditional chemotherapies have added toxicities, particularly related to hematology. Having said that, the combination of ATR inhibitors with immune-checkpoint inhibitors is better tolerated thus making it an attractive approach.

1.10.2 Wee1 inhibitors for cancer therapy

Cancers often have a deregulated G1 checkpoint. As a result, they are heavily reliant on the G2/M checkpoint for survival and mitosis. Consequently, Wee1 is often highly expressed in many cancers including breast (Iorns *et al.* 2009, Murrow *et al.* 2010), glioma (Mir *et al.* 2010), melanoma (Magnussen *et al.* 2012), lung (Iorns *et al.* 2009), leukemia (Porter *et al.* 2012, Tibes *et al.* 2012), osteosarcoma (PosthumaDeBoer *et al.* 2011), and squamous cell carcinoma (Magnussen *et al.* 2013). As most cancer therapies induce lethal amounts of DNA damage in cancer cells, Wee1 overexpression promotes cell survival by reinforcing DNA damage checkpoints and preventing mitotic catastrophe (Mir *et al.* 2010). The indispensable role of Wee1 in regulating the G2/M

checkpoint in response to DNA damage has made it an attractive target for cancer therapy. Despite its appeal, to date only one selective and highly potent small molecule Wee1 inhibitor, AZD1775 (also known as Adavosertib or MK-1775) (Hirai *et al.* 2009), has been widely reported and is being evaluated against various advanced cancers in phase I/II clinical trials either as a monotherapy (Do *et al.* 2015, Leijen *et al.* 2016, Sanai *et al.* 2018) or in combination with other chemotherapies (Leijen *et al.* 2016, Leijen *et al.* 2016, Mendez *et al.* 2018).

Wee1 inhibition by AZD1775 has been shown to induce *in vitro* and *in vivo* synergistic tumor cell killing with several DNA damaging therapies including IR (Bridges *et al.* 2011) and chemotherapeutics like cisplatin, paclitaxel doxorubicin, 5-fluorouracil, and gemcitabine (Hirai *et al.* 2010, Aarts *et al.* 2012, Lewis *et al.* 2017, Zheng *et al.* 2017). Given the role of p53 in regulating the G1 cell cycle checkpoint, treatment with AZD1775 has been reported to selectively target cancers harboring p53 mutations or loss of gene function (Hirai *et al.* 2009, Rajeshkumar *et al.* 2011). Having said that, a few studies have also shown that AZD1775 sensitizes cancer cells to DNA damaging therapies independent of p53 status (Kreahling *et al.* 2012, Van Linden *et al.* 2013, Harris *et al.* 2014). Additionally, DNA damaging agents that specifically interfere with DNA synthesis and arrest cells in S-phase show high synergy with AZD1775 (Aarts *et al.* 2012, Hauge *et al.* 2017). Overall, these preclinical studies support that AZD1775 has antitumor effects in a wide range of tumors both as a monotherapy and in combination with other chemotherapeutics.

There are 57 clinical trials listed on clinicaltrials.gov (accessed April 2021) for AZD1775 where it is being evaluated against a wide range of cancer types including breast cancer, cervical cancer, leukemia, lung cancer, ovarian cancer, pancreatic cancer, pediatric and adult brain tumors. Findings of the phase I clinical trial show that AZD1775 is well tolerated with acceptable toxicity profiles both as a single agent and in combination with other therapies (Do *et al.* 2015). As a

monotherapy, the maximum tolerated dose was determined as 225 mg, which was administered orally twice per day for 2.5 days per week, for 2 weeks per 21 day cycle (Do *et al.* 2015). The dose limiting toxicities included hematologic events, nausea, vomiting, and fatigue (Do *et al.* 2015, Leijen *et al.* 2016). Interestingly, two of the nine patients harboring *BRCAl* mutation recorded partial response, but none of the patients with documented p53 mutation exhibited a response (Do *et al.* 2015). Early indications from a phase II trial evaluating AZD1775 plus carboplatin in p53 mutant ovarian cancer refractory or therapy-resistant patients show encouraging antitumor activity with one (5%) complete response and eight (38%) partial responses (Leijen *et al.* 2016). Moreover, the overall response rate (43%) far exceeded the results that could be expected with second-line single agent treatments (11% to 21%) (Leijen *et al.* 2016).

The indispensable role of ATR and Wee1 in promoting cancer cell survival prompted us to exploit their combined pharmacological inhibition as a therapeutic strategy for the treatments of breast cancer. The research presented in this thesis shows that combined inhibition of ATR and Wee1 abrogates the S- and G2-checkpoint in cancer cells, triggering premature entry into mitosis, and ultimately causing cell death *via* mitotic catastrophe. In an orthotopic breast cancer xenograft model, we show that this neoadjuvant therapy results in tumor control and suppression of metastasis. We also report the application of [¹⁸F]-FLT-PET as a theranostic biomarker to identify responders to this novel treatment strategy. Lastly, we provide preliminary evidence on using combined ATR and Wee1 as a radiosensitizer. Preliminary findings also suggest that combined ATR, Wee1, and IR treatment modulates the tumor microenvironment to improve antitumor immunity, as indicated by reduced expression of PD-1 and other markers of T-cell exhaustion (TIM-3 and LAG-3). As these inhibitors of ATR and Wee1 are currently undergoing phase I/II

clinical trials, this knowledge could soon be translated into the clinic, especially as we showed that the combination treatment targets a wide range of tumor cells.

Chapter 2: Inhibiting Wee1 and ATR Kinases Produces Tumor- Selective Synthetic Lethality and Suppresses Metastasis

2.1 Introduction

The DDR senses DNA damage and replication stress and orchestrates the cellular response to protect the cell and organism from genotoxic insults. These signal transduction pathways include the choreography of DNA repair, cell cycle control, and cell fate decision among others (Ciccia and Elledge 2010). Due to their dysregulated proliferation, the genomic integrity of cancer cells is particularly threatened by DNA damage and replication stress, but also by metabolic, mitotic, oxidative and proteotoxic stresses (Luo *et al.* 2009). Furthermore, during tumorigenesis cells often lose DDR mechanisms leading to increased genomic instability (Drosos *et al.* 2017). These DNA repair/DNA damage signaling defects and/or the increased genotoxic stress make cancer cells heavily dependent on the (remaining) intact DDR pathways.

Synthetic lethality refers to an interaction between two genes when the perturbation of either gene alone is viable, but the simultaneous perturbation of both genes leads to cell death. The discovery that breast cancer cells with mutations in homologous recombination proteins BRCA1 or BRCA2 are hypersensitive to PARP inhibitors (Bryant *et al.* 2005, Farmer *et al.* 2005) led to therapeutic approaches targeting cancer cells with deficiencies in one DDR pathway by inhibition of an alternative DDR pathway. However, as this approach only targets cells with a defective DDR, it is bound to only affect a subset of cancers or populations within a tumor. Resistance can arise by reactivation of the defective pathway. Conditional synthetic lethality refers to synthetic lethality observed only under certain circumstances, such as genetic background or metabolic state of cells or cellular environment (O'Neil *et al.* 2017). In view of the inter- and intratumor heterogeneity commonly observed, to achieve the necessary therapeutic window for a wide range of tumors it is necessary to identify a common “condition” upon which to base cancer-selective conditional synthetic lethality. Oncogene-induced DNA damage is a common feature of cancer cells leading

to high levels of replication stress as well as mitotic stress in cancer cells compared to normal proliferating cells (Halazonetis *et al.* 2008, Lecona and Fernandez-Capetillo 2014). Based on this tumor-specific property, we tested whether increasing genotoxic stress and simultaneously inhibiting an important rescue pathway would lead to cancer cell-selective death by evaluating the efficacy of combined ATR and Wee1 inhibition on cancer cell eradication. Wee1 is a kinase controlling G/M and S phase checkpoints *via* phosphorylation of the cyclin dependent kinases CDK1 and CDK2. Furthermore Wee1 inhibition prolongs mitosis in a range of cancer cells and makes them more susceptible to chemotherapy-induced mitotic catastrophe (Lewis *et al.* 2017). ATR is the apical kinase of a DDR pathway. ATR is considered the main mediator in the DDR to replication stress (Lecona and Fernandez-Capetillo 2014), including signaling to cell cycle checkpoints *via* Chk1 and regulating repair by promoting extensive DNA end-resection needed for homologous recombination (Gamper *et al.* 2013, Kibe *et al.* 2016, Buisson *et al.* 2017). Bioavailable selective ATR inhibitors (AZD6738 by AstraZeneca; VX-970 and VX-803 by Merck) as well as the Wee1 inhibitor AZD1775 have recently entered phase I/II clinical trials in combination with radiation or chemotherapeutics.

Here we report that tumor-selective synthetic lethality between ATR and Wee1 inhibitors leads to tumor shrinkage and suppresses metastasis. Using an orthotopic breast cancer xenograft mouse model we show that combination treatment leads to complete remission in 6/9 cases, inhibits tumor spread and prolongs survival. Our toxicity studies show that the combination treatment is associated with minimal side effects. Fast proliferating tissues, such as the ileum or the bone marrow, showed no signs of renewal defects. Synergistic cell killing by inhibition of ATR and Wee1 is observed in cancer cells from various tissue origins, but not in untransformed cells. Mechanistic studies using pulses of reversible inhibition during the cell cycle show that combined

ATR/Wee1 inhibition during S and G2/M phase cooperate to kill cancer cells. Furthermore, live cell imaging studies reveal that combined ATR/Wee1 inhibition causes cells to enter mitosis with unrepaired/under-replicated DNA leading to mitotic catastrophe. As the studied ATR and Wee1 inhibitors are already in phase I/II clinical trials, this knowledge could soon be translated into the clinic.

2.2 Materials and Methods

2.2.1 Cell lines and plasmids

Cell lines were purchased from American Type Cell Culture (ATCC) and regularly tested for mycoplasma. MDA-MB-231-*fluc2-tdT* cells were engineered by stable transfection with pcDNA3.1(+)/Luc2-tdT (Addgene, #32904) and maintained under 400 µg/mL G418 selection.

2.2.2 Antibodies and reagents

Anti-pChk1 (Ser345) (133D3; #2348), anti-Chk1 (2G1D5; #2360), anti-pCDK1 (Tyr15) (10A11; #4539), anti-β-actin (13E5; #4970), anti-pHistone H2A.X (Ser139) (20E3; #9718), anti-Ki-67 (D3B5; #12202), anti-mouse IgG HRP-linked (#7076) and anti-rabbit IgG HRP-linked (#7074) were purchased from Cell Signalling, anti-pATR (Thr1989) (#GTX128145) from GeneTex. Immunoblotting was performed as previously described (Gamper *et al.* 2013).

AZD6738 and AZD1775 were kindly provided by AstraZeneca. VE-821, ETP-46464, UCN-01 and Verapamil were purchased from Sigma.

2.2.3 Crystal violet assay

5000 cells per well were seeded into 96 well plates 4 h prior to drug treatment. Cells were treated with indicated concentrations of AZD6738 (100 nM to 4000 nM) and AZD1775 (50 nM to 2000 nM) for 96 h. For siRNA treatment, cells were seeded into 96 well plates at a density of 4000 cells per well and cultured for 24 h prior to treatment. Cells were transfected with siRNA against Wee1 (Ambion; #s21) with 0.2% Lipofectamine RNAiMAX (ThermoFisher; #13778075) in multiples of 8 at the following final pM concentrations: 78.125, 156.25, 312.5, 625, 1250, 2500, 5000, 10000, and 20000, as well as no-siRNA control. Transfected cells were then treated in quadruplicate with either AZD6738 (500 or 1000 nM) or vehicle (DMSO) for 96 h. After 96 h,

cells were washed twice with 1X PBS and stained with 0.5% crystal violet (in 20% methanol) for 20 mins. Cells were then washed with water for 4 times, plates were air dried overnight. 200 μ L methanol was added per well and incubated for 20 mins at room temperature. Optical density was measured at 584 nm using the FLUOstar Omega plate reader (BMG Labtech). Background values were subtracted using blank OD₅₈₄. Data was calculated in terms of percent surviving attached cells (% crystal violet OD) compared to vehicle control treated cells. Experiments were performed in triplicates at least 3 times. To ensure that the Crystal Violet assay reflects cell survival, we compared some of the survival data measured by this method to cell survival observed by live cell imaging over the same period. We found that the two methods yielded very similar survival rates.

2.2.4 Cell synchronization and cell cycle analysis

U-2 OS cells were treated with 2 mM thymidine for 16 h, released into fresh medium for 4 h followed by nocodazole (100 ng/mL) treatment for 8 h. 6 h after release from nocodazole in to fresh medium, cells were treated with DMSO, AZD6738 (1 μ M), AZD1775 (0.3 μ M), or a combination of AZD6738 and AZD1775.

MDA-MB-231 cells were treated with 2 mM thymidine for 18 h, followed by release into fresh medium for 8 h and a second treatment with 2 mM thymidine for 18 h. After release, cells were treated with either DMSO, AZD6738 (1 μ M), AZD1775 (0.3 μ M), or combined AZD6738 and AZD1775.

For cell cycle analysis, cells were harvested at 2 h intervals and fixed with 70% chilled ethanol for at least 24 h at -20°C before a wash with 1X PBS. Pelleted cells (1500 rpm, 5 mins) were resuspended in propidium iodide (PI) buffer (50 μ g/mL) containing RNase A (10 μ g/mL) and incubated at 37°C for 30 mins. Samples were analyzed on a BD FACSCanto II flow cytometer.

2.2.5 Side population assay

Trypsinized MCF7 or MDA-MB-231 cells were counted using a hemocytometer. 1×10^6 cells were incubated for 15 mins at 37°C with 50 µg/mL Verapamil, a membrane transport blocker, and used as a negative control for gating. After 15 mins, cells in the negative control tube and the sample tube were stained with 0.5 µL DyeCycle Violet (DCV) dye (Thermofisher, USA) per million cells and incubated at 37°C for 90 mins with intermittent shaking. Cells were washed twice with 1X PBS (1500 rpm, 5 mins) and resuspended in sorting buffer. Samples were sorted using a BD FACSAria III flow cytometer.

2.2.6 Mammosphere assay

1000 MCF7 and MDA-MB-231 side population (SP) and non-side population (NSP) sorted cells were seeded on 24-well ultra-low attachment plates (Corning, USA) in serum free DMEM/F12 medium containing a cocktail of EGF (10 ng/mL), Insulin (20 ng/mL), Lf1 (10 ng/mL; all from Sigma), and basic human FGF (20 ng/mL; Goldbio). Medium was replenished every 3 days and mammospheres were cultured for 3 passages. Mammospheres were imaged at 10X magnification using a Zeiss Axiovert 200M inverted microscope (Carl Zeiss, Germany). Total number of mammospheres were counted under a light microscope.

For limiting dilution (LD50) assays, SP/NSP sorted MCF7 and MDA-MB-231 cells were seeded in increasing concentrations (1, 2, 5, 10, 100, and 1000 cells/well) on 24-well ultra-low attachment plates in serum free media as described above. Wells were examined for mammospheres after 10 days under a light microscope and the observations were recorded as the number of wells containing mammospheres for each cell concentration.

2.2.7 Immunofluorescence

Cells were seeded on coverslips and synchronized using a double thymidine block. Released synchronized cells were treated with either vehicle, 1 μ M AZD6738, 0.3 μ M AZD1775, or a combination of AZD6738 and AZD1775 for 4 h and fixed with 4% paraformaldehyde (Sigma, USA) for 10 minutes at 37°C. Cells were then permeabilized in 4% paraformaldehyde with 0.2% Triton X-100 (Fisher Scientific, USA) for 10 minutes and blocked with 2% BSA for 30 minutes at room temperature. Cells were incubated with anti-centromere (ACA sera were kind gifts from Dr. M. Fritzler, University of Calgary, Calgary, Alberta, Canada) and anti-tubulin (Sigma; #T5168) antibodies at 37°C for 1 h each. Cells were washed with PBS and incubated with the dye-conjugated antibodies anti-human Alexa Fluor 647 and anti-rat Alexa Fluor 488 (ThermoFisher, USA). Nuclei were counterstained with DAPI (5 μ g/mL). Coverslips were mounted using the VECTASHIELD mounting medium for fluorescence (Vector Laboratories Inc., CA). Images were captured at 63X magnification using a Zeiss LSM 710 Meta Confocal Microscope (Carl Zeiss, Germany).

2.2.8 Live cell imaging

For analysis of mitotic timing, MDA-MB-231 stably expressing mCherry-H2B and GFP-Tubulin (Moudgil *et al.* 2015) were seeded in a 35 mm glass bottom dish (MatTek Corporation) and treated with vehicle, AZD6738, AZD1775, or combined AZD6738 and AZD1775. Plates were placed on a motor-controlled stage within an incubator chamber maintained at 37°C and 5% CO₂. Images were acquired using a spinning disc confocal inverted microscope (Axiovert 200M; Carl Zeiss) using the 40X objective lens and captured at 5 mins interval for 24 h (using the Volocity software). Movie files were exported as OME-TIFF files and further processed in Imaris 9.0.1 for background subtraction and noise reduction.

2.2.9 High-content screening microscopy

Images were taken with a High-content automated microscopy imaging system (MetaXpress Micro XLS, software version 6, Molecular Devices, Sunnyvale, CA, USA). Briefly, MDA-MB-231 cells were seeded onto a 96 well plate at a density of 4000 cells per well. Single images were captured in each well with a 20× (NA 0.75) objective equipped sCMOS camera using bandpass filters of 624/40 nm for mCherry. On average 200 cell images per well were manually analyzed with the MetaXpress software using mCherry-H2B to identify changes in DNA organization. Mitotic timing was calculated as the interval between nuclear envelope break down (NEBD, indicated by the first evidence of chromosome condensation) to the onset of anaphase (or chromosome decondensation in the case of mitotic slippage). The fates of cells (and resulting daughter cells) were tracked for the duration of the experiment (48 h). Cell death was determined by the formation of apoptotic bodies, loss of cell attachment, and/or loss of membrane integrity.

2.2.10 Assessment of mouse hematopoietic progenitor cells

6 to 8 weeks old C57BL/6 mice were treated with inhibitors as described above for 26 days (n = 3 per group). Body weight was measured every 4 days as an indicator of toxicity. On the 27th day, mice were euthanized by CO₂ asphyxiation and bone marrow was isolated from the femur by centrifugation at 14,000 rpm for 15 secs. Isolated bone marrow cells were resuspended in FACS buffer (1X PBS + 1% FBS) and cells were counted using a hemocytometer. 1 x 10⁶ cells were stained with either PE anti-mouse CD117 (c-Kit) antibody (#105807) and/or Pacific Blue anti-mouse Lineage Cocktail (#133310) and/or FITC anti-mouse Ly-6A/E (Sca1) antibody (#108105) or PE rat IgG2b isotype (#400608) or Pacific Blue rat IgG2a isotype (#400527) or FITC rat IgG2a isotype (#400505; all from Biolegend) controls. Samples were analyzed on a BD FACSCanto II flow cytometer.

2.2.11 Orthotopic breast cancer xenografts and drug treatments

All mice were obtained from breeding colonies at the University of Alberta. All animal studies described were carried out under protocol number AC16225 approved by the Cross Cancer Institute's Animal Care Committee, Edmonton, Canada. For tumor formation, 2×10^6 MDA-MB-231-*fluc2-tdT* cells were mixed with Matrigel (Corning, USA) and PBS (1:1) and injected in 50 μ L volume orthotopically into the inguinal mammary fat pad of 6 to 8 weeks old female NOD.Cg-*Prkdc^{scid} Il2rg^{tm1Wjl}/SzJ* (NSG) mice. Tumor growth was measured every 4 days using a Vernier caliper and volume was assessed as $[\text{length} \times (\text{width})^2]/2$. When the tumor volumes reached approx. 40-50 mm^3 , mice were randomly segregated into 4 groups (n = 9 per group). Mice were treated daily with vehicle, 25 mg/kg AZD6738 (in 10% DMSO, 40% polypropylene glycol, and 50% ddH₂O), 60 mg/kg AZD1775 (in 0.5% methylcellulose), or a combination of AZD6738 and AZD1775 *via* oral gavage for 26 days. Body weight was measured every 4 days as an indicator of toxicity. Mice were euthanized when the tumor volume reached a total of 1000 mm^3 , after a > 10% reduction in body weight, or any other indications of physical discomfort.

For histological studies, tumor bearing mice (approx. 250 mm^3 tumor volume) were treated with either vehicle or 25 mg/kg AZD6738 or 60 mg/kg AZD1775 or a combination of AZD6738 and AZD1775 *via* oral gavage for 5 (short term) or 26 (long term) days. Tumors and small intestines (ileum), lungs, livers, kidneys, and spleen were harvested and fixed with 10% formalin for 48 h prior to embedding.

2.2.12 Bioluminescence imaging

In vivo bioluminescence imaging was carried out as previously described (Rengan *et al.* 2015). Briefly, mice were imaged using the Bruker In-Vivo Xtreme after intraperitoneal injection of D-Luciferin (3 mg/mouse). *Ex vivo* bioluminescence imaging was performed on major organs

by immersing them in the D-Luciferin substrate. Sequential scans were acquired to capture the maximum kinetics of the luciferase reaction. Images of the luciferase scans were overlaid on the X-ray images acquired in the background. The light output was quantified using the Bruker MI SE software. Pseudocolor bars represent photon flux captured by the CCD camera.

2.2.13 Immunohistochemistry

Immunohistochemistry was performed on formalin fixed paraffin embedded (FFPE) tissue samples using standard procedures as previously described (Varghese *et al.* 2014). Briefly, 4 μm slices were sectioned on precleaned Colorfrost Plus microscope slides (Fisher Scientific, USA) using a microtome (Leica, Germany). Tissue samples were baked at 60°C for 2 h and deparaffinized 3 times in xylene for 10 mins each and subsequently rehydrated in a gradient of ethanol washes. Tissue sections were subjected to antigen retrieval in a pressure cooker using 0.05% citraconic anhydride antigen retrieval buffer (pH – 7.4). Tissue samples were blocked with 4% BSA for 30 mins and incubated with respective primary antibodies overnight at 4°C. Next day, endogenous peroxidase activity was blocked for 30 mins using 3% H₂O₂, followed by incubation with anti-rabbit HRP labelled secondary antibody (Dako EnVision+ System; K4007) for 1 h at room temperature in the dark. Samples were incubated with DAB (3,3'-diaminobenzidine) + substrate chromogen (Dako, USA) for brown color development, counter stained with hematoxylin, and mounted with DPX mounting medium (Sigma, USA). Images were captured using the Zeiss Axioskop2 plus upright microscope (Zeiss, Germany) equipped with AxioCam color camera (images on Figures 2.10 and 2.12), later upgraded to AxioCam 512 color camera (images on Figure 2.14, 2.15, 2.17-2.19). Villi length (3 mice / treatment group) was measured using Fiji software (Schindelin *et al.* 2012).

2.2.14 TUNEL assay

TUNEL assay was performed for apoptosis detection using DeadEnd Fluorometric TUNEL System kit (G3250, Promega, USA) as per manufacturer's instructions. Briefly, 4 μm slices were sectioned on precleaned Colorfrost Plus microscope slides (Fisher Scientific, USA) using a microtome (Leica, Germany). Samples were baked at 60°C for 2 h and deparaffinized by washing 2 times in xylene for 5 mins each and subsequently rehydrated in a gradient of ethanol washes followed by washing in 0.85% NaCl and 1x PBS solutions. Samples were then fixed with 4% methanol free formaldehyde for 15 mins and permeabilized with Proteinase K solution (20 $\mu\text{g}/\text{mL}$) at room temperature for 8 minutes. Samples were washed with PBS and fixed again with methanol-free formaldehyde solution. Samples were then allowed to equilibrate at room temperature using equilibration buffer. For labelling purposes, TdT reaction mix was added to the tissue area and covered with plastic coverslips to allow equal distribution. Samples were incubated for 60 mins at 37°C in a dark humidified chamber. Reaction was stopped by immersing slides in 2x SSC for 15 minutes. Tissue sections were counter stained with DAPI (5 $\mu\text{g}/\text{mL}$) and mounted using the VECTASHIELD mounting medium for fluorescence (Vector Laboratories Inc., CA). Images were captured at 40X magnification using a Zeiss LSM 710 Meta Confocal Microscope (Carl Zeiss, Germany).

2.2.15 Statistical analysis

All statistical analysis was performed using GraphPad Prism 7 software (GraphPad Software, La Jolla, California, USA). All experiments were performed at least 3 times in triplicates or quadruplicates. *P*-values were calculated using one-way ANOVA, two-way ANOVA, and Log-rank (Mantel-Cox) test. *P*-values of < 0.05 were considered significant, and *P*-values of < 0.001 were considered highly significant.

2.3 Results

2.3.1 Synergistic cell killing of cancer cells by ATR and Wee1 inhibition *in vitro*

CDK1/2 activity is regulated by inhibitory phosphorylation at tyrosine 15 by the protein kinase Wee1 that is counteracted by the phosphatase cdc25. CDK1 activity regulates entry into and exit out of mitosis (Malumbres and Barbacid 2005, Chow *et al.* 2011, Visconti *et al.* 2012, Vassilopoulos *et al.* 2015, Visconti *et al.* 2015), and we recently showed that Wee1 inhibition in breast cancer cells promotes premature mitosis, prolongs mitosis, and promotes paclitaxel-induced mitotic catastrophe (Lewis *et al.* 2017). In addition to regulating entry into mitosis, screens identified an important role for Wee1 in the maintenance of genome integrity during DNA replication. Both Wee1 knockdown or inhibition lead to upregulation of phosphorylated H2AX (γ H2AX), a readout for DNA damage, in S phase cells (Beck *et al.* 2010, Dominguez-Kelly *et al.* 2011, Hauge *et al.* 2017). The underlying mechanisms remain poorly understood and seemingly conflicting data led to two models proposing either that Wee1 controls genomic stability during replication by regulating origin firing (Hauge *et al.* 2017), or that it regulates the processing of stalled replication forks by the Mus81-Eme1 endonuclease (Dominguez-Kelly *et al.* 2011).

The protein kinase ATR is constitutively bound by ATRIP (ATR-interacting protein) and is activated by replication protein A (RPA)-coated single-stranded DNA, structures that can arise from stalled replication forks or resected DNA double-strand breaks (Ciccia and Elledge 2010). Unsurprisingly, ATR plays a crucial role in the response to replication stress – likely the reason for it being an essential gene (Brown and Baltimore 2000, de Klein *et al.* 2000) – and to ionizing radiation-induced DNA double-strand breaks. ATR activation is important for S and G2/M checkpoint signaling and DNA damage repair by homologous recombination (Gamper *et al.* 2013).

To test whether Wee1 inhibition activates ATR, we incubated cancer cells for 2 hours with the Wee1 inhibitor AZD1775. Immunoblots of cell lysates show that AZD1775 treatment leads to phosphorylation of Chk1 Serine 345, a target site of ATR (**Fig. 2.1A**). ATR activation was confirmed by co-treatment with two ATR selective inhibitors, AZD6738 and ETP-46464, which suppressed AZD1775-induced Chk1 phosphorylation (**Fig. 2.1A, lanes 1-4**), and is observed in breast cancer (MDA-MB-231) and osteosarcoma (U-2 OS) cells, indicating that it is unlikely cancer type specific (**Fig. 2.1A, Suppl. Fig. 2.1**). ATR activation by AZD1775 is potentiated by DNA damaging agents, such as ionizing radiation (**Suppl. Fig. 2.1**). The activation of ATR by Wee1 inhibition prompted us to study the combinatorial effect of Wee1 and ATR inhibition on cancer cell killing. 5,000 cells were plated and incubated with different concentrations of AZD1775 and AZD6738 for 4 days before measuring surviving cells by Crystal Violet staining and colorimetry (Feoktistova *et al.* 2016). We observe *synergistic* cell killing by ATR and Wee1 inhibition in all tested cancer cell lines (**Table 2.1, Suppl. Fig. 2.3C**), including the human breast cancer cell lines MDA-MB-231, MCF7, and Zr-75-1 (**Fig. 2.1B-D**), but not in non-tumorigenic MCF 10A and immortalized mammary epithelial cells (hTERT-HME1) (**Fig. 2.1E, F**), as demonstrated in Loewe plots and calculated Bliss combination indices (CI) (Fouquier and Guedj 2015). A CI below 1 indicates synergy. The synergistic cell killing we observe with Wee1 and ATR inhibitors is unlikely due to off-target effects, because several ATR inhibitors (including ETP-46464 and VE-821, **Suppl. Fig. 2.3**) and knockdown of Wee1 with siRNA (**Suppl. Fig. 2.2D**) show cooperative lethality as well. Importantly, and in agreement with a conditional synthetic lethality of Wee1 and ATR based on DNA damage, a favorable therapeutic window for the combination treatment is provided by the increased oncogenic stress in cancer cells, as no cooperative lethality is observed in MCF 10A and hTERT-HME1. This is in stark contrast to

inhibition of the ATR downstream target Chk1. MCF 10A and hTERT-HME1 are very sensitive to the Chk1 inhibitor UCN-01 alone and to combined Wee1 and Chk1 inhibition (**Suppl. Fig. 2.4**). Depletion or inhibition of Chk1, but not of ATR, has previously been shown to cause DNA damage in normal cells (Techer *et al.* 2016), likely explaining the toxicity of Chk1 inhibitors observed in the clinic (Seto *et al.* 2013, Sausville *et al.* 2014). Several studies have shown that in the absence of exogenous genotoxic stress ATR inhibitors are well tolerated (Reaper *et al.* 2011, Toledo *et al.* 2011) and cells from Seckel syndrome patients, who have hypomorphic levels of ATR, do not show increased DNA damage levels (O'Driscoll *et al.* 2003), indicating that low ATR activity is sufficient to respond to the endogenous genotoxic stress in normal cells.

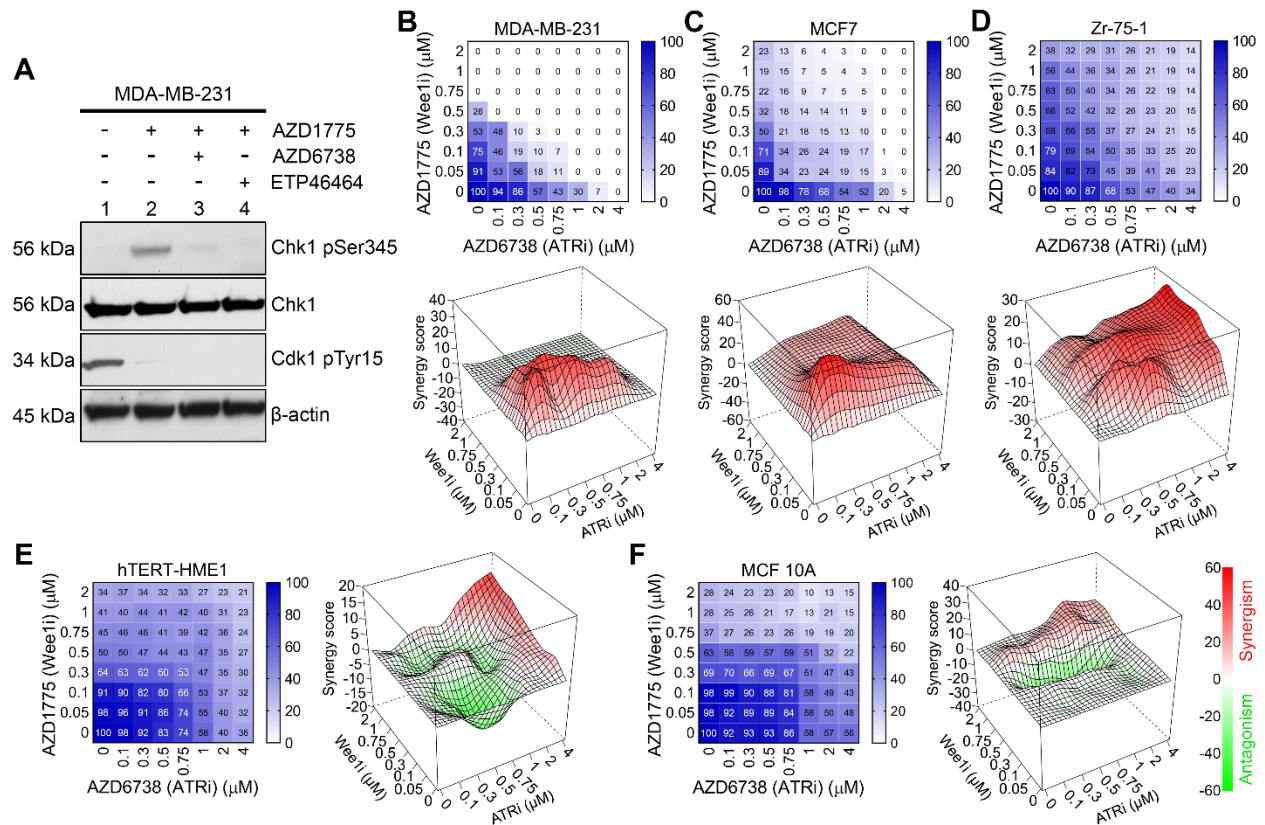


Figure 2.1. Wee1 inhibition activates ATR and shows synergistic cancer cell killing with ATR inhibition.

(A) MDA-MB-231 cells were incubated with the indicated inhibitors for Wee1 (AZD1775) or ATR (AZD6738, ETP46464). After 2 hours, cell lysates were harvested and probed for Chk1 and CDK1 phosphorylation by immunoblotting. (B–F) MDA-MB-231, MCF7, Zr-75-1, hTERT-HME1, or MCF10A cells were treated for 4 days with a combination of up to 4 μ M AZD6738 and up to 2 μ M AZD1775. Survival was assayed by crystal violet staining and each experiment was repeated at least 4 times. Color bars indicate percentage survival normalized to untreated cells. Representative cooperativity screens and Loewe plots for drug cooperativity are shown.

<i>Cell line</i>	<i>AZD6738 (ATRi)</i>	<i>AZD1775 (Wee1i)</i>	<i>Bliss CI</i>	<i>ATRi IC₅₀</i>	<i>Wee1i IC₅₀</i>
<i>MDA-MB-231</i>	300 nM	100 nM	0.60	540 nM	190 nM
<i>MCF7</i>	300 nM	100 nM	0.65	840 nM	280 nM
<i>Zr-75-1</i>	500 nM	300 nM	0.74	1120 nM	1270 nM
<i>T-47D</i>	750 nM	500 nM	0.83	1120 nM	340 nM
<i>MDA-MB-468</i>	300 nM	100 nM	0.56	2580 nM	520 nM
<i>MDA-MB-175-VII</i>	300 nM	100 nM	0.34	3740 nM	460 nM
<i>Sk-Br-3</i>	300 nM	100 nM	0.57	5165 nM	570 nM
<i>U-2 OS</i>	300 nM	100 nM	0.54	550 nM	160 nM
<i>hTERT-HME1</i>	300 nM	100 nM	1.07	2400 nM	660 nM
	750 nM	500 nM	1.11	2400 nM	660 nM
<i>MCF 10A</i>	300 nM	100 nM	1.09	3790 nM	615 nM
	750 nM	500 nM	1.08	3790 nM	615 nM

Table 2.1. Synergistic cancer cell killing by ATR and Wee1 inhibition.

2.3.2 Combination treatment of cancer cells with ATR and Wee1 inhibitors leads to centromere fragmentation and mitotic catastrophe

Several reproductive cell death modes can lead to the inability of a cell to reproduce after exposure to genotoxic stress (Eriksson and Stigbrand 2010, Surova and Zhivotovsky 2013). While treated cells with intact cell cycle checkpoint function tend to senesce, the major death mechanism after exposure to DNA damaging agents for cells with defects in cell cycle checkpoints and impaired DNA repair mechanisms is *mitotic catastrophe*. Mitotic catastrophe occurs when cells enter mitosis prematurely before the completion of DNA repair and/or DNA replication, resulting in dysregulated/failed mitosis, and can lead to delayed apoptosis, senescence or even necrosis.

We used live cell microscopy to address whether cell death by Wee1 and/or ATR inhibition requires cells to enter mitosis. Cancer cell lines display variable intra-line (within their population) response to drug treatments (Gascoigne and Taylor 2008). Therefore, monitoring individual cell fates with time-lapse microscopy is essential to understanding the cell cycle response of cancer cells to drug treatment. Breast cancer cell lines stably expressing GFP-tubulin and mCherry-histone H2B enabled us to track the fates of individual cells and their progenies. Our data for MDA-MB-231 show that, unlike Wee1 inhibition ($P = 0.0387$, one-way ANOVA) (Lewis *et al.* 2017), ATR inhibition alone does not prolong mitosis (**Fig. 2.2A, B**). Yet when ATR and Wee1 inhibition are combined, mitosis is significantly longer ($P < 0.0001$, one-way ANOVA) (**Fig. 2.2A, B**) and commonly leads to cell death (**Fig. 2.2C, D**). The median time between nuclear envelope breakdown to anaphase in control cells, cells treated with AZD6738, AZD1775, or the combination is 35, 45, 160, or 325 minutes, respectively (**Fig. 2.2B**). Cell death is observed during failed mitosis, after mitotic slippage (when cells have aborted mitosis as evidenced by the disappearance of the mitotic spindle without cytokinesis), or in interphase after cytokinesis (often

with visible micronucleation) (**Fig. 2.2C, D; Suppl. Fig. 2.5A**). Mitotic duration seems to correlate with cell death observed during mitosis, with 0, 3.6, 28.6, or 64.3 percent of MDA-MB-231 cells dying in mitosis when treated with vehicle, AZD6738, AZD1775, or combined AZD6738/AZD1775, respectively (**Fig. 2.2D**). While ATR inhibition kills 44.6% of the cells, most of the cell deaths occur during interphase in daughter cells. We do not observe interphase death in cells before aborted or completed mitosis. This clearly indicates the importance of cells entering mitosis, presumably with unrepaired or under-replicated DNA, for cell death and shows that mitotic defects can lead to delayed cell death in daughter cells.

Mitotic cells with under-replicated genome (MUG) were discovered 30 years ago (Brinkley *et al.* 1988). Mitotic defects observed in these cells commonly include centromere fragmentation (Beeharry *et al.* 2013), characterized by the formation of centromere clusters spatially separated from the main mass of chromosomes. As the majority of cells treated with combined ATR and Wee1 inhibitors died in mitosis, we synchronized cells in S phase by a double thymidine block and inhibited ATR and/or Wee1 after release. Four hours after G1/S release, cells were fixed and stained for tubulin, centromeres, and DNA (**Fig. 2.2E**). Wee1 inhibition, but particularly combined ATR/Wee1 inhibition, leads to an increase in mitotic cells (**Fig. 2.2F**) in the breast cancer cell lines MDA-MB-231 and T-47D, as well as in HeLa cells (**Suppl. Fig. 2.5B**). Furthermore, the majority of the mitotic cells in the combination treatment group show centromere fragmentation, as seen by the clustering of centromeres and kinetochores and their separation from the bulk condensed chromatin (compare mitotic cells treated with combined AZD6738 and AZD1775 to DMSO control in **Fig. 2.2E, Suppl. Fig. 2.5B**).

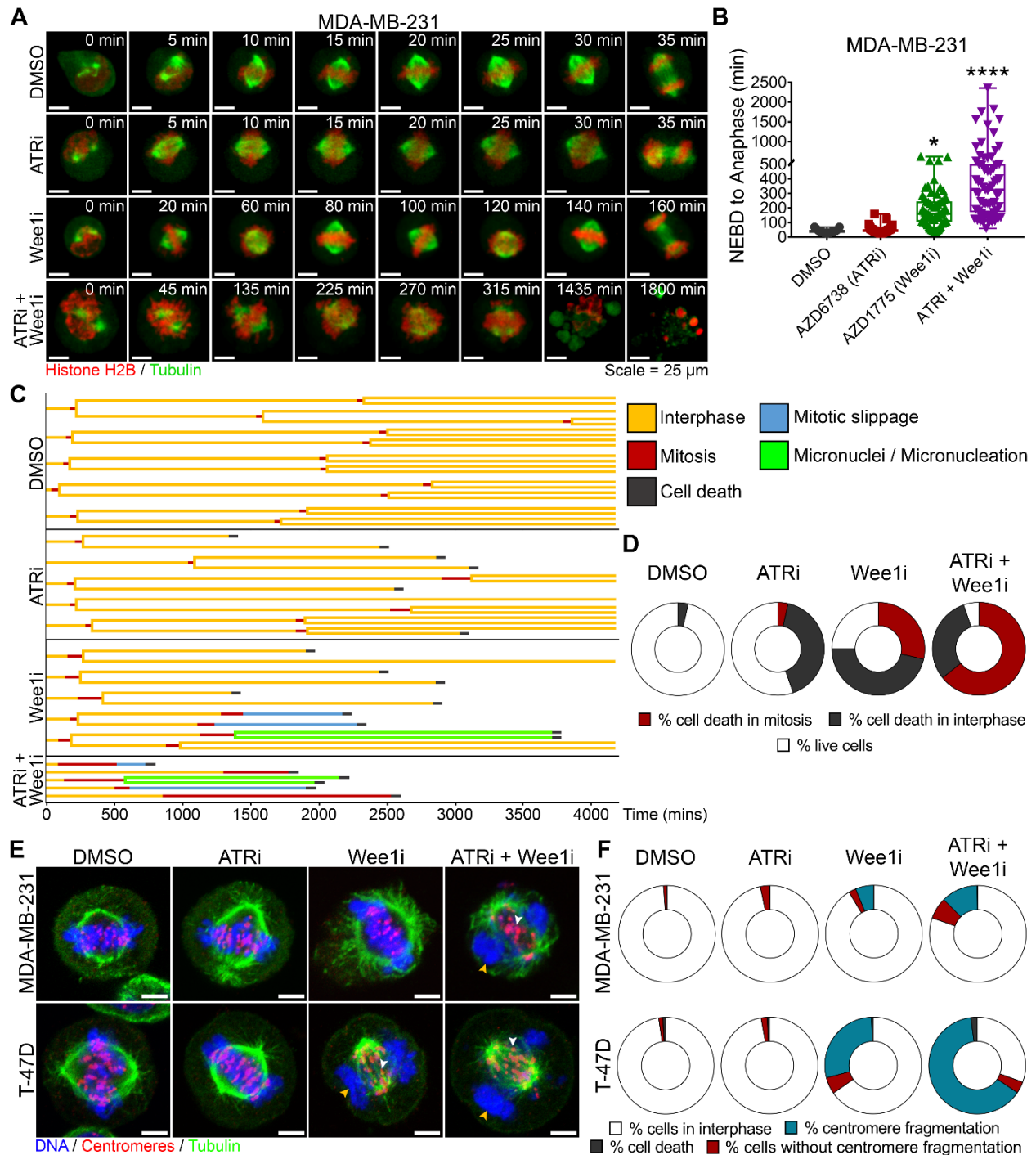


Figure 2.2. Combined ATR and Wee1 inhibition leads to mitotic defects and cancer cell death.

(A–D) Live cell imaging of MDA-MB-231 expressing mCherry–histone H2B and GFP-tubulin. (A) Cells treated as indicated (ATRi = 1 μ M AZD6738, Wee1i = 0.3 μ M AZD1775) were monitored by spinning-disk confocal microscopy. Representative images of cells following nuclear envelope breakdown (NEBD) are shown. (B) Quantification of the time from NEBD to anaphase. (C) Representative fates of 5 cells in the 4 treatment groups. (D) Quantification of

observed cell fates ($n = 56$). Of note, when cell death occurred in interphase, the dying cells had previously undergone mitosis following drug addition. **(E)** Representative images of MDA-MB-231 or T-47D mitotic cells treated as in **A**. Fixed cells were stained for centromeres (red) and tubulin (green) by immunofluorescence and for DNA with DAPI (blue). Drug-induced clustering of centromeres (white arrows) spatially separated from the main mass of chromosomes (yellow arrow), a feature of centromere fragmentation, is clearly visible. Scale bars: 10 μm . **(F)** Quantification of cells that are in mitosis (red and blue) and display centromere fragmentation (blue) ($n > 1,000$), after fixing cells 4 hours after release from a double thymidine block in the presence of the indicated inhibitors. $*P < 0.05$, $****P < 0.0001$ (one-way ANOVA).

2.3.3 Events in S phase and G2/M phase contribute to the synergistic cancer cell killing by the combination treatment of cancer cells with ATR and Wee1 inhibitors

To estimate the contribution of abrogation of cell cycle checkpoints and DNA damage repair to overall cell killing, we evaluated the impact of ATR and/or Wee1 activity during phases of the cell cycle on cancer cell survival. As this requires the ability to switch ATR and Wee1 activity on and off, we tested the reversible nature of inhibition by AZD6738 and AZD1775. Mock or AZD6738 treated cells were UV-irradiated and ATR activation measured by Chk1 phosphorylation (**Fig. 2.3A**). AZD6738 washout leads to ATR reactivation within 1 h, as evidenced by restoration of high Chk1 pS345 levels. AZD1775 treatment of cells reduces CDK1 phospho-Y15 levels, confirming that Wee1 is the primary kinase phosphorylating CDK1 at tyrosine 15 (**Fig. 2.3B**). Washout of AZD1775 restores Wee1 kinase activity to full levels in less than two hours, as shown by the reestablishment of normal CDK1 phospho-Y15 levels. Having established that ATR and Wee1 inhibition can be reversed within approximately one hour, we next synchronized U-2 OS cells by a thymidine-nocodazole block (**Fig. 2.3C**) as described (Gamper *et al.* 2013). At various times after nocodazole release and for different durations, cells were pulse-treated with 1 μ M AZD6739 and/or 300 nM AZD1775 by addition and subsequent washout as indicated: from +10 to +16 h (roughly late G1 to G2), from +18 to +22 h (late G2 into mitosis), from +10 to +22 h, for a full cell cycle starting from late G1, or for the entire period of 4 days. All cells were assayed for survival after 4 days by measuring Crystal Violet staining compared to mock treated cells. As discussed previously, treatment for the entire time window with a combination of AZD6738 and AZD1775 leads to strong synergy (**Fig. 2.3D**, right panel). Inhibition of ATR or Wee1 alone for short intervals, during S phase or late G2/mitosis (**Fig. 2.3D**, first two left panels), had no significant effect on survival, indicating that cells were able to recover from transient ATR

or Wee1 inhibition for the indicated time intervals. Prolonged inhibition, from late G1 into mitosis, on the other hand, leads to significant cell killing by the single agents ($P < 0.0001$, one-way ANOVA), comparable to inhibition for an entire cell cycle. Interestingly, combined ATR and Wee1 inhibition for just the short periods encompassing S phase (+10 to +16 h) or from late G2 into mitosis (+18 to +22 h) leads to killing of approximately half of the cells ($P < 0.0001$, one-way ANOVA). Yet when ATR and Wee1 are both inhibited from late G1 into mitosis (+10 to +22 h), less than 10% of the cells survive, indicating not only a strong synergy between the two inhibitors, but also the contribution of events during both cell cycle intervals (G1 to G2; G2 and mitosis) the inhibitors were active (compare the three left panels in **Fig. 2.3D**). Combination treatment for an entire normal cell cycle interval further increased cell killing to levels comparable to treatment for the entire 4 days.

We also tested inhibitor-induced changes in cell cycle profiles in cells synchronized by a thymidine-nocodazole block, if AZD6738 and/or AZD1775 were added to G1 cells 6 hours after release. Flow cytometry of propidium iodide stained cells show a significant increase of cells with DNA content between $2n$ and $4n$ at 14 hours after nocodazole release in the combined ATR and Wee1 inhibitor treated group compared to control (**Fig. 2.3C**). The DNA content indicates delayed S phase or entry into G2/mitosis with under-replicated genomes. The latter is more likely, because many cells retain a DNA content below $4n$ even several hours later. Combined with our observation that cells treated with both ATR and Wee1 inhibitor show frequent centromere fragmentation in mitosis (**Fig. 2.2E, F**), a hallmark of under-replicated cells entering mitosis, the inhibitor-induced shift in DNA content profile underlines the synergistic contribution of reversible ATR/Wee1 inhibition during S and G2/M phases in causing mitotic catastrophe.

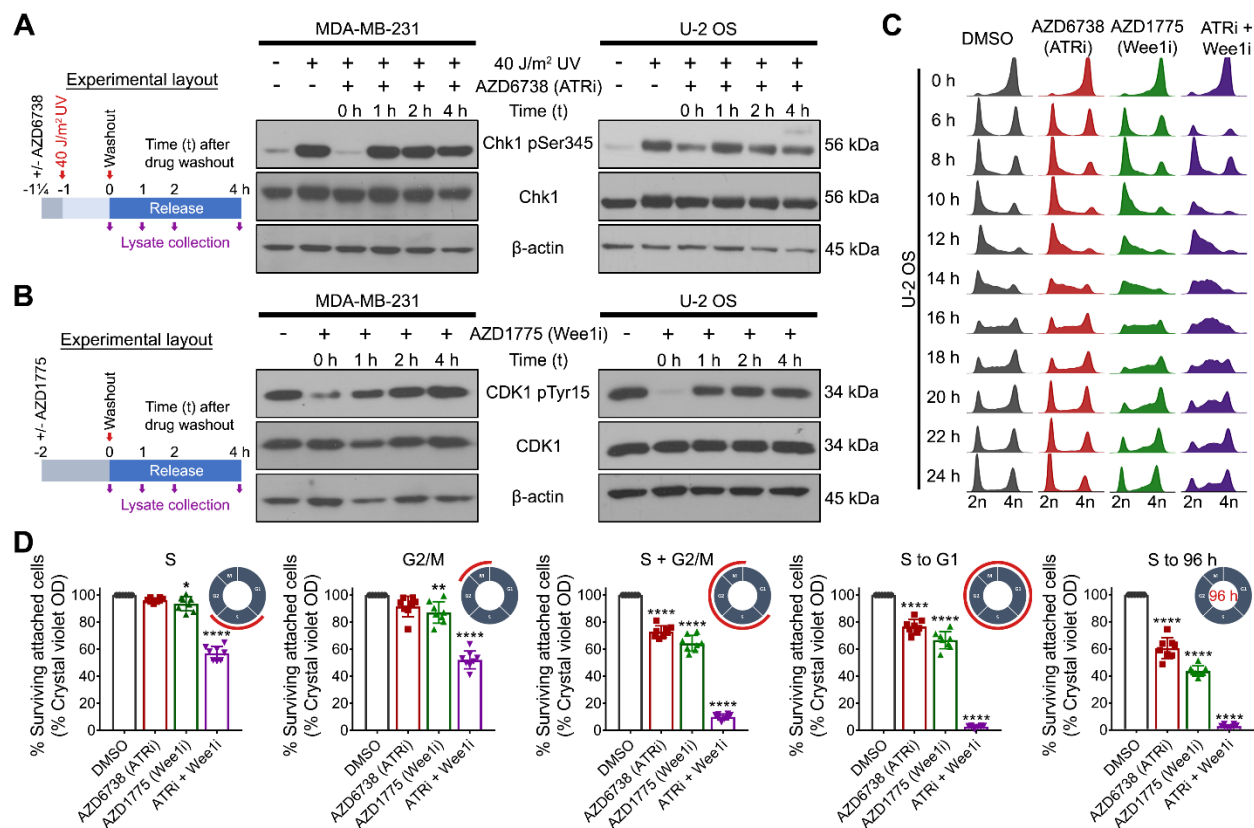


Figure 2.3. Contribution of cell cycle phases, during which ATR and/or Wee1 was inhibited, to overall cell killing.

(A and B) AZD6738 and AZD1775 are reversible inhibitors. Immunoblots of MDA-MB-231 and U-2 OS cells treated as indicated. (A) The ATR inhibitor AZD6738 (1 μ M) was added to cells 15 minutes before irradiation with 40 J/m² UV, a strong activator of ATR. One hour after irradiation, AZD6738 was removed, and the cells were washed and harvested at indicated times after drug removal. Restoration of ATR activity is observed 1 hour after AZD6738 washout. (B) Cells were incubated for 2 hours with 300 nM Wee1 inhibitor AZD1775, leading to a strong reduction in phospho-CDK1. AZD1775 was then removed, and cells washed, leading to restoration of Wee1 activity within 1–2 hours. (C) U-2 OS cells were synchronized by a thymidine-nocodazole block. Six hours after release, cells were treated with 1 μ M AZD6738 and/or 300 nM AZD1775. Cell cycle profiles were analyzed by propidium iodide staining and flow cytometry. (D) ATR and/or Wee1 in synchronized cancer cells were transiently inhibited with 1 μ M AZD6738 and/or 300 nM AZD1775 during the indicated cell cycle intervals. Survival of drug-treated cells relative to vehicle control was measured after 4 days. Data represent mean \pm SD. * P < 0.05, ** P < 0.005, and **** P < 0.0001 (one-way ANOVA).

2.3.4 Combined inhibition of ATR and Wee1 leads to increased DNA damage in tumors in vivo

AZD1775 and AZD6738 are both bioavailable and can be administered to mice by oral gavage. To test synthetic lethality between Wee1 and ATR inhibitors in tumors, we established a human breast cancer xenograft model in mice. Due to the tumor (micro)environment, drugs that sensitize *in vitro* face additional challenges in selectively killing cancer cells *in vivo*. The different growth kinetics *in vivo*, hypoxia, intra-tumoral heterogeneity, interaction with the stroma, and of course drug delivery, influence efficacy. Moreover, side effects such as injury to normal tissues are of great concern.

We derived from MDA-MB-231, a triple negative human breast cancer cell line (p53 mutated, BRCA wild type), a cell line that expresses the second-generation, less immunogenic firefly luciferase and the red-fluorescent protein tdTomato (Shaner *et al.* 2004) (**Suppl. Fig. 2.6**). In our orthotopic xenograft model these MDA-MB-231-*fluc2-tdTomato* cells are injected into the fourth mammary fat pad of 6-8 week old female NOD.Cg-*Prkdc^{scid} Il2rg^{tm1Wjl}/SzJ* (NSG) mice according to our approved animal protocol (AC16225). Once tumors reach a volume of 40-50 mm³ they are randomly allocated to treatment or vehicle arms. For our initial biomarker study to validate *in vivo* inhibition of ATR and Wee1 by our inhibitors and to test DNA damage induction in tumors, we administered 25 mg/kg AZD6738 and 60 mg/kg AZD1775 by oral gavage daily over 5 days. One hour after the last drug treatment [the approximate T_{max}, when these drugs show maximal plasma concentrations (Stewart *et al.* 2017), (personal communication by AstraZeneca)] we harvested the tumors. Excised tumors (n = 3 mice per treatment group) were tested for ATR and Wee1 activity by immunohistochemistry, assessing phosphorylation of the respective Wee1 and ATR substrates CDK1 Y15 and ATR T1989 (**Fig. 2.4A, B**) [As all Chk1 pS345 antibodies we tested did not work for immunohistochemistry, we used ATR auto-phosphorylation on Thr1989

as alternative readout for ATR activation (Nam *et al.* 2011) (**Suppl. Fig. 2.7**)]. Interestingly we not only confirmed ATR and Wee1 inhibition by AZD6738 and AZD1775, respectively, but also observed ATR activation *in vivo* in Wee1 inhibitor-treated tumors (**Fig. 2.4A**). Our data also indicate that ATR or Wee1 inhibition over the same period leads to a significant increase in tumor cells with DNA damage, assayed by γ H2AX staining (**Fig. 2.4C, D**). Of note, combination treatment with the two kinase inhibitors seems to synergistically enhance the number of cells staining for γ H2AX in the tumor ($P < 0.0001$, one-way ANOVA) (**Fig. 2.4D**). It also reduces the fraction of proliferating tumor cells, as measured by Ki-67 staining ($P < 0.0001$, one-way ANOVA) (**Fig. 2.4E, F**). We also note a significant increase in the number of apoptotic cells as measured by an increase in the number of TUNEL positive tumor cells ($P < 0.001$, one-way ANOVA) (**Fig. 2.4G, H**).

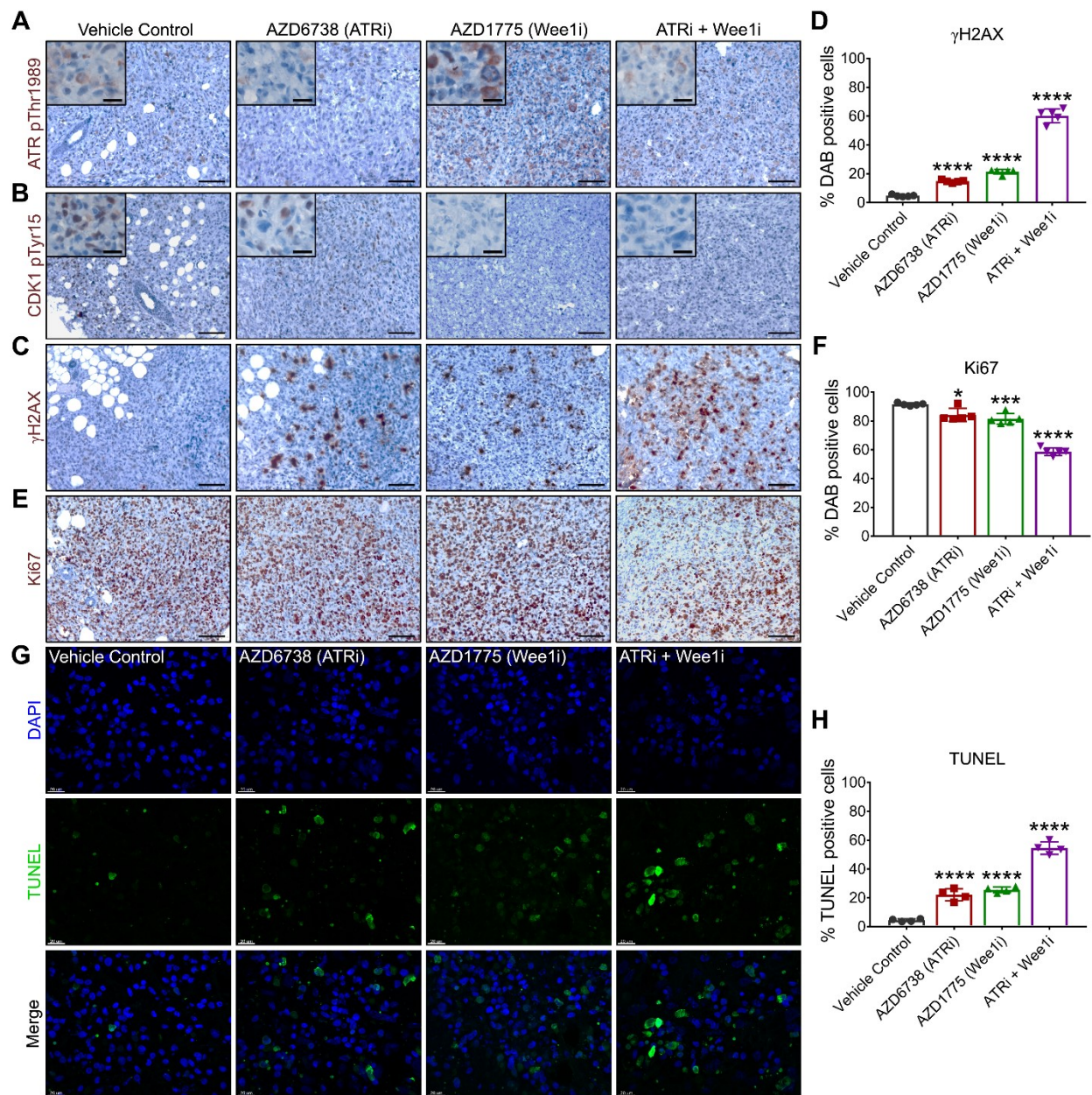


Figure 2.4. AZD6738 and AZD1775 inhibit ATR and Wee1, respectively, *in vivo*.

MDA-MB-231-*fluc2-tdTomato* xenografts were excised for immunohistochemistry 1 hour after the last administration of the inhibitors to the mice by oral gavage for 5 days (25 mg/kg AZD6738 and/or 60 mg/kg AZD1775 daily). ATR (A) and Wee1 activity (B) was tested by probing for phosphorylation of their respective substrates, ATR Thr1989 and CDK1 Tyr15 (insets show tumor tissue at $\times 40$ magnification). (C and D) DNA damage was tested for with antibodies against γ H2AX. (E and F) Ki-67 staining was used as a readout for proliferating cells. Scale bars: 100 μ m and 25 μ m (insets). (G and H) TUNEL assay was used to quantify cell death in excised tumor sections. Scale bars: 20 μ m. Data represent mean \pm SD. * $P < 0.05$, *** $P < 0.001$, and **** $P < 0.0001$ (one-way ANOVA). DAB = 3,3'-diaminobenzidine.

2.3.5 Combined ATR and Wee1 inhibition is well tolerated

As the aim of the conditional synthetic lethality approach is to spare normal tissue, we studied potential toxicities in treated mice, particularly in tissues with fast-proliferating cells and relying on stem cells for regeneration. We first tested tumor bearing immune-compromised NSG mice (n = 9 per group), used for our xenografts, and immune-competent C57BL/6 mice (n = 6 per group) for rudimentary indicators of side effects after treatment with 25 mg/kg AZD6738 and/or 60 mg/kg AZD1775 daily over a period of 26 days (**Fig. 2.5A**). None of the mice showed significant changes in body weight (**Fig. 2.5B, C**), behavior (including food intake) or feces consistency (data not shown). Postmortem analyses revealed no signs of inflammation or changes in spleen size. Only one mouse (in the ATR alone treatment group) showed signs of partial hair loss (**Suppl. Fig. 2.8**).

Due to renewal kinetics, tissues relying on fast-proliferating cells are particularly endangered by drugs that increase replication stress. Crypt intestinal stem cells support the continuous regeneration of the small intestine epithelium, the most rapidly self-renewing tissue in adult mammals (Barker *et al.* 2007). We therefore examined intestinal cells for DNA damage and measured the villi length of ilea from NSG mice. Due to abrasion villi are constantly replenished by the progenitor cells sitting in the crypt. Although we see an increase in crypt cells staining for γ H2AX (**Fig. 2.5D**) in mice treated with Wee1 inhibitor alone or in combination, but not with ATR inhibitor alone, no treatment group showed a decrease in villi length by day 26 (**Fig. 2.5E**). In mice crypt stem cell depletion, e.g. by ionizing radiation, can lead to observable changes in villi within 4 days (Withers 1971), yet the combination treatment over a period of 26 days is well tolerated in our mouse intestines, in agreement with no signs of diarrhea or changes in body weight. To test for changes in another tissue sensitive to genotoxic stress, we isolated the bone marrow from

immune-competent C57BL/6 mice after 26 days of inhibitor treatment. Bone marrow injury is one of the most common dose-limiting adverse effects of cancer therapy with genotoxic agents. Radiation and chemotherapy induce hematopoietic cell apoptosis, particularly in multipotent progenitor and hematopoietic progenitor cells, which proliferate and have lower DNA repair capacity than the quiescent hematopoietic stem cells they derive from (Mohrin *et al.* 2010). Hematopoietic stem and progenitor cells can be identified by surface markers (Kondo *et al.* 1997, Akashi *et al.* 2000). We used flow cytometry to quantify stem and progenitor cells from bone marrow using two different marker combinations, CD117+/Sca1+ (hematopoietic stem and multipotent progenitor cells) (**Fig. 2.5F, G**) and CD117+/Lin- (which additionally include myeloid progenitor cells) (**Fig. 2.5H, I**) (Mohrin *et al.* 2010). We did not see any significant changes in the percentage of these subpopulations in bone marrows from inhibitor treated mice compared to control mice (**Fig. 2.5G, I**).

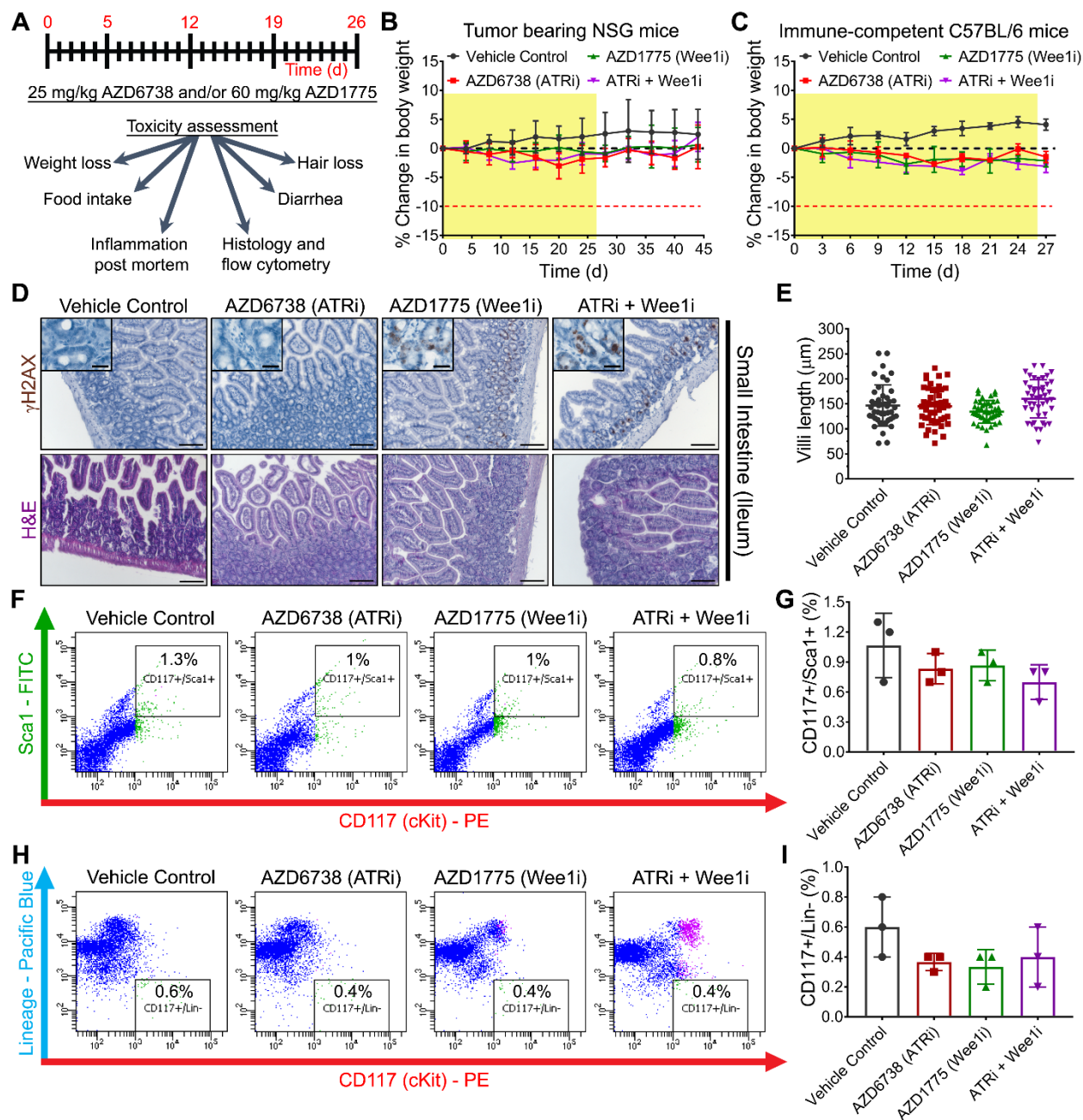


Figure 2.5. Combination treatment with ATR and Wee1 inhibitors and normal tissue toxicity.

(A) Mice were treated for 26 days daily with 25 mg/kg AZD6738 and/or 60 mg/kg AZD1775 and tested for adverse effects. (B and C) No significant body weight changes are observed in tumor-bearing immune-deficient NSG or in immunocompetent C57BL/6 mice. (D and E) Although Wee1 inhibition leads to some γ H2AX staining in the crypts of NSG mouse ilea (see insets) (D), no significant change in villi length is observed (E). $n = 50$ refers to 50 measurements in each of 3 mice per group. Scale bars: 100 μ m and 25 μ m (insets). (F–I) No significant depletion of hematopoietic stem and progenitor cells isolated from treated C57BL/6 mice is observed. Bone

marrow cells were isolated from C57BL/6 mice treated as described in **A** and analyzed with the indicated surface markers by flow cytometry. (**F** and **G**) Hematopoietic stem and multipotent progenitor cells stained for CD117 and Sca1. (**H** and **I**) The CD117⁺Lin⁻ population additionally includes myeloid progenitor cells. Data represent mean \pm SD.

To rigorously test for drug-induced damage to normal tissue we harvested additional tissues from tumor bearing immune-compromised NSG mice (n = 3 per group) and immune-competent C57BL/6 mice (n = 3 per group) immediately after the 26 day (“26 d”) drug treatment, or one (“33 d”) or two weeks after the last day of drug administration (**Fig. 2.6**). Only in the ileum and in the spleen of mice at the end of the drug treatment did we observe an increase of γ H2AX-staining cells. No DNA damage was observable e.g., in lungs, kidneys or livers from either NSG or C57BL/6 mice (**Fig. 2.6** and **Suppl. Fig. 2.9-2.13**). Remarkably after a period of just 7 days after last drug administration, the number of DNA damaged cells in the ilea or the spleens returned to background levels (**Fig. 2.6**, left panel). We also analyzed the blood of mice at the end of and 1 or 2 weeks after drug treatment. Pathological evaluations did not reveal any significant changes in complete blood cell count (**Suppl. Table 2.1, 2.2**), in agreement with the lack of observable hematopoietic stem cell depletion (**Fig. 2.5 F-I**). In summary, the increased endogenous DNA damage in cancer cells compared to even actively proliferating normal cells seems to provide a significant therapeutic window for the combination treatment.

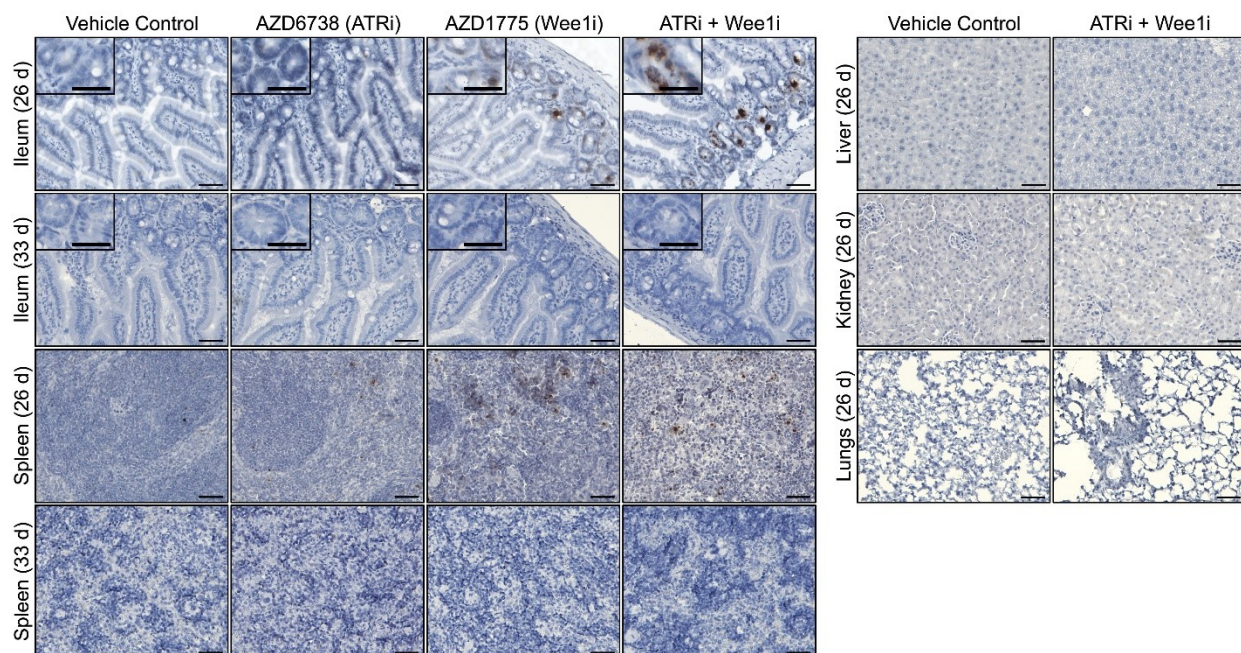


Figure 2.6. Evaluation of normal tissue DNA damage.

Tissues from tumor-bearing NSG mice (or immunocompetent C57BL/6 mice without tumors, shown in Suppl. Figure 2.13) were harvested on the last day (26 d) or 1 week after (33 d) the last day of a 26-day treatment period with AZD6738 and/or AZD1775. While lung, liver, and kidney did not show any signs of DNA damage, some cells in the ileum and spleen were found to stain for γ H2AX at the end of the treatment (26 d). However, 1 week later (33 d), ilea and spleens recovered from the drug treatment, as measured by staining for γ H2AX. Scale bars: 25 μ m and 20 μ m (insets).

2.3.6 Combined inhibition of ATR and Wee1 leads to tumor remission, increased survival and inhibition of metastasis

To test drug efficacy in longitudinal studies using our xenograft model, once tumors reached a volume of 40-50 mm³ mice were randomly allocated to treatment or vehicle arms (n = 9 mice per treatment group). These mice were administered 25 mg/kg AZD6738 and/or 60 mg/kg AZD1775 daily over a period of 26 days (**Fig. 2.5A**, yellow shades in **Fig. 2.7B, C, F**) and tumor growth was followed by caliper measurement every second day and metastasis by weekly inspection with a bioluminometer (**Fig. 2.7A**). We observed significant inhibition of tumor growth ($P < 0.0001$, two-way ANOVA) (**Fig. 2.7B**) by treatment with AZD6738 and AZD1775. While treatment with AZD6738 or AZD1775 alone delays tumor growth, tumor expansion resumes rapidly when drug treatment is stopped. However, combination treatment leads to tumor shrinkage below 1 mm³, in 6/9 cases even to complete remission as measured by impalpable tumor levels. Although we have not observed complete eradication so far (the high sensitivity of bioluminescence allows for the visualization of residual MDA-MB-231-*fluc2*), we speculate that a proportionate level of cell killing in immunocompetent patients could lead to tumor control. In our immunocompromised NSG mice that have been treated with the inhibitor combination, tumors do eventually recur (**Suppl. Fig. 2.14**). Nevertheless, and although mice were only treated for 26 days, mice treated with AZD6738+AZD1775 lived significantly longer ($P < 0.0001$, Log-rank Mantel-Cox; median survival after start of treatment: AZD6738 – 60 days; AZD1775 – 62 days; AZD6738+AZD1775 – 103 days; vehicle control treated – 53 days) (**Fig. 2.7C**), paralleling the cancer-selective synthetic lethality observed *in vitro*.

Tagging MDA-MB-231 cells with firefly luciferase also allowed us to follow metastasis by non-invasive bioluminescence imaging. As can be seen by representative images of mice at

week 7 (16 days after the last drug administration) and the statistical analysis of bioluminescence at distant sites, combined Wee1 and ATR inhibition strongly suppressed metastasis (**Fig. 2.7D**). While Wee1 or ATR inhibitor stand-alone treatment did not show any significant inhibition of metastasis, bioluminescence levels at distant sites in the combination treatment are below the background threshold ($P = 0.0383$, one-way ANOVA) (**Fig. 2.7E**).

To further investigate inhibition of metastasis we treated a set of mice (n = 4 mice per treatment group) only when tumors reached a volume of around 250 mm³. At that point micrometastasis should already have occurred, as the corresponding time relates to approximately 4-5 weeks later in tumor growth compared to the previous experiments (Compare tumor volumes and metastasis at week 7 for control mice in **Fig. 2.7B, D**). Again, mice were randomly allocated to treatment arms, consisting of a 26 day period of daily administration of 25 mg/kg AZD6738 and/or 60 mg/kg AZD1775. As seen before, AZD6738 and AZD1775 single treatment led to tumor growth delay ($P < 0.0001$, two-way ANOVA), but combined treatment led to tumor shrinkage ($P < 0.0001$, two-way ANOVA) (**Fig. 2.7F**). Secondary tumors were observed in the thoracic lymph nodes of control, AZD6738 or AZD1775 treated mice, but not in animals receiving the combination treatment ($P = 0.0061$, one-way ANOVA) (**Fig. 2.7G**). Even more compelling, tissues from the mice euthanized at the end of the treatment were inspected for micrometastases by bioluminescence, a technique that allows us to detect clusters of as few as 20 cells. Unlike in the case of control or single inhibitor treated mice, which showed metastasis to lymph nodes, lungs, liver, bone, gut, and in some case also to the brain and ovaries, tissues from combined ATR and Wee1 inhibitor treated animals showed no detectable micrometastases (**Table 2.2**).

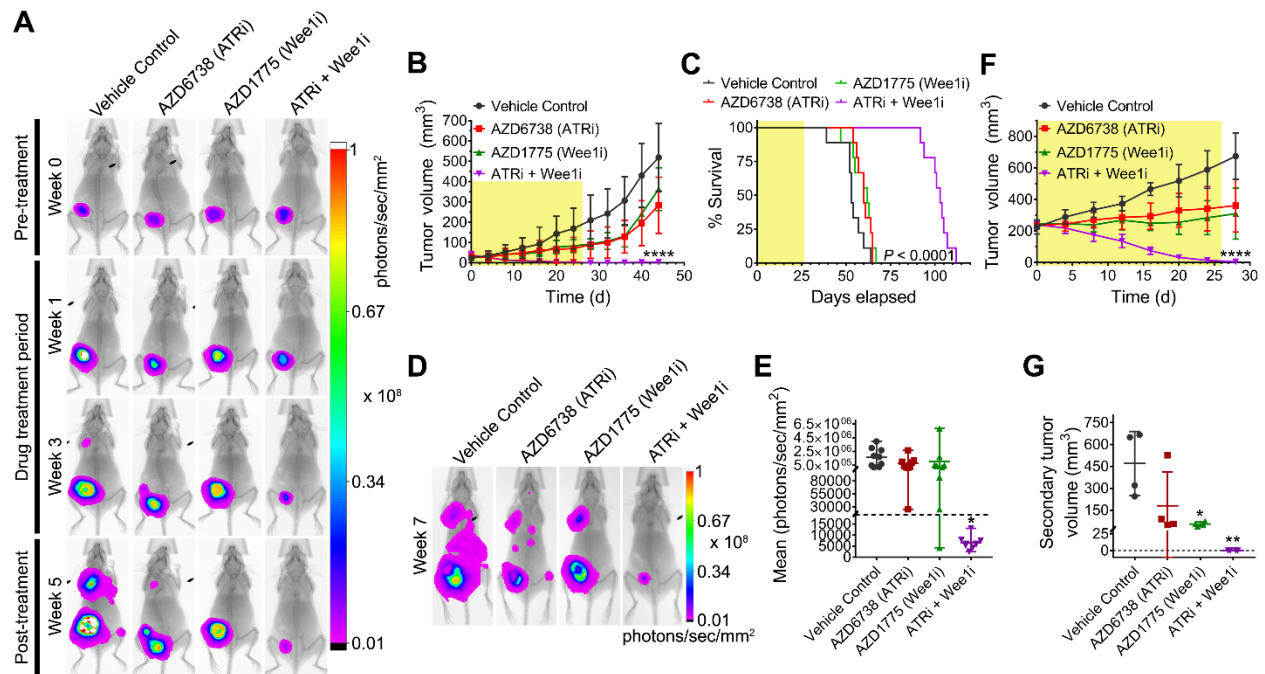


Figure 2.7. Combination treatment with ATR and Wee1 inhibitors and tumor control.

(A–E) NSG mice were injected orthotopically with MDA-MB-231-*fluc2-tdTomato*-labeled breast cancer cells and treated for 26 days (indicated by yellow shades) with 25 mg/kg AZD6738 and/or 60 mg/kg AZD1775 after tumors reached approximately 40 mm³. (A) Tumor progression was monitored weekly by bioluminescence imaging. (B) Tumor growth of mice in the 4 treatment arms ($n = 9$ per group). (C) Kaplan-Meier survival curves of treated mice ($n = 9$ per group). (D and E) Metastasis in regions distal to the primary tumor was assessed 7 weeks after treatment initiation ($n = 9$ per group). The dotted line indicates background threshold (E). (F and G) To further investigate inhibition of metastasis, a group of MDA-MB-231-*fluc2-tdTomato* tumors ($n = 4$ per group) were allowed to grow to approximately 250 mm³ before treatment as in A. Combination treatment leads to tumor shrinkage (F). Unlike control or single-agent-treated mice, those treated with AZD6738 and AZD1775 had no detectable secondary tumors (G). Data represent mean \pm SD. * $P < 0.05$, ** $P < 0.01$, **** $P < 0.0001$ by 2-way ANOVA (B and F), log-rank Mantel-Cox test (C), or 1-way ANOVA (E and G).

<i>Tissue</i>	<i>Vehicle Control</i>	<i>AZD6738 (ATRi)</i>	<i>AZD1775 (Wee1i)</i>	<i>ATRi + Wee1i</i>
<i>Lungs</i>	4/4	4/4	4/4	0/4
<i>Lymph node</i>	4/4	4/4	4/4	0/4
<i>Bone</i>	4/4	2/4	1/4	0/4
<i>Liver</i>	4/4	4/4	4/4	0/4
<i>Brain</i>	2/4	1/4	0/4	0/4
<i>Gut</i>	4/4	4/4	4/4	0/4
<i>Ovaries</i>	4/4	3/4	1/4	0/4

Table 2.2. Metastases in animals treated with ATR and Wee1 inhibitors.

Ex vivo bioluminescence imaging of excised tissues revealed micrometastases in several organs from control or single inhibitor treated mice, but no micrometastases were observed in the AZD6738/AZD1775 combination treatment group.

2.3.7 ATR and Wee1 activity are critical for breast cancer stem cell survival

Our observation that combined ATR and Wee1 inhibition suppresses metastasis of highly invasive MDA-MB-231 (**Fig. 2.7D-F** and **Table 2.2**) could be explained by inhibition of the process of metastasis *per se* or a depletion of cells able to spread and to initiate tumors at distant sites. Breast cancer stem cells have been implicated in metastasis due to their high cellular plasticity, enabling them to undergo epithelial-mesenchymal transition, and their tumor initiating potential. This prompted us to isolate a subpopulation enriched in cancer stem cells from cell lines of two different breast cancer subtypes, MCF7 (luminal B) and MDA-MB-231 (claudin low), by their dye efflux propensity (Telford *et al.* 2007) (**Fig. 2.8A**). Cancer stem cells often show upregulation of transporter proteins in the ATP-binding cassette family, such as ABCG2. Confirming the stem cell character of the isolated subpopulation, a much lower number of seeded cells from the fraction with high dye efflux capacity (“side population”, SP) is required to form mammospheres than cells with low efflux capacity (“non-side population”, NSP) (**Table 2.3** and **Fig. 2.8B**). We next compared cooperative cell killing by ATR and Wee1 inhibitors in the cancer stem cell-enriched side population to a non-side population. MCF7 and MDA-MB-231 cancer stem cells (SP) are more resistant than the control subpopulation (NSP) to either AZD6738 or AZD1775 alone, but surprisingly showed similar sensitivities to the combined treatment (**Fig. 2.8C, D**). This unexpected finding is due to higher synergistic effects in cancer stem cells than in cancer cells without stem cell features (e.g., lower Bliss combination indices (CI) at 300 nM AZD6738 and 100 nM AZD1775 of 0.40 versus 0.90 for MCF7 and 0.41 versus 0.75 for MDA-MB-231). To our knowledge this is the first reported observation of increased synergistic effects of cytotoxic agents in cancer stem cells compared to bulk cancer cells. The increased synergy in

cancer stem cells, although they are more resistant to the single agents, could explain the strong anti-metastatic effect by the combination treatment observed in our animal model.

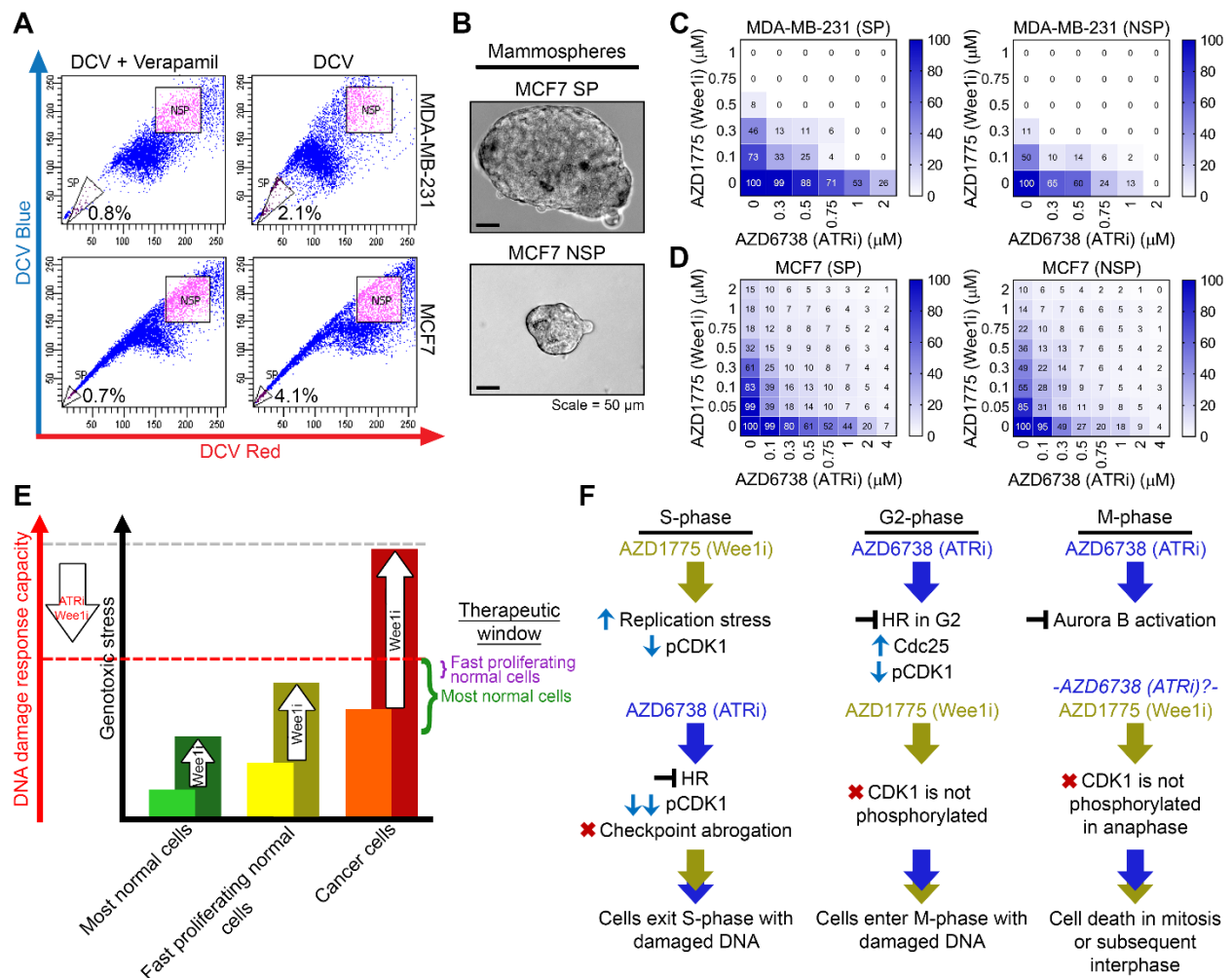


Figure 2.8. Synergistic killing of breast cancer stem cells by ATR and Wee1 inhibitors.

(A) Isolation of cancer stem cell-enriched subpopulations (side population, SP) from MDA-MB-231 or MCF7 based on their increased dye (DyeCycle Violet, DCV) efflux properties. Verapamil, an inhibitor of drug efflux pump proteins, particularly of the ABC transporter family, served as negative control. (B) Isolated SPs show an increased ability to form mammospheres compared with control subpopulations (non-side population, NSP). Representative images of mammospheres are shown. (C and D) Four-day survival assays of cancer stem cell-enriched SPs and control cells (NSPs) isolated from MDA-MB-231 (C) and MCF7 (D). Plated cells were treated with indicated concentrations of AZD1775 and/or AZD6738. Color bars indicate percentage survival normalized to untreated cells. (E) Model of cancer-selective synergistic cell killing by combined ATR and Wee1 inhibition. Cancer cells have higher baseline levels of genotoxic stress than normal cells. Wee1 inhibition increases genotoxic stress, while ATR and Wee1 inhibition together lower cellular DNA-damage response capacity (in the simplified model to the same extent, but potentially higher in cancer cells relying on these 2 kinases for survival). A therapeutic window is created for the selective killing of cancer cells. (F) Cell cycle-dependent effects of ATR

and Wee1 inhibition contributing to overall cell death following mitotic catastrophe. HR, homologous recombination.

		<i>MDA-MB-231</i>	<i>MCF7</i>
	<i>Cells plated per well</i>	<i>Number of wells positive for mammospheres</i>	<i>Number of wells positive for mammospheres</i>
<i>Side Population (SP)</i>	1	0/6	2/6
	2	0/6	2/6
	5	0/6	3/6
	10	0/6	4/6
	100	5/6	5/6
	1000	6/6	6/6
<i>Non-Side Population (NSP)</i>	1	0/6	0/6
	2	0/6	0/6
	5	0/6	0/6
	10	0/6	0/6
	100	1/6	0/6
	1000	5/6	4/6

Table 2.3. Mammosphere-forming capabilities of SP and NSP cells.

Isolated “side population” cells demonstrate higher mammosphere forming capabilities as compared to the “non-side population” cells.

2.4 Discussion

Tumor heterogeneity constitutes one of the biggest barriers to effective cancer therapies. Therapies merely targeting the bulk of cancer cells are often destined to fail because induced clonal drifts and the formation of dormant cells decrease tumor control probability. Furthermore, activation of alternative pathways to counteract targeted therapies can lead to drug resistance. Here we describe a strategy designed to take advantage of the cancer-intrinsic property of DNA damage (Halazonetis *et al.* 2008), a feature shared by all clones (albeit potentially to different extents). Genomic instability is a driver of tumorigenesis and has been designated as a hallmark of cancer (Hanahan and Weinberg 2011). Cancer cells typically show oncogene-driven genome changes such as an aberrant number or structure of chromosomes (chromosomal instability), microsatellite instability, and/or the mutagenic load. While the impairment of checkpoints that should prevent these events are drivers of tumorigenesis, the increase in accumulated DNA damage leads to replication stress (Kotsantis *et al.* 2018) and a high risk of mitotic failure, making the survival of cancer cells heavily reliant on an often partially defective DNA damage response.

The gene products of Ataxia telangiectasia mutated (ATM) and ATR are apical kinases of pathways activated by DNA damage. Unlike ATM, which is frequently lost in cancers (Greenman *et al.* 2007), ATR is an essential gene for the response to DNA damage (Brown and Baltimore 2000, de Klein *et al.* 2000) and ATR activity is often upregulated in cancer cells (Parikh *et al.* 2014, Abdel-Fatah *et al.* 2015). ATR activation is important for DNA damage repair by homologous recombination (Gamper *et al.* 2013, Kibe *et al.* 2016, Buisson *et al.* 2017). Furthermore ATR (*via* Chk1) together with Wee1 negatively regulates the activity of CDK2 and especially of CDK1, the only essential CDK in mammals (Santamaria *et al.* 2007). Likely due to the reliance of cancer cells on the G2/M checkpoint to protect them from mitotic catastrophe as a

consequence of excessive DNA damage, Wee1 was found to be upregulated in several cancer types (Matheson *et al.* 2016). The importance that Wee1 and ATR were found to have in cancer cell survival make them attractive therapeutic targets.

2.4.1 A model for the synergistic cell killing by ATR and Wee1 inhibition

Here we report cancer-selective synergistic killing by ATR and Wee1 inhibition. (While this manuscript was in preparation, another group reported synergistic killing of triple-negative breast cancer cells by Wee1 and ATR inhibitors (Jin *et al.* 2018)). Our data support a model, where synergistic killing by ATR and Wee1 inhibitors is triggered by Wee1 inhibition-induced DNA damage during replication, abrogation of ATR-mediated S phase checkpoint activation, inhibition of ATR-dependent homologous recombination, and amplified by increased entry into mitosis with defective genomes due to combined inhibition of ATR and Wee1 (**Suppl. Fig. 2.15**). High replication stress in cancer cells could be due to the high level of baseline DNA damage *per se*, but also to the resulting exhaustion of factors needed for both repair and replication, such as RPA (Toledo *et al.* 2013). ATR plays an essential role for cancer cells to survive replication stress. Already hypersensitive to ATR inhibition, we propose that Wee1 inhibition leads to even higher replication stress in cancer cells making them unable to avoid DNA damage during replication at ATR inhibitor doses tolerable to the animals (or patients). Highly proliferative normal tissues by contrast do not have such high baseline replication stress and can tolerate the combination treatment (**Fig. 2.8E**). This model is supported by our observation that reversal of ATR or Wee1 inhibition alone following S phase leads to minimal cell death (**Fig. 2.8D**), indicating that the resulting increase in replication stress can be rescued by repair before entry into mitosis. Combined inhibition during replication on the other hand, even if reversed after S phase, leads to substantial cell killing, likely due to extensive genome damage that cannot be repaired before cells enter

mitosis. Similarly, combined ATR and Wee1 inhibition after S phase completion leads to extensive cell death. This might be due to G2/M checkpoint abrogation and the consequent premature entry into mitosis with unrepaired endogenous DNA damage, but also to functions of ATR and Wee1 during mitosis. ATR was reported to contribute to faithful chromosome segregation by promoting Aurora B activation at centromeres (Kabeche *et al.* 2018). Also Wee1 has a role in mitosis beyond regulating the G2/M checkpoint, as residual Wee1 (potentially together with ATR) inhibits CDK1 activity in anaphase, which controls mitotic exit (Lewis *et al.* 2017). The abrogation of ATR and Wee1 activity during different phases of the cell cycle cooperatively leads to cell death caused by mitotic defects (**Fig. 2.8F**). Cell death can occur in mitosis or in interphase after aborted or completed mitosis. As a consequence of coordinated effects that Wee1 and ATR have on faithful cell cycle progression, particularly in cells with high baseline DNA damage, a therapeutic window opens to lower the activity of these two kinases to levels lethal for cancer cells, but tolerable to normal tissues. This is in stark contrast to Chk1 inhibition, which – particularly when combined with Wee1 inhibition (**Suppl. Fig. 2.2**) – shows high toxicity in non-transformed cells. As previously pointed out by us and others, Chk1 inhibition is not phenotypically identical with ATR inhibition (Gamper *et al.* 2013, Techer *et al.* 2016, Forment and O'Connor 2018).

2.4.2 Cancer-selective synthetic lethality, tumor remission and inhibition of metastasis

Our preclinical mouse data indicate that at doses leading to strong tumor shrinkage, combined ATR and Wee1 inhibition shows minimal adverse effects. The absence of diarrhea or villi change in the ilea as well as of a significant loss of hematopoietic stem and progenitor cells, indicators of intestinal damage or bone marrow injury respectively, suggest that tissues relying on fast proliferating cells for homeostasis are less sensitive to the combination treatment than tumor cells. Phase I studies of AZD6738 (as well as other ATR inhibitors) are currently being undertaken.

AZD1775 (currently the only Wee1 inhibitor in clinical development) has already progressed to several phase II trials, usually in combination with genotoxic agents such as carboplatin or gemcitabine (Forment and O'Connor 2018). The strong synergistic effects on tumor control described here, leading to complete remission in 6/9 cases by the AZD6738/AZD1775 combination treatment, provide an ideal base for phase I clinical trials. Even more striking is our observation that combined Wee1/ATR inhibition leads to a strong inhibition of metastasis. We observe both inhibition of tumor spread by a 26 day AZD6738/AZD1775 treatment started when tumors are still small as well as the absence of metastatic lesions following the same treatment in mice, when the treatment was initiated after micrometastasis already has happened (**Fig. 2.7D-G** and **Table 2.2**). This observation could be explained by our surprising finding that breast cancer stem cell-enriched populations, although more resistant to either ATR or Wee1 inhibition alone, show a higher synergy in cell killing by co-treatment with AZD6738 and AZD1775, than bulk cells. Cancer stem cells from a variety of tissues were found to display elevated radiation and chemoresistance (Vitale *et al.* 2017). Interestingly, glioma, colon and lung cancer stem cells were found to have a stronger ATR response to genotoxic agents than bulk cancer cells (Bao *et al.* 2006, Gallmeier *et al.* 2011, Bartucci *et al.* 2012), and glioma stem cells were found to be more sensitive to Wee1 inhibition than neural stem cells (Toledo *et al.* 2015). It could be that the reliance of cancer stem cells on ATR or Wee1 to withstand genotoxic insults makes them particularly vulnerable to combined Wee1/ATR inhibition. Because metastasis is the main cause of death in cancer patients, the anti-metastatic activity, and the propensity to kill cancer stem cells could make a combined AZD6738/AZD1775 regimen suitable for stand-alone treatment or for adjuvant therapy.

2.4.3 Potential strategies for patient selection

Unlike recently reported by Jin *et al.* (Jin *et al.* 2018), we observe *in vitro* synthetic lethality of ATR and Wee1 inhibition not only in triple-negative breast cancer cells, but in a wide range of breast cancer cell lines, including luminal A and B cells (MCF7, T47-D, MDA-MB-175-VII, Zr-75-1) and Her2-amplified Sk-BR-3. While Jin *et al.* speculate that p53 mutation sensitizes cancer cells to combined ATR/Wee1 inhibition, we noticed strong synthetic lethality also in p53 wild type cells, such as MDA-MB-175-VII, Zr-75-1, and MCF7, and the osteosarcoma cell line U-2 OS. Based on our model, where ATR and Wee1 inhibition leads to decreased S, S/G2 and G2/M checkpoint activation, supported by the recent finding that ATR is an important regulator of the S/G2 checkpoint (Saldivar *et al.* 2018), and subsequently leads to mitotic catastrophe, we speculate that p53 status is less of a predictor of therapeutic outcome by the drug combination than baseline levels of DNA damage and alterations in the mechanisms regulating CDK1/2 activity. Indeed, our unpublished data show that factors besides Chk1 and Wee1 regulating CDK1 activity, such as the Wee1-related kinase Myt1, or factors involved in processing replication stress intermediates, play important roles in cellular sensitivity to Wee1/ATR combination treatment *in vitro*. Initial clinical trials are expected in cancer types known for their genomic instability, such as cancers with ATM loss, which we previously showed to sensitize to ATR inhibition (Gamper *et al.* 2013), and certain breast, ovarian or colorectal cancers, where Homologous Recombination (e.g. by BRCA loss) or other repair pathways are impaired. Yet the conditional synthetic lethality underlying combined AZD1775/AZD6738 treatment is based on the increased DNA damage *per se* in cancer cells compared to normal tissue. This genotoxic stress can have various origins, from aneuploidy to gene or epigenetic defects, but will result in replication stress. Unfortunately, while several candidate predictive biomarkers have been identified for cellular sensitivity to ATR or Wee1

inhibitors (reviewed in (Brandsma *et al.* 2017)), clinical biomarkers for DNA replication stress are still lacking. Whereas *in vitro* FANCD2 or RAD51 foci resulting from the recruitment of these proteins to common fragile sites are good surrogate markers for replication stress (Schwartz *et al.* 2005, Chan *et al.* 2009), attempts to use Ki-67, cyclin E, POLD3, γ H2AX, and FANCD2 staining in cancer specimens by IHC have been disappointing (Ren *et al.* 2017). Incidentally, ATR activation should correlate with replication stress and future studies will assess whether ATR phosphorylation at T1989 in cancer biopsies, used as marker of ATR activation in our xenografts, is a predictive biomarker for combined ATR/Wee1 inhibitor treatment.

2.5 Acknowledgements

We thank Dr. Kristi Baker for the C57BL/6 mice; Dr. David Murray for helpful suggestions on the manuscript; Powel Crosley for help with R programming; John Lewis for the use of the *in vivo* imaging system; Dr. Xuejun Sun and Geraldine Barron for assistance in the cell imaging facility; Sabina Baghirova and Dr. Aja Rieger for assistance with flow cytometry; and AstraZeneca for compounds AZD6738 and AZD1775. ABB and CWL are supported by Alberta Cancer Foundation's Dr. Cyril M. Kay Graduate Scholarship and NSERC Alexander Graham Bell Canada Graduate Scholarship respectively. This research is funded by a startup grant from the University of Alberta and a CIHR grant in the Gamper laboratory, and by NSERC and the Cancer Research Society in the Chan laboratory.

2.6 Conflict of interest

The authors have declared that no conflict of interest exists.

2.7 References

- Abdel-Fatah, T. M., F. K. Middleton, A. Arora, D. Agarwal, T. Chen, P. M. Moseley, C. Perry, R. Doherty, S. Chan, A. R. Green, E. Rakha, G. Ball, I. O. Ellis, N. J. Curtin and S. Madhusudan (2015). "Untangling the ATR-CHEK1 network for prognostication, prediction and therapeutic target validation in breast cancer." *Mol Oncol* **9**(3): 569-585.
- Akashi, K., D. Traver, T. Miyamoto and I. L. Weissman (2000). "A clonogenic common myeloid progenitor that gives rise to all myeloid lineages." *Nature* **404**(6774): 193-197.
- Bao, S., Q. Wu, R. E. McLendon, Y. Hao, Q. Shi, A. B. Hjelmeland, M. W. Dewhirst, D. D. Bigner and J. N. Rich (2006). "Glioma stem cells promote radioresistance by preferential activation of the DNA damage response." *Nature* **444**(7120): 756-760.
- Barker, N., J. H. van Es, J. Kuipers, P. Kujala, M. van den Born, M. Cozijnsen, A. Haegebarth, J. Korving, H. Begthel, P. J. Peters and H. Clevers (2007). "Identification of stem cells in small intestine and colon by marker gene Lgr5." *Nature* **449**(7165): 1003-1007.
- Bartucci, M., S. Svensson, P. Romania, R. Dattilo, M. Patrizii, M. Signore, S. Navarra, F. Lotti, M. Biffoni, E. Pillozzi, E. Duranti, S. Martinelli, C. Rinaldo, A. Zeuner, M. Maugeri-Sacca, A. Eramo and R. De Maria (2012). "Therapeutic targeting of Chk1 in NSCLC stem cells during chemotherapy." *Cell Death Differ* **19**(5): 768-778.
- Beck, H., V. Nahse, M. S. Larsen, P. Groth, T. Clancy, M. Lees, M. Jorgensen, T. Helleday, R. G. Syljuasen and C. S. Sorensen (2010). "Regulators of cyclin-dependent kinases are crucial for maintaining genome integrity in S phase." *J Cell Biol* **188**(5): 629-638.
- Beeharry, N., J. B. Rattner, J. P. Caviston and T. Yen (2013). "Centromere fragmentation is a common mitotic defect of S and G2 checkpoint override." *Cell Cycle* **12**(10): 1588-1597.
- Brandsma, I., E. D. G. Fleuren, C. T. Williamson and C. J. Lord (2017). "Directing the use of DDR kinase inhibitors in cancer treatment." *Expert Opin Investig Drugs* **26**(12): 1341-1355.
- Brinkley, B. R., R. P. Zinkowski, W. L. Mollon, F. M. Davis, M. A. Pisegna, M. Pershouse and P. N. Rao (1988). "Movement and segregation of kinetochores experimentally detached from mammalian chromosomes." *Nature* **336**(6196): 251-254.
- Brown, E. J. and D. Baltimore (2000). "ATR disruption leads to chromosomal fragmentation and early embryonic lethality." *Genes Dev* **14**(4): 397-402.
- Bryant, H. E., N. Schultz, H. D. Thomas, K. M. Parker, D. Flower, E. Lopez, S. Kyle, M. Meuth, N. J. Curtin and T. Helleday (2005). "Specific killing of BRCA2-deficient tumours with inhibitors of poly(ADP-ribose) polymerase." *Nature* **434**(7035): 913-917.
- Buisson, R., J. Niraj, A. Rodrigue, C. K. Ho, J. Kreuzer, T. K. Foo, E. J. Hardy, G. Dellaire, W. Haas, B. Xia, J. Y. Masson and L. Zou (2017). "Coupling of Homologous Recombination and the Checkpoint by ATR." *Mol Cell* **65**(2): 336-346.
- Chan, K. L., T. Palmari-Pallag, S. Ying and I. D. Hickson (2009). "Replication stress induces sister-chromatid bridging at fragile site loci in mitosis." *Nat Cell Biol* **11**(6): 753-760.

Chow, J. P., R. Y. Poon and H. T. Ma (2011). "Inhibitory phosphorylation of cyclin-dependent kinase 1 as a compensatory mechanism for mitosis exit." Mol Cell Biol **31**(7): 1478-1491.

Ciccia, A. and S. J. Elledge (2010). "The DNA damage response: making it safe to play with knives." Mol Cell **40**(2): 179-204.

de Klein, A., M. Muijtjens, R. van Os, Y. Verhoeven, B. Smit, A. M. Carr, A. R. Lehmann and J. H. Hoeijmakers (2000). "Targeted disruption of the cell-cycle checkpoint gene ATR leads to early embryonic lethality in mice." Curr Biol **10**(8): 479-482.

Dominguez-Kelly, R., Y. Martin, S. Koundrioukoff, M. E. Tanenbaum, V. A. Smits, R. H. Medema, M. Debatisse and R. Freire (2011). "Wee1 controls genomic stability during replication by regulating the Mus81-Eme1 endonuclease." J Cell Biol **194**(4): 567-579.

Drosos, Y., D. Escobar, M. Y. Chiang, K. Roys, V. Valentine, M. B. Valentine, J. E. Rehg, V. Sahai, L. A. Begley, J. Ye, L. Paul, P. J. McKinnon and B. Sosa-Pineda (2017). "ATM-deficiency increases genomic instability and metastatic potential in a mouse model of pancreatic cancer." Sci Rep **7**(1): 11144.

Eriksson, D. and T. Stigbrand (2010). "Radiation-induced cell death mechanisms." Tumour Biol **31**(4): 363-372.

Farmer, H., N. McCabe, C. J. Lord, A. N. Tutt, D. A. Johnson, T. B. Richardson, M. Santarosa, K. J. Dillon, I. Hickson, C. Knights, N. M. Martin, S. P. Jackson, G. C. Smith and A. Ashworth (2005). "Targeting the DNA repair defect in BRCA mutant cells as a therapeutic strategy." Nature **434**(7035): 917-921.

Feoktistova, M., P. Geserick and M. Leverkus (2016). "Crystal Violet Assay for Determining Viability of Cultured Cells." Cold Spring Harb Protoc **2016**(4): pdb prot087379.

Forment, J. V. and M. J. O'Connor (2018). "Targeting the replication stress response in cancer." Pharmacol Ther.

Fouquier, J. and M. Guedj (2015). "Analysis of drug combinations: current methodological landscape." Pharmacol Res Perspect **3**(3): e00149.

Gallmeier, E., P. C. Hermann, M. T. Mueller, J. G. Machado, A. Ziesch, E. N. De Toni, A. Palagyi, C. Eisen, J. W. Ellwart, J. Rivera, B. Rubio-Viqueira, M. Hidalgo, F. Bunz, B. Goke and C. Heeschen (2011). "Inhibition of ataxia telangiectasia- and Rad3-related function abrogates the in vitro and in vivo tumorigenicity of human colon cancer cells through depletion of the CD133(+) tumor-initiating cell fraction." Stem Cells **29**(3): 418-429.

Gamper, A. M., R. Rofougaran, S. C. Watkins, J. S. Greenberger, J. H. Beumer and C. J. Bakkenist (2013). "ATR kinase activation in G1 phase facilitates the repair of ionizing radiation-induced DNA damage." Nucleic Acids Res **41**(22): 10334-10344.

Gascoigne, K. E. and S. S. Taylor (2008). "Cancer cells display profound intra- and interline variation following prolonged exposure to antimetabolic drugs." Cancer Cell **14**(2): 111-122.

Greenman, C., P. Stephens, R. Smith, G. L. Dalgliesh, C. Hunter, G. Bignell, H. Davies, J. Teague, A. Butler, C. Stevens, S. Edkins, S. O'Meara, I. Vastrik, E. E. Schmidt, T. Avis, S. Barthorpe, G. Bhamra, G. Buck, B. Choudhury, J. Clements, J. Cole, E. Dicks, S. Forbes, K. Gray, K. Halliday,

R. Harrison, K. Hills, J. Hinton, A. Jenkinson, D. Jones, A. Menzies, T. Mironenko, J. Perry, K. Raine, D. Richardson, R. Shepherd, A. Small, C. Tofts, J. Varian, T. Webb, S. West, S. Widaa, A. Yates, D. P. Cahill, D. N. Louis, P. Goldstraw, A. G. Nicholson, F. Brasseur, L. Looijenga, B. L. Weber, Y. E. Chiew, A. DeFazio, M. F. Greaves, A. R. Green, P. Campbell, E. Birney, D. F. Easton, G. Chenevix-Trench, M. H. Tan, S. K. Khoo, B. T. Teh, S. T. Yuen, S. Y. Leung, R. Wooster, P. A. Futreal and M. R. Stratton (2007). "Patterns of somatic mutation in human cancer genomes." Nature **446**(7132): 153-158.

Halazonetis, T. D., V. G. Gorgoulis and J. Bartek (2008). "An oncogene-induced DNA damage model for cancer development." Science **319**(5868): 1352-1355.

Hanahan, D. and R. A. Weinberg (2011). "Hallmarks of cancer: the next generation." Cell **144**(5): 646-674.

Hauge, S., C. Naucke, G. Hasvold, M. Joel, G. E. Rodland, P. Juzenas, T. Stokke and R. G. Syljuasen (2017). "Combined inhibition of Wee1 and Chk1 gives synergistic DNA damage in S-phase due to distinct regulation of CDK activity and CDC45 loading." Oncotarget **8**(7): 10966-10979.

Jin, J., H. Fang, F. Yang, W. Ji, N. Guan, Z. Sun, Y. Shi, G. Zhou and X. Guan (2018). "Combined Inhibition of ATR and WEE1 as a Novel Therapeutic Strategy in Triple-Negative Breast Cancer." Neoplasia **20**(5): 478-488.

Kabeche, L., H. D. Nguyen, R. Buisson and L. Zou (2018). "A mitosis-specific and R loop-driven ATR pathway promotes faithful chromosome segregation." Science **359**(6371): 108-114.

Kibe, T., M. Zimmermann and T. de Lange (2016). "TPP1 Blocks an ATR-Mediated Resection Mechanism at Telomeres." Mol Cell **61**(2): 236-246.

Kondo, M., I. L. Weissman and K. Akashi (1997). "Identification of clonogenic common lymphoid progenitors in mouse bone marrow." Cell **91**(5): 661-672.

Kotsantis, P., E. Petermann and S. J. Boulton (2018). "Mechanisms of Oncogene-Induced Replication Stress: Jigsaw Falling into Place." Cancer Discov.

Lecona, E. and O. Fernandez-Capetillo (2014). "Replication stress and cancer: it takes two to tango." Exp Cell Res **329**(1): 26-34.

Lewis, C. W., Z. Jin, D. Macdonald, W. Wei, X. J. Qian, W. S. Choi, R. He, X. Sun and G. Chan (2017). "Prolonged mitotic arrest induced by Wee1 inhibition sensitizes breast cancer cells to paclitaxel." Oncotarget **8**(43): 73705-73722.

Luo, J., N. L. Solimini and S. J. Elledge (2009). "Principles of cancer therapy: oncogene and non-oncogene addiction." Cell **136**(5): 823-837.

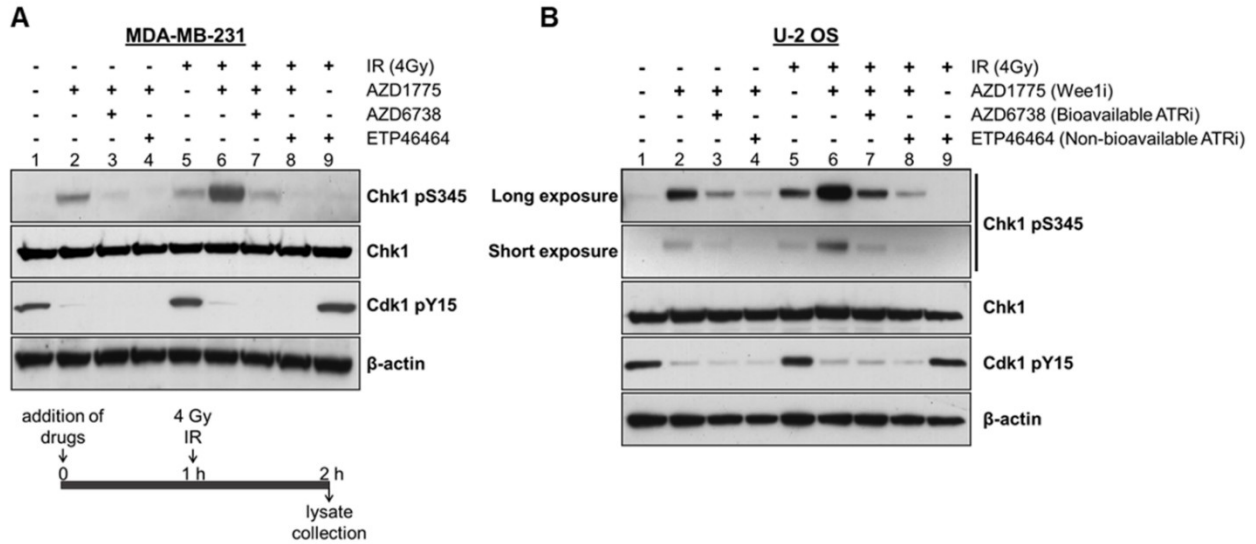
Malumbres, M. and M. Barbacid (2005). "Mammalian cyclin-dependent kinases." Trends Biochem Sci **30**(11): 630-641.

Matheson, C. J., D. S. Backos and P. Reigan (2016). "Targeting WEE1 Kinase in Cancer." Trends Pharmacol Sci **37**(10): 872-881.

- Mohrin, M., E. Bourke, D. Alexander, M. R. Warr, K. Barry-Holson, M. M. Le Beau, C. G. Morrison and E. Passegue (2010). "Hematopoietic stem cell quiescence promotes error-prone DNA repair and mutagenesis." Cell Stem Cell **7**(2): 174-185.
- Nam, E. A., R. Zhao, G. G. Glick, C. E. Bansbach, D. B. Friedman and D. Cortez (2011). "Thr-1989 phosphorylation is a marker of active ataxia telangiectasia-mutated and Rad3-related (ATR) kinase." J Biol Chem **286**(33): 28707-28714.
- O'Driscoll, M., V. L. Ruiz-Perez, C. G. Woods, P. A. Jeggo and J. A. Goodship (2003). "A splicing mutation affecting expression of ataxia-telangiectasia and Rad3-related protein (ATR) results in Seckel syndrome." Nat Genet **33**(4): 497-501.
- O'Neil, N. J., M. L. Bailey and P. Hieter (2017). "Synthetic lethality and cancer." Nat Rev Genet **18**(10): 613-623.
- Parikh, R. A., L. J. Appleman, J. E. Bauman, M. Sankunny, D. W. Lewis, A. Vlad and S. M. Gollin (2014). "Upregulation of the ATR-CHEK1 pathway in oral squamous cell carcinomas." Genes Chromosomes Cancer **53**(1): 25-37.
- Reaper, P. M., M. R. Griffiths, J. M. Long, J. D. Charrier, S. Maccormick, P. A. Charlton, J. M. Golec and J. R. Pollard (2011). "Selective killing of ATM- or p53-deficient cancer cells through inhibition of ATR." Nat Chem Biol **7**(7): 428-430.
- Ren, L., L. Chen, W. Wu, L. Garribba, H. Tian, Z. Liu, I. Vogel, C. Li, I. D. Hickson and Y. Liu (2017). "Potential biomarkers of DNA replication stress in cancer." Oncotarget **8**(23): 36996-37008.
- Saldivar, J. C., S. Hamperl, M. J. Bocek, M. Chung, T. E. Bass, F. Cisneros-Soberanis, K. Samejima, L. Xie, J. R. Paulson, W. C. Earnshaw, D. Cortez, T. Meyer and K. A. Cimprich (2018). "An intrinsic S/G2 checkpoint enforced by ATR." Science **361**(6404): 806-810.
- Santamaria, D., C. Barriere, A. Cerqueira, S. Hunt, C. Tardy, K. Newton, J. F. Caceres, P. Dubus, M. Malumbres and M. Barbacid (2007). "Cdk1 is sufficient to drive the mammalian cell cycle." Nature **448**(7155): 811-815.
- Sausville, E., P. Lorusso, M. Carducci, J. Carter, M. F. Quinn, L. Malburg, N. Azad, D. Cosgrove, R. Knight, P. Barker, S. Zabludoff, F. Agbo, P. Oakes and A. Senderowicz (2014). "Phase I dose-escalation study of AZD7762, a checkpoint kinase inhibitor, in combination with gemcitabine in US patients with advanced solid tumors." Cancer Chemother Pharmacol **73**(3): 539-549.
- Schwartz, M., E. Zlotorynski, M. Goldberg, E. Ozeri, A. Rahat, C. le Sage, B. P. Chen, D. J. Chen, R. Agami and B. Kerem (2005). "Homologous recombination and nonhomologous end-joining repair pathways regulate fragile site stability." Genes Dev **19**(22): 2715-2726.
- Seto, T., T. Esaki, F. Hirai, S. Arita, K. Nosaki, A. Makiyama, T. Kometani, C. Fujimoto, M. Hamatake, H. Takeoka, F. Agbo and X. Shi (2013). "Phase I, dose-escalation study of AZD7762 alone and in combination with gemcitabine in Japanese patients with advanced solid tumours." Cancer Chemother Pharmacol **72**(3): 619-627.
- Shaner, N. C., R. E. Campbell, P. A. Steinbach, B. N. Giepmans, A. E. Palmer and R. Y. Tsien (2004). "Improved monomeric red, orange and yellow fluorescent proteins derived from *Discosoma* sp. red fluorescent protein." Nat Biotechnol **22**(12): 1567-1572.

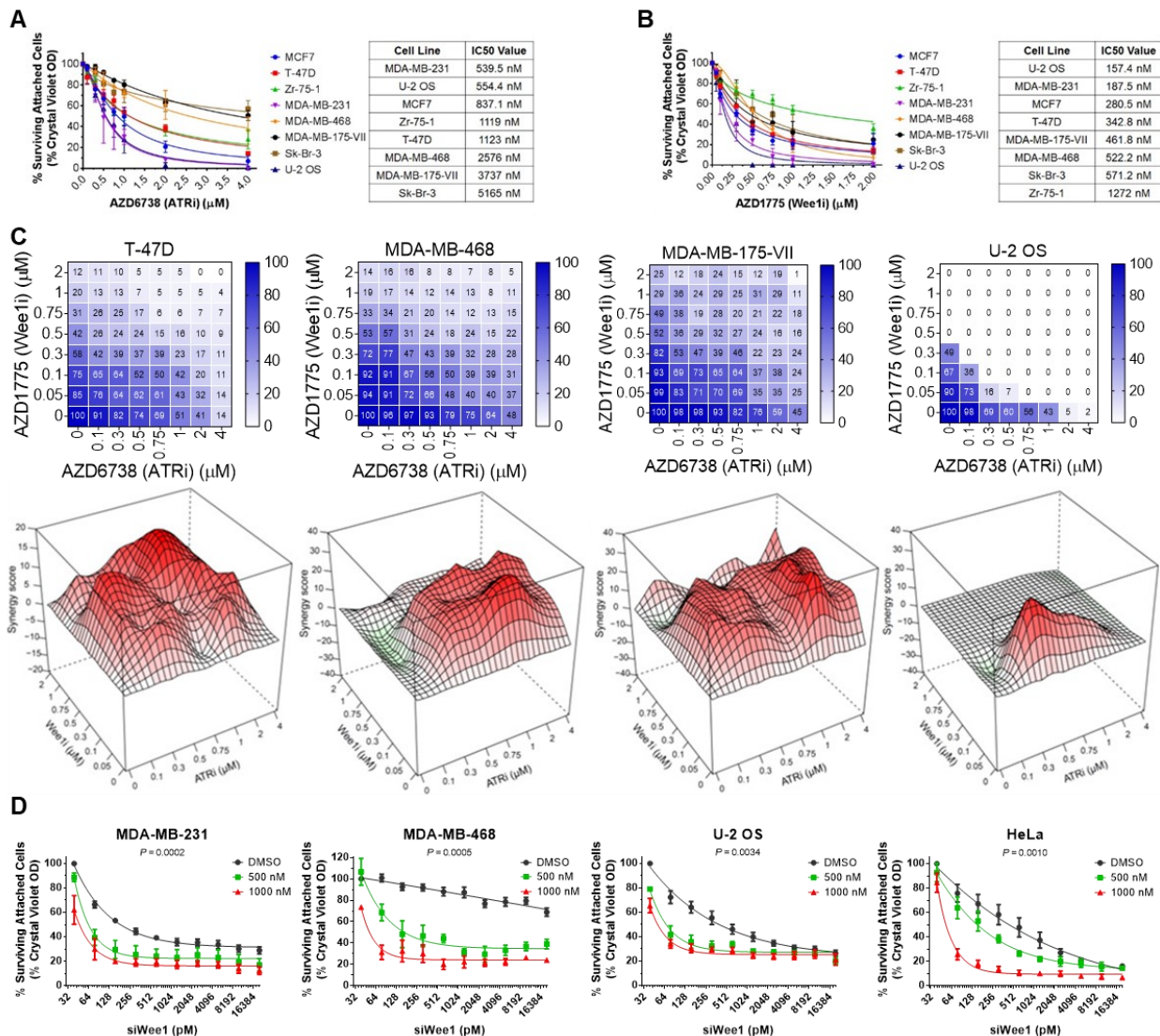
- Stewart, E., S. M. Federico, X. Chen, A. A. Shelat, C. Bradley, B. Gordon, A. Karlstrom, N. R. Twarog, M. R. Clay, A. Bahrami, B. B. Freeman, 3rd, B. Xu, X. Zhou, J. Wu, V. Honnell, M. Ocarz, K. Blankenship, J. Dapper, E. R. Mardis, R. K. Wilson, J. Downing, J. Zhang, J. Easton, A. Pappo and M. A. Dyer (2017). "Orthotopic patient-derived xenografts of paediatric solid tumours." Nature **549**(7670): 96-100.
- Surova, O. and B. Zhivotovsky (2013). "Various modes of cell death induced by DNA damage." Oncogene **32**(33): 3789-3797.
- Techer, H., S. Koundrioukoff, S. Carignon, T. Wilhelm, G. A. Millot, B. S. Lopez, O. Brison and M. Debatisse (2016). "Signaling from Mus81-Eme2-Dependent DNA Damage Elicited by Chk1 Deficiency Modulates Replication Fork Speed and Origin Usage." Cell Rep **14**(5): 1114-1127.
- Telford, W. G., J. Bradford, W. Godfrey, R. W. Robey and S. E. Bates (2007). "Side population analysis using a violet-excited cell-permeable DNA binding dye." Stem Cells **25**(4): 1029-1036.
- Toledo, C. M., Y. Ding, P. Hoellerbauer, R. J. Davis, R. Basom, E. J. Girard, E. Lee, P. Corrin, T. Hart, H. Bolouri, J. Davison, Q. Zhang, J. Hardcastle, B. J. Aronow, C. L. Plaisier, N. S. Baliga, J. Moffat, Q. Lin, X. N. Li, D. H. Nam, J. Lee, S. M. Pollard, J. Zhu, J. J. Delrow, B. E. Clurman, J. M. Olson and P. J. Paddison (2015). "Genome-wide CRISPR-Cas9 Screens Reveal Loss of Redundancy between PKMYT1 and WEE1 in Glioblastoma Stem-like Cells." Cell Rep **13**(11): 2425-2439.
- Toledo, L. I., M. Altmeyer, M. B. Rask, C. Lukas, D. H. Larsen, L. K. Povlsen, S. Bekker-Jensen, N. Mailand, J. Bartek and J. Lukas (2013). "ATR prohibits replication catastrophe by preventing global exhaustion of RPA." Cell **155**(5): 1088-1103.
- Toledo, L. I., M. Murga, R. Zur, R. Soria, A. Rodriguez, S. Martinez, J. Oyarzabal, J. Pastor, J. R. Bischoff and O. Fernandez-Capetillo (2011). "A cell-based screen identifies ATR inhibitors with synthetic lethal properties for cancer-associated mutations." Nat Struct Mol Biol **18**(6): 721-727.
- Vassilopoulos, A., Y. Tominaga, H. S. Kim, T. Lahusen, B. Li, H. Yu, D. Gius and C. X. Deng (2015). "WEE1 murine deficiency induces hyper-activation of APC/C and results in genomic instability and carcinogenesis." Oncogene **34**(23): 3023-3035.
- Visconti, R., R. Della Monica, L. Palazzo, F. D'Alessio, M. Raia, S. Improta, M. R. Villa, L. Del Vecchio and D. Grieco (2015). "The Fcp1-Wee1-Cdk1 axis affects spindle assembly checkpoint robustness and sensitivity to antimicrotubule cancer drugs." Cell Death Differ **22**(9): 1551-1560.
- Visconti, R., L. Palazzo, R. Della Monica and D. Grieco (2012). "Fcp1-dependent dephosphorylation is required for M-phase-promoting factor inactivation at mitosis exit." Nat Commun **3**: 894.
- Vitale, I., G. Manic, R. De Maria, G. Kroemer and L. Galluzzi (2017). "DNA Damage in Stem Cells." Mol Cell **66**(3): 306-319.
- Withers, H. R. (1971). "Regeneration of intestinal mucosa after irradiation." Cancer **28**(1): 75-81.

2.8 Supplementary information



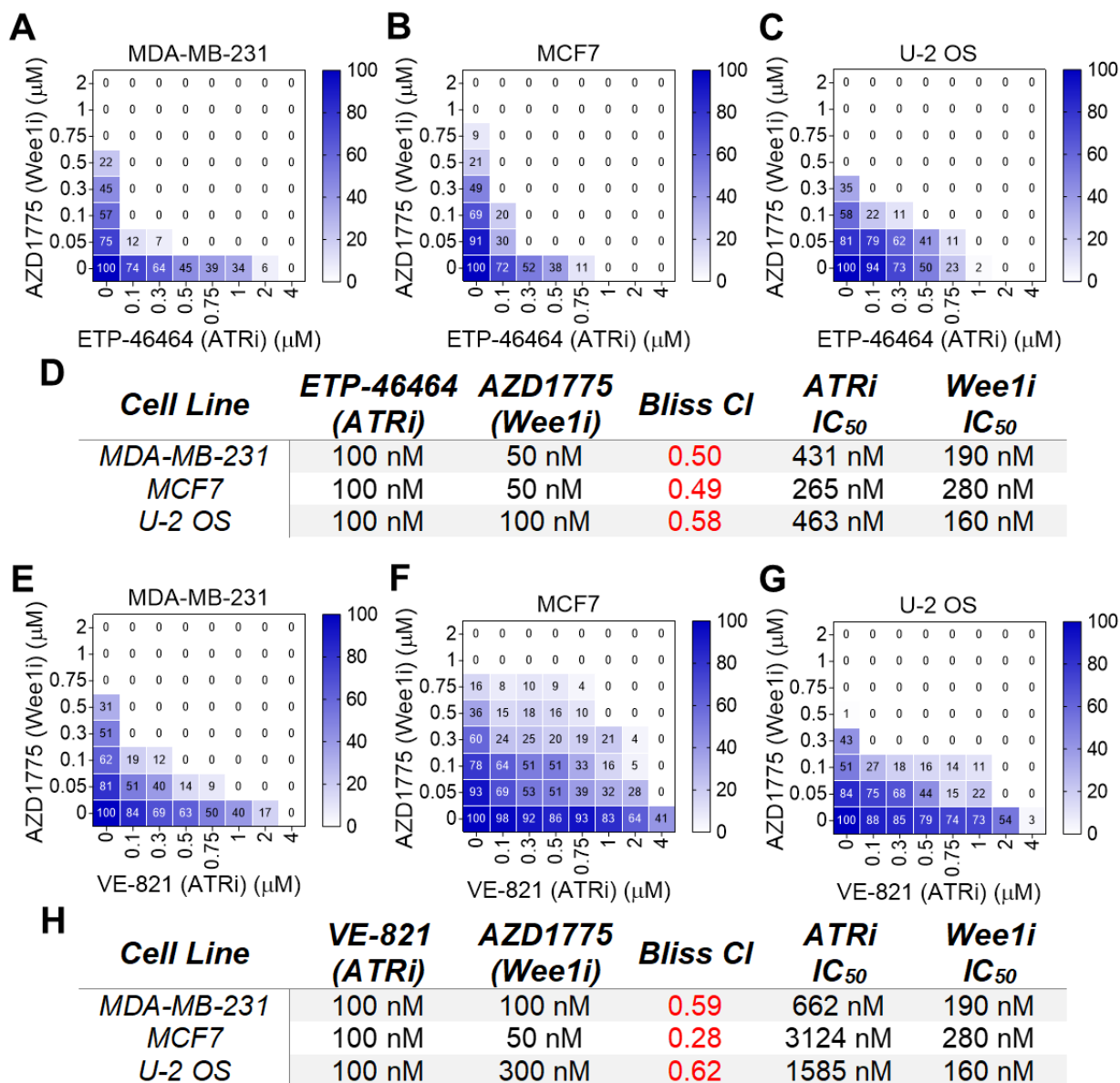
Supplementary Figure 2.1. Wee1 inhibition activates ATR.

MDA-MB-231 (A) and U-2 OS (B) cells were incubated with the indicated inhibitors. After 1 hour cells were irradiated with 4 Gy or mock treated. After another hour cell lysates were harvested and probed for Chk1 and CDK1 phosphorylation by immunoblotting. Inhibition of Wee1 by AZD1775 leads to activation of ATR (see decrease in phospho-CDK1 levels and increase in phospho-Chk1 in lane 2). AZD6738 and ETP46464 are selective ATR inhibitors. DNA damaging agents such as ionizing radiation (IR) can combine with Wee1 inhibition in activating ATR. Figure 2.1A is a subset of this figure derived from the same experiment.



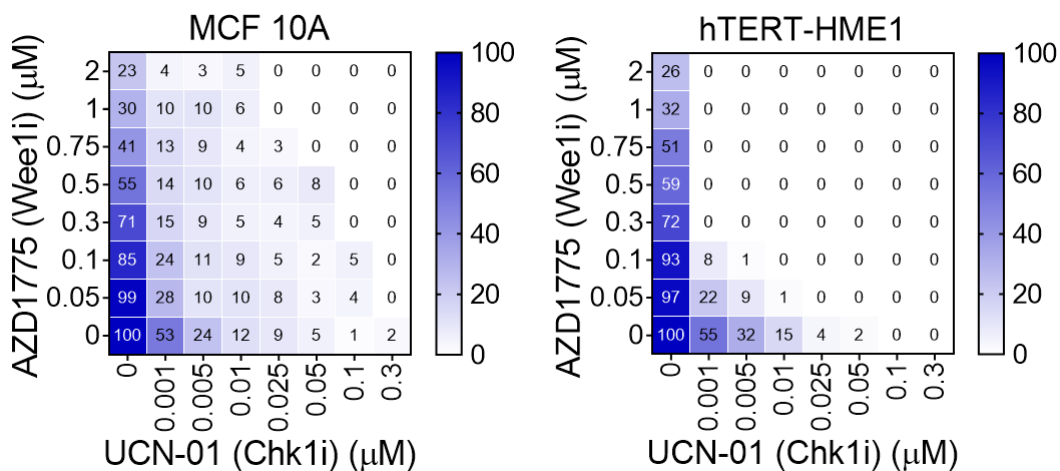
Supplementary Figure 2.2. Wee1 and ATR inhibition synergistically kills cancer cells.

(A) IC₅₀ values for AZD6738 in cancer cells. Cells were treated for 4 days with up to 4 µM AZD6738 and survival was assayed by Crystal Violet staining. (B) IC₅₀ values for AZD1775 in cancer cells. Four day survival relative to control was measured like in (A). (C) Synergistic killing of cancer cells by AZD6738 and AZD1775. Cooperative cell killing was measured by treating cells with the indicated drug concentrations or vehicle control. Color bars indicate % survival normalized to vehicle treated cells. Representative cooperativity screens and Loewe plots for drug cooperativity are shown. Bliss combination indices (CI) at indicated drug concentrations are shown in Table 1. (D) Cooperative cell killing by Wee1 knockdown and ATR inhibition. Control or cells treated with AZD6738 at indicated concentrations were transfected with increasing doses of siRNA against Wee1 and assayed for viability after 4 days by Crystal Violet staining as described (Lewis *et al.* 2017). Statistical analysis was performed using two-way ANOVA.



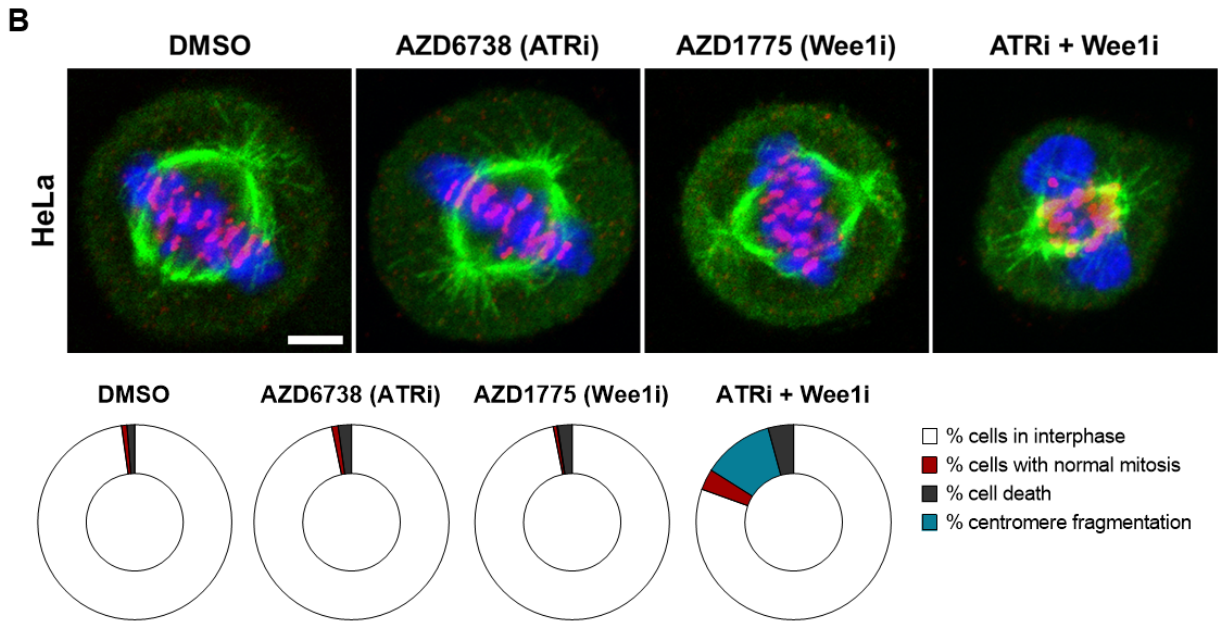
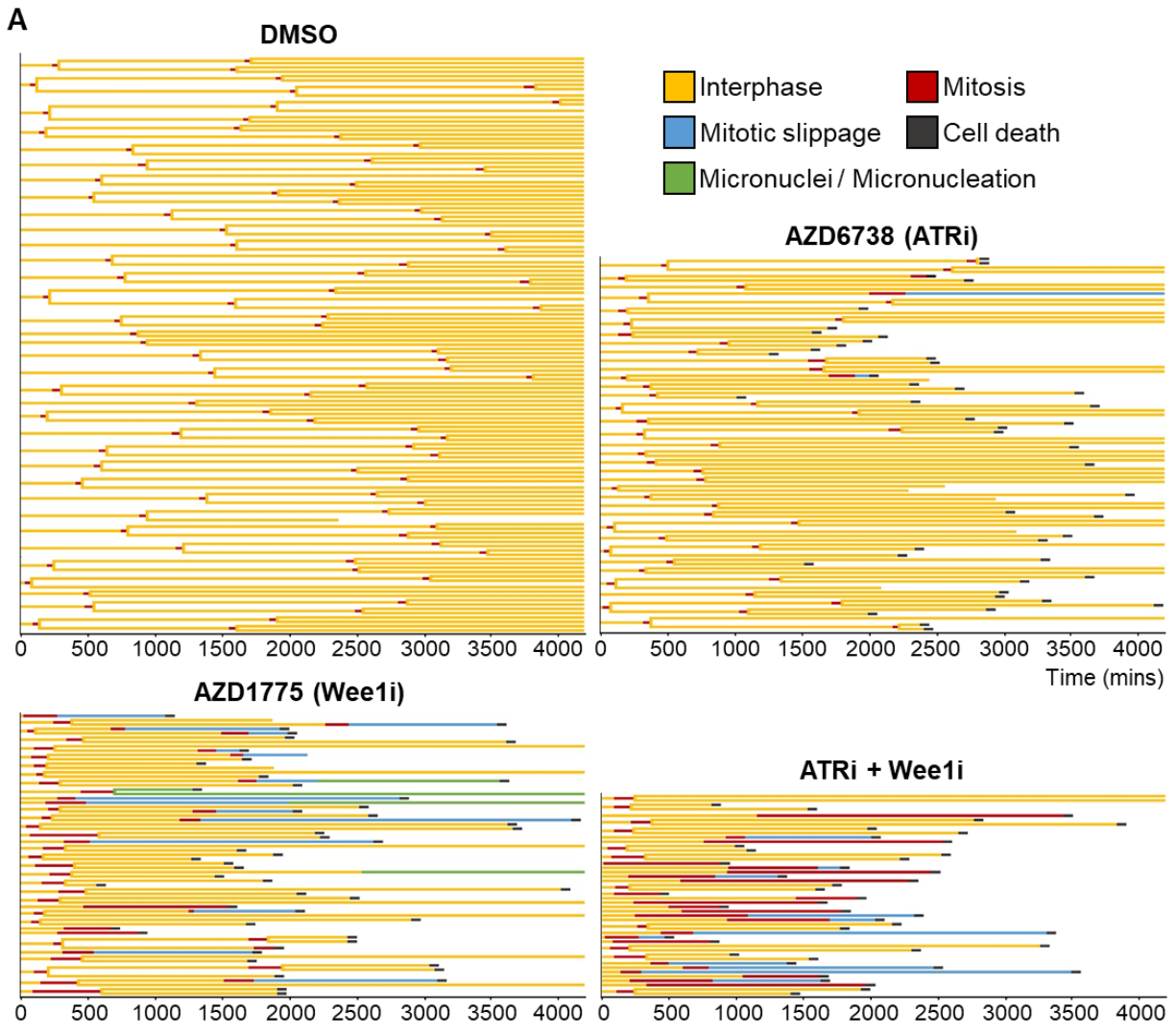
Supplementary Figure 2.3. Wee1 and ATR inhibition synergistically kills cancer cells.

(A-C) Synergistic killing of cancer cells by ETP-46464 and AZD1775. Cooperative cell killing was measured by treating cells with the indicated drug concentrations or vehicle control. Color bars indicate % survival normalized to vehicle treated cells. (D) Table shows Bliss combination indices (CI) at indicated drug concentration. (E-G) Plots show synergistic killing of cancer cells by VE-821 and AZD1775. (H) Table shows Bliss CI at indicated drug concentrations.



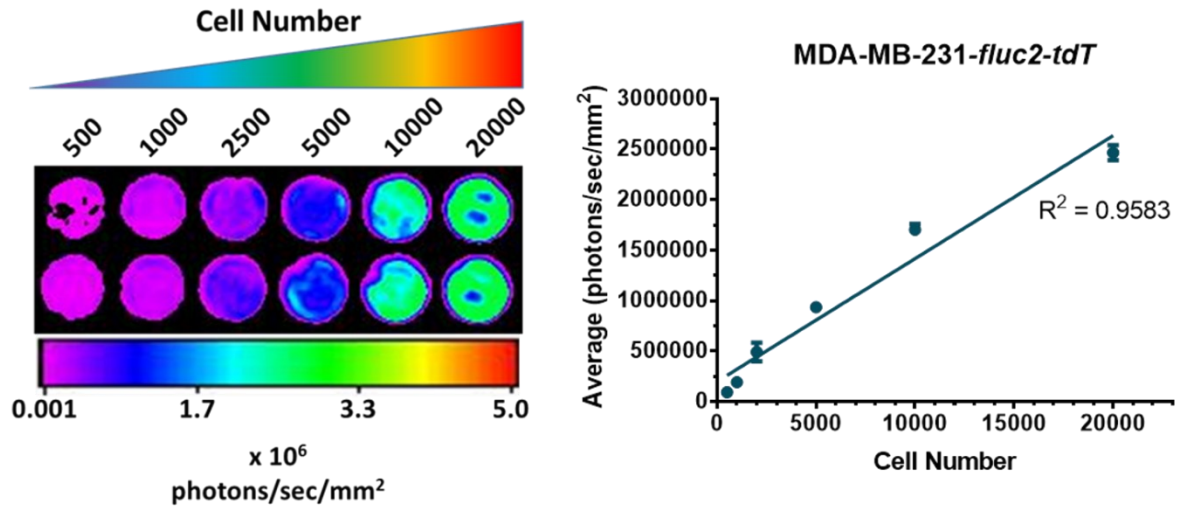
Supplementary Figure 2.4. The Chk1 inhibitor UCN-01 is highly toxic in MCF10A and hTERT-HME1, alone and in combination with AZD1775.

Synergistic killing of “normal” cells by UCN-01 and AZD1775. Cooperative cell killing was measured by treating cells with the indicated drug concentrations or vehicle control. Color bars indicate % survival normalized to vehicle treated cells. Representative cooperativity screens are shown.



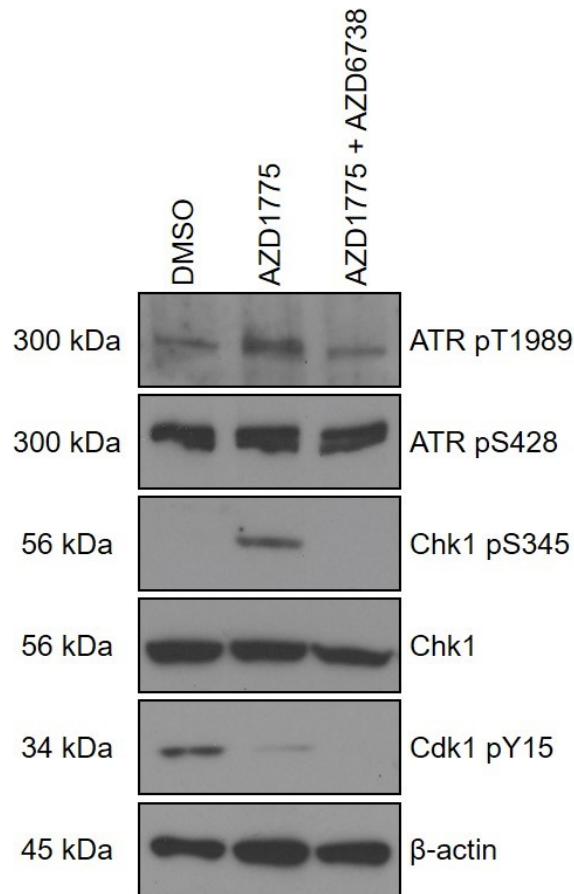
Supplementary Figure 2.5. Combined ATR and Wee1 inhibition leads to mitotic defects and cancer cell death.

(A) Representative fates of MDA-MB-231 cells ($n = 35$) in the 4 treatment groups. (B) Representative images of mitotic HeLa cells treated with ATR and/or Wee1 inhibitor (ATR_i = 1 μ M AZD6738, Wee1_i = 0.3 μ M AZD1775). Fixed cells were stained for centromeres (red) and tubulin (green) by immunofluorescence and for DNA with DAPI (blue). Drug-induced clustering of centromeres spatially separated from the main mass of chromosome, a feature of centromere fragmentation, is clearly visible. Quantification of cells ($n > 1000$) fixed 4 h after release from a double thymidine block in the presence of the indicated inhibitors, that are in mitosis (red and blue) and display centromere fragmentation (blue).



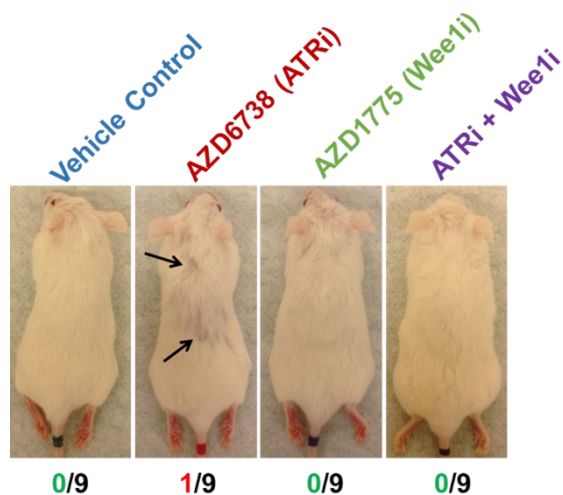
Supplementary Figure 2.6. Quantification of photon flux for MDA-MB-231-fluc2-tdTomato cells *in vitro*.

Increasing numbers of cells were plated, D-luciferin was added, and images were taken using the Bruker In-Vivo Xtreme optical imager to measure linearity of the signal.



Supplementary Figure 2.7. ATR phosphorylation at T1989 is a marker of ATR activation.

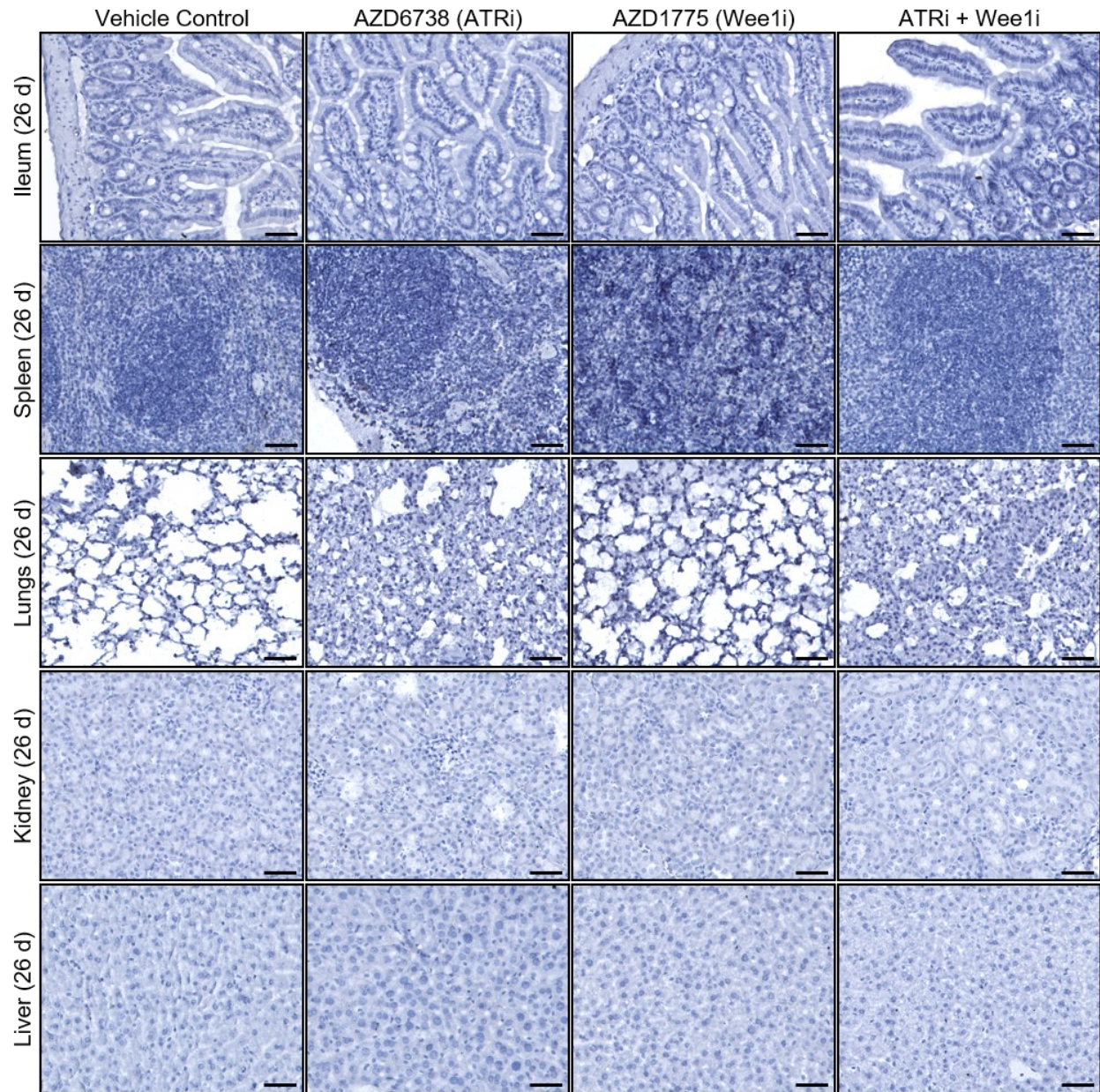
MDA-MB-231 cells were treated for 24 h with AZD1775 (300 nM), AZD1775 combined with AZD6738 (1 μ M), or vehicle control (DMSO) before harvesting and analysing their lysates by immunoblotting. Unlike phosphorylation of ATR at Serine 428, phosphorylation at Threonine 1989 correlates with the phosphorylation of Chk1 at Serine 345, indicating that the phosphorylation status of ATR T1989 can be used as biomarker for ATR activation in agreement with Nam *et al.* (Nam *et al.* 2011).



Supplementary Figure 2.8. Hair growth changes in mice treated with ATR and/or Wee1 inhibitors.

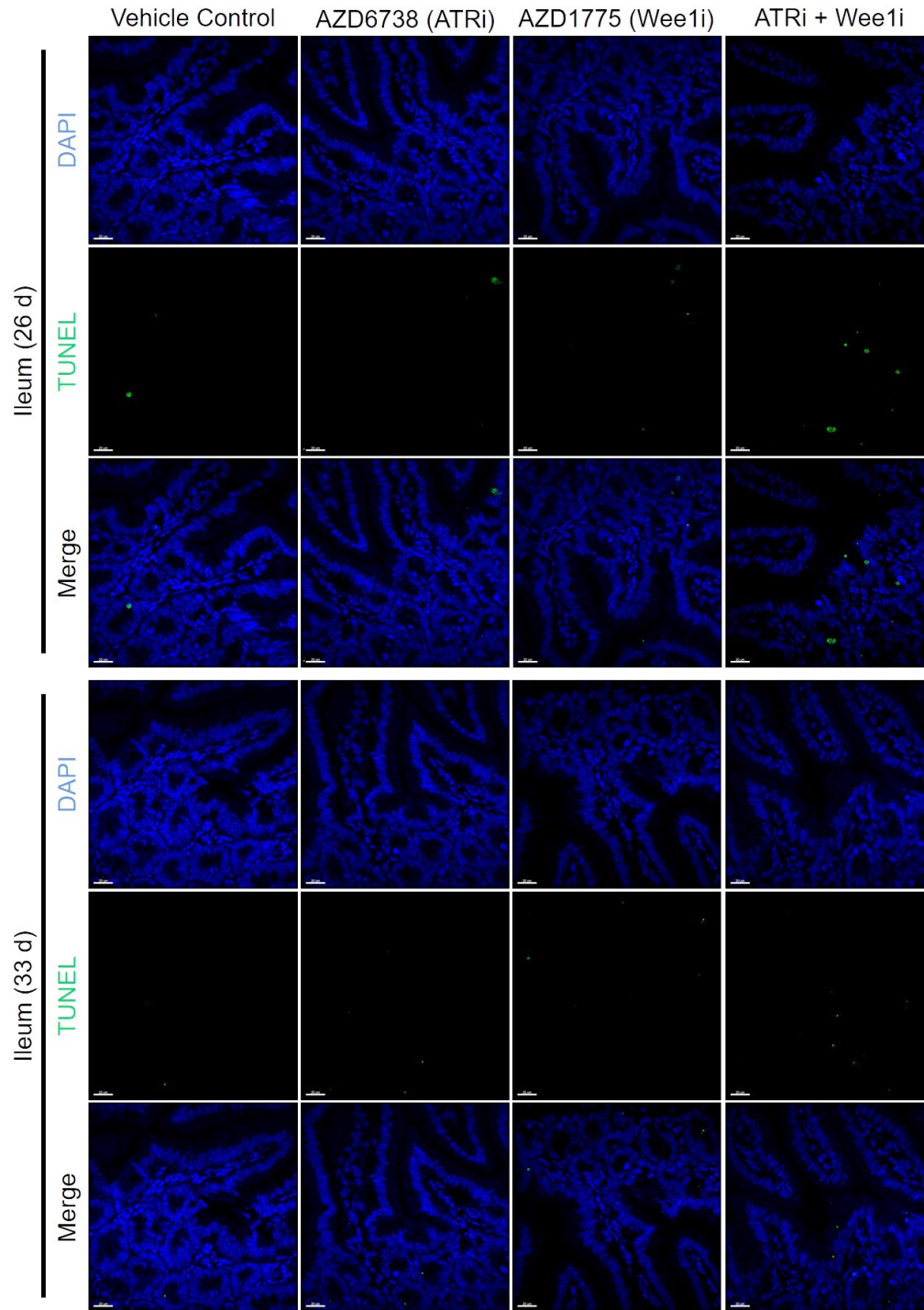
Tumor-bearing NSG mice were randomly assigned to treatment groups and treated for 26 days with 25 mg/kg AZD6738 and/or 60 mg/kg AZD1775 daily for longitudinal studies as described later in Figure 2.14 A-E. Only one mouse (depicted) showed signs of partial hair loss.

None of the NSG mice (n = 4 per cohort) used for experiments described in Figure 2.14F-H or C57BL/6 mice used in experiments described in Figure 2.12C showed any signs of hair loss, despite being treated 26 days with 25 mg/kg AZD6738 and/or 60 mg/kg AZD1775 per diem.

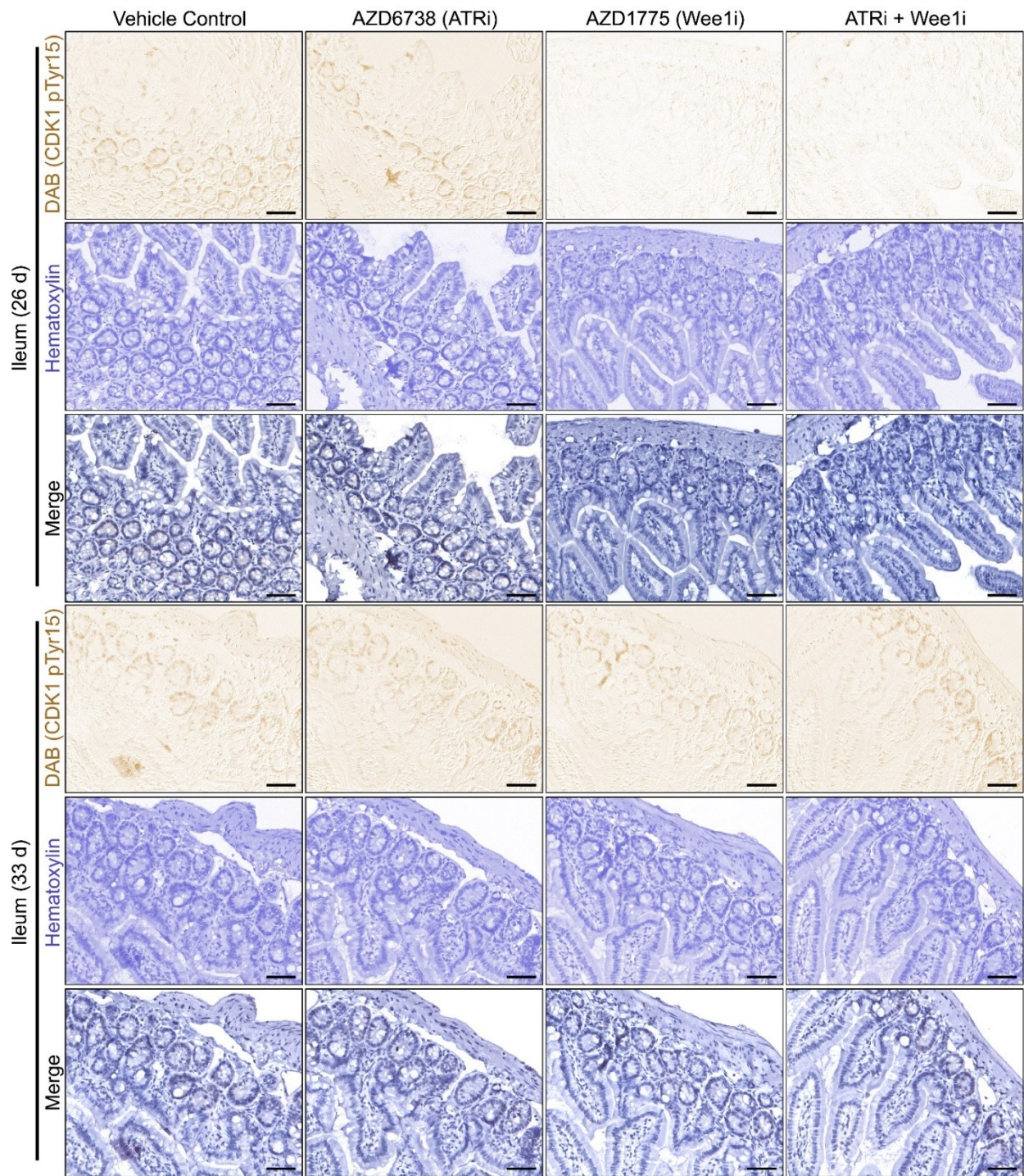


Supplementary Figure 2.9. Immunohistochemistry evaluation of ATR pThr1989 levels in normal tissues of NSG mice.

Figure shows immunohistochemical evaluation of ATR pThr1989 levels in normal tissues of NSG mice with or without treatment with ATR and/or Wee1 inhibitors for 26 days. Scale = 25 μ m

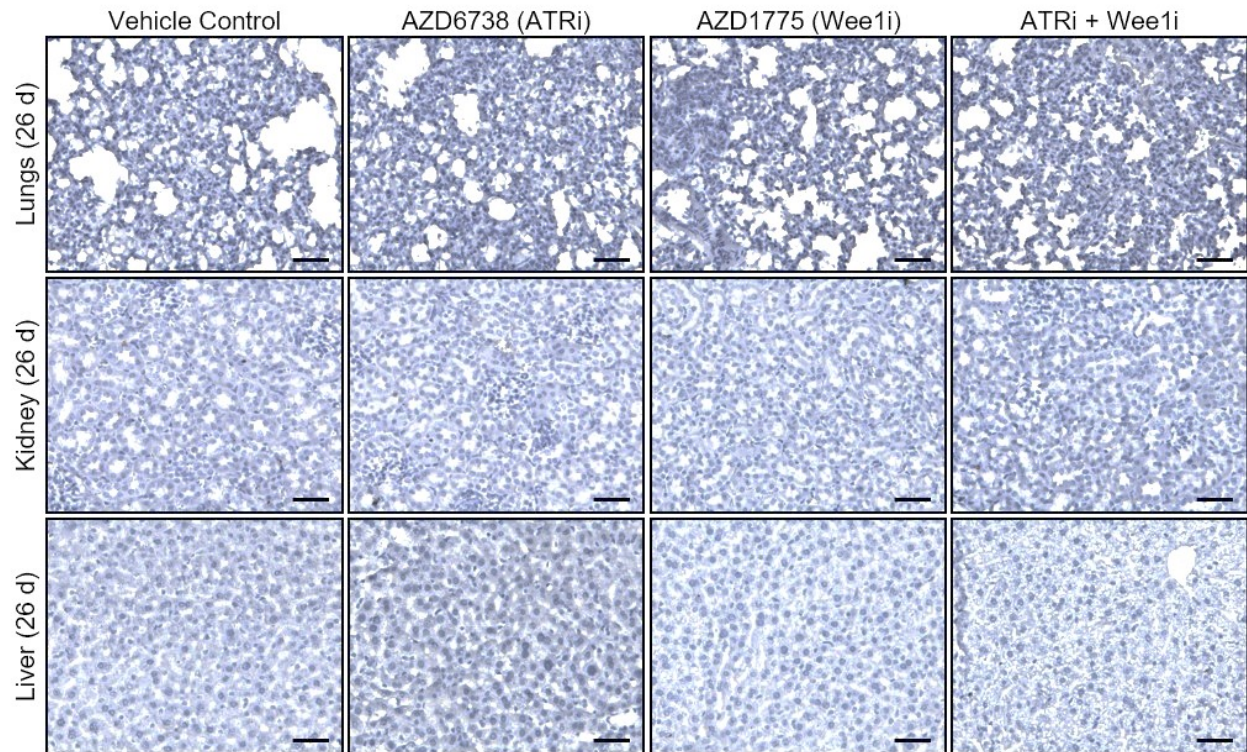


Supplementary Figure 2.10. Evaluation of apoptotic cells by TUNEL assay in ileum. Evaluation of apoptotic cells by TUNEL assay in ileum at 26- and 33-day time points post-treatment with ATR and/or Wee1 inhibitors. Scale = 20 μ m.



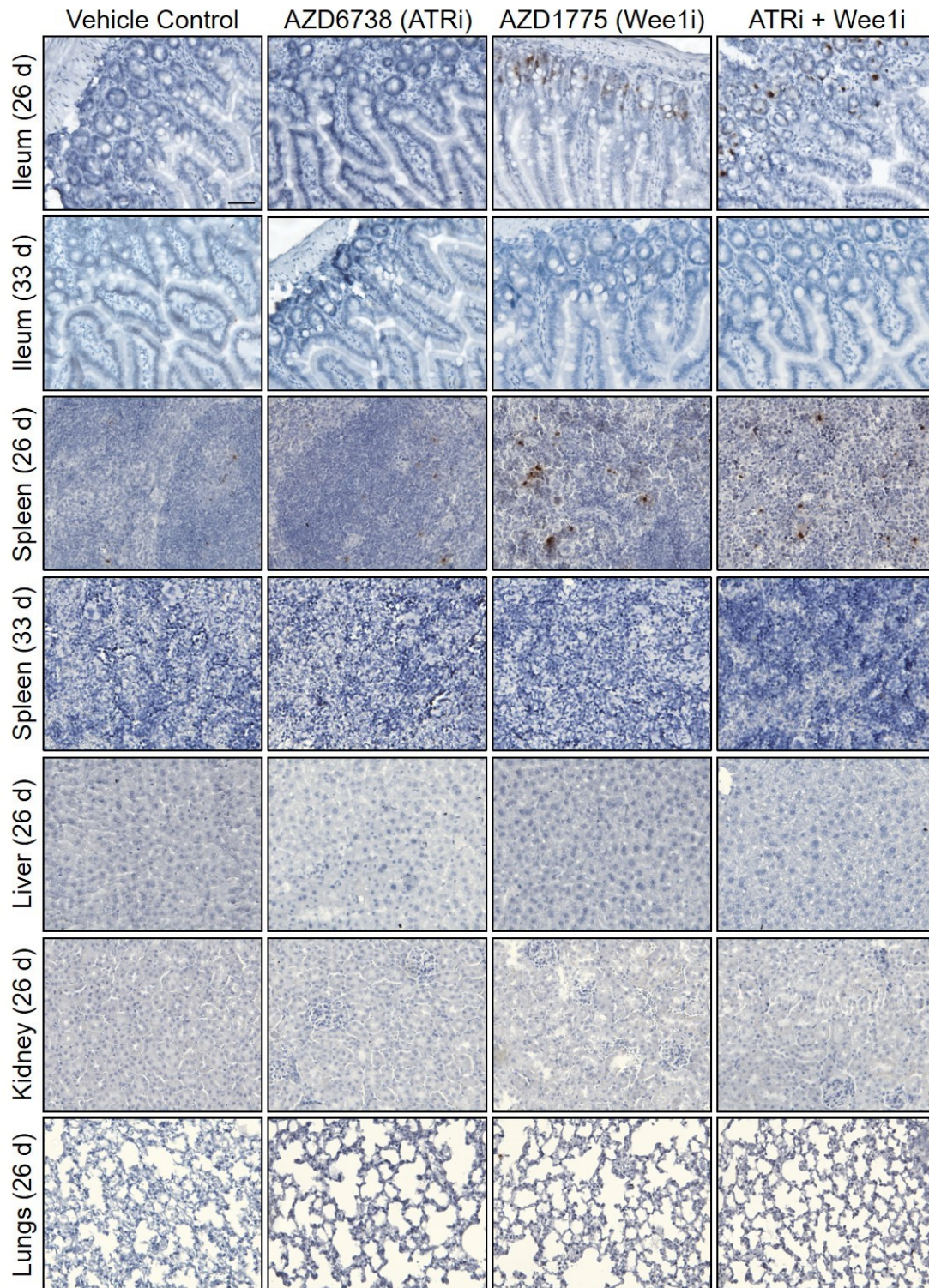
Supplementary Figure 2.11. Immunohistochemistry evaluation of CDK1 pTyr15 levels.

Immunohistochemistry evaluation of CDK1 pTyr15 levels in Ileum of NSG mice at 26- and 33-days post-treatment with ATR and/or Wee1 inhibitors. Scale = 25 μ m.



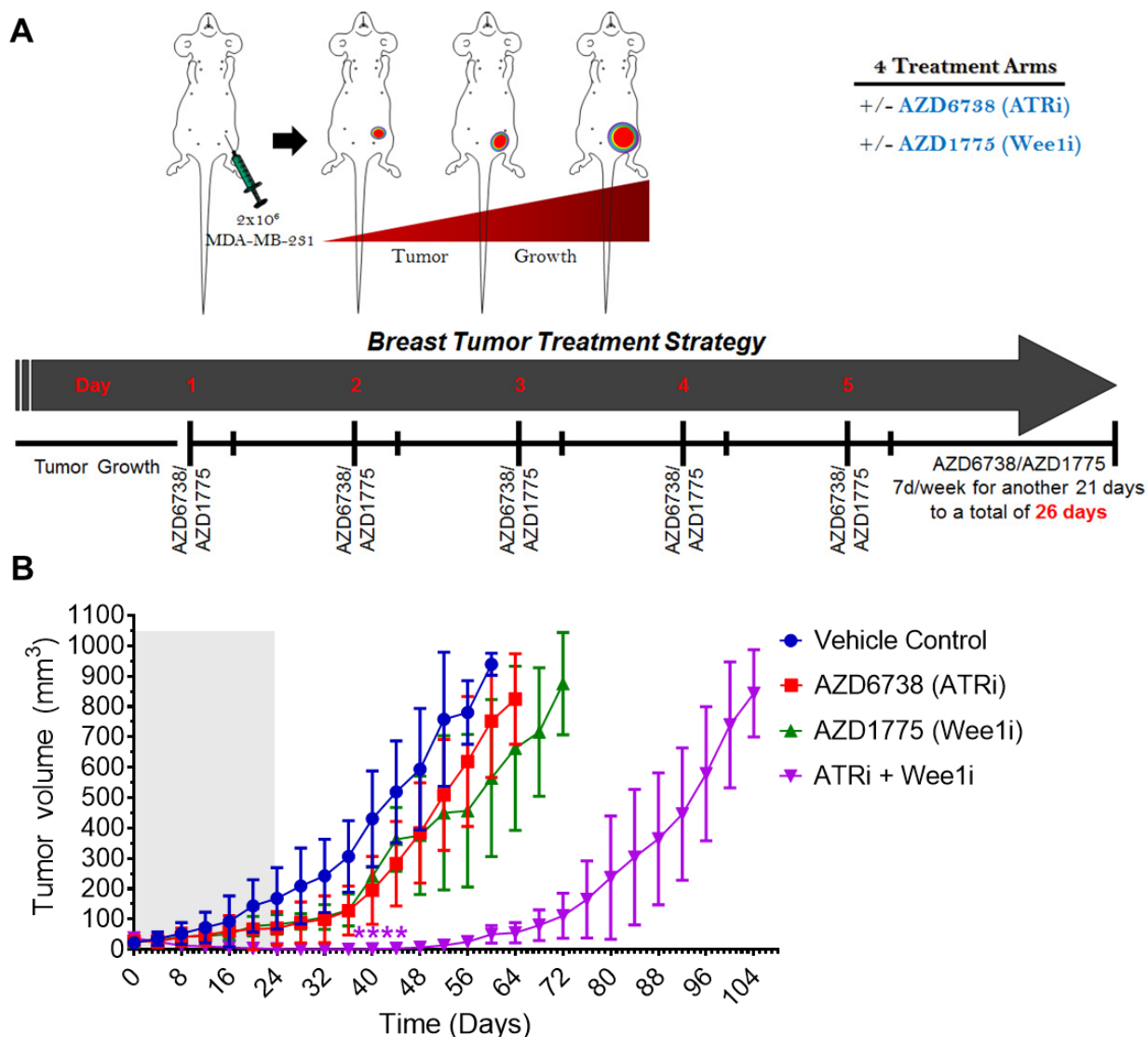
Supplementary Figure 2.12. Immunohistochemistry evaluation of CDK1 pTyr15 in other normal tissues.

Immunohistochemistry evaluation of CDK1 pTyr15 in normal tissue of NSG mice 26 days post-treatment with ATR and/or Wee1 inhibitors. Scale = 25 μ m.



Supplementary Figure 2.13. Immunohistochemistry evaluation of γ H2AX staining in normal tissue.

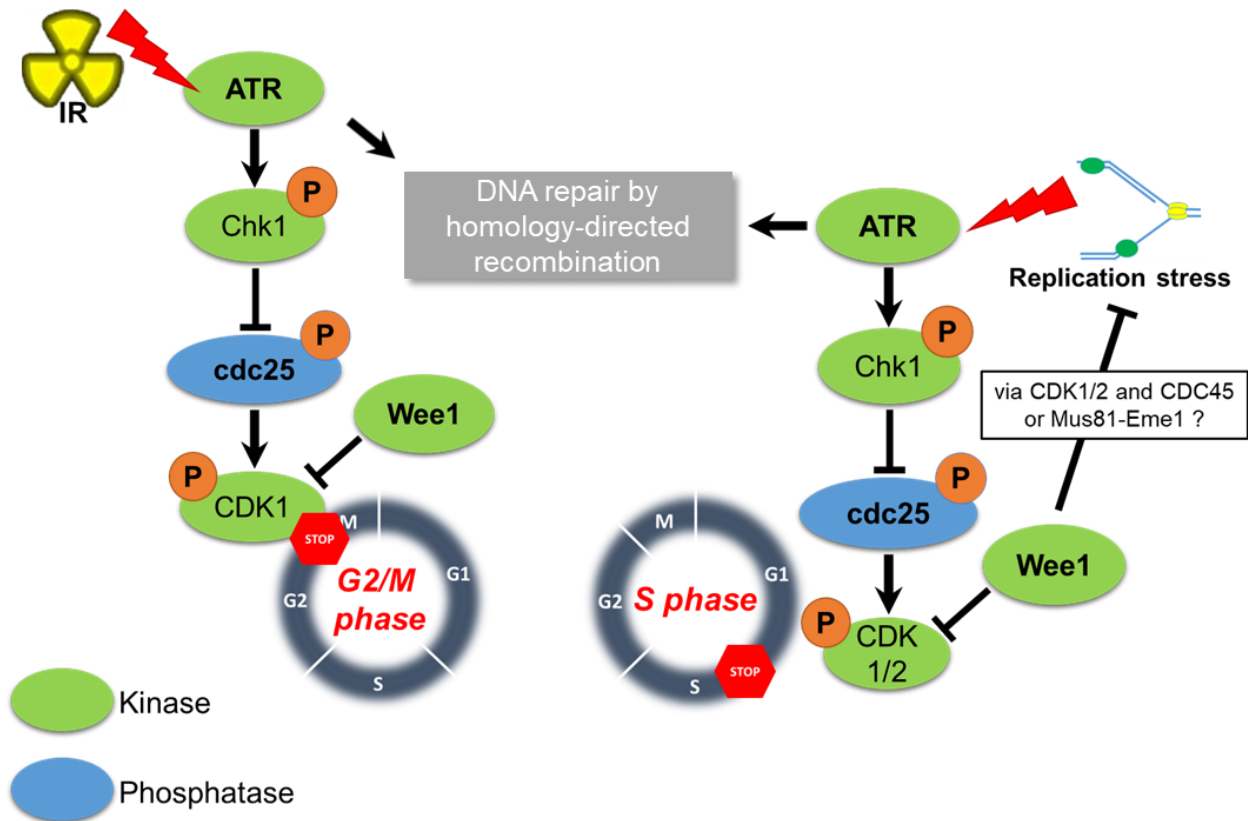
Immunohistochemistry evaluation of γ H2AX staining in normal tissue of C57BL/6 mice 26 days post-treatment with ATR and/or Wee1 inhibitors. Scale = 25 μ m.



Supplementary Figure 2.14. Longitudinal studies of tumor-bearing mice treated with ATR and Wee1 inhibitors.

(A) Treatment plan. NSG mice were injected with MDA-MB-231-*fluc2-tdTomato* labelled breast cancer cells in an orthotopic xenograft mouse model, randomly assigned to treatment groups when tumors reached 40-50 mm^3 and treated for 26 days with 25 mg/kg AZD6738 and/or 60 mg/kg AZD1775. (B) Tumor growth of mice in the four treatment arms ($n = 9$). The shaded area indicates duration of the treatment.

Checkpoint signaling by ATR and Wee1



Supplementary Figure 2.15. G2/M and S phase checkpoint regulation by ATR and Wee1.

The activity of the cyclin-dependent kinases CDK1 and CDK2 regulates the G2/M and S phase cell cycle checkpoints. Besides by binding to the appropriate cyclins (not shown), the activity of these CDKs is regulated by their phosphorylation state, which in turn is determined by the protein kinase Wee1 and the counter-acting protein phosphatase cdc25.

Activation of ATR by RPA-coated single-stranded DNA, structures resulting from replication fork uncoupling or resection of DNA double strand breaks (e.g., after ionizing radiation), leads to activating phosphorylation of Chk1 at serines 317 and 345. Chk1 in turn phosphorylates cdc25 leading to cdc25 inhibition and targeting for degradation. ATR activation thus leads to increased phosphorylation and inhibition of CDK1/2. Of note, Wee1 inhibition was reported to increase replication stress, by a still poorly understood mechanism.

ATR also positively regulates homology-directed recombination, an important DNA repair mechanism during S and G2 phase.

HEMATOLOGY									
Sample ID	WBC (x10 ⁹ /L)	RBC (x10 ¹² /L)	Hemoglobin (g/L)	Hematocrit (L/L)	MCV (fl)	MCF (pg)	MCHC (g/L)	RDW (%CV)	Platelets (x10 ⁹ /L)
Vehicle Control (26 d)	2.55±0.6	10.75±0.6	167±12	0.48±0.01	44.45±1.4	15.5±0.28	349±18	22.7±2.1	904±370
Vehicle Control (33 d)	4.6±1.13	10.75±0.63	167±12	0.48±0.01	44.45±1.48	15.5±0.28	325±2	21.85±0.07	817±540
Vehicle Control (40 d)	4.4±2.26	9.9±0.56	150±7	0.45±0.02	45.65±0.7	15.15±0.2	332±1	21.45±0.7	840±405
AZD6738 (ATRi) (26 d)	6.8±0.28	10.4±1.2	156±15	0.49±0.05	47.9±1.41	15±0.42	314±1	22.35±1.6	524±186
AZD6738 (ATRi) (33 d)	7.75±3.46	9.4±0.28	142±5	0.44±0.007	47.35±1.34	15±0.21	319±14	21±1.13	619±332
AZD6738 (ATRi) (40 d)	7.75±2.3	9.75±0.07	146±1	0.45±0.007	46.6±0.14	15±0.14	321±4	23.4±0.7	513±255
AZD1775 (Wee1i) (26 d)	7.05±2.2	10.6±0.56	160±4	0.51±0.03	48.6±0.7	15.2±0.42	313±13	22.5±0.7	670±190
AZD1775 (Wee1i) (33 d)	4.3±2.5	9.85±0.07	150±1	0.44±0.007	45.5±0.3	15.45±0.35	334±2	21.8±0.42	694±29
AZD1775 (Wee1i) (40 d)	9.4±0.7	10.25±0.63	157±12	0.48±0.03	47.2±0.2	15.3±0.28	324±7	22.75±1.06	763±394
ATRi + Wee1i (26 d)	5±2.4	10.3±0.14	162±2	0.48±0.01	46.15±1.2	15.6±0.14	338±12	22.35±0.07	778±423
ATRi + Wee1i (33 d)	8.6±2.7	10.25±0.63	160±11	0.5±0.03	48.9±0.56	15.65±0.21	319±7	22.1±0.14	1023±365
ATRi + Wee1i (40 d)	9.1±3.1	10.65±0.35	163±6	0.5±0.007	47.45±0.91	15.15±0.21	322±6	22.1±0.14	1085±566

Supplementary Table 2.1. Complete blood count (CBC) analysis of mice treated with ATR and/or Wee1 inhibitors.

Table represents complete blood count (CBC) analysis of C57BL/6 mice treated for 26 days with either vehicle control or AZD6738 (ATRi) or AZD1775 (Wee1i) or combined treatment of AZD6738 and AZD1775 (n = 3 per group). Whole blood samples were collected by cardiac puncture at day 26, 33, and 40. Pathological evaluation revealed no signs of abnormalities.

Sample ID	Neutrophils		Lymphocytes		Monocytes		Eosinophils		Basophils	
	%	abs	%	abs	%	abs	%	Abs	%	abs
Vehicle Control (26 d)	10±2.8	0.25±0.07	87.5±5	2.2±0.6	2.5±2.1	0.3±0.2	0	0	0	0
Vehicle Control (33 d)	5.5±0.7	0.25±0.07	87±7	3.9±0.6	6.5±4.9	0.3±0.2	1±1	0.05±0.07	0	0
Vehicle Control (40 d)	15±11.3	0.8±0.8	77.5±13	3.2±1.2	7±2.8	0.3±0.2	0.3±0.5	0	0	0
AZD6738 (ATRi) (26 d)	8±4.2	0.5±0.3	83±2.8	5.6±0.07	8±1.4	0.5±0.07	1±0	0.1±0	0	0
AZD6738 (ATRi) (33 d)	8±2.1	0.6±0.4	86±1.4	6.6±2.9	5±2.1	0.4±0	1±0.3	0.1±0	0	0
AZD6738 (ATRi) (40 d)	14±4.2	1.2±0.6	81±2.1	6.3±1.7	4±1.4	0.3±0	1±0.3	0.1±0	0	0
AZD1775 (Wee1i) (26 d)	9.5±2.1	0.7±0.1	78.5±1	5.5±1.7	8.5±2.1	0.6±0	3.5±3	0.3±0.2	0	0
AZD1775 (Wee1i) (33 d)	8±1.4	0.4±0.2	81.5±4	3.5±1.9	6±0.7	0.3±0.1	4±1.4	0.2±0.1	0	0
AZD1775 (Wee1i) (40 d)	5.6±0.5	0.6±0.1	81±6	7.6±0.5	7.1±1.2	0.7±0.1	5.7±4.6	0.5±0.4	0	0
ATRi + Wee1i (26 d)	11±2.8	0.6±0.4	78±2.1	3.9±1.8	4±0.7	0.3±0.1	6±0	0.3±0.1	0	0
ATRi + Wee1i (33 d)	11±3.5	0.9±0.2	78±1.4	6.7±2.1	4±0	0.4±0.1	6±2	0.6±0.4	0	0
ATRi + Wee1i (40 d)	11±8.4	0.9±0.4	76±14.1	7.2±3.6	5±0	0.5±0.2	8±5.6	0.7±0.2	0	0

Supplementary Table 2.2. Manual differential analysis of mice treated with ATR and/or Wee1 inhibitors.

Table represents manual differential analysis of C57BL/6 mice treated for 26 days with either vehicle control or AZD6738 (ATRi) or AZD1775 (Wee1i) or combined treatment of AZD6738 and AZD1775 (n = 3 per group) performed by a pathologist at IDEXX laboratories. Whole blood samples were collected by cardiac puncture at day 26, 33, and 40. Pathological evaluation revealed no signs of abnormalities.

Chapter 3: [¹⁸F]-FLT-PET as a Predictive Biomarker for Combined ATR and Wee1 Inhibitor Treatment

3.1 Introduction

The development and clinical use of inhibitors of the DDR are one of the most exciting and impactful advances in cancer therapy. As a leading example, PARP inhibitors have revolutionized the treatment of a range of tumors, particularly of breast cancers with deficiencies in homologous recombination based on mutations in the BRCA1 and BRCA2 genes. The success of PARP inhibitors has heightened the interest in inhibitors of enzymes in the DDR, particularly protein kinases involved in DNA damage signaling, as well as their combination with DNA damaging agents or cell cycle regulators. Recent preclinical and clinical studies have shown the efficacy of DDR inhibitors also in tumors with no known underlying genetic signatures, showcasing the urgency of novel biomarkers for treatment plans based on the principle of targeting the DDR. Of particular interest are non-invasive biomarkers that predict treatment response at an early stage of therapy.

The response to neoadjuvant chemotherapy is typically evaluated by physical examination of gross tumor size estimates and conventional imaging, such as mammography or ultrasonography for breast cancers (Fowler *et al.* 2017). Pre-clinical and clinical research aimed at evaluating chemotherapy response in neoadjuvant settings take advantage of combining imaging techniques with histological findings to measure pathological response, identify potential prognostic biomarkers, and tailor personalized therapies. However, accurate measurement of treatment effectiveness to stratify cancer patients into responders and non-responders remains a challenge in the clinic. Early classification of non-responders may allow exploration of alternative therapies to avoid unnecessary side-effects of ineffective treatments. This requires reliable biomarkers that functionally correlate early treatment-related changes in tumor biology with treatment outcome.

In that regard, imaging of solid tumors by positron emission tomography (PET) imaging has become a widely used tool in the clinic and is accompanied by a continuous development of new PET tracers and new applications for existing ones (Gambhir 2002, Derlin *et al.* 2018). Based on the radiotracer used, PET imaging provides quantifiable data for tracer uptake in the form of standardized uptake values (SUV) as a measure of the various underlying biological processes (Chalkidou *et al.* 2012). PET-based imaging biomarkers allow for non-invasive longitudinal assessment of comprehensive spatial information across the entire tumor and body. For example, the glucose analog [^{18}F]2'-fluoro-2'-deoxyglucose (FDG) is a widely used PET tracer for metabolic imaging to sensitively detect malignant tumors from various origins based on increased glucose uptake and glycolysis of cancer cells (Buck *et al.* 2009, Jensen and Kjaer 2015). However, treatment induced inflammation can reduce the specificity of [^{18}F]-FDG-PET and may result in overestimation of the percentage of the remaining tumor burden (Kubota *et al.* 2006, Bollineni *et al.* 2012, Bollineni *et al.* 2016).

To overcome this pitfall and measure cell proliferation status *in vivo*, Shields and colleagues introduced a [^{18}F] labelled thymidine analog, [^{18}F]3'-deoxy-3'-fluorothymidine (FLT) (Shields *et al.* 1998). [^{18}F]-FLT cellular uptake is mediated *via* the equilibrative nucleoside transporters 1 (ENT1) and deletion of ENT1 in mouse models significantly affects [^{18}F]-FLT tumor and normal tissue uptake (Paproski *et al.* 2010). [^{18}F]-FLT can be incorporated into DNA during DNA synthesis, but due to the lack of a 3' hydroxyl group FLT is a replication chain terminator and incorporated FLT is likely removed by DNA repair enzymes. As the first step of the pyrimidine salvage pathway involves phosphorylation of thymidine by thymidine kinase 1 (TK1), the conversion of the thymidine analogue to [^{18}F]-FLT-monophosphate traps the phosphorylated form inside the cell (Been *et al.* 2004). TK1 is expressed during the S-phase of the

cell cycle and remains inactive in quiescent cells (Munch-Petersen *et al.* 1995, Jagarlamudi and Shaw 2018). [¹⁸F]-FLT uptake was reported to positively correlate with TK1 activity (Sherley and Kelly 1988, Rasey *et al.* 2002) and the tracer uptake was proposed to be a surrogate marker for cell proliferation status (Jensen and Kjaer 2015). To further validate this, several groups have reported a significant correlation between Ki-67 expression – the clinical gold standard for evaluating cell proliferation status – and [¹⁸F]-FLT uptake in many cancers (Francis *et al.* 2003, Chen *et al.* 2005, Choi *et al.* 2005, Richard *et al.* 2011), including those of the breast (Chalkidou *et al.* 2012, Woolf *et al.* 2014, Kostakoglu *et al.* 2015).

In this pre-clinical study, we evaluated the use of changes in [¹⁸F]-FLT uptake as a non-invasive prognostic biomarker to identify early responders to combined AZD6738 (ATRi) and AZD1775 (Wee1i) treatment in a neoadjuvant setting. AZD6738 and AZD1775 are bioavailable inhibitors of the kinases ataxia telangiectasia and Rad3 related (ATR) and Wee1, respectively. ATR is an apical kinase in the DNA damage response, and Wee1 kinase regulates cell cycle progression. By combining inhibition of ATR and Wee1, we recently showed cancer cell-specific synergistic cell killing which resulted in tumor control, metastasis inhibition, and increased overall survival of breast cancer xenograft bearing mice (Bukhari *et al.* 2019). Here, using a syngeneic orthotopic mouse model of triple negative breast cancer, we show that early post-treatment changes in [¹⁸F]-FLT uptake help predict treatment response to combined ATRi and Wee1i neoadjuvant chemotherapy. Furthermore, we evaluated by histology whether the changes in FLT-uptake correlated with Ki-67 expression in tumors. We found a significant reduction in the percentage of Ki-67 positive cells following neoadjuvant chemotherapy. Since AZD6738 and AZD1775 are currently being evaluated in clinical trials as monotherapy agents or in combination with various other genotoxic therapies, our preclinical findings will have direct implications for

future clinical trials to identify patient responders and non-responders to this combination treatment regime. While this study focuses on the combined inhibition of ATR and Wee1 as treatment strategies, we envision that changes in FLT uptake could be utilized also for other therapeutic strategies targeting the DNA damage response and become an integral part of an effort to use functional biomarkers for therapy dynamics at an early stage for precision medicine.

3.2 Materials and Methods

3.2.1 Antibodies and chemicals

anti-Ki-67 (D3B5; #12202) was purchased from Cell Signalling Technologies. The bioavailable inhibitors AZD6738 and AZD1775 were kindly provided by AstraZeneca.

3.2.2 Cell lines

4T1 and EMT6 cell lines were purchased from the American Type Cell Culture (ATCC) and cultured in DMEM high glucose medium supplemented with 10% fetal calf serum. These cell lines were regularly tested for mycoplasma.

3.2.3 Crystal violet assay

3000 cells per well were seeded into 96 well plates 4 h prior to drug treatment. Cells were treated with indicated concentrations of AZD6738 (100 nM to 4000 nM) and AZD1775 (50 nM to 2000 nM) for 96 h. After 96 h, cells were washed twice with 1X PBS and stained with 0.5% crystal violet (in 20% methanol) for 20 mins. Cells were then washed with water for 4 times, plates were air dried overnight. 200 μ L methanol was added per well and incubated for 20 mins at room temperature. Optical density was measured at 584 nm using the FLUOstar Omega plate reader (BMG Labtech). Background values were subtracted using blank OD584. Data was calculated in terms of % surviving attached cells (% crystal violet OD) compared to vehicle control treated cells. Experiments were performed in triplicates in at least 3 independent experiments.

3.2.4 Orthotopic breast cancer syngeneic mouse models and drug treatment

6 week old female BALB/c mice were obtained from Charles Rivers, Canada. For tumor formation, 1×10^5 4T1 and 2×10^5 EMT6 cells were mixed with Matrigel (Corning) and PBS (1:1) and injected in 40 μ L orthotopically into the thoracic mammary fat pad of 8-10 week old female

BALB/c mice. Tumor growth was measured every 3 days using a Vernier caliper and volume was assessed as $(\text{length} \times \text{width}^2)/2$.

When the tumor reached an approximate volume of 25-35 mm³ for 4T1 model or 60-80 mm³ for the EMT6 model, mice were randomly segregated into 2 groups (n = 9 per group) for each model. Because EMT6 tumors grew faster than 4T1 tumors, treatment starting points had to be adjusted accordingly. Mice were treated daily with vehicle or 25 mg/kg AZD6738 (in 10% DMSO, 40% polypropylene glycol, and 50% ddH₂O) and 60 mg/kg AZD1775 (in 0.5% methylcellulose) combination *via* oral gavage for 5 days. Body weight was measured pre- and post-treatment as an indicator of toxicity. Mice were euthanized 12 hours post [¹⁸F]-FLT-PET scan to allow radioactivity decay and tumors were harvested for histology. All experiments were done in accordance with our animal care protocol (AC20251).

Treatment efficacy was categorized according to guidelines adapted from Response Evaluation Criteria in Solid Tumors (RECIST) (Eisenhauer *et al.* 2009, Schwartz *et al.* 2016). The treatment efficacy was defined by the percentage change in tumor volume measured at the end of the treatment over the tumor volume measured before treatment by a Vernier calliper. Treatment response was classified as partial response (PR) if the reduction in total tumor size was > 30%; stable disease (SD) if the reduction in total tumor size was < 30% and tumor growth was < 20%; progressive disease (PD) if the growth in total tumor size exceeded 20% or new lesions were identified; and complete response (CR) if disappearance of tumor lesions was observed.

3.2.5 Immunohistochemistry

Immunohistochemistry was performed on formalin fixed paraffin embedded (FFPE) tissue samples using standard procedures as previously described (3). Briefly, tumors were sectioned into 5 μm slices on precleaned Colorfrost Plus microscope slides (Fisher Scientific, USA) using a

microtome (Leica, Germany). Tissue samples were baked at 60°C for 2 h and deparaffinized 3 times in xylene for 10 min each and subsequently rehydrated in a gradient of ethanol washes. For antigen retrieval, tissue sections were subjected to heat in a pressure cooker and 0.05% citraconic anhydride antigen retrieval buffer (pH – 7.4). Tissue samples were then blocked with 4% BSA for 30 min and incubated with the respective primary antibodies overnight at 4°C. The next day, endogenous peroxidase activity was blocked for 30 min using 3% H₂O₂, followed by incubation with anti-rabbit HRP labelled secondary antibody (Dako EnVision+ System; K4007) for 1 h at room temperature in the dark. Samples were incubated with DAB (3,3'-diaminobenzidine) + substrate chromogen (Dako, USA) for brown color development, counterstained with hematoxylin, and mounted with DPX mounting medium (Sigma, USA). Images were captured using the Zeiss Axioskop2 plus upright microscope (Zeiss, Germany) equipped with Axiocam 512 color camera.

3.2.6 Radiosynthesis

[¹⁸F]3'-deoxy-3'-fluorothymidine (FLT) was synthesized by the method described by Machulla *et al.* (Machulla *et al.* 2000) at the Cross Cancer Institute's cyclotron facility using the GE TracerLab-FX-automated synthesis unit (GE Healthcare, United Kingdom) with 5'-O-(4,4'-dimethoxytrityl)-2,3'-anhydrothymidine (ABX GmbH, Radeberg, Germany) as the labeling precursor.

3.2.7 PET imaging

4T1 and EMT6 tumor-bearing BALB/c mice were anesthetized with isoflurane and placed on a 37°C heated bed to regulate their body temperature. They were positioned and immobilized in prone position at the centre of the field of view of the INVEON® PET scanner (Siemens Preclinical Solutions, Knoxville, TN, USA). The presence of radioactivity in the injection solution

was determined using a dose calibrator (Atomlab™ 300, Biodex Medical Systems, New York, NY, USA), which was cross-calibrated with the scanner. 4-8 MBq [¹⁸F]-FLT in 100 μL saline solution was injected through the lateral tail vein using a needle catheter after the emission scan was started. A dynamic PET scan was acquired 60 minutes post-radioactivity injection in the three dimensions list mode for 10 minutes. Imaging data were reconstructed using the maximum a *posteriori* algorithm. The imaging data files were then processed using the ROVER v2.0.51 software (ABX GmbH, Radeberg, Germany). Masks defining the three dimensional regions of interest (ROI) over the tumor were set at a threshold of 50% of radioactivity uptake. Mean standardized uptake values were calculated for each ROI as $SUV_{\text{mean}} = (\text{measured radioactivity in the ROI} / \text{mL tumor tissue}) / (\text{total injected radioactivity} / \text{body weight of mouse})$.

3.2.8 Statistical analysis

All statistical analysis was performed using the GraphPad Prism 7 software. All experiments were performed at least 3 times with triplicate samples. *P* values were calculated using one-way ANOVA test or two-way ANOVA. *P* < 0.05 was considered significant, and *P* < 0.001 was considered highly significant.

3.3 Results

3.3.1 Combined ATR and Wee1 inhibitor treatment leads to synergistic cell killing in 4T1 but not in the EMT6 murine breast cancer cell line

The serine/threonine kinase Wee1 regulates the inhibitory phosphorylation of CDK1 at tyrosine 15 to delay mitotic entry until suitable conditions have been met (Malumbres and Barbacid 2005). Inhibition of Wee1 results in increased entry and prolonged mitosis making cancer cells more vulnerable to therapy induced mitotic catastrophe (Lewis *et al.* 2017). ATR, the central kinase of the DNA damage response to replication stress, controls cell cycle checkpoints by pathways initiated by the phosphorylation of the downstream kinase Chk1 in response to DNA damage. We recently showed that combined inhibition of ATR and Wee1 kinases results in synergistic cell killing in a variety of cancer cell lines (Bukhari *et al.* 2019). Our additional screening identified a murine breast cancer cell line, EMT6, that showed low ATR inhibitor sensitivity and did not display significant synergistic cell killing by ATR and Wee1 inhibition. As seen in **Fig. 3.1A, B**, in a crystal violet assay with different concentrations of AZD6738 and AZD1775 for 4 days, the murine breast cancer cell lines EMT6 and 4T1 show different sensitivities to the ATR inhibitor AZD6738. Furthermore, unlike the 4T1 cell line [and over two dozen cell lines assayed previously (**see Chapter 2**)], EMT6 does not show synergistic cell killing by ATR and Wee1 inhibition as confirmed by calculating Bliss combination indices, represented as a 3D matrix (CIs) in **Fig. 3.1C, D**. A CI value lower than 1 indicates synergy, and a value greater than 1 indicates antagonism (**Table 3.1**). We do not know yet the reason behind the ATR inhibitor resistance and absence of synthetic lethality of ATR and Wee1 inhibition in EMT6. While several groups have reported that cells with p53 and/or ATM defects are more sensitive to ATR inhibition (Nghiem *et al.* 2001, Peasland *et al.* 2011, Reaper *et al.* 2011, Toledo *et al.* 2011, Gamper *et al.*

2013) likely due to the impaired G1 checkpoint and/or the increased replication stress that occurs due to relaxed S-phase entry (Toledo *et al.* 2011), we did not see any correlation between p53 status and sensitivity to ATR inhibition in the human cancer cell lines tested in our previous study (Bukhari *et al.* 2019). We therefore suspect that the p53 wild type state of the EMT6 murine breast cancer cell line could be just one of several factors contributing to lower sensitivity to ATR inhibition (**Table 3.2**).

The differing response of 4T1 and EMT6 to the drug combination treatment *in vitro* prompted us to use these cell lines as treatment responsive and refractory models in comparative *in vivo* studies. To investigate the drug efficacy and to test PET imaging as non-invasive biomarker for treatment response we used an immune competent mouse model facilitated by the fact that 4T1 and EMT6 are both derived from tumors in BALB/c mice.

<i>Cell Line</i>	<i>AZD6738 (ATRi)</i>	<i>AZD1775 (Weeli)</i>	<i>Bliss CI</i>	<i>ATRi IC₅₀</i>	<i>Weeli IC₅₀</i>
<i>4T1</i>	100 nM	50 nM	0.39	736 nM	308 nM
	100 nM	100 nM	0.10		
	300 nM	50 nM	0.34		
	300 nM	100 nM	0.33		
<i>EMT6</i>	100 nM	50 nM	1.04	2578 nM	162 nM
	100 nM	100 nM	1.06		
	300 nM	50 nM	1.03		
	300 nM	100 nM	1.02		

Table 3.1. Synergistic murine breast cancer cell killing by ATR and Wee1 inhibition.

IC₅₀ values and Bliss combination indices (CI) at indicated drug concentrations calculated from at least three independent experiments. A Bliss CI of less than 1 indicates synergy, a CI of < 0.7 strong synergy, and a CI of > 1 antagonism.

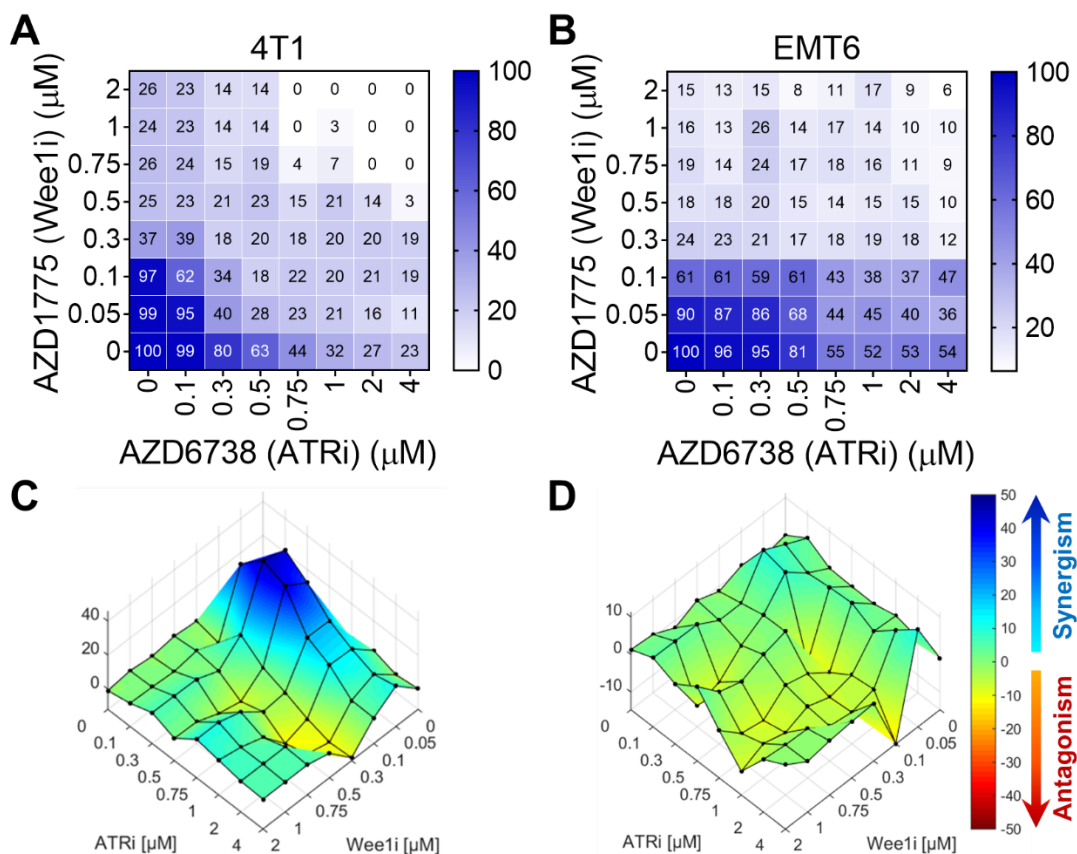


Figure 3.1. ATR and Wee1 inhibition leads to synergistic cell killing in 4T1, but not in EMT6. Murine breast cancer cell lines 4T1 (**A**) and EMT6 (**B**) were treated with increasing concentrations and different combinations of AZD6738 (up to 4 μM) and AZD1775 (up to 2 μM) for four days. Survival was assayed by crystal violet staining and experiments were repeated at least three times. The color bar indicates percent survival normalized to vehicle control-treated cells. (**C** and **D**) 3D plots were generated using Combenefit software to represent the calculated Bliss distribution in a 3D matrix. The blue color scale at low doses indicates strong synergy in 4T1 cells. No synergy was observed in EMT6 cells.

3.3.2 [^{18}F]-FLT-PET imaging can be used as a biomarker to assess combined ATRi and Wee1 inhibitor therapy response in breast tumors *in vivo*

To evaluate the therapeutic response of combined ATRi and Wee1i treatment *in vivo*, we established syngeneic orthotopic mouse breast tumors in BALB/c mice. The EMT6 and 4T1 allografts in BALB/c mice allows for a robust evaluation of the drug response of metastatic triple negative breast cancer cells by including an immune response, which was lacking in our previous xenograft models (Bukhari *et al.* 2019). Tumors were developed by injecting 4T1 or EMT6 cells (**Table 3.2**) (Schrors *et al.* 2020) in the thoracic mammary fat pad of 8-10 week old female BALB/c mice. In our previous study we treated tumors for 25 days with the inhibitor combination (Bukhari *et al.* 2019). To validate [^{18}F]-FLT as a potential biomarker for *early* therapy response, mice were administered 25 mg/kg ATRi and 60 mg/kg Wee1i by oral gavage over just 5 days (days 1-5).

Pre- (day 0) and post-treatment (day 7 and 14) PET scans were acquired to assess changes in [^{18}F]-FLT uptake (**Fig. 3.2A**). Representative maximum intensity projection images are shown in **Fig. 3.2B, E**. Interestingly, in the case of 4T1, 5 days of treatment with ATRi and Wee1i showed a significant reduction in [^{18}F]-FLT tumor uptake compared to control mice post-treatment (day 7), with SUV_{mean} of 1.335 ± 0.097 for vehicle control mice and SUV_{mean} of 0.7061 ± 0.264 for treatment group mice ($P < 0.001$; one-way ANOVA; $n = 9$ mice per group) (**Fig. 3.2C**). 5 mice were randomly selected from each group for further PET imaging a week later (day 14). As anticipated, [^{18}F]-FLT tumor uptake continued to be significantly lower in mice treated with ATRi and Wee1i for just 5 days (SUV_{mean} of 0.729 ± 0.413) compared to mice receiving just the vehicle (SUV_{mean} of 1.244 ± 0.195) ($P = 0.0403$; one-way ANOVA; $n = 5$ mice per group) (**Fig. 3.2C**). Of note, mice treated with ATRi and Wee1i had a significant reduction in tumor size on day 7 and 14 ($P < 0.005$; one-way ANOVA) (**Fig. 3.2D**). Interestingly, of the 5 mice followed longer, one

animal even showed complete regression (or complete response as per RECIST criteria) of the primary tumor following just 5 days of the drug treatment as determined by the absence of a palpable tumor at the primary site.

Based on our *in vitro* findings, we expected EMT6 tumors to be poor responders to ATRi and Wee1i treatment *in vivo*. To validate this and to probe whether [¹⁸F]-FLT can indeed be used as a biomarker to evaluate therapy response, BALB/c mice bearing orthotopic EMT6 tumors were treated with ATRi and Wee1i as described above. As expected, EMT6 tumors did not respond to the 5 days ATRi and Wee1i treatment regimen as no significant change in primary tumor volume between the vehicle and treatment groups was observed on day 7 (**Fig. 3.2G**). Of note, also the [¹⁸F]-FLT uptake measured either shortly after treatment (day 7; SUV_{mean} of 0.953 ± 0.096 for ATRi + Wee1i versus SUV_{mean} of 0.924 ± 0.061 for vehicle) or during the follow-up (day 14; SUV_{mean} of 0.96 ± 0.079 for ATRi + Wee1i versus SUV_{mean} of 0.896 ± 0.096 for vehicle) showed no significant changes (**Fig. 3.2E, F**), supporting [¹⁸F]-FLT imaging as suitable candidate biomarker for early drug response.

<i>Gene</i>	<i>4T1</i>	<i>EMT6</i>
<i>TP53</i>	Mutant	Wildtype
<i>ATM</i>	Wildtype	Wildtype
<i>BRCA1</i>	Wildtype	Wildtype
<i>BRCA2</i>	Wildtype	Wildtype
<i>PIK3CG</i>	Mutant	?
<i>PTEN</i>	Wildtype	Mutant (G209*)

Table 3.2. Mutation status in 4T1 and EMT6 murine breast cancer cell lines of genes with potential impact on ATR inhibitor sensitivity.

Data courtesy of Charles River.

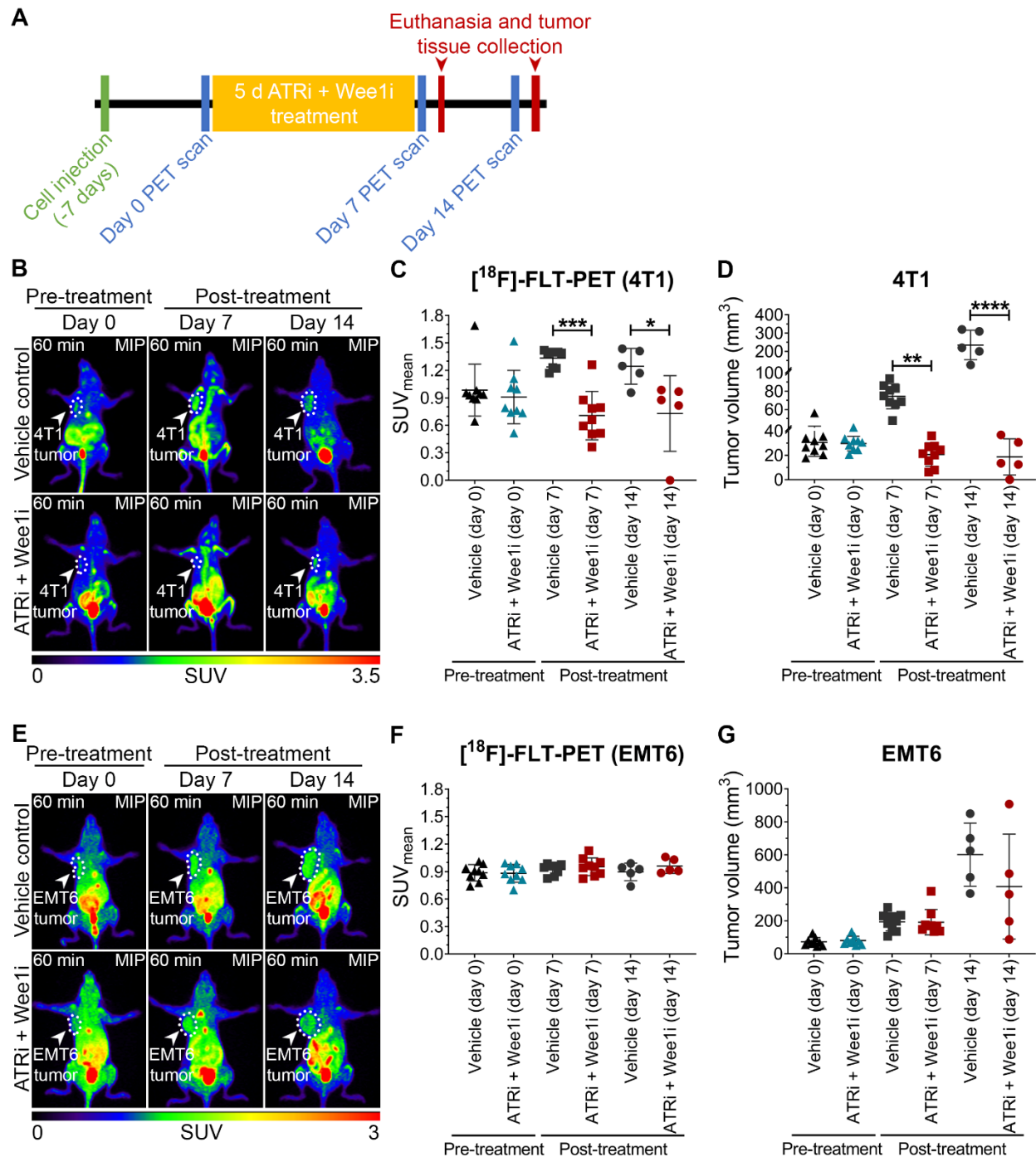


Figure 3.2. Combination treatment with ATR and Wee1 inhibitors and non-invasive monitoring of treatment response with $[^{18}\text{F}]$ -FLT-PET imaging.

BALB/c mice were injected orthotopically with 4T1 or EMT6 cells and treated for 5 days. Pre- and post-treatment $[^{18}\text{F}]$ -FLT-PET scans were acquired to evaluate therapy response. **(A)** Schematic representation of the experimental outline. **(B and E)** Representative mouse images showing maximum intensity projection (MIP) of $[^{18}\text{F}]$ -FLT uptake 60 minutes post tracer injection. **(C and F)** Quantitative $[^{18}\text{F}]$ -FLT uptake represented as mean standardized uptake values (SUV_{mean}). **(D and G)** Graph represents pre- and post-treatment tumor growth in mice treated with

ATRi + Wee1i combination or vehicle for 5 days. Data represented as scatter dot plot showing all experimental data points. Error bars represent SD. * indicates $P < 0.05$, ** indicates $P < 0.01$, *** indicates $P < 0.001$, **** indicates $P < 0.0001$ as calculated by one-way ANOVA.

3.3.3 Early changes in [¹⁸F]-FLT uptake translate to tumor volume response

To evaluate treatment response, we adapted the Response Evaluation Criteria in Solid Tumors (RECIST) that is routinely used in the clinic to estimate treatment efficacy. While the clinical assessment of RECIST uses tumor volume estimates based on CT scans, here we relied on measurements using a caliper, which is a standard practice in pre-clinical studies. Based on this, we found that 5 out of 9 (~55%) 4T1 tumor-bearing mice showed PR (indicated in blue) to combined ATRi and Wee1i treatment for just 5 days and 4 (~45%) presented with SD (indicated in orange) on day 7. Interestingly, 2 out of 5 (40%) 4T1 tumor bearing mice continued to show PR even one week after treatment completion (day 14) and 1 out of 5 (20%) had CR (indicated in green) (**Fig. 3.3A**). These responses were in line with the early changes noticed with [¹⁸F]-FLT-PET scans performed after treatment completion. As expected, 9 out of 9 (100%) EMT6 tumor bearing mice indicated PD (indicated in black) at day 7 measurements and 4 out of 5 (80%) continued to show PD with one mouse (20%) showing indication of SD (**Fig. 3.3B**).

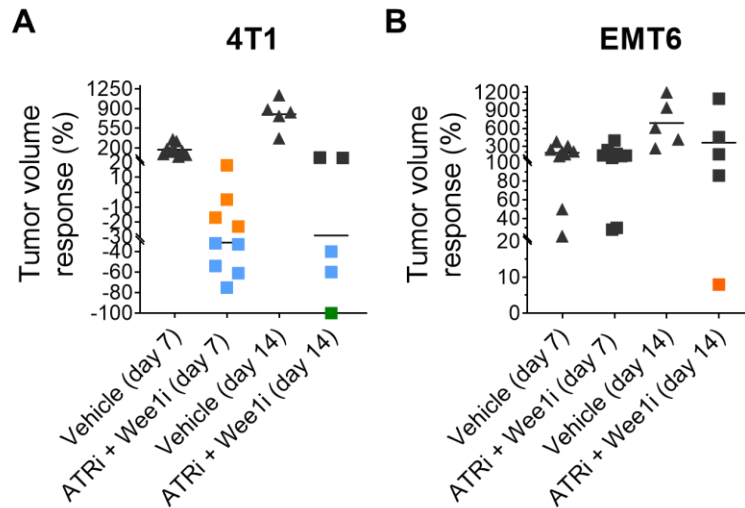


Figure 3.3. Effect of ATR and Wee1 inhibitors on tumor volume response.

Graph represents tumor volume response calculated based on an adapted RECIST criteria for 4T1 (A) and EMT6 (B) tumor bearing mice treated with ATRi and Wee1i for 5 days. Disappearance of all lesions indicates complete response (CR; indicated in green); tumor volume reduction > 30% indicates partial response (PR; indicated in blue) and < 30% stable disease (SD; indicated in orange), whereas growth > 20% classifies as progressive disease (PD; indicated in black) (Notice the difference in the y-axis).

3.3.4 [¹⁸F]-FLT uptake correlates with Ki-67 immunohistochemical staining

Although an indirect biomarker for proliferation, Ki-67 has become the gold standard for measuring cell proliferation status of biopsy samples in the clinic. Recently, Ki-67 was reported to be constitutively expressed during the S, G2, and M phases of the cell cycle, whereas – while Ki-67 expression during the G0/quiescent and G1 phases is generally lower – the dynamics of Ki-67 levels in non-proliferating cells vary (Miller *et al.* 2018). [¹⁸F]-FLT uptake was originally proposed as an imaging biomarker for cell proliferation status based on its entrapment by TK1 in the thymidine salvage pathway (Shields *et al.* 1998). Nevertheless, the correlation between [¹⁸F]-FLT uptake and TK1 levels or activity or Ki-67 levels remains unclear. Several contradictory findings reported indicate a more complex relationship between these parameters (Brockenbrough *et al.* 2011). To correlate [¹⁸F]-FLT uptake in our *in vivo* experiments with Ki-67 staining, we performed immunohistochemistry in 4T1 (**Fig. 3.4A**) and EMT6 (**Fig. 3.4D**) tumors post-imaging. Tumor tissues were excised on day 8, 12 hours after [¹⁸F]-FLT-PET scans from vehicle control mice and mice treated with the ATRi and Wee1i combination for 5 days (n = 4 mice per group). In support of a correlation of [¹⁸F]-FLT-PET uptake with proliferation *in vivo* ($R^2 = 0.7459$), we found a significant reduction in Ki-67 positive cells in 4T1 tumors treated with ATRi and Wee1i for just 5 days ($P = 0.0136$; two-way ANOVA) compared to control tumors (**Fig. 3.4A-C**). As anticipated, no differences were observed in Ki-67 staining between vehicle or ATRi and Wee1i treated EMT6 tumors (**Fig. 3.4D, E**).

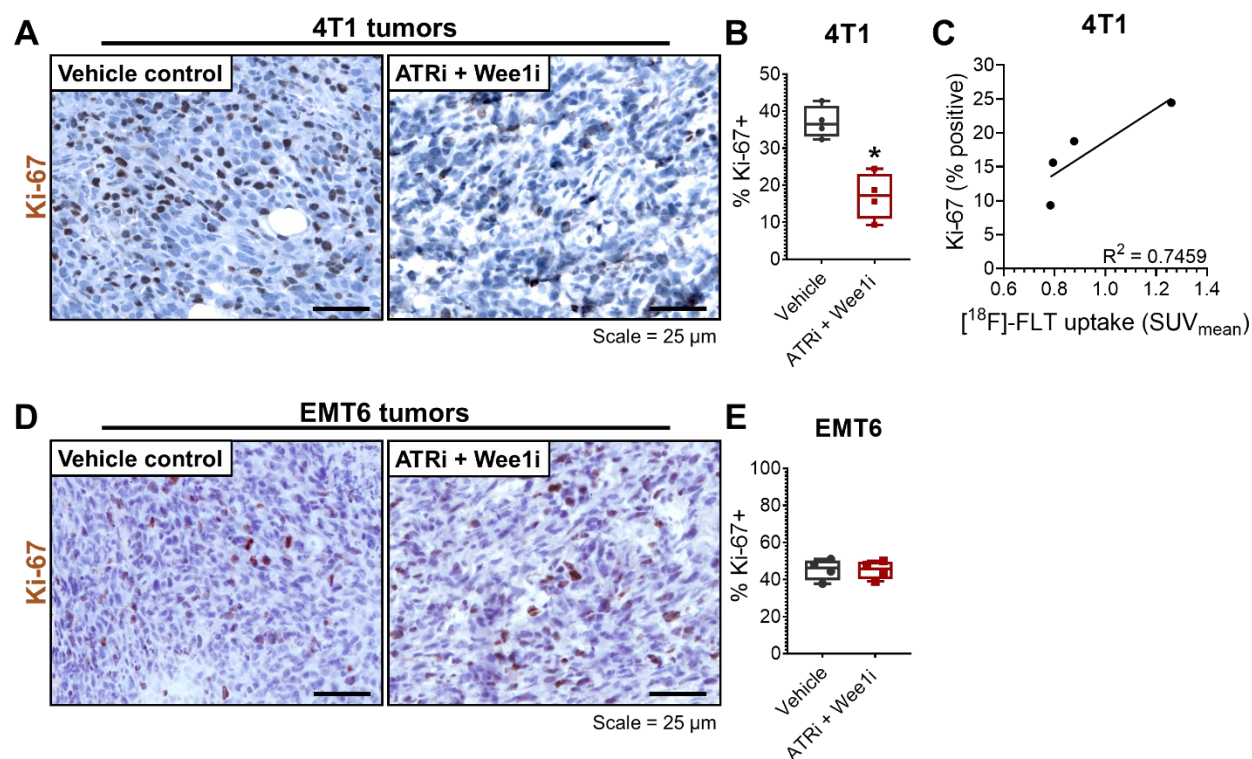


Figure 3.4. Histological evaluation of cell proliferation status.

5 day treated ATRi + Wee1i or vehicle tumors were harvested 12 hours after $[^{18}\text{F}]\text{-FLT-PET}$ scan and processed for immunohistochemistry. **(A and D)** Representative images of the 4T1 and EMT6 tumor sections stained with Ki-67 marker to evaluate cell proliferation status. **(B and E)** The graph represents percentage of Ki-67 positive cells per 1000 cells. **(C)** The graph shows correlation between Ki-67 staining and $[^{18}\text{F}]\text{-FLT}$ uptake. Data represents evaluation from 4 independent tumors in each group. * indicates $P < 0.05$ (two-way ANOVA).

3.3.5 Early changes in [¹⁸F]-FLT uptake correlate with tumor growth delay and longer overall survival of mice treated with combined ATR and Wee1 inhibitors

Lastly, to test treatment response in terms of overall outcomes in our syngeneic mouse models, we evaluated tumor growth kinetics. As expected, in 4T1 tumor bearing BALB/c mice treatment with combined ATRi and Wee1i for just 5 days significantly delayed tumor growth in comparison to the vehicle treatment ($P < 0.0001$, two-way ANOVA) (**Fig. 3.5A**). On the other hand, EMT6 tumor bearing BALB/c mice failed to show any differences in tumor growth between drug combination and vehicle treatment (**Fig. 3.5B**). Furthermore, the 4T1 tumor bearing mice treated with combined ATRi and Wee1i lived significantly longer despite being treated for just 5 days ($P = 0.0084$, log-rank Mantel-Cox test) – median survival of 41 days versus 28.5 days of the vehicle treated mice (**Fig. 3.5C**). The overall survival of the EMT6 tumor bearing mice was similar in both the vehicle and combined ATRi and Wee1i treatment groups (**Fig. 3.5D**).

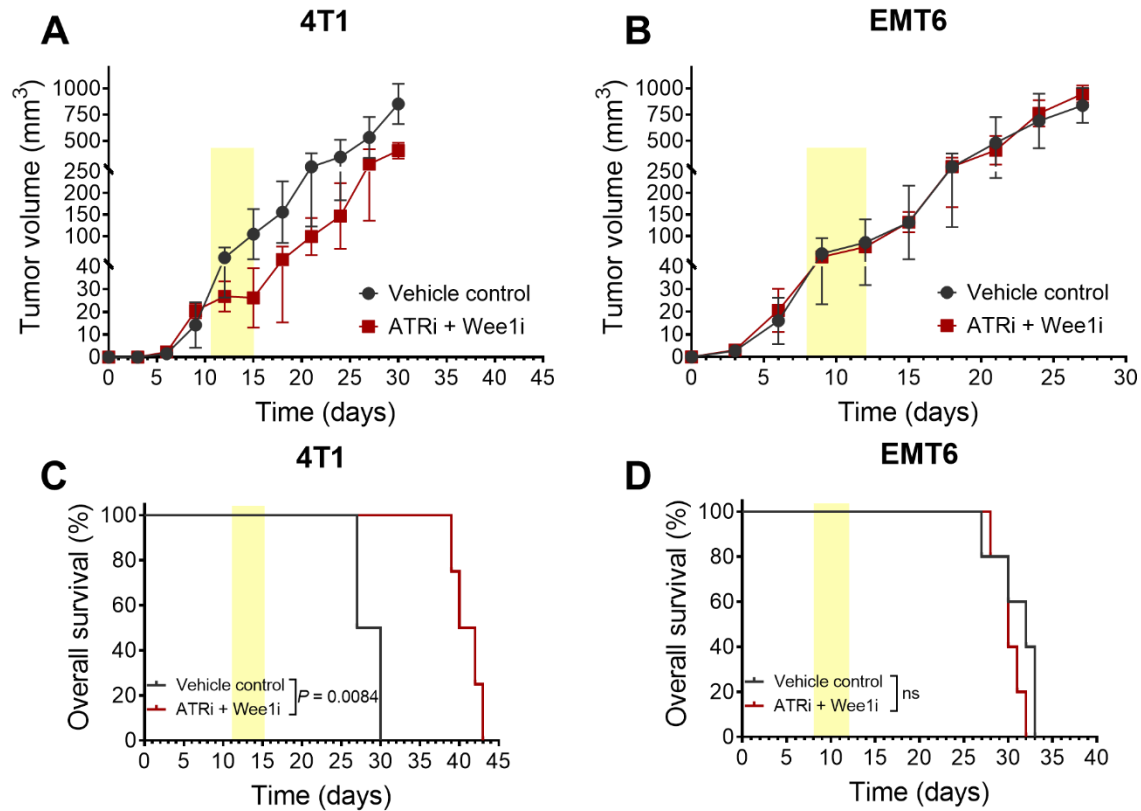


Figure 3.5. Combined treatment with ATR and Wee1 inhibitors and tumor response.

(A and B) The graphs show tumor growth curves of 4T1 (n = 4 mice per group) and EMT6 (n = 5 mice per group) tumor bearing BALB/c mice treated with either vehicle or combined ATR and Wee1 inhibitors for 5 days (indicated by yellow shades). (C and D) Kaplan-Meier survival curves of the treated mice (n = 4 mice per group for 4T1 tumors, and n = 5 per mice group for EMT6 tumors).

3.4 Discussion

AZD6738 and AZD1775 are currently being evaluated in Phase I/II clinical trials in combination with several other genotoxic agents (Forment and O'Connor 2018). In addition, several studies have reported that AZD6738 or AZD1775 in combination with radiation therapy not only results in radiosensitization of the treated tumor but also triggers an immune response in immune-competent mice (Cuneo *et al.* 2016, Dillon *et al.* 2017, Vendetti *et al.* 2018, Lee *et al.* 2019, Sheng *et al.* 2020, Wang *et al.* 2020, Yang *et al.* 2020). These early findings are encouraging for future studies using this drug combination also as an adjuvant to radiation therapy. Therefore, identifying ways to accurately predict treatment response and classify patients as responders or non-responders at an early stage of clinical treatment has the potential to greatly impact cancer health care. Early identification of non-responders can help avoid unnecessary therapy induced side effects and help clinicians opt for alternative treatment options. Molecular imaging of tumors provide excellent alternatives to visualize treatment outcomes non-invasively. In that regard, functional PET imaging is a particularly attractive approach due to its ability to assess molecular changes within tumors before size related physical changes manifest.

3.4.1 EMT6 as model cell line for cancers refractory to ATR and Wee1 inhibitor treatment

The triple negative subtype of breast cancer is invasive and extremely aggressive. Our *in vitro* drug screen using triple negative breast cancers identified the EMT6 cell line as resistant to ATR inhibition compared to other cell lines, including 4T1. Interestingly, EMT6 was also the only cell line we found so far that failed to show synergistic killing when ATR and Wee1 inhibitors were combined. We verified that these findings extended to *in vivo* treatment, as EMT6 tumors responded poorly to the combination treatment (unlike 4T1). The underlying reason for EMT6 resistance remain unclear, yet a recent report identified several genes in a genome-wide screen that

promote ATR inhibitor resistance (Schleicher *et al.* 2020). Schleicher *et al.* reported that individual inactivation of seven genes (KNTC1, EEF1B2, LUC7L3, SOD2, MED12, RETSAT, and LIAS) among the top 40 candidates identified by CRISPR knockout screens promoted resistance to two different ATR inhibitors – AZD6738 and M6620 (Schleicher *et al.* 2020). While the status of these genes in the murine breast cancer cell lines EMT6 and 4T1 is currently unknown, these genes may serve as a starting point for future studies evaluating drug resistance mechanisms to combined ATR and Wee1 inhibitor treatments. Yet caution is advised, as the reported screen relied on single gene knockout. It is likely that multifactorial genetic changes during carcinogenesis and associated changes in expression levels, not necessarily complete loss, of genes are determining drug resistance. As an example, we previously identified increased expression of the kinase PKMYT1 as mechanism of acquired Wee1 inhibitor resistance (Lewis *et al.* 2019).

3.4.2 Changes in FLT uptake during early treatment stage as biomarker for tumor response

Our pre-clinical results indicate that early changes in [¹⁸F]-FLT uptake following just 5 days of combined ATR and Wee1 inhibitor treatment were able to predict responders to the therapy. Using an adapted RECIST criteria, we were able to correlate the initial reduction in tracer uptake to a partial response to therapy in 5 out of 9 mice in our “responder” model, one of whom showed complete response at a later timepoint. Moreover, we found [¹⁸F]-FLT to be a functional measure of changes in cell proliferation status unrelated to tumor size as [¹⁸F]-FLT uptake in EMT6 tumors did not change over time despite tumor growth (**Fig. 3.2E-G**). This could be particularly beneficial when evaluating response to cytostatic therapies where tumors may not regress radiologically despite effective treatment. An example of this would be in pre-clinical and clinical studies evaluating inhibition of the mammalian target of rapamycin (mTOR), a regulator of cell proliferation. mTOR inhibition results in cell cycle arrest in mid to late G1 phase (Costa

2007). As TK1 upregulates in S-phase, mTOR inhibition may affect [^{18}F]-FLT uptake. Indeed, imaging cell proliferation status with [^{18}F]-FLT can directly measure the effect of cytostatic treatments (like mTOR inhibition) and identify responders (Brepoels *et al.* 2009). Of note, further analysis of our findings suggest a correlation between change in SUV (ΔSUV_{0-7}) and change in tumor volume ($\Delta\text{Volume}_{0-7}$) at day 7 ($R^2 = 0.5472$) (**Fig. 3.6**). Indeed, only the mice that had lower [^{18}F]-FLT uptake post-treatment (at day 7), had reductions in tumor volume (samples highlighted in teal) due to the 5 day combined ATRi and Wee1i treatment. In two mice, although the growth rate was drastically reduced, we saw a positive change (samples highlighted in red) in tumor volume, and this further correlated with an increase in [^{18}F]-FLT uptake. It should be pointed out that pre-treatment SUV can not be used as predictor for treatment response. For example, both 4T1 and EMT tumors showed similar SUVs for [^{18}F]-FLT at the onset of treatment (around 0.9), but as discussed EMT failed to respond to the drug combination (**Fig. 3.2C, F**).

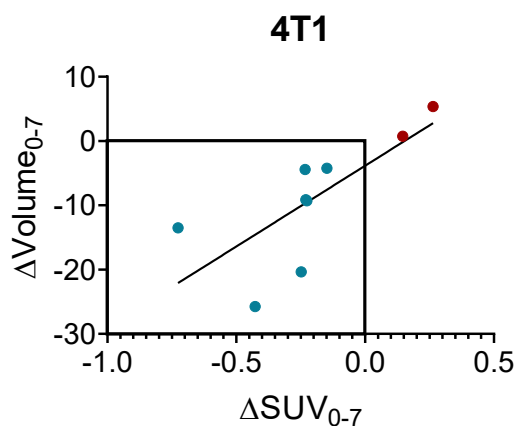


Figure 3.6. Changes in SUV_{mean} correlates with changes in tumor volume.

Graph shows change in SUV_{mean} ($\Delta\text{SUV}_{\text{mean}}$) versus change in tumor volume (ΔVolume) post-treatment with combined ATR and Wee1 inhibitors for 5 days. Lower [^{18}F]-FLT uptake correlated with reduced tumor volumes in seven out of nine mice (indicated in teal) whereas no tumor shrinkage was seen in two mice (indicated in red).

Several groups have evaluated the diagnostic potential of [¹⁸F]-FLT-PET imaging for monitoring treatment response in various preclinical (reviewed in (Jensen and Kjaer 2015, Schelhaas *et al.* 2017)) and clinical studies (reviewed in (Bollineni *et al.* 2016)). In a triple negative MDA-MB-468 breast cancer xenograft, [¹⁸F]-FDG and [¹⁸F]-FLT had similar indications in predicting tumor response to paclitaxel treatment (Raccagni *et al.* 2018). More recently, two independent pilot studies, limited by their sample size (n = 15 and n = 16 patients, respectively), found that early changes in [¹⁸F]-FLT-PET could not only identify responders and non-responder to neoadjuvant chemotherapy with anthracycline or taxane-based regimens but also predict long-term survival (Crippa *et al.* 2015, Ueberroth *et al.* 2019). In addition, a report by Troost *et al.* demonstrated the use of [¹⁸F]-FLT-PET imaging to examine tumor response as early as one week after start of radiation treatment, and these early changes were found to precede the CT tumor volume response (Troost *et al.* 2010). Furthermore, Lin *et al.* reported reduction of [¹⁸F]-FLT uptake as early as 24 hours after charged particle radiation therapy in xenografts (Lin *et al.* 2015). Such early changes in [¹⁸F]-FLT uptake and retention after radiation therapy are encouraging to the future studies using combined ATRi and Wee1i treatments adjuvant to radiation therapy. A few reports also showed that [¹⁸F]-FLT-PET can monitor treatment (with Herceptin or aromasin) related changes in patients with metastatic breast cancer wherein changes in [¹⁸F]-FLT uptake at the primary or metastatic site significantly correlated with overall therapy response (Pio *et al.* 2006) and that the tracer uptake was more prominent in large axillary lymph-node metastasis (Been *et al.* 2006). Based on our previous finding, we expect combined treatment with ATRi and Wee1i to target metastasis as well (Bukhari *et al.* 2019), and [¹⁸F]-FLT-PET could serve as an excellent biomarker in future clinical trials to monitor therapy response not only at the primary site, but also of metastatic lesions.

With regards to radiation therapy, it is noteworthy that even though [^{18}F]-FDG is more popular for treatment response monitoring due to signal robustness, [^{18}F]-FLT has two potential advantages over it with regards to radiation therapy: (1) [^{18}F]-FLT-PET has higher specificity than [^{18}F]-FDG-PET as it does not accumulate in therapy-induced inflammatory regions, which usually have higher glucose metabolism (which is measured by [^{18}F]-FDG uptake) (Been *et al.* 2004, van Waarde *et al.* 2004, Kubota *et al.* 2006); and (2) proliferation related changes in thymidine metabolism are more strongly associated with radiation injury than those in glycolysis (Tehrani and Shields 2013). Yet for diagnostic purposes, [^{18}F]-FLT is not regarded as an ideal tracer for tumor detection or staging due to its high physiological uptake in the bone marrow and liver, limiting its potential to accurately detect distant metastasis at those sites (Been *et al.* 2004, Kenny *et al.* 2011).

3.4.3 [^{18}F]-FLT uptake correlates with Ki-67 immunohistochemical staining

Previous reports from breast cancer have shown a correlation between [^{18}F]-FLT-PET uptake and Ki-67 in pilots involving 20, 12, and 8 patients (Kenny *et al.* 2005, Contractor *et al.* 2011, Woolf *et al.* 2014). In line with our findings, a meta-analysis of 27 studies in a variety of tumor types showed a strong correlation between Ki-67 staining and FLT uptake (Chalkidou *et al.* 2012). However, data from another pilot of 12 breast cancer patients failed to see a correlation (Smyczek-Gargya *et al.* 2004). Although high levels of Ki-67 pre-neoadjuvant chemotherapy are regarded as a predictor for chemotherapy response due to a better chance of achieving pathological complete response (pCR), they are also associated with poorer long-term outcomes particularly if pCR is not achieved (Jones *et al.* 2009, Weigel and Dowsett 2010). Given the small sample size of our study and the aggressive nature of our murine breast cancer cell lines mimicking stage IV

human metastatic breast cancers, the purposely short drug treatment could not achieve pCR except in one 4T1 tumor bearing mouse.

Chapter 4: Combined ATR and Wee1 Inhibition as Adjuvant to Breast Cancer Radiotherapy or Surgery

4.1 Introduction

Radiation therapy plays an essential role in the multidisciplinary management of breast cancer with the aim of eradicating minimal residual disease after surgical removal of the evident primary tumor. Advances in radiotherapy modalities allow for imaging-based planning and directed tumor delivery of the radiation dose, thereby minimizing damage to the surrounding tissue. The discovery of radiosensitizers, drugs that increase radiation-mediated tumor cell killing while having a smaller effect on normal tissue, may decrease radiation doses used for the treatment of patients and/or increase cell killing of the radioresistant tumor subpopulations (Wardman 2007). In this regard, inhibitors of the DNA damage response like ATR and Wee1 kinase inhibitors have been shown to radiosensitize tumors of various backgrounds (Bridges *et al.* 2011, Gamper *et al.* 2013, Cuneo *et al.* 2016, Dillon *et al.* 2017, Tu *et al.* 2018, Lee *et al.* 2019). ATR is an apical kinase in the DNA damage response, and Wee1 regulates cell cycle progression. More recently, ATR and Wee1 inhibitors were shown to additionally enhance the antitumor immune response when tumors were treated in combination with radiation.

Immune cells within the tumor microenvironment are composed of lymphoid and myeloid cells, and their activation state and phenotype can either promote or inhibit various aspects of tumor development (Coussens *et al.* 2013, Edechi *et al.* 2019). Antitumor immunity is mainly imposed by antigen specific CD8⁺ T cells (Davis and Bjorkman 1988). Antigen naïve T cells interact with antigen peptides bound to major histocompatibility complex class I molecules (MHC I) on the surface of antigen presenting cells (APCs) *via* their T cell receptors (TCR). CD8⁺ T cells utilize the TCR to recognize the peptides presented by MHC I, which subsequently leads to the activation and proliferation of CD8⁺ T cells that play a crucial role in pathogen response, autoimmunity, and tumor suppression (Zoete *et al.* 2013, Gros *et al.* 2014, Gubin *et al.* 2014,

Linnemann *et al.* 2014, Tran *et al.* 2014, Linnemann *et al.* 2015). One of the hallmarks of cancer cells is their ability to avoid immunosurveillance (Hanahan and Weinberg 2011), whereby tumor cells escape the antitumor immune response or actively suppress it (Dunn *et al.* 2006, Koebel *et al.* 2007, Swann and Smyth 2007). Tumor cells often achieve this by expressing suppressive cytokines such as interleukin (IL)-10 (Saraiva and O'Garra 2010) and arginase (Crittenden *et al.* 2014), increased expression of programmed death-1 ligand (PD-L1) (Pardoll 2012), downregulation of MHC I on tumor cells (Leone *et al.* 2013), or secreting other immune-suppressive factors within the tumor microenvironment (Zou 2005). In addition, the inhibitory receptor PD-1 is expressed on the surface of T cells, B cells, natural killer (NK) cells, macrophages, and dendritic cells (Petrovas *et al.* 2006, Liu *et al.* 2009). Activation of TCR induces PD-1 expression on naïve T cells (Chikuma *et al.* 2009). Moreover, constitutive PD-1 expression on T cells is associated with the expression of additional inhibitory receptors like TIM-3 and LAG-3 (Grosso *et al.* 2009, Fourcade *et al.* 2010), which leads to impaired T cell function and tumor immune evasion upon ligation of PD-1 with the PD-L1 ligand on tumor cells (Ahmadzadeh *et al.* 2009).

Treatment of various cancers with cytotoxic chemotherapeutics or DNA damaging agents has been shown to enhance the cytotoxic CD8⁺ T cell (CTLs) response (Klemm and Joyce 2015, Ruffell and Coussens 2015). Wee1 kinase inhibition was shown to sensitize tumors to PD-1 mAb immune checkpoint blockade *in vivo*, resulting in CTL mediated tumor cell killing (Sun *et al.* 2018). More recently, inhibition of Wee1 was also shown to suppress PD-L1 expression on breast tumors and enhance CTL mediated tumor cell killing when combined with radiation (Patel *et al.* 2019, Wang *et al.* 2020). In addition to CTLs, NK cells also mediate tumor cell death and are affected by chemotherapeutics. In immunocompetent mice bearing aggressive head and neck

tumors, concurrent treatment with adoptively transferred high affinity NK cells and the Wee1 inhibitor AZD1775 prolonged survival compared to either treatment alone (Friedman *et al.* 2018). We should note that, as NK cells represent 2% or less of the circulating white blood cells, NK-based cell therapies have not garnered attention similar to T-lymphocyte-based cellular therapies (Klingemann *et al.* 2016).

In addition to chemotherapeutic agents, radiation therapy can also increase immunogenic properties of tumor cells by enhancing the expression of MHC I molecules, thereby increasing their vulnerability to CTL (Reits *et al.* 2006, Mouw *et al.* 2017). Single high dose ionizing radiation (IR) (10 Gy) was also found to activate tumor-associated dendritic cells (DCs), which in turn support the accumulation of tumor-specific CD8⁺ effector T cells (Gupta *et al.* 2012). Furthermore, IR has also been reported to activate chemokine release that stimulates DCs (Hallahan *et al.* 1989), to promote cross-presentation of tumor antigens (Sharabi *et al.* 2015), to lead to proinflammatory chemokines secretion by cancer cells and thus to attract tumor infiltrating lymphocytes (TILs) (Matsumura *et al.* 2008), and to enhance TIL extravasation *via* upregulation of cell adhesion molecules (Hallahan *et al.* 1996). IR also facilitates immunogenic cell death (ICD) (Golden *et al.* 2014, Golden and Apetoh 2015). Sublethal doses of IR were implicated in stimulating the release of danger-associated molecular patterns (DAMPs) such as HMGB1 (Gameiro *et al.* 2014) and in increasing FAS expression to promote caspase-mediated apoptosis (Chakraborty *et al.* 2003, Garnett *et al.* 2004). On the other hand, radiation can also enhance immunosuppressive aspects of the tumor microenvironment by recruiting Tregs and inducing PD-L1 expression (Kachikwu *et al.* 2011, Deng *et al.* 2014, Dovedi *et al.* 2014). Some of these IR-induced immune-suppressive effects may be countered or attenuated by ATR or Wee1 inhibition. Regarding ATR inhibition, it was found that DNA damage following ATR inhibitor (AZD6738) treatment combined with radiation

led to immunomodulatory effects in the tumor microenvironment by increasing innate immune cell infiltration (Dillon *et al.* 2019). AZD6738 was also found to attenuate radiation-induced interferon- γ (IFN- γ) mediated PD-L1 expression which resulted in an increased proliferation of tumor-infiltrating CD8⁺ T cells in a syngeneic as well as a genetically engineered mouse model of non-small cell lung cancer (Vendetti *et al.* 2018).

In this preliminary study, we show that combined treatment of ATR and Wee1 inhibitors with radiation results in *in vivo* radiosensitization of 4T1 tumors, a highly metastatic murine breast cancer cell line. Consequently, we observe tumor growth delay and prolonged overall survival of 4T1 tumor bearing BALB/c mice. We provide preliminary evidence that combined treatment with ATR and Wee1 inhibitors plus radiation potentiates the ability of conformal radiotherapy to elicit an antitumor immune response. Lastly, we present findings that combined treatment with ATR and Wee1 inhibitors as an adjuvant to surgery may achieve better tumor control in highly aggressive tumors where surgery is non-curative.

4.2 Materials and Methods

4.2.1 Antibodies and chemicals

anti-CD3 (APC conjugate; Catalog #100222), anti-CD8a (APC conjugate; Catalog #17-008183), anti-PD-1 (FITC conjugate; Catalog #135214), anti-LAG-3 (PE-Cy7 conjugate; Catalog #125226), anti-TIM-3 (Brilliant Violet 421 conjugate; Catalog #134019), antibodies were purchased from BioLegend, anti-CD4 (PE-Cy5.5 conjugate; Catalog #35-0042-82) antibody was purchased from eBiosciences, anti-IFN γ (PE conjugate; Catalog #12-7311-82) and anti-FoxP3 (PE conjugate; Catalog #00-5523) were purchased from ThermoFisher. The respective isotype controls were purchased along with the conjugates.

The bioavailable inhibitors AZD6738 and AZD1775 were kindly provided by AstraZeneca.

4.2.2 Cell lines

The 4T1 cell line was purchased from the American Type Cell Culture (ATCC) and cultured in DMEM high glucose medium supplemented with 10% fetal calf serum. The cell line was regularly tested for mycoplasma.

4.2.3 Orthotopic mouse model, drug, and radiation treatments

6 week old female BALB/c mice were obtained from Charles Rivers, Canada. For tumor formation, 1×10^5 4T1 cells were mixed with PBS and injected in 40 μ L orthotopically into the inguinal mammary fat pad of 8-10 week old female BALB/c mice. Tumor growth was measured every 3 days using a Vernier caliper and volume was assessed as $(\text{length} \times \text{width}^2)/2$.

When the tumors reached an approximate volume of 25-35 mm^3 , mice were randomly segregated into 8 groups ($n = 4$ per group). Mice were treated daily with vehicle or 25 mg/kg

AZD6738 (in 10% DMSO, 40% polypropylene glycol, and 50% ddH₂O) and/or 60 mg/kg AZD1775 (in 0.5% methylcellulose) *via* oral gavage for 5 days 1 hour prior to radiation treatment on the Small Animal Radiation Research Platform (SARRP). For radiation treatment, mice were anesthetized using isoflurane and placed supine on the polystyrene bed. Cone Beam Computed Tomography (CBCT) images were acquired at low resolution (360 frames). A two-beam treatment plan was designed using the MuriPlan software (Xstrahl) and conformal radiation was delivered accordingly at a dose of 200 cGy per fraction for a total of 5 fractions. The dose volume histogram (DVH) showed greater than 95% of the tumor receiving target dose. Body weight was measured pre- and post-treatment as an indicator of toxicity. Mice were euthanized when the tumor volume reached a total of 1000 mm³, after a > 10% reduction in body weight, or any other indications of physical discomfort. All experiments were done in accordance with our animal care protocol (AC20251).

4.2.4 Tumor infiltrating lymphocytes isolation and staining

Mice were euthanized at day 3 or 7 by CO₂ asphyxiation and tumors were harvested in 2 ml tubes. Tumors were then dissociated into smaller pieces with scissors and the dissociated fragments were then transferred to a 15 ml tube containing 5 mL prewarmed enzyme cocktail (0.5 mg/mL Collagenase IV and 10 µg/mL DNase I mixed in RPMI / 10% FBS and preheated at 37 °C). Tubes were then tightly sealed and incubated on a shaker at 37 °C for 30 mins. The fragments were mixed with a pipette for further dissociation. Next, the fragments were filtered through a 100 µm strainer in a 15 mL tube, the tube was filled with 2% FBS/PBS solution and centrifuged at 1500 rpm at 4 °C for 5 mins. The supernatant was discarded, and the pellet was resuspended in 1 mL 2% FBS/PBS solution using a 1 mL pipette. The samples were washed again with 2%

FBS/PBS solution by centrifugation at 1500 rpm at 4 °C for 5 mins. Lastly, cells were resuspended in 200 µL of RPMI medium before proceeding with flow cytometry staining.

All flow cytometry staining was performed in 96-well round bottom plates. Cells from each tumor sample were added to individual wells and the plate was centrifuged at 1500 rpm at 4 °C for 5 mins. Prior to staining with the respective antibodies, cells were stained with Zombie Aqua viability dye (BioLegend) in 1x PBS in the dark for 30 mins. For IFN- γ stimulation, samples were treated with phorbol myristate acetate (PMA) (1:10000) and Ionomycin (1:1000) diluted in RPMI medium. 200 µL of PMA/Ionomycin was added to each well, mixed, and incubated at 37 °C for 2 hours. Next, 50 µL Monensin (1:1000 in RPMI medium) was added to each well, mixed, and incubated at 37 °C for 2 hours. Samples were washed twice with 200 µL 1x PBS by centrifugation at 1500 rpm at 4 °C for 5 mins. Intracellular staining of Forkhead Box Protein 3 (FoxP3) was performed as per manufacturers instructions. Briefly, cells were mixed with fixation/permeabilization solution and incubated at 4 °C for 18 hours in the dark. Following incubation, samples were washed twice with permeabilization buffer and incubated with 50 µL primary antibody against FoxP3 in 1x permeabilization buffer at 4 °C for 30 mins in the dark. Samples were then washed twice with 1x permeabilization buffer and resuspended in 150 µL FACS buffer. All other samples were stained with 100 µL antibody cocktail (Panel 1: CD3, CD4, CD8, IFN- γ , PD-1, LAG-3, TIM-3; Panel 2: CD3, CD4, PD-1, LAG-3, TIM-3) at room temperature for 30 mins in the dark. Samples were then washed twice in 200 µL ice cold FACS buffer (1x PBS, 2% FBS, 1 mM EDTA) by centrifugation at 1500 rpm at 4 °C for 5 mins. The pellet was resuspended in 150 µL of FACS buffer and analyzed on a flow cytometer (Beckman Cytoflex S). The acquired data was exported as FCS files and analyzed using FlowJo v10.

4.2.5 Primary tumor removal surgeries

4T1 tumor removal surgeries were performed when primary tumor reached $\sim 25 \text{ mm}^3$, $\sim 50 \text{ mm}^3$, or $\sim 100 \text{ mm}^3$ ($n = 4$ mice per group). Prior to anesthesia, mice were orally administered Metacam for pain management. Mice were then anesthetized using isoflurane and placed supine under constant anesthesia on a warm surgical waterbed. Hair was removed using a hair removal cream and the area was sterilized with 70% isopropanol and a betadine scrub was applied. Using scissors, an incision was made medial to the tumor and extended dorsally in a superior direction. Next, using forceps and a No. 11 surgical blade, the tumor tissue was cut away from the skin and much of the surrounding mammary fat pad was also removed. The incision site was sealed using 5-0 monocryl sutures (Johnson & Johnson), tissue adhesive (3M Vetbond), and surgical staples. Mice were kept warm until recovery from anesthesia and returned to their cages. Metacam was administered for two additional days post surgery. Mice were inspected daily for any signs of discomfort or bleeding at the surgery site.

4.2.6 Statistical analysis

All statistical analysis was performed using GraphPad Prism 8 software (GraphPad Software, La Jolla, California, USA). *P*-values were calculated using two-way ANOVA, and Log-rank (Mantel-Cox) test. *P*-values of < 0.05 were considered significant, and *P*-values of < 0.001 were considered highly significant.

4.3 Results

4.3.1 Combined inhibition of ATR and Wee1 radiosensitizes 4T1 tumors, leads to growth delay and prolongs survival

Our *in vitro* findings suggest that combined treatment with AZD6738 (ATRi) and AZD1775 (Wee1i) results in synergistic cell killing of 4T1 murine breast cancer cells (**Fig 3.1A, C; see Chapter 3**). Furthermore, our group had previously found that ATR and Wee1 inhibition radiosensitized a variety of cancer cell lines *in vitro*, both as single agents and as a drug combination (unpublished data). To test radiosensitization following drug treatments *in vivo*, 4T1 tumor bearing BALB/c mice were randomly allocated to treatment or vehicle arms (n = 4 mice per treatment group) once the tumors reached a volume of 25-35 mm³. These mice were treated with 25 mg/kg AZD6738 and/or 60 mg/kg AZD1775 and/or conformal IGRT (5 consecutive daily doses of 2 Gy) for just 5 days and tumor growth was measured by caliper measurements (**Fig. 4.1A-C**). We see a significant tumor growth delay in all treatment arms ($P < 0.0001$, two-way ANOVA) except those that received ATRi or Wee1i alone (**Fig. 4.1D**). Interestingly, mice that received treatment with either ATRi and/or Wee1i in combination with IR continued to show delayed tumor growth kinetics for over two weeks after the 5 day treatment while tumor growth in all other treatment arms resumed rapidly when the treatment was stopped. Consequently, treatment for just 5 days significantly prolonged overall survival in ATRi and/or Wee1i and/or IR groups with median survivals as – ATRi + Wee1i, 40.5 days; IR (5 x 2 Gy), 37.5 days; ATRi + IR, 47.5 days; Wee1i + IR, 44 days; ATRi + Wee1i + IR, 56.5 days; and vehicle control, 28.5 days (**Fig. 4.1E**). Mono-treatments with ATRi (median survival - 30.5 days) or Wee1i (median survival - 27.5 days) did not prolong overall survival (**Fig. 4.1E**).

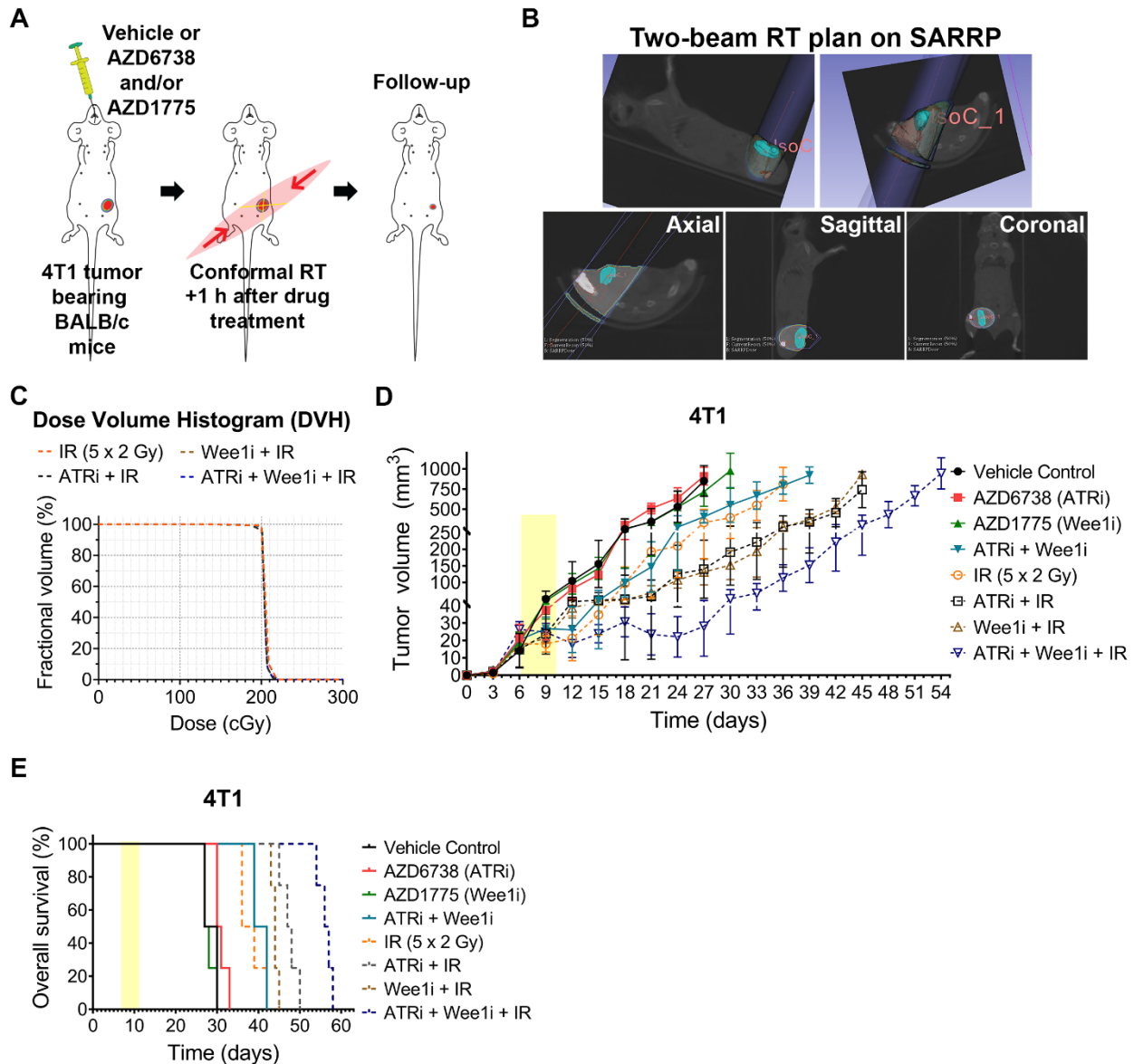


Figure 4.1. Combined inhibition of ATR and Wee1 kinases radiosensitizes 4T1 tumors and prolongs survival.

(A) Schematic shows that mice were treated with vehicle or AZD6738 and/or AZD1775 for 5 days 1 hour before radiation therapy (RT). (B) Sample CBCT image of a mouse showing the two-beam treatment plan, the tumor isocenter, and the two incident beams hitting the planning target volume. (C) Dose volume histogram (DVH) shows that at least 95% of the target volume being irradiated with the target dose (200 cGy). (D) Graph shows tumor growth of mice in the 8 treatment arms (n = 4 per group). (E) Kaplan-Meier survival curve of treated mice (n = 4 per group).

4.3.2 Combined inhibition of ATR and Wee1 attenuates expression of CD8⁺ T cell exhaustion markers following radiation

Our observation that combined ATRi and/or Wee1i treatment with IR resulted in prolonged tumor growth delay could be explained by the loss of clonogenicity *in vivo* as well as a potential trigger of an antitumor immune response in our immune-competent BALB/c mice. Although the results of phase I trials combining ATRi or Wee1i with conformal radiotherapy have not been disclosed, a few patients receiving either ATRi or Wee1i as a monotherapy confirmed partial response (tumor volume reductions) with increased immune cell infiltrates (Do *et al.* 2015, Dillon *et al.* 2019). In view of these early clinical findings and of the observed delay in tumor growth in our pre-clinical model, we evaluated the impact of the drug combination on the immune system. PD-1 is an inhibitory receptor frequently expressed on CD4⁺ and CD8⁺ T cells, B cells, monocytes, and NK cells (Ahmadzadeh *et al.* 2009). T cell exhaustion refers to a T cell state with reduced proliferation and cytokine secretion capability, and increased expression of inhibitory receptors (Blank *et al.* 2019). Overexpression of PD-1 is associated with T cell exhaustion, resulting in an immune-suppressive tumor microenvironment (Barber *et al.* 2006). Other markers that regulate T cell exhaustion in cancer include TIM-3 and LAG-3 (Jiang *et al.* 2015). We examined PD-1 (CD3⁺ CD8⁺ PD-1⁺), TIM-3 (CD3⁺ CD8⁺ TIM-3⁺) and LAG-3 (CD3⁺ CD8⁺ LAG-3⁺) expression on TILs by flow cytometry at day 3 and day 7 post 5 day-treatment with ATRi + Wee1i ± IR (5 x 2 Gy). Combined treatment with ATRi + Wee1i reduced PD-1 or TIM-3 expression on CD8⁺ T cells in comparison to the vehicle control at the day 3 time point, but PD-1 and TIM-3 staining 7 days after treatment was similar in the control, IR, and ATRi + Wee1 groups (**Fig. 4.2A, B**). Interestingly, combined ATRi + Wee1i treatment with IR attenuated radiation-induced PD-1 or TIM-3 expression on CD8⁺ T cells at both the tested time points (PD-1 day 3: $P = 0.0066$; TIM-3 day 3:

$P = 0.0106$, two-way ANOVA) (**Fig. 4.2A, B**). Regarding LAG-3, we observed a tendency for the combined ATRi + Wee1i treatment to reduce LAG-3 expression at both timepoints, day 3 and 7 after treatment, when comparing the radiation treatment groups (day 7: $P = 0.0397$, two-way ANOVA) (**Fig. 4.2C**)

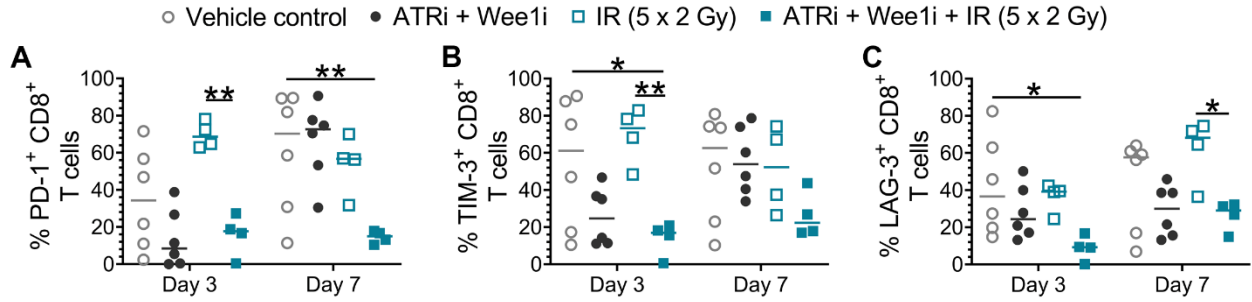


Figure 4.2. Combined inhibition of ATR and Wee1 attenuates expression of T cell exhaustion markers.

(A) Graph shows the percentage of CD8⁺ T cells expressing PD-1 at days 3 and 7 after the 5 day treatment. (B) Graph shows the percentage of CD8⁺ T cells expressing TIM-3 at days 3 and 7 after the 5 day treatment. (C) Graph shows the percentage of CD8⁺ T cells expressing LAG-3 at days 3 and 7 after the 5 day treatment. * indicates $P < 0.05$, ** indicates $P < 0.01$.

4.3.3 IR but not combined inhibition of ATR and Wee1 alone, temporarily reduces the ratio of Tregs in the tumors

To assess the impact of combined ATRi + Wee1i + IR treatment on TIL in the tumor microenvironment, we analysed the proportion of CD8⁺ and CD4⁺ T cells by flow cytometry. Treatment with IR increased the proportion of both CD8⁺ and CD4⁺ lymphocytes in the tumor compared to the other treatment groups (**Fig. 4.3A, B**). We see a reduction in the percentage of CD8⁺ (CD3⁺ CD8⁺) and CD4⁺ (CD3⁺ CD4⁺) TIL in tumors treated with ATRi + Wee1i + IR compared to vehicle treated tumors 3 days post-treatment (**Fig. 4.3A, B**). However, no change was observed between the two groups 7 days post-treatment.

Tregs are an immune suppressive subset of CD4⁺ T cells that are characterized by the expression of FoxP3 (Hori *et al.* 2003). Tregs mainly migrate to sites of inflammation and suppress effector T cell (CD8⁺ and CD4⁺) function. (Togashi *et al.* 2019). In the tumor, Tregs thus can decrease antitumor immunity (Togashi *et al.* 2019). To evaluate if combined treatment with ATRi + Wee1i + IR promotes an immune-activating or immune-suppressive state in the tumor microenvironment, we analyzed the proportion of Tregs in excised tumors by flow cytometry. At day 3, we see a significant reduction in the percentage of Tregs (CD3⁺ CD4⁺ FoxP3⁺) among TILs in tumors treated with combined ATRi + Wee1i + IR compared to vehicle control treated tumors ($P = 0.0132$, two-way ANOVA) (**Fig. 4.3C**). By day 7 post-treatment, the percentage of tumor infiltrating Tregs had significantly increased in tumors treated with combined ATRi + Wee1i + IR treatment (**Fig. 4.3C**).

Interestingly, overall IR with or without combined treatment with ATRi + Wee1i resulted in an elevated CD8⁺/Treg ratio at day 3 (**Fig. 4.3D**). However, at day 7, treatment with ATRi + Wee1i in combination with IR showed a lower CD8⁺/Treg ratio than IR alone. Similarly, the

CD4⁺/Treg ratio showed a trend to be increased in the IR groups at day 3, but no significant differences were seen at day 7 (**Fig. 4.3E**). Taken together, these findings suggest that at least on day 3 after treatment, IR has a greater impact on the proportion of Tregs among the lymphocytes in the tumor microenvironment than the drug combination alone.

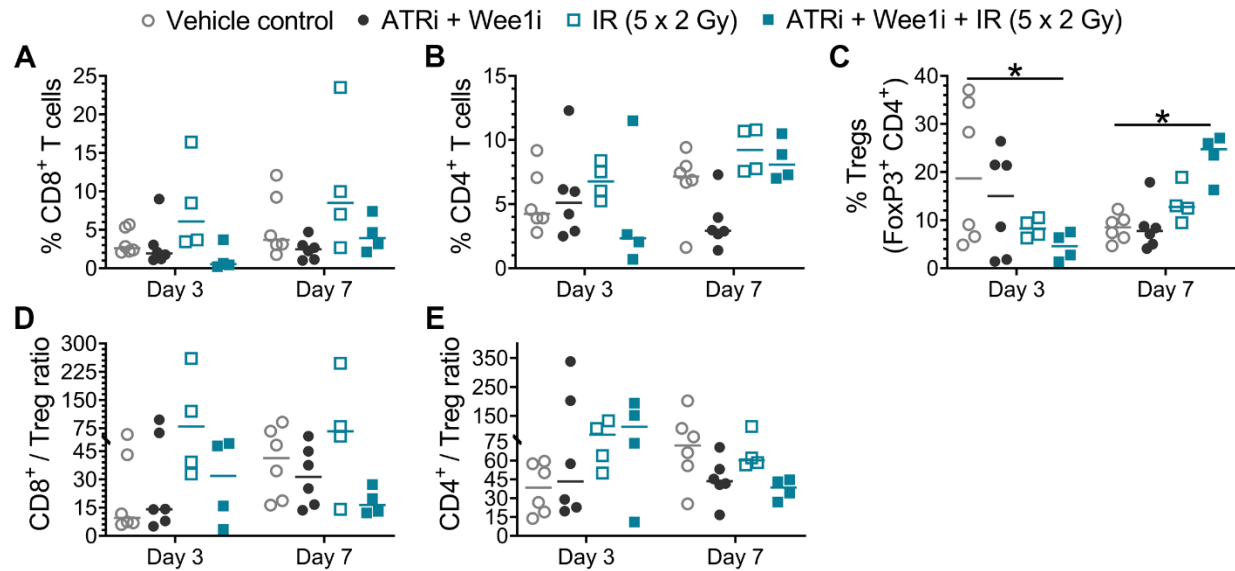


Figure 4.3. Radiation reduces the proportion of Tregs among TILs.

(A) The graph represents the percentage of CD8⁺ (CD3⁺ CD8⁺) tumor infiltrating cells. (B) The graph represents the percentage of tumor infiltrating CD4⁺ (CD3⁺ CD4⁺) T cells. (C) The graph represents the percentage of tumor infiltrating FoxP3⁺ (CD3⁺ CD4⁺ FoxP3⁺) Tregs. (D) The graph represents the CD8⁺ to Treg ratio. (E) The graph represents the CD4⁺ to Treg ratio. * indicates $P < 0.05$.

4.3.4 Combined inhibition of ATR and Wee1 concomitant with radiation diminishes CD8⁺ T cell effector function in 4T1 tumors in a time dependent manner

Based on our results so far, we see that combined treatment with ATRi + Wee1i + IR results in decreased expression of T cell exhaustion markers – PD-1, LAG-3, and TIM-3 – as well a reduction in the percentage of tumor infiltrating Tregs compared to vehicle control on day 3. IFN- γ is predominantly produced by T cells and NK cells in response to immune stimuli. IFN- γ activation can promote antitumor functions by augmenting the function of TIL and suppressing Treg cell function (Ivashkiv 2018). However, as unstimulated T lymphocytes produce little to no cytokine spontaneously, PMA and ionomycin are commonly used as stimulants *in vitro* to test the ability to produce IFN- γ (Baran *et al.* 2001). To assess if reduced T cell exhaustion marker expression and the percentage of Tregs result in increased effector T cell function, we evaluated the production of IFN- γ following stimulation with PMA and ionomycin at days 3 and 7 after the combined ATRi + Wee1i \pm IR 5 day-treatments. We see a striking reduction in the percentage of CD8⁺ T cells that produced IFN- γ in all our treatment groups at 3 days post-treatment in the radiation groups (\pm ATRi and Wee1i) (**Fig. 4.4**). Interestingly, 7 days post-treatment, the percentage of CD8⁺ T cells secreting IFN- γ was similar in all the treatment groups with no statistical significance observed (**Fig. 4.4**). Although puzzling, these findings indicate that if the antitumor immune response is truly CD8⁺ T cell mediated, it is likely *via* an alternative mechanism resulting in their activation (such as *via* TNF- α or IL-2) (Croft 2009, Ross and Cantrell 2018).

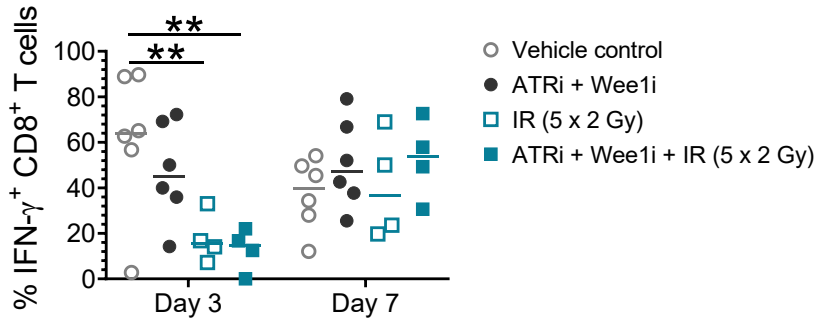


Figure 4.4. Impact of combined ATR, Wee1, and radiation treatment on CD8⁺ T cell effector function.

Graph shows the percentage of CD8⁺ T cells secreting IFN- γ . ** indicates $P < 0.01$.

4.3.5 Combined inhibition of ATR and Wee1 as an adjuvant to surgery prolongs overall survival of BALB/c mice

Surgery is a mainstay in treatment of early stage breast cancer and is an option for advanced stage patients with lower metastatic disease burden. We previously described that treatment of MDA-MB-231 tumor bearing immunocompromised mice with combined AZD6738 and AZD1775 for 26 days results in tumor regression to impalpable levels as well as suppression of (micro) metastasis (see **Chapter 2** (Bukhari *et al.* 2019)). However, once the treatment regime was completed, the presence of minimal residual disease eventually resulted in tumor recurrence in that immune-compromised mouse model (NSG mice). Based on this we hypothesized that surgical resection of primary tumor followed with adjuvant AZD6738 and AZD1775 over 3 weeks might result in tumor cure in our immune-competent mouse models of locally advanced disease.

A recent study found that surgery with negative margins can elicit an immune response to eliminate disseminated tumor cells and is curative in EMT6, but not the 4T1 tumor bearing mice (Piranlioglu *et al.* 2019). For this reason, we chose 4T1 as a model for our study. To identify tumor volumes at which surgery is non-curative, i.e., when tumor spread has likely already occurred, we performed mastectomies on 4T1 orthotopic tumor bearing mice (n = 4 mice per group) when the primary tumors were ~25 mm³, ~50 mm³, or ~100 mm³ (**Fig. 4.5A, B**). We see all mice in the ~100 mm³ surgery group had tumor recurrence either in the adjacent mammary fat pad or in the peritoneal cavity within 12-18 days post surgery (**Fig. 4.5C**). On the other hand, in some mice receiving surgery in the ~25 mm³ or the ~50 mm³ groups tumor recurrence was delayed, and a few mice showed indications of cure during the 3 month follow-up post surgery (**Fig. 4.5C**).

Since we know that surgeries on mice bearing ~100 mm³ 4T1 tumors is not curative in all cases and thus micro-metastasis must have already occurred, we used this point to evaluate the

impact of AZD6738 and AZD1775 as an adjuvant therapy to surgery for advanced (metastatic) breast cancer. Primary tumor removal surgeries were performed on 4T1 tumor bearing mice when the primary tumor volume reached $\sim 100 \text{ mm}^3$. These mice were then treated with either vehicle or combined AZD6738 (25 mg/kg) and AZD1775 (60 mg/kg) for 26 days (n = 4 mice per group). We note a dramatic increase in the overall survival of mice treated with ATRi and Wee1i with median survival of 65.5 days as compared to vehicle treated mice with median survival 34 days (**Fig. 4.5D**). Interestingly, one mouse showed no indication of tumor recurrence during 4 months of follow-up post-treatment. Taken together these findings, although limited by sample size, indicate that combined treatment with ATRi and Wee1i as an adjuvant to surgery prolongs survival, and in some cases, may even lead to tumor “cure” of BALB/c mice.

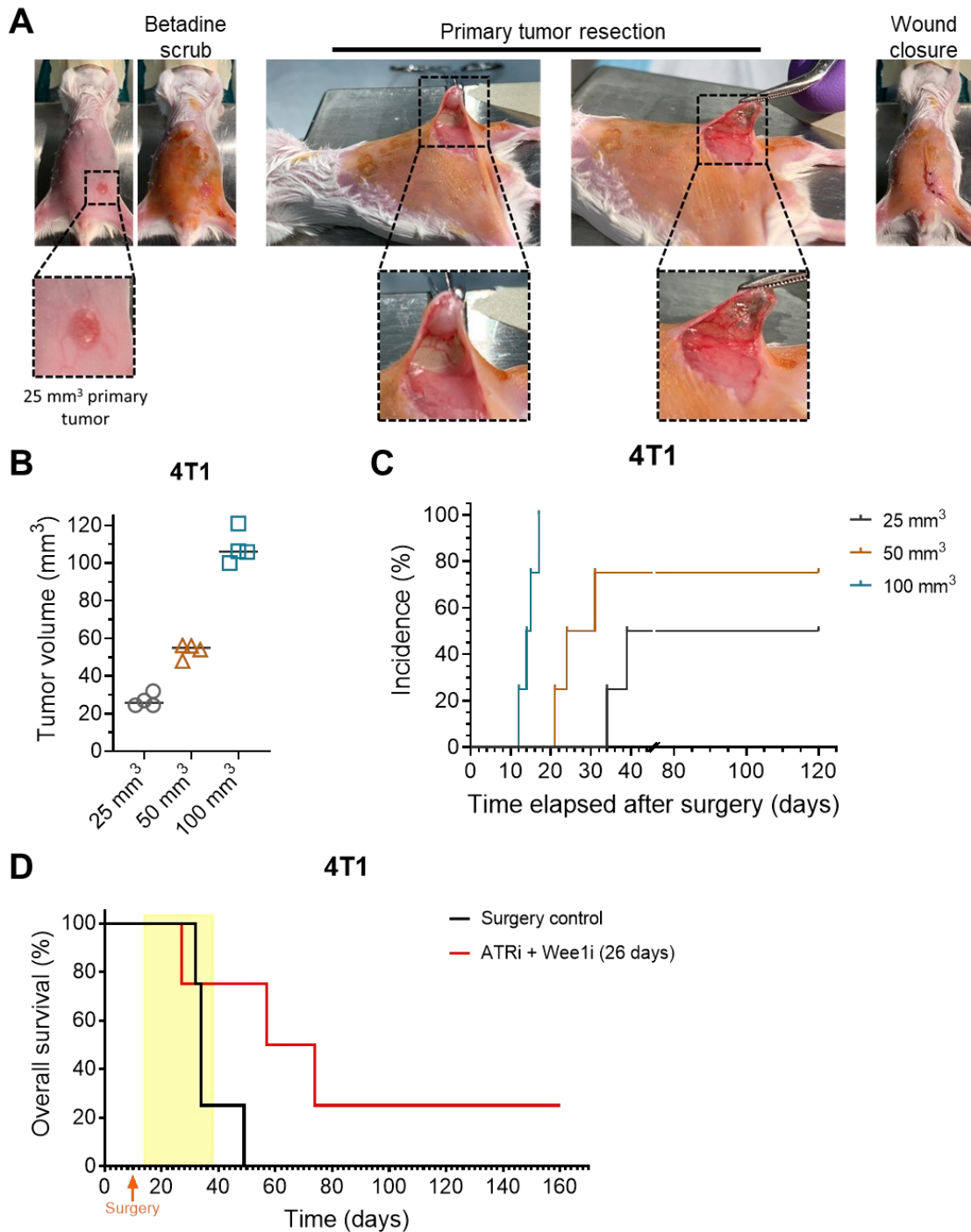


Figure 4.5. Combined inhibition of ATR and Wee1 as adjuvant therapy to surgery.

(A) Representative images of the surgery process of primary tumor removal. (B) The graph shows the tumor volume distribution in the three groups before surgery. (C) The incident curve shows the time it took for tumors to recur after surgery in the respective groups. (D) Kaplan-Meier survival curve of mice treated with either vehicle or combined ATR and Wee1 inhibitors for 26 days. The time of surgery (red arrow) and of drug treatment (yellow shaded area) are shown.

4.4 Discussion

Surgery and radiotherapy are central pillars in the multidisciplinary management of breast cancers. However, despite the advances in imaging guided conformal radiotherapy, normal tissue complications limit dose escalation. Additionally, in cancers, DDR pathways are often upregulated, ultimately resulting in radioresistance. In this regard, several small molecule inhibitors targeting the DDR are being tested as radiosensitizers to improve responses to radiotherapy by increasing tumor cell killing or eliciting an antitumor immune response. It is well established that radiotherapy can trigger immune responses to promote antitumor immunity (Weichselbaum *et al.* 2017), but can also enhance the infiltration of immune suppressive cells such as Tregs, tumor associated macrophages, and myeloid derived suppressor cells (Grassberger *et al.* 2019). Recent studies have shown that IR-induced antitumor immunity is improved when combined with ATR, Wee1, or immune checkpoint blockade inhibitors as single adjuvant agents (Deng *et al.* 2014, Twyman-Saint Victor *et al.* 2015, Vendetti *et al.* 2018, Dillon *et al.* 2019, Patel *et al.* 2019, Sheng *et al.* 2020, Wang *et al.* 2020).

In this preliminary study, we evaluated the impact of combined ATR inhibitor and Wee1 inhibitor treatment as radiosensitizers, and as an adjuvant to surgery. Here, we also provide preliminary evidence that ATRi + Wee1i + IR may promote an antitumor immune response resulting in delayed tumor growth and prolonged overall survival *in vivo*.

4.4.1 ATR and Wee1 inhibitors as radiosensitizers

Our preclinical syngeneic mouse model indicates that combination treatment with ATRi and Wee1i with conformal radiation therapy radiosensitizes 4T1 murine breast tumors, ultimately prolonging life span of these tumor bearing mice. While we acknowledge that this model does not accurately reflect clinical management of breast cancers, we believe it to be a good starting point

before we attempt to use an advanced model where surgery is performed prior to treatment with radiotherapy. Although there are no studies that report the use of combined ATRi and Wee1i as radiosensitizers, based on our published study (see **Chapter 2** (Bukhari *et al.* 2019)), these inhibitors work by abrogating the S and G2/M checkpoints and promoting premature mitotic entry. The addition of radiation increases DNA damage and enhances cell killing by combined ATR and Wee1 inhibition. There already are a few studies that have demonstrated radiosensitization by either ATRi or Wee1i (Bridges *et al.* 2011, Gamper *et al.* 2013, Dillon *et al.* 2017, Tu *et al.* 2018, Lee *et al.* 2019). A common mechanistic finding from these studies was that ATRi or Wee1i attenuate the radiation-induced G2/M checkpoint activation and induces cell death in p53 defective tumors. As we did not observe any correlation of synergistic cell killing with p53 status in our previous study (see **Chapter 2** (Bukhari *et al.* 2019)), we postulate that many tumors will benefit from combined ATRi and Wee1i treatment with IR. Phase I/II studies with AZD6738 (ATRi; Ceralasertib) and AZD1775 (Wee1i; Adavosertib) are currently underway where they are being evaluated as single agents in combination with various genotoxic agents including radiotherapy. The observed radiosensitization in our model may have significant implications for future clinical trials with the drug combination.

4.4.2 ATR and Wee1 inhibitors as activators of the immune response

An interesting observation made in the radiosensitization experiments *in vivo* was that tumor growth was delayed for over two weeks post-treatment in mice treated with just a 5 day treatment of ATRi + Wee1i + IR (**Fig. 4.1D**). Together with the lower expression of inhibitory ligands on CD8⁺ T cells (PD-1, TIM-3, and LAG-3) compared to the IR alone group (**Fig. 4.2A-C**), the growth delay indicates not just a stronger, but also a prolonged antitumor immune response. Radiation-induced DNA damage can promote the expression of markers like PD-L1 in cancer cells

in a ATR/Chk1-dependent manner (Sato *et al.* 2017). Although we did not test the expression of PD-L1 on tumor cells in our model, 4T1 tumors have been reported to have inherently high expression of PD-L1 to start with (Lian *et al.* 2019). This makes our model an attractive avenue for future studies evaluating the response of combined ATRi and Wee1i with immune checkpoint blockade therapies (like anti-PD-1/PD-L1) especially in breast cancers. Regarding immune cells, the combined ATRi and Wee1i treatment with radiotherapy also attenuated the expression of T cell exhaustion markers (PD-1, LAG-3, and TIM-3), which is consistent with recent reports evaluating the impact of ATRi or Wee1i (as individual drugs) plus radiotherapy on immune activation *in vivo* (Vendetti *et al.* 2018, Wang *et al.* 2020).

The PD-1/PD-L1 pathway can promote the development of Tregs and regulate their maintenance *via* the Treg-specific FoxP3 transcription factor (Francisco *et al.* 2009). In line with this finding, treatment with ATRi and Wee1i plus radiation dramatically reduced the proportion of tumor infiltrating Tregs among CD4⁺ cells at day 3, possibly due to the attenuation of PD-1 expressing CD8⁺ T cells (**Fig. 4.3C**). In agreement with other reports (Vendetti *et al.* 2018, Dillon *et al.* 2019), the reduction in the percentage of Tregs was transient, and we see an increase in the percentage of tumor infiltrating Tregs at day 7 in tumors treated with ATRi + Wee1i plus radiation. At day 3, ATRi + Wee1i plus radiation treatment resulted in elevated CD8⁺/Treg ratios compared to vehicle control, although this effect was not seen on day 7. It remains unclear whether ATRi + Wee1i ± radiation treatment impairs Treg proliferation or selectively kills the existing proliferating Tregs (Ghiringhelli *et al.* 2004). A recent report suggested that activated CD8⁺ T cells were more susceptible to killing by Chk1/2 and Wee1 inhibitors (McNally *et al.* 2017), and this could potentially explain the reduction in CD8⁺/Treg ratios at day 7. We suspect that combined treatment with ATRi and Wee1i may either selectively kill the rapidly proliferating CD8⁺ T cells or may

transiently impair activation of CD8⁺ T cells. Either way, it appears that combined ATRi and Wee1i treatment following radiation may delay the adaptive immune response, and later time points of analysis would be required for verification.

As previously mentioned, IFN- γ is secreted by T cells and NK cells in response to a variety of inflammatory or immune stimuli and can lead to antitumor functions (Ivashkiv 2018). However, like many cytokines, IFN- γ can also induce inhibitory mechanisms to limit the immune response (Hu and Ivashkiv 2009). With regard to this, IFN- γ has been shown to inhibit CD8⁺ T cell mediated antitumor immune response through Treg dependent suppression of the immune system, upregulation of PD-L1 on tumor cells, and upregulation of suppressor of cytokine signaling 2 (SOCS2) in dendritic cells (Spranger *et al.* 2013, Garcia-Diaz *et al.* 2017, Nirschl *et al.* 2017). We see that combined ATRi and Wee1i treatment reduced the proportion of CD8⁺ T cells secreting IFN- γ in the tumor microenvironment at day 3 and this likely resulted in the reduction of IFN- γ mediated PD-1 expression following radiation treatment (Spranger *et al.* 2013, Deng *et al.* 2014). Indeed, these results did not hold true at day 7 and we see a similar percentage of CD8⁺ T cells secreting IFN- γ . Besides IFN- γ , TNF- α has been shown to promote the activation and proliferation of naïve and effector T cells (Croft 2009). Additionally, another cytokine, IL-2 has been reported to promote T cell differentiation into effector T cells and memory T cells (Ross and Cantrell 2018). Therefore, it seems plausible that these factors may be playing a role in CD8⁺ T cell activation. Having said that, although not tested during our preliminary study, a secondary possibility is a NK cell mediated antitumor immune response. Moreover, Wee1 inhibition has been shown to sensitize head and neck cancers to NK cell based therapies (Friedman *et al.* 2018). Although, our study is limited by the small sample size (n = 4 mice per group) and absence of longer time points for analysis, collectively, our data provides preliminary evidence that combined ATRi and Wee1i

treatment with radiation promotes antitumor immunity and results in delayed tumor growth kinetics. Moreover, these early observations are valuable as neoadjuvant treatment with ATRi and Wee1i may also help reduce the number of Tregs in future clinical evaluations of this combination treatment. Future studies will also evaluate the role of NK cells in promoting antitumor immune response. Studies depleting CD8⁺ T cells and NK cells *in vivo* would enhance our understanding of major influencers in antitumor immunity following combined ATR and Wee1 inhibitor treatments.

4.4.3 A model for pre-clinical evaluation of ATR and Wee1 inhibitors as adjuvant therapy

The failure to completely eradicate minimal residual disease eventually results in tumor recurrence and metastasis. In fact, this was also evident in our previous study where we saw eventual tumor recurrence and metastasis on completion of treatment regime (Bukhari *et al.* 2019). Moreover, it has been long understood that dissemination of tumor cells from the primary tumor to distant sites occurs early during tumor development. However, the role of these early disseminated tumor cells in developing clinically significant metastasis remained unclear (Chambers *et al.* 2002, Hosseini *et al.* 2016). In this preliminary study, we assessed the impact of combined ATRi and Wee1i treatment as an adjuvant to surgery. Non-curative surgeries were performed at advanced tumor volumes to see if combined treatment with ATRi and Wee1i could eliminate metastasis. We used an immune-competent model of breast cancer to mimic the clinical setting where the immune response can aid cytotoxic agents in achieving a positive outcome. At present, there are no reported studies evaluating either ATR or Wee1 inhibitors as an adjuvant to surgery. A recent study demonstrated that surgical resection of primary tumor with negative margins allows the immune response to eradicate disseminated tumor cells in EMT6, but not in 4T1 tumors (Piranlioglu *et al.* 2019). Given that ATRi or Wee1i in combination with radiation

elicits an antitumor immune response (Vendetti *et al.* 2018, Wang *et al.* 2020), it would be worthwhile to combine radiation in this surgical model to not only eradicate any microscopic minimal residual disease but also to trigger an immune response in the process. While our study was limited to a small sample size, one mouse showed no indication of tumor recurrence following treatment with ATRi and Wee1i suggesting tumor “cure”. These early findings are encouraging for studies evaluating the impact of combined ATRi and Wee1i treatment in an adjuvant setting.

Chapter 5: General Discussion and Future Directions

5.1 ATR and Wee1 inhibition as a promising approach for breast cancer treatment

In our study, we exploited breast cancer's reliance on ATR and Wee1 for survival by using bioavailable inhibitors targeting these kinases to force cancer cells with damaged DNA into mitosis prematurely causing mitotic catastrophe in cancer cells, resulting in significant tumor control *in vivo*. An interesting finding from our study was that combined ATR and Wee1 inhibitor treatment resulted in highly synergistic killing of cancer stem-like "side population" cells. Of note, the cancer stem cell enriched populations isolated from MCF7 or MDA-MB-231 breast cancer cell lines were less sensitive to Wee1 or ATR inhibition as monotherapy compared to bulk populations from those cell lines. Future studies evaluating the mechanism underlying this effect would be of great interest especially because cancer stem-like cells are assumed to be the culprits of cancer therapy resistance, relapse, and metastasis. Additionally, these studies will confirm our findings by assessing the tumorigenic potential of side population cells in limiting dilution assays *in vivo*. Unpublished preliminary findings from our lab also show that inhibiting ATR or Wee1 radiosensitizes breast cancer side population cells, as assessed by clonogenic assays. Evaluation of this finding *in vivo* would be of additional interest as radiotherapy has implications for cancer stem cell plasticity (i.e., inducing a breast cancer stem-like phenotype in previously non-tumorigenic breast cancer cells) *via* activation of Notch signaling (Lagadec *et al.* 2012).

To mimic clinical scenarios in a preclinical setting, we also evaluated the impact of combined ATR and Wee1 inhibitor treatment in combination with radiation or as an adjuvant to surgery. Although preliminary, our findings are exciting because treatment with ATR and Wee1 inhibitors in combination with radiation for just 5 days results in significant tumor growth delay. The reason we treated for 5 days concomitantly is that we wanted to test ATR or Wee1 inhibition

for radiosensitization. Future studies will compare the 5 day ATRi + Wee1i + IR with IR followed by ATRi + Wee1i or vice versa, to estimate the radiosensitization effect by reducing the DNA repair capacity in cancer cells. In addition, we also see early evidence for activation of an antitumor immune response. IR has been shown to induce immunogenic cell death, a form of cell regulated tumor cell death that triggers an adaptive immune response and is reliant on the antigenicity or adjuvanticity of the dying tumor cells (Golden and Apetoh 2015). Moreover, when combined ATR and Wee1 inhibitor treatment is used as an adjuvant to surgery in locally advanced metastatic breast cancers, complete response to therapy may be achievable in at least a few cases. This is particularly exciting because advanced (metastatic) breast cancer remains virtually incurable in the clinic.

Our ongoing collaboration with AstraZeneca has promoted talks of a phase I clinical trial to evaluate the safety and efficacy of combined ATR and Wee1 inhibitor treatment. However, there have been delays as AstraZeneca expressed concerns about the toxicity of the Wee1 inhibitor in the ongoing Phase I/II clinical trials. Of note, the response to combined ATR and Wee1 inhibitor treatment we observed in our study was for a treatment regimen far below the maximum tolerated dose for the individual drugs provided to us by AstraZeneca. Despite this, we see strong synergy *in vitro* and *in vivo*. However, a clinical trial would need a dose escalation phase to evaluate the toxicity of different doses of AZD6738 and AZD1775 (likely in a standard 3 x 3 design). In addition, as [¹⁸F]-FLT is already used in the clinic as a PET tracer, trials evaluating combined ATR and Wee1 inhibitor could also employ [¹⁸F]-FLT for imaging to further validate our preclinical indications as a suitable non-invasive biomarker and potentially identify responders and non-responders.

5.2 Identification of potential biomarkers to predict sensitivity to ATR and Wee1 inhibitor treatment

Several studies have reported that treatment with ATR or Wee1 inhibitors can selectively target p53-deficient cancers (Hirai *et al.* 2009, Rajeshkumar *et al.* 2011, Reaper *et al.* 2011). However, we did not see this correlation in our breast cancer cell lines. Importantly, findings from phase I clinical trials of ATR or Wee1 inhibitors also showed poor correlation between drug sensitivity and p53 status (Do *et al.* 2015, Yap *et al.* 2021). Although, there are no clinical trials evaluating ATR and Wee1 inhibition as a combination treatment yet, we believe findings from pre-clinical and clinical studies evaluating either ATR or Wee1 inhibitors as single drugs may help us predict sensitivity biomarkers that could respond to this combination as well.

In a genome-wide CRISPR/Cas9 screen, 117 genes targets were identified, whose mutations result in hypersensitivity to two different ATR inhibitors, VE-821 and AZD6738 (Hustedt *et al.* 2019). The 11 targets validated in the study included *APEX2*, *ATM*, *ATRIP*, *C16orf72*, *C17orf53*, *CIP2A*, *POLE3*, *POLE4*, *RNASEH2A*, *RNASEH2B*, and *RNASEH2C* (Hustedt *et al.* 2019). Indeed, studies have previously shown sensitization of ATM-, ATRIP-, RNASEH2-deficient cells to ATR inhibition (Zou and Elledge 2003, Reaper *et al.* 2011, Gamper *et al.* 2013, Wang *et al.* 2019). Moreover, the overexpression of RNASEH2 was recently found to promote ATR inhibitor resistance (Wang *et al.* 2019). Another study recently performed a genome-wide CRISPR knockout and CRISPR activation screen to identify genes whose loss conferred resistance to ATR inhibitors (M6620 and AZD6738) (Schleicher *et al.* 2020). This study identified 118 overlapping targets between the two ATR inhibitors and validated seven common genes amongst the top 40 candidates, which include *KNTC1*, *EEF1B2*, *LUC7L3*, *SOD2*, *MED12*, *RETSAT*, and *LIAS* (Schleicher *et al.* 2020). Loss of any of these gene targets did not restore Chk1

phosphorylation following ATR inhibition indicating that these genes did not interfere with drug activity per se. In fact, resistance to both ATR inhibitors was induced by suppressing ATR inhibitor-induced apoptosis (loss of *LUC7L3*), stabilization of the replication fork following ATR inhibition (loss of *MED12* and *LIAS*), and activation of the TGF β pathway (*MED12* depletion) (Schleicher *et al.* 2020). Although we see synergy to combined ATR and Wee1 inhibitor treatment in all the tested human cancer cell lines in our study, future mechanistic studies in the combination therapy-resistant EMT6 murine breast cancer could provide insights on how to overcome resistance to combined ATR and Wee1 inhibitor treatment. During tumorigenesis, TGF β can act as an oncogene and promote cancer cell proliferation, tumor-initiating cell self-renewal, epithelial-to-mesenchymal transition, metastasis, and immune evasion (Ciardiello *et al.* 2020). Additionally, TGF β signaling is activated following radio- or chemotherapy (Kakeji *et al.* 1997) and tumors with high levels of TGF β are resistant to chemotherapy (Teicher *et al.* 1997). As several TGF β inhibitors are undergoing clinical trials (Ciardiello *et al.* 2020), it would be of great interest to assess the impact of ATR and Wee1 inhibition in combination with TGF β inhibitors particularly with regards to overcoming therapeutic resistance. Furthermore, a recent clinical study evaluating over 10,000 Chinese patients with 25 different tumor subtypes suggests that mutations in *ARID1A*, *ATM*, *BRCA1/2*, *MYC* amplification, and *CCNE1* amplification can help predict sensitivity to ATR inhibitors in the clinic (Shen *et al.* 2020).

With regard to the Wee1 kinase, a recent report studying breast cancers suggests that loss of PTEN may be one of the strongest markers of Wee1 inhibitor sensitivity in human breast cancers (Brunner *et al.* 2020). Interestingly, Wee1 inhibition in cells with PTEN loss also displayed decreased Chk1 activation suggesting reduced ATR activation. Hence, PTEN status could be a candidate predictive biomarker for combined ATR and Wee1 inhibitor treatment. Moreover, we

recently showed that the overexpression of PKMYT1 promotes intrinsic and acquired resistance to the Wee1 inhibitor AZD1775 (Adavosertib) in a variety of cancer cell lines (Lewis *et al.* 2019). Because Wee1 and PKMYT1 negatively regulate the mitotic checkpoint by regulating CDK1 expression, PKMYT1 could be used as a predictive biomarker to evaluate response to AZD1775 treatment. Furthermore, PKMYT1 was recently shown to be essential for cell survival in a subset of patient-derived glioblastoma cells with downregulated Wee1 expression (Toledo *et al.* 2015). The first selective and orally bioavailable PKMYT1 inhibitor (RP-6306, Repare Therapeutics) has just entered phase I clinical trials for safety and efficacy evaluation (Gallo *et al.* 2021). In a newly established collaboration with Repare Therapeutics, we will exploit the impact of RP-6306 in previously established Wee1 inhibitor resistant cell lines as well as in cancers with high expression of PKMYT1. Furthermore, as RP-3306 was identified as selectively toxic to cyclin E-overexpressing cancer cells (Gallo *et al.* 2021), and overexpression of cyclin E (*via* increased replication stress) also sensitizes to ATR inhibition, we expect PKMYT1 inhibition to synergize with ATR inhibition.

5.3 ATR and Wee1 inhibitor treatment in combination with other DDR targets

While several preclinical cancer models have demonstrated the impact of ATR or Wee1 inhibitors as monotherapy agents, their clinical use will likely be integrated into combination regimens with additional therapies. Indeed, chemotherapeutics that induce excess replication stress or DNA interstrand crosslinks have shown to synergize well with either ATR or Wee1 inhibitors. However, clinical trials have reported dose limiting toxicities relating to hematological malignancies when either ATR or Wee1 inhibitors are used in combination with platinum-based chemotherapeutics (Cuneo *et al.* 2019, Yap *et al.* 2020).

Given the crucial role of DDR pathways in promoting cancer cell survival in response to genotoxic stress, inhibitors of DDR become attractive targets for cancer therapy. In this regard, in addition to ATR and Wee1 inhibitors, ATM inhibitors have also made their way into the clinic. Furthermore, PARP inhibitors (Olaparib, Talazoparib, Rucaparib, and Niraparib) have already been approved for their clinical use in breast and ovarian cancers with BRCA mutation. The strong synergy observed in our study at low dose treatments with combined ATRi and Wee1i supports the idea of favourable clinical outcomes without reaching dose-limiting toxicities by resorting to synergistic interventions selective to cancer cells and at the same time opens room for combining this approach with other DDR targets and/or radiotherapy. Inhibition of ATR and Wee1 not only results in the abrogation of the S and G2/M cell cycle checkpoints by forced activation of CDK1 (see **Chapter 2**), but it also results in inhibition of HR (Gamper *et al.* 2013, Krajewska *et al.* 2013, Bukhari *et al.* 2019). The induction of this HR deficient state presents a unique opportunity to evaluate the effects of ATR and Wee1 inhibitors in combination with PARP inhibitors. Moreover, a few studies have used ATR or Wee1 inhibitors in combination with PARP inhibitors. Combined inhibition of ATR and PARP resulted in greater sensitization of the *BRCA* defective ovarian cancer cells beyond the sensitization already observed owing to their HR status (Huntoon *et al.* 2013, Kim *et al.* 2017). Similarly, combined inhibition of Wee1 and PARP has shown to radiosensitize pancreatic and *KRAS* mutant non-small cell lung cancer cells greater than when either are used as monotherapies (Karnak *et al.* 2014, Parsels *et al.* 2018). With strong support from these pre-clinical studies, nine clinical trials are investigating the use of ATR ± PARP inhibitors and two clinical trials are investigating the use of Wee1 ± PARP inhibitors (clinicaltrials.gov).

Besides PARP inhibitors, ATM inhibitors have also been shown to greatly radiosensitize cancer cells from various backgrounds when used in combination with ATR inhibitors (Sarkaria

et al. 1999, Gamper *et al.* 2013). At present, there are three ATM inhibitors being tested in clinical trials in combination with palliative radiotherapy, Olaparib, and irinotecan (clinicaltrials.gov). Of note, combining ATM inhibitors with other DDR targets has not gained enough attention likely due to the frequency of ATM or p53 defects in cancers. Additionally, there has been significant interest surrounding Chk1 inhibitors. However, their clinical progression was hindered due to associated cardiac toxicities (Sausville *et al.* 2014). Having said that, inhibition of multiple DNA repair pathways prevents cancer cells from compensating DNA damage, but care must be taken regarding the therapeutic index. Only targeting pathways cancer cells selectively rely on will avoid normal tissue complications. Furthermore, the key to successful combination regimes in terms of dose-limiting hematological toxicities will also be optimizing dose and scheduling.

5.4 ATR and Wee1 inhibitors in combination with radiotherapy and immune checkpoint blockade inhibitors

Radiotherapy is a staple in the treatment of cancer, and it has long been known to cause immune-activating as well as immune-suppressive effects on the tumor microenvironment. In the clinic, immune checkpoint blockade therapies targeting cytotoxic T lymphocyte-associated protein 4 (CTLA-4) and PD-1 have demonstrated impressive outcomes in patients with metastatic cancer and pre-existing antitumor immunity. However, in patients that lack pre-existing antitumor immunity, responses remain poor (Gajewski *et al.* 2013). In these patients, treatment with immune checkpoint inhibitors in combination with other therapies (like IR or ATRi or Wee1i in our case) can induce *de novo* antitumor immunity (Formenti and Demaria 2012). Exposure of tumor cells to cellular stressors (such as conventional chemotherapies or radiotherapy) can expose tumor-associated antigens on dying tumor cells for recognition and elimination by an adaptive immune response (Golden *et al.* 2014). This form of regulated tumor cell death is reliant on the antigenicity

and adjuvanticity of dying tumor cells and is termed immunogenic cell death (Golden *et al.* 2014). Here, the antigenic determinants of dying tumor cells could include tumor-associated antigens or expression of mutated genes among many others (Golden and Apetoh 2015). Similarly, the adjuvant components of dying tumor cells can cause the upregulation or release of DAMPs to alert the immune cells of potential threats (Kepp *et al.* 2009, Frey *et al.* 2015). The release of DAMPs following IR-induced tumor cell death can in turn recruit and activate dendritic cells to uptake and cross-present tumor antigens to naïve T cells thus triggering antitumor immune responses (Hernandez *et al.* 2016). Additionally, tumor cell recognition and killing by cytotoxic T cells can also be enhanced by IR-mediated upregulation of MHC I, FAS/CD95, and stress-induced natural killer group 2D-ligands on tumor cells (Chakraborty *et al.* 2003, Reits *et al.* 2006, Sridharan *et al.* 2016).

In regard to immune-suppression, several studies have shown upregulation of PD-L1 on tumor cells following radiotherapy and use of anti-PD-1/PD-L1 antibodies can block this aberrant upregulation of PD-L1 to enhance tumor control (Deng *et al.* 2014, Dovedi *et al.* 2014, Vendetti *et al.* 2018). PD-1 is a key immune checkpoint receptor mediating immune suppression on activated T cells by interaction with its ligand, PD-L1, which is commonly expressed on tumor cells (Pardoll 2012). Moreover, PD-L1 expression on tumor cells has been suggested as a predictive biomarker (Borghaei *et al.* 2015, Reck *et al.* 2016). Clinical trials of anti-PD-1/PD-L1 based immunotherapies have been encouraging and have led to their accelerated clinical approval for melanomas, non small cell lung cancers, and renal cancers (Garon *et al.* 2015, Gettinger *et al.* 2015, Robert *et al.* 2015, Robert *et al.* 2015). Recently, it was shown that tumor cells upregulate PD-L1 in response to DNA damage (Sato *et al.* 2017). Interestingly, Sato *et al.* found that ATM/ATR/Chk1 signaling upregulates PD-L1 expression on cancer cells in response to DNA

damage by activation of JAK/STAT/IRF1 pathway (Sato *et al.* 2017). In support of this report, a few other studies have recently shown that ATR inhibition downregulates PD-L1 expression on tumor cells and promotes CD8⁺ T cell mediated antitumor immune response (Sun *et al.* 2018, Vendetti *et al.* 2018, Sheng *et al.* 2020). Phase I trials of ATR or Wee1 inhibitors in combination with durvalumab (anti-PD-L1 antibody) are currently underway in patients with advanced stage cancers (clinicaltrials.gov). Future studies combining ATRi + Wee1i + IR with anti-PD-1/PD-L1 antibodies could promote a stronger antitumor immune response and prove to be a viable strategy for a variety of tumors. Moreover, combining local radiotherapy with systemic ATRi + Wee1i + anti-PD-1/PD-L1 could increase the likelihood of an abscopal effect and bring closer the goal of *in situ* cancer vaccination. Of note, pre-clinical studies combining local radiotherapy with systemic PD-1/PD-L1 blockade have demonstrated enhanced T cell response in the primary tumor and at metastatic lesions *via* abscopal effect (Deng *et al.* 2014, Park *et al.* 2015).

5.5 Conclusions

Combined ATR and Wee1 inhibition is a promising approach for the treatment of breast cancers, with excellent safety profiles at the dose used in our pre-clinical study. Nevertheless, it is to be expected that not all cancers respond to the combination treatment, as exemplified by EMT6 murine breast cancers which we identified as poor responders to combined ATR and Wee1 inhibitor treatment. Similar challenges are likely to arise in the clinic and use of imaging biomarkers (like [¹⁸F]-FLT) to identify responders and non-responders would allow for prompt treatment planning decisions. Having said that, even in highly metastatic cancers, combining ATR and Wee1 inhibitors with radiotherapy could promote an antitumor immune response with favourable outcome in the clinic. As the ATR and Wee1 inhibitors used in our study are currently undergoing phase I/II clinical trials, our approach could soon find application in the clinic.

Bibliography

- Aarts, M., R. Sharpe, I. Garcia-Murillas, H. Gevensleben, M. S. Hurd, S. D. Shumway, C. Toniatti, A. Ashworth and N. C. Turner (2012). "Forced mitotic entry of S-phase cells as a therapeutic strategy induced by inhibition of WEE1." Cancer Discov **2**(6): 524-539.
- Abdel-Fatah, T. M., F. K. Middleton, A. Arora, D. Agarwal, T. Chen, P. M. Moseley, C. Perry, R. Doherty, S. Chan, A. R. Green, E. Rakha, G. Ball, I. O. Ellis, N. J. Curtin and S. Madhusudan (2015). "Untangling the ATR-CHEK1 network for prognostication, prediction and therapeutic target validation in breast cancer." Mol Oncol **9**(3): 569-585.
- Abe, S., K. Nagasaka, Y. Hirayama, H. Kozuka-Hata, M. Oyama, Y. Aoyagi, C. Obuse and T. Hirota (2011). "The initial phase of chromosome condensation requires Cdk1-mediated phosphorylation of the CAP-D3 subunit of condensin II." Genes Dev **25**(8): 863-874.
- Acheampong, T., R. D. Kehm, M. B. Terry, E. L. Argov and P. Tehranifar (2020). "Incidence Trends of Breast Cancer Molecular Subtypes by Age and Race/Ethnicity in the US From 2010 to 2016." JAMA Netw Open **3**(8): e2013226.
- Ahmadzadeh, M., L. A. Johnson, B. Heemskerk, J. R. Wunderlich, M. E. Dudley, D. E. White and S. A. Rosenberg (2009). "Tumor antigen-specific CD8 T cells infiltrating the tumor express high levels of PD-1 and are functionally impaired." Blood **114**(8): 1537-1544.
- Akashi, K., D. Traver, T. Miyamoto and I. L. Weissman (2000). "A clonogenic common myeloid progenitor that gives rise to all myeloid lineages." Nature **404**(6774): 193-197.
- Alderton, G. K., H. Joenje, R. Varon, A. D. Borglum, P. A. Jeggo and M. O'Driscoll (2004). "Seckel syndrome exhibits cellular features demonstrating defects in the ATR-signalling pathway." Hum Mol Genet **13**(24): 3127-3138.
- Alonzi, R. (2015). "Functional Radiotherapy Targeting using Focused Dose Escalation." Clin Oncol (R Coll Radiol) **27**(10): 601-617.
- Bagnardi, V., M. Rota, E. Botteri, I. Tramacere, F. Islami, V. Fedirko, L. Scotti, M. Jenab, F. Turati, E. Pasquali, C. Pelucchi, C. Galeone, R. Bellocco, E. Negri, G. Corrao, P. Boffetta and C. La Vecchia (2015). "Alcohol consumption and site-specific cancer risk: a comprehensive dose-response meta-analysis." Br J Cancer **112**(3): 580-593.
- Ball, H. L., J. S. Myers and D. Cortez (2005). "ATRIP binding to replication protein A-single-stranded DNA promotes ATR-ATRIP localization but is dispensable for Chk1 phosphorylation." Mol Biol Cell **16**(5): 2372-2381.
- Bao, S., Q. Wu, R. E. McLendon, Y. Hao, Q. Shi, A. B. Hjelmeland, M. W. Dewhirst, D. D. Bigner and J. N. Rich (2006). "Glioma stem cells promote radioresistance by preferential activation of the DNA damage response." Nature **444**(7120): 756-760.
- Baran, J., D. Kowalczyk, M. Ozog and M. Zembala (2001). "Three-color flow cytometry detection of intracellular cytokines in peripheral blood mononuclear cells: comparative analysis of phorbol myristate acetate-ionomycin and phytohemagglutinin stimulation." Clin Diagn Lab Immunol **8**(2): 303-313.

- Barber, D. L., E. J. Wherry, D. Masopust, B. Zhu, J. P. Allison, A. H. Sharpe, G. J. Freeman and R. Ahmed (2006). "Restoring function in exhausted CD8 T cells during chronic viral infection." Nature **439**(7077): 682-687.
- Barker, N., J. H. van Es, J. Kuipers, P. Kujala, M. van den Born, M. Cozijnsen, A. Haegebarth, J. Korving, H. Begthel, P. J. Peters and H. Clevers (2007). "Identification of stem cells in small intestine and colon by marker gene *Lgr5*." Nature **449**(7165): 1003-1007.
- Barnieh, F. M., P. M. Loadman and R. A. Falconer (2021). "Progress towards a clinically-successful ATR inhibitor for cancer therapy." Current Research in Pharmacology and Drug Discovery **2**: 100017.
- Bartucci, M., S. Svensson, P. Romania, R. Dattilo, M. Patrizii, M. Signore, S. Navarra, F. Lotti, M. Biffoni, E. Pillozzi, E. Duranti, S. Martinelli, C. Rinaldo, A. Zeuner, M. Maugeri-Sacca, A. Eramo and R. De Maria (2012). "Therapeutic targeting of Chk1 in NSCLC stem cells during chemotherapy." Cell Death Differ **19**(5): 768-778.
- Beck, H., V. Nahse, M. S. Larsen, P. Groth, T. Clancy, M. Lees, M. Jorgensen, T. Helleday, R. G. Syljuasen and C. S. Sorensen (2010). "Regulators of cyclin-dependent kinases are crucial for maintaining genome integrity in S phase." J Cell Biol **188**(5): 629-638.
- Beeharry, N., J. B. Rattner, J. P. Caviston and T. Yen (2013). "Centromere fragmentation is a common mitotic defect of S and G2 checkpoint override." Cell Cycle **12**(10): 1588-1597.
- Been, L. B., P. H. Elsinga, J. de Vries, D. C. Cobben, P. L. Jager, H. J. Hoekstra and A. J. Suurmeijer (2006). "Positron emission tomography in patients with breast cancer using (18)F-3'-deoxy-3'-fluoro-l-thymidine ((18)F-FLT)-a pilot study." Eur J Surg Oncol **32**(1): 39-43.
- Been, L. B., A. J. Suurmeijer, D. C. Cobben, P. L. Jager, H. J. Hoekstra and P. H. Elsinga (2004). "[18F]FLT-PET in oncology: current status and opportunities." Eur J Nucl Med Mol Imaging **31**(12): 1659-1672.
- Blank, C. U., W. N. Haining, W. Held, P. G. Hogan, A. Kallies, E. Lugli, R. C. Lynn, M. Philip, A. Rao, N. P. Restifo, A. Schietinger, T. N. Schumacher, P. L. Schwartzberg, A. H. Sharpe, D. E. Speiser, E. J. Wherry, B. A. Youngblood and D. Zehn (2019). "Defining 'T cell exhaustion'." Nat Rev Immunol **19**(11): 665-674.
- Bollineni, V. R., G. M. Kramer, E. P. Jansma, Y. Liu and W. J. Oyen (2016). "A systematic review on [(18)F]FLT-PET uptake as a measure of treatment response in cancer patients." Eur J Cancer **55**: 81-97.
- Bollineni, V. R., J. Widder, J. Pruijm, J. A. Langendijk and E. M. Wiegman (2012). "Residual (1)(8)F-FDG-PET uptake 12 weeks after stereotactic ablative radiotherapy for stage I non-small-cell lung cancer predicts local control." Int J Radiat Oncol Biol Phys **83**(4): e551-555.
- Booher, R. N., P. S. Holman and A. Fattaey (1997). "Human Myt1 is a cell cycle-regulated kinase that inhibits Cdc2 but not Cdk2 activity." J Biol Chem **272**(35): 22300-22306.
- Borghaei, H., L. Paz-Ares, L. Horn, D. R. Spigel, M. Steins, N. E. Ready, L. Q. Chow, E. E. Vokes, E. Felip, E. Holgado, F. Barlesi, M. Kohlhaufl, O. Arrieta, M. A. Burgio, J. Fayette, H. Lena, E. Poddubskaya, D. E. Gerber, S. N. Gettinger, C. M. Rudin, N. Rizvi, L. Crino, G. R. Blumenschein, Jr., S. J. Antonia, C. Dorange, C. T. Harbison, F. Graf Finckenstein and J. R. Brahmer (2015).

"Nivolumab versus Docetaxel in Advanced Nonsquamous Non-Small-Cell Lung Cancer." N Engl J Med **373**(17): 1627-1639.

Brandsma, I., E. D. G. Fleuren, C. T. Williamson and C. J. Lord (2017). "Directing the use of DDR kinase inhibitors in cancer treatment." Expert Opin Investig Drugs **26**(12): 1341-1355.

Brepoels, L., S. Stroobants, G. Verhoef, T. De Groot, L. Mortelmans and C. De Wolf-Peeters (2009). "(18)F-FDG and (18)F-FLT uptake early after cyclophosphamide and mTOR inhibition in an experimental lymphoma model." J Nucl Med **50**(7): 1102-1109.

Bridges, K. A., H. Hirai, C. A. Buser, C. Brooks, H. Liu, T. A. Buchholz, J. M. Molkenkine, K. A. Mason and R. E. Meyn (2011). "MK-1775, a novel Wee1 kinase inhibitor, radiosensitizes p53-defective human tumor cells." Clin Cancer Res **17**(17): 5638-5648.

Brinkley, B. R., R. P. Zinkowski, W. L. Mollon, F. M. Davis, M. A. Pisegna, M. Pershouse and P. N. Rao (1988). "Movement and segregation of kinetochores experimentally detached from mammalian chromosomes." Nature **336**(6196): 251-254.

Brizuela, L., G. Draetta and D. Beach (1989). "Activation of human CDC2 protein as a histone H1 kinase is associated with complex formation with the p62 subunit." Proc Natl Acad Sci U S A **86**(12): 4362-4366.

Brockenbrough, J. S., T. Souquet, J. K. Morihara, J. E. Stern, S. E. Hawes, J. S. Rasey, A. Leblond, L. W. Wiens, Q. Feng, J. Grierson and H. Vesselle (2011). "Tumor 3'-deoxy-3'-(18)F-fluorothymidine ((18)F-FLT) uptake by PET correlates with thymidine kinase 1 expression: static and kinetic analysis of (18)F-FLT PET studies in lung tumors." J Nucl Med **52**(8): 1181-1188.

Brown, E. J. and D. Baltimore (2000). "ATR disruption leads to chromosomal fragmentation and early embryonic lethality." Genes Dev **14**(4): 397-402.

Brunner, A., A. Suryo Rahmanto, H. Johansson, M. Franco, J. Viiliainen, M. Gazi, O. Frings, E. Fredlund, C. Spruck, J. Lehtio, J. K. Rantala, L. G. Larsson and O. Sangfelt (2020). "PTEN and DNA-PK determine sensitivity and recovery in response to WEE1 inhibition in human breast cancer." Elife **9**.

Bryant, H. E., N. Schultz, H. D. Thomas, K. M. Parker, D. Flower, E. Lopez, S. Kyle, M. Meuth, N. J. Curtin and T. Helleday (2005). "Specific killing of BRCA2-deficient tumours with inhibitors of poly(ADP-ribose) polymerase." Nature **434**(7035): 913-917.

Buck, A. K., K. Herrmann, C. Shen, T. Dechow, M. Schwaiger and H. J. Wester (2009). "Molecular imaging of proliferation in vivo: positron emission tomography with [18F]fluorothymidine." Methods **48**(2): 205-215.

Buisson, R., J. Niraj, A. Rodrigue, C. K. Ho, J. Kreuzer, T. K. Foo, E. J. Hardy, G. Dellaire, W. Haas, B. Xia, J. Y. Masson and L. Zou (2017). "Coupling of Homologous Recombination and the Checkpoint by ATR." Mol Cell **65**(2): 336-346.

Bukhari, A. B., C. W. Lewis, J. J. Pearce, D. Luong, G. K. Chan and A. M. Gamper (2019). "Inhibiting Wee1 and ATR kinases produces tumor-selective synthetic lethality and suppresses metastasis." J Clin Invest **129**(3): 1329-1344.

- Caldecott, K. W. (2008). "Single-strand break repair and genetic disease." Nat Rev Genet **9**(8): 619-631.
- Cardoso, F., S. Paluch-Shimon, E. Senkus, G. Curigliano, M. S. Aapro, F. Andre, C. H. Barrios, J. Bergh, G. S. Bhattacharyya, L. Biganzoli, F. Boyle, M. J. Cardoso, L. A. Carey, J. Cortes, N. S. El Saghir, M. Elzayat, A. Eniu, L. Fallowfield, P. A. Francis, K. Gelmon, J. Gligorov, R. Haidinger, N. Harbeck, X. Hu, B. Kaufman, R. Kaur, B. E. Kiely, S. B. Kim, N. U. Lin, S. A. Mertz, S. Neciosup, B. V. Offersen, S. Ohno, O. Pagani, A. Prat, F. Penault-Llorca, H. S. Rugo, G. W. Sledge, C. Thomssen, D. A. Vorobiof, T. Wiseman, B. Xu, L. Norton, A. Costa and E. P. Winer (2020). "5th ESO-ESMO international consensus guidelines for advanced breast cancer (ABC 5)." Ann Oncol **31**(12): 1623-1649.
- Carey, L. A., C. M. Perou, C. A. Livasy, L. G. Dressler, D. Cowan, K. Conway, G. Karaca, M. A. Troester, C. K. Tse, S. Edmiston, S. L. Deming, J. Geradts, M. C. Cheang, T. O. Nielsen, P. G. Moorman, H. S. Earp and R. C. Millikan (2006). "Race, breast cancer subtypes, and survival in the Carolina Breast Cancer Study." JAMA **295**(21): 2492-2502.
- Chakraborty, M., S. I. Abrams, K. Camphausen, K. Liu, T. Scott, C. N. Coleman and J. W. Hodge (2003). "Irradiation of tumor cells up-regulates Fas and enhances CTL lytic activity and CTL adoptive immunotherapy." J Immunol **170**(12): 6338-6347.
- Chalkidou, A., D. B. Landau, E. W. Odell, V. R. Cornelius, M. J. O'Doherty and P. K. Marsden (2012). "Correlation between Ki-67 immunohistochemistry and 18F-fluorothymidine uptake in patients with cancer: A systematic review and meta-analysis." Eur J Cancer **48**(18): 3499-3513.
- Chambers, A. F., A. C. Groom and I. C. MacDonald (2002). "Dissemination and growth of cancer cells in metastatic sites." Nat Rev Cancer **2**(8): 563-572.
- Chan, K. L., T. Palmai-Pallag, S. Ying and I. D. Hickson (2009). "Replication stress induces sister-chromatid bridging at fragile site loci in mitosis." Nat Cell Biol **11**(6): 753-760.
- Chao, K. S., J. O. Deasy, J. Markman, J. Haynie, C. A. Perez, J. A. Purdy and D. A. Low (2001). "A prospective study of salivary function sparing in patients with head-and-neck cancers receiving intensity-modulated or three-dimensional radiation therapy: initial results." Int J Radiat Oncol Biol Phys **49**(4): 907-916.
- Charrier, J. D., S. J. Durrant, J. M. Golec, D. P. Kay, R. M. Knegt, S. MacCormick, M. Mortimore, M. E. O'Donnell, J. L. Pinder, P. M. Reaper, A. P. Rutherford, P. S. Wang, S. C. Young and J. R. Pollard (2011). "Discovery of potent and selective inhibitors of ataxia telangiectasia mutated and Rad3 related (ATR) protein kinase as potential anticancer agents." J Med Chem **54**(7): 2320-2330.
- Chen, W., T. Cloughesy, N. Kamdar, N. Satyamurthy, M. Bergsneider, L. Liau, P. Mischel, J. Czernin, M. E. Phelps and D. H. Silverman (2005). "Imaging proliferation in brain tumors with 18F-FLT PET: comparison with 18F-FDG." J Nucl Med **46**(6): 945-952.
- Chen, W. Y., B. Rosner, S. E. Hankinson, G. A. Colditz and W. C. Willett (2011). "Moderate alcohol consumption during adult life, drinking patterns, and breast cancer risk." JAMA **306**(17): 1884-1890.

Chikuma, S., S. Terawaki, T. Hayashi, R. Nabeshima, T. Yoshida, S. Shibayama, T. Okazaki and T. Honjo (2009). "PD-1-mediated suppression of IL-2 production induces CD8⁺ T cell anergy in vivo." *J Immunol* **182**(11): 6682-6689.

Choi, S. J., J. S. Kim, J. H. Kim, S. J. Oh, J. G. Lee, C. J. Kim, Y. S. Ra, J. S. Yeo, J. S. Ryu and D. H. Moon (2005). "[¹⁸F]3'-deoxy-3'-fluorothymidine PET for the diagnosis and grading of brain tumors." *Eur J Nucl Med Mol Imaging* **32**(6): 653-659.

Chow, E., Y. M. van der Linden, D. Roos, W. F. Hartsell, P. Hoskin, J. S. Wu, M. D. Brundage, A. Nabid, C. J. Tissing-Tan, B. Oei, S. Babington, W. F. Demas, C. F. Wilson, R. M. Meyer, B. E. Chen and R. K. Wong (2014). "Single versus multiple fractions of repeat radiation for painful bone metastases: a randomised, controlled, non-inferiority trial." *Lancet Oncol* **15**(2): 164-171.

Chow, J. P., R. Y. Poon and H. T. Ma (2011). "Inhibitory phosphorylation of cyclin-dependent kinase 1 as a compensatory mechanism for mitosis exit." *Mol Cell Biol* **31**(7): 1478-1491.

Ciardiello, D., E. Elez, J. Tabernero and J. Seoane (2020). "Clinical development of therapies targeting TGFbeta: current knowledge and future perspectives." *Ann Oncol* **31**(10): 1336-1349.

Ciccia, A. and S. J. Elledge (2010). "The DNA damage response: making it safe to play with knives." *Mol Cell* **40**(2): 179-204.

Clarke, M., R. Collins, S. Darby, C. Davies, P. Elphinstone, V. Evans, J. Godwin, R. Gray, C. Hicks, S. James, E. MacKinnon, P. McGale, T. McHugh, R. Peto, C. Taylor, Y. Wang and G. Early Breast Cancer Trialists' Collaborative (2005). "Effects of radiotherapy and of differences in the extent of surgery for early breast cancer on local recurrence and 15-year survival: an overview of the randomised trials." *Lancet* **366**(9503): 2087-2106.

Cline, M. S., R. G. Liao, M. T. Parsons, B. Paten, F. Alquaddoomi, A. Antoniou, S. Baxter, L. Brody, R. Cook-Deegan, A. Coffin, F. J. Couch, B. Craft, R. Currie, C. C. Dlott, L. Dolman, J. T. den Dunnen, S. O. M. Dyke, S. M. Domchek, D. Easton, Z. Fischmann, W. D. Foulkes, J. Garber, D. Goldgar, M. J. Goldman, P. Goodhand, S. Harrison, D. Haussler, K. Kato, B. Knoppers, C. Markello, R. Nussbaum, K. Offit, S. E. Plon, J. Rashbass, H. L. Rehm, M. Robson, W. S. Rubinstein, D. Stoppa-Lyonnet, S. Tavtigian, A. Thorogood, C. Zhang, M. Zimmermann, B. C. Authors, J. Burn, S. Chanock, G. Ratsch and A. B. Spurdle (2018). "BRCA Challenge: BRCA Exchange as a global resource for variants in BRCA1 and BRCA2." *PLoS Genet* **14**(12): e1007752.

Combes, E., A. F. Andrade, D. Tosi, H. A. Michaud, F. Coquel, V. Garambois, D. Desigaud, M. Jarlier, A. Coquelle, P. Pasero, N. Bonnefoy, J. Moreaux, P. Martineau, M. Del Rio, R. L. Beijersbergen, N. Vezzio-Vie and C. Gongora (2019). "Inhibition of Ataxia-Telangiectasia Mutated and RAD3-Related (ATR) Overcomes Oxaliplatin Resistance and Promotes Antitumor Immunity in Colorectal Cancer." *Cancer Res* **79**(11): 2933-2946.

Committee, C. C. S. A. (2019). Canadian Cancer Statistics 2019. Toronto, ON, Canadian Cancer Society.

Contractor, K. B., L. M. Kenny, J. Stebbing, A. Challapalli, A. Al-Nahhas, C. Palmieri, S. Shousha, J. S. Lewis, K. Hogben, Q. De Nguyen, R. C. Coombes and E. O. Aboagye (2011). "Biological basis of [(1)(1)C]choline-positron emission tomography in patients with breast cancer:

comparison with [(1)(8)F]fluorothymidine positron emission tomography." Nucl Med Commun **32**(11): 997-1004.

Cortez, D., S. Guntuku, J. Qin and S. J. Elledge (2001). "ATR and ATRIP: partners in checkpoint signaling." Science **294**(5547): 1713-1716.

Costa, L. J. (2007). "Aspects of mTOR biology and the use of mTOR inhibitors in non-Hodgkin's lymphoma." Cancer Treat Rev **33**(1): 78-84.

Coussens, L. M., L. Zitvogel and A. K. Palucka (2013). "Neutralizing tumor-promoting chronic inflammation: a magic bullet?" Science **339**(6117): 286-291.

Creighton, C. J. (2012). "The molecular profile of luminal B breast cancer." Biologics **6**: 289-297.

Crippa, F., R. Agresti, M. Sandri, G. Mariani, B. Padovano, A. Alessi, G. Bianchi, E. Bombardieri, I. Maugeri, M. Rampa, M. L. Carcangiu, G. Trecate, C. Pascali, A. Bogni, G. Martelli and F. de Braud (2015). "(1)(8)F-FLT PET/CT as an imaging tool for early prediction of pathological response in patients with locally advanced breast cancer treated with neoadjuvant chemotherapy: a pilot study." Eur J Nucl Med Mol Imaging **42**(6): 818-830.

Crittenden, M. R., T. Savage, B. Cottam, J. Baird, P. C. Rodriguez, P. Newell, K. Young, A. M. Jackson and M. J. Gough (2014). "Expression of arginase I in myeloid cells limits control of residual disease after radiation therapy of tumors in mice." Radiat Res **182**(2): 182-190.

Croft, M. (2009). "The role of TNF superfamily members in T-cell function and diseases." Nat Rev Immunol **9**(4): 271-285.

Cuneo, K. C., M. A. Morgan, M. A. Davis, L. A. Parcels, J. Parcels, D. Karnak, C. Ryan, N. Liu, J. Maybaum and T. S. Lawrence (2016). "Wee1 Kinase Inhibitor AZD1775 Radiosensitizes Hepatocellular Carcinoma Regardless of TP53 Mutational Status Through Induction of Replication Stress." Int J Radiat Oncol Biol Phys **95**(2): 782-790.

Cuneo, K. C., M. A. Morgan, V. Sahai, M. J. Schipper, L. A. Parsels, J. D. Parsels, T. Devasia, M. Al-Hawaray, C. S. Cho, H. Nathan, J. Maybaum, M. M. Zalupski and T. S. Lawrence (2019). "Dose Escalation Trial of the Wee1 Inhibitor Adavosertib (AZD1775) in Combination With Gemcitabine and Radiation for Patients With Locally Advanced Pancreatic Cancer." J Clin Oncol **37**(29): 2643-2650.

Curtin, N. J. (2012). "DNA repair dysregulation from cancer driver to therapeutic target." Nat Rev Cancer **12**(12): 801-817.

Dai, Y. and S. Grant (2010). "New insights into checkpoint kinase 1 in the DNA damage response signaling network." Clin Cancer Res **16**(2): 376-383.

Davis, M. M. and P. J. Bjorkman (1988). "T-cell antigen receptor genes and T-cell recognition." Nature **334**(6181): 395-402.

de Klein, A., M. Muijtjens, R. van Os, Y. Verhoeven, B. Smit, A. M. Carr, A. R. Lehmann and J. H. Hoeijmakers (2000). "Targeted disruption of the cell-cycle checkpoint gene ATR leads to early embryonic lethality in mice." Curr Biol **10**(8): 479-482.

- Debeb, B. G., W. Xu and W. A. Woodward (2009). "Radiation resistance of breast cancer stem cells: understanding the clinical framework." J Mammary Gland Biol Neoplasia **14**(1): 11-17.
- Delacroix, S., J. M. Wagner, M. Kobayashi, K. Yamamoto and L. M. Karnitz (2007). "The Rad9-Hus1-Rad1 (9-1-1) clamp activates checkpoint signaling via TopBP1." Genes Dev **21**(12): 1472-1477.
- Deng, L., H. Liang, B. Burnette, M. Beckett, T. Darga, R. R. Weichselbaum and Y. X. Fu (2014). "Irradiation and anti-PD-L1 treatment synergistically promote antitumor immunity in mice." J Clin Invest **124**(2): 687-695.
- Denkert, C., C. Liedtke, A. Tutt and G. von Minckwitz (2017). "Molecular alterations in triple-negative breast cancer-the road to new treatment strategies." Lancet **389**(10087): 2430-2442.
- Denkert, C., S. Loibl, A. Noske, M. Roller, B. M. Muller, M. Komor, J. Budczies, S. Darb-Esfahani, R. Kronenwett, C. Hanusch, C. von Torne, W. Weichert, K. Engels, C. Solbach, I. Schrader, M. Dietel and G. von Minckwitz (2010). "Tumor-associated lymphocytes as an independent predictor of response to neoadjuvant chemotherapy in breast cancer." J Clin Oncol **28**(1): 105-113.
- Derlin, T., V. Grunwald, J. Steinbach, H. J. Wester and T. L. Ross (2018). "Molecular Imaging in Oncology Using Positron Emission Tomography." Dtsch Arztebl Int **115**(11): 175-181.
- Dillon, M., J. Guevara, K. Mohammed, S. A. Smith, E. Dean, L. McLellan, Z. Boylan, J. Spicer, M. D. Forster and K. J. Harrington (2019). "A phase I study of ATR inhibitor, AZD6738, as monotherapy in advanced solid tumours (PATRIOT part A, B)." Annals of Oncology **30**: v165-v166.
- Dillon, M. T., H. E. Barker, M. Pedersen, H. Hafsi, S. A. Bhide, K. L. Newbold, C. M. Nutting, M. McLaughlin and K. J. Harrington (2017). "Radiosensitization by the ATR Inhibitor AZD6738 through Generation of Acentric Micronuclei." Mol Cancer Ther **16**(1): 25-34.
- Dillon, M. T., K. F. Bergerhoff, M. Pedersen, H. Whittock, E. Crespo-Rodriguez, E. C. Patin, A. Pearson, H. G. Smith, J. T. E. Paget, R. R. Patel, S. Foo, G. Bozhanova, C. Ragulan, E. Fontana, K. Desai, A. C. Wilkins, A. Sadanandam, A. Melcher, M. McLaughlin and K. J. Harrington (2019). "ATR Inhibition Potentiates the Radiation-induced Inflammatory Tumor Microenvironment." Clin Cancer Res **25**(11): 3392-3403.
- Dillon, M. T., K. F. Bergerhoff, M. Pedersen, H. Whittock, E. Crespo-Rodriguez, E. C. Patin, A. Pearson, H. G. Smith, J. T. E. Paget, R. R. Patel, S. Foo, G. Bozhanova, C. Ragulan, E. Fontana, K. Desai, A. C. Wilkins, A. Sadanandam, A. Melcher, M. McLaughlin and K. J. Harrington (2019). "ATR Inhibition Potentiates the Radiation-induced Inflammatory Tumor Microenvironment." Clin Cancer Res.
- Dillon, M. T., Z. Boylan, D. Smith, J. Guevara, K. Mohammed, C. Peckitt, M. Saunders, U. Banerji, G. Clack, S. A. Smith, J. F. Spicer, M. D. Forster and K. J. Harrington (2018). "PATRIOT: A phase I study to assess the tolerability, safety and biological effects of a specific ataxia telangiectasia and Rad3-related (ATR) inhibitor (AZD6738) as a single agent and in combination with palliative radiation therapy in patients with solid tumours." Clin Transl Radiat Oncol **12**: 16-20.

- Do, K., J. H. Doroshow and S. Kummar (2013). "Wee1 kinase as a target for cancer therapy." Cell Cycle **12**(19): 3159-3164.
- Do, K., D. Wilsker, J. Ji, J. Zlott, T. Freshwater, R. J. Kinders, J. Collins, A. P. Chen, J. H. Doroshow and S. Kummar (2015). "Phase I Study of Single-Agent AZD1775 (MK-1775), a Wee1 Kinase Inhibitor, in Patients With Refractory Solid Tumors." J Clin Oncol **33**(30): 3409-3415.
- Dominguez-Kelly, R., Y. Martin, S. Koundrioukoff, M. E. Tanenbaum, V. A. Smits, R. H. Medema, M. Debatisse and R. Freire (2011). "Wee1 controls genomic stability during replication by regulating the Mus81-Eme1 endonuclease." J Cell Biol **194**(4): 567-579.
- Donegan, W. L. (1997). "Tumor-related prognostic factors for breast cancer." CA Cancer J Clin **47**(1): 28-51.
- Donzelli, M. and G. F. Draetta (2003). "Regulating mammalian checkpoints through Cdc25 inactivation." EMBO Rep **4**(7): 671-677.
- Dovedi, S. J., A. L. Adlard, G. Lipowska-Bhalla, C. McKenna, S. Jones, E. J. Cheadle, I. J. Stratford, E. Poon, M. Morrow, R. Stewart, H. Jones, R. W. Wilkinson, J. Honeychurch and T. M. Illidge (2014). "Acquired resistance to fractionated radiotherapy can be overcome by concurrent PD-L1 blockade." Cancer Res **74**(19): 5458-5468.
- Drosos, Y., D. Escobar, M. Y. Chiang, K. Roys, V. Valentine, M. B. Valentine, J. E. Rehg, V. Sahai, L. A. Begley, J. Ye, L. Paul, P. J. McKinnon and B. Sosa-Pineda (2017). "ATM-deficiency increases genomic instability and metastatic potential in a mouse model of pancreatic cancer." Sci Rep **7**(1): 11144.
- Dunn, G. P., C. M. Koebel and R. D. Schreiber (2006). "Interferons, immunity and cancer immunoediting." Nat Rev Immunol **6**(11): 836-848.
- Early Breast Cancer Trialists' Collaborative, G., S. Darby, P. McGale, C. Correa, C. Taylor, R. Arriagada, M. Clarke, D. Cutter, C. Davies, M. Ewertz, J. Godwin, R. Gray, L. Pierce, T. Whelan, Y. Wang and R. Peto (2011). "Effect of radiotherapy after breast-conserving surgery on 10-year recurrence and 15-year breast cancer death: meta-analysis of individual patient data for 10,801 women in 17 randomised trials." Lancet **378**(9804): 1707-1716.
- Early Breast Cancer Trialists' Collaborative, G., C. Davies, J. Godwin, R. Gray, M. Clarke, D. Cutter, S. Darby, P. McGale, H. C. Pan, C. Taylor, Y. C. Wang, M. Dowsett, J. Ingle and R. Peto (2011). "Relevance of breast cancer hormone receptors and other factors to the efficacy of adjuvant tamoxifen: patient-level meta-analysis of randomised trials." Lancet **378**(9793): 771-784.
- Ebctcg, P. McGale, C. Taylor, C. Correa, D. Cutter, F. Duane, M. Ewertz, R. Gray, G. Mannu, R. Peto, T. Whelan, Y. Wang, Z. Wang and S. Darby (2014). "Effect of radiotherapy after mastectomy and axillary surgery on 10-year recurrence and 20-year breast cancer mortality: meta-analysis of individual patient data for 8135 women in 22 randomised trials." Lancet **383**(9935): 2127-2135.
- Edechi, C. A., N. Ikeogu, J. E. Uzonna and Y. Myal (2019). "Regulation of Immunity in Breast Cancer." Cancers (Basel) **11**(8).
- Eisenhauer, E. A., P. Therasse, J. Bogaerts, L. H. Schwartz, D. Sargent, R. Ford, J. Dancey, S. Arbuck, S. Gwyther, M. Mooney, L. Rubinstein, L. Shankar, L. Dodd, R. Kaplan, D. Lacombe

- and J. Verweij (2009). "New response evaluation criteria in solid tumours: revised RECIST guideline (version 1.1)." Eur J Cancer **45**(2): 228-247.
- Elston, C. W. and I. O. Ellis (1991). "Pathological prognostic factors in breast cancer. I. The value of histological grade in breast cancer: experience from a large study with long-term follow-up." Histopathology **19**(5): 403-410.
- Eriksson, D. and T. Stigbrand (2010). "Radiation-induced cell death mechanisms." Tumour Biol **31**(4): 363-372.
- Farmer, H., N. McCabe, C. J. Lord, A. N. Tutt, D. A. Johnson, T. B. Richardson, M. Santarosa, K. J. Dillon, I. Hickson, C. Knights, N. M. Martin, S. P. Jackson, G. C. Smith and A. Ashworth (2005). "Targeting the DNA repair defect in BRCA mutant cells as a therapeutic strategy." Nature **434**(7035): 917-921.
- Feng, S., Y. Zhao, Y. Xu, S. Ning, W. Huo, M. Hou, G. Gao, J. Ji, R. Guo and D. Xu (2016). "Ewing Tumor-associated Antigen 1 Interacts with Replication Protein A to Promote Restart of Stalled Replication Forks." J Biol Chem **291**(42): 21956-21962.
- Feoktistova, M., P. Geserick and M. Leverkus (2016). "Crystal Violet Assay for Determining Viability of Cultured Cells." Cold Spring Harb Protoc **2016**(4): pdb prot087379.
- Fokas, E., R. Prevo, E. M. Hammond, T. B. Brunner, W. G. McKenna and R. J. Muschel (2014). "Targeting ATR in DNA damage response and cancer therapeutics." Cancer Treat Rev **40**(1): 109-117.
- Fong, P. C., D. S. Boss, T. A. Yap, A. Tutt, P. Wu, M. Mergui-Roelvink, P. Mortimer, H. Swaisland, A. Lau, M. J. O'Connor, A. Ashworth, J. Carmichael, S. B. Kaye, J. H. Schellens and J. S. de Bono (2009). "Inhibition of poly(ADP-ribose) polymerase in tumors from BRCA mutation carriers." N Engl J Med **361**(2): 123-134.
- Forment, J. V. and M. J. O'Connor (2018). "Targeting the replication stress response in cancer." Pharmacol Ther.
- Forment, J. V. and M. J. O'Connor (2018). "Targeting the replication stress response in cancer." Pharmacol Ther **188**: 155-167.
- Formenti, S. C. and S. Demaria (2012). "Radiation therapy to convert the tumor into an in situ vaccine." Int J Radiat Oncol Biol Phys **84**(4): 879-880.
- Fouquier, J. and M. Guedj (2015). "Analysis of drug combinations: current methodological landscape." Pharmacol Res Perspect **3**(3): e00149.
- Foulkes, W. D. (2008). "Inherited susceptibility to common cancers." N Engl J Med **359**(20): 2143-2153.
- Fourcade, J., Z. Sun, M. Benallaoua, P. Guillaume, I. F. Luescher, C. Sander, J. M. Kirkwood, V. Kuchroo and H. M. Zarour (2010). "Upregulation of Tim-3 and PD-1 expression is associated with tumor antigen-specific CD8+ T cell dysfunction in melanoma patients." J Exp Med **207**(10): 2175-2186.

- Fowler, A. M., D. A. Mankoff and B. N. Joe (2017). "Imaging Neoadjuvant Therapy Response in Breast Cancer." Radiology **285**(2): 358-375.
- Fowler, J. F. (1989). "The linear-quadratic formula and progress in fractionated radiotherapy." Br J Radiol **62**(740): 679-694.
- Francis, D. L., A. Freeman, D. Visvikis, D. C. Costa, S. K. Luthra, M. Novelli, I. Taylor and P. J. Ell (2003). "In vivo imaging of cellular proliferation in colorectal cancer using positron emission tomography." Gut **52**(11): 1602-1606.
- Francisco, L. M., V. H. Salinas, K. E. Brown, V. K. Vanguri, G. J. Freeman, V. K. Kuchroo and A. H. Sharpe (2009). "PD-L1 regulates the development, maintenance, and function of induced regulatory T cells." J Exp Med **206**(13): 3015-3029.
- Frey, B., S. Hehlhans, F. Rodel and U. S. Gaipl (2015). "Modulation of inflammation by low and high doses of ionizing radiation: Implications for benign and malign diseases." Cancer Lett **368**(2): 230-237.
- Friedman, J., M. Morisada, L. Sun, E. C. Moore, M. Padget, J. W. Hodge, J. Schlom, S. R. Gameiro and C. T. Allen (2018). "Inhibition of WEE1 kinase and cell cycle checkpoint activation sensitizes head and neck cancers to natural killer cell therapies." J Immunother Cancer **6**(1): 59.
- Fujimitsu, K., M. Grimaldi and H. Yamano (2016). "Cyclin-dependent kinase 1-dependent activation of APC/C ubiquitin ligase." Science **352**(6289): 1121-1124.
- Gajewski, T. F., H. Schreiber and Y. X. Fu (2013). "Innate and adaptive immune cells in the tumor microenvironment." Nat Immunol **14**(10): 1014-1022.
- Gallmeier, E., P. C. Hermann, M. T. Mueller, J. G. Machado, A. Ziesch, E. N. De Toni, A. Palagyi, C. Eisen, J. W. Ellwart, J. Rivera, B. Rubio-Viqueira, M. Hidalgo, F. Bunz, B. Goke and C. Heeschen (2011). "Inhibition of ataxia telangiectasia- and Rad3-related function abrogates the in vitro and in vivo tumorigenicity of human colon cancer cells through depletion of the CD133(+) tumor-initiating cell fraction." Stem Cells **29**(3): 418-429.
- Gallo, D., J. T. F. Young, J. Fourtounis, G. Martino, A. Álvarez-Quilón, C. Bernier, N. M. Duffy, R. Papp, A. Roulston, R. Stocco, J. Szychowski, A. Veloso, H. Alam, P. S. Baruah, A. B. Fortin, J. Bowlan, N. Chaudhary, J. Desjardins, E. Dietrich, S. Fournier, C. Fugère-Desjardins, T. G. de Rugy, M.-E. Leclaire, B. Liu, H. Melo, O. Nicolas, A. Singhanian, R. K. Szilard, J. Tkáč, S. Y. Yin, S. J. Morris, M. Zinda, C. Gary Marshall and D. Durocher (2021). "CCNE1 amplification is synthetic-lethal with PKMYT1 kinase inhibition." bioRxiv: 2021.2004.2008.438361.
- Gambhir, S. S. (2002). "Molecular imaging of cancer with positron emission tomography." Nat Rev Cancer **2**(9): 683-693.
- Gameiro, S. R., M. L. Jammeh, M. M. Wattenberg, K. Y. Tsang, S. Ferrone and J. W. Hodge (2014). "Radiation-induced immunogenic modulation of tumor enhances antigen processing and calreticulin exposure, resulting in enhanced T-cell killing." Oncotarget **5**(2): 403-416.
- Gamper, A. M., R. Rofougaran, S. C. Watkins, J. S. Greenberger, J. H. Beumer and C. J. Bakkenist (2013). "ATR kinase activation in G1 phase facilitates the repair of ionizing radiation-induced DNA damage." Nucleic Acids Res **41**(22): 10334-10344.

Garcia-Diaz, A., D. S. Shin, B. H. Moreno, J. Saco, H. Escuin-Ordinas, G. A. Rodriguez, J. M. Zaretsky, L. Sun, W. Hugo, X. Wang, G. Parisi, C. P. Saus, D. Y. Torrejon, T. G. Graeber, B. Comin-Anduix, S. Hu-Lieskovan, R. Damoiseaux, R. S. Lo and A. Ribas (2017). "Interferon Receptor Signaling Pathways Regulating PD-L1 and PD-L2 Expression." *Cell Rep* **19**(6): 1189-1201.

Garnett, C. T., C. Palena, M. Chakraborty, K. Y. Tsang, J. Schlom and J. W. Hodge (2004). "Sublethal irradiation of human tumor cells modulates phenotype resulting in enhanced killing by cytotoxic T lymphocytes." *Cancer Res* **64**(21): 7985-7994.

Garon, E. B., N. A. Rizvi, R. Hui, N. Leighl, A. S. Balmanoukian, J. P. Eder, A. Patnaik, C. Aggarwal, M. Gubens, L. Horn, E. Carcereny, M. J. Ahn, E. Felip, J. S. Lee, M. D. Hellmann, O. Hamid, J. W. Goldman, J. C. Soria, M. Dolled-Filhart, R. Z. Rutledge, J. Zhang, J. K. Lunceford, R. Rangwala, G. M. Lubiniecki, C. Roach, K. Emancipator, L. Gandhi and K.-. Investigators (2015). "Pembrolizumab for the treatment of non-small-cell lung cancer." *N Engl J Med* **372**(21): 2018-2028.

Gascoigne, K. E. and S. S. Taylor (2008). "Cancer cells display profound intra- and interline variation following prolonged exposure to antimetabolic drugs." *Cancer Cell* **14**(2): 111-122.

Gettinger, S. N., L. Horn, L. Gandhi, D. R. Spigel, S. J. Antonia, N. A. Rizvi, J. D. Powderly, R. S. Heist, R. D. Carvajal, D. M. Jackman, L. V. Sequist, D. C. Smith, P. Leming, D. P. Carbone, M. C. Pinder-Schenck, S. L. Topalian, F. S. Hodi, J. A. Sosman, M. Sznol, D. F. McDermott, D. M. Pardoll, V. Sankar, C. M. Ahlers, M. Salvati, J. M. Wigginton, M. D. Hellmann, G. D. Kollia, A. K. Gupta and J. R. Brahmer (2015). "Overall Survival and Long-Term Safety of Nivolumab (Anti-Programmed Death 1 Antibody, BMS-936558, ONO-4538) in Patients With Previously Treated Advanced Non-Small-Cell Lung Cancer." *J Clin Oncol* **33**(18): 2004-2012.

Ghiringhelli, F., N. Larmonier, E. Schmitt, A. Parcellier, D. Cathelin, C. Garrido, B. Chauffert, E. Solary, B. Bonnotte and F. Martin (2004). "CD4+CD25+ regulatory T cells suppress tumor immunity but are sensitive to cyclophosphamide which allows immunotherapy of established tumors to be curative." *Eur J Immunol* **34**(2): 336-344.

Gianni, L., T. Pienkowski, Y. H. Im, L. M. Tseng, M. C. Liu, A. Lluch, E. Staroslawska, J. de la Haba-Rodriguez, S. A. Im, J. L. Pedrini, B. Poirier, P. Morandi, V. Semiglazov, V. Srimuninnimit, G. V. Bianchi, D. Magazzu, V. McNally, H. Douthwaite, G. Ross and P. Valagussa (2016). "5-year analysis of neoadjuvant pertuzumab and trastuzumab in patients with locally advanced, inflammatory, or early-stage HER2-positive breast cancer (NeoSphere): a multicentre, open-label, phase 2 randomised trial." *Lancet Oncol* **17**(6): 791-800.

Golden, E. B. and L. Apetoh (2015). "Radiotherapy and immunogenic cell death." *Semin Radiat Oncol* **25**(1): 11-17.

Golden, E. B., D. Frances, I. Pellicciotta, S. Demaria, M. Helen Barcellos-Hoff and S. C. Formenti (2014). "Radiation fosters dose-dependent and chemotherapy-induced immunogenic cell death." *Oncoimmunology* **3**: e28518.

Grassberger, C., S. G. Ellsworth, M. Q. Wilks, F. K. Keane and J. S. Loeffler (2019). "Assessing the interactions between radiotherapy and antitumour immunity." *Nat Rev Clin Oncol* **16**(12): 729-745.

Greenman, C., P. Stephens, R. Smith, G. L. Dalgliesh, C. Hunter, G. Bignell, H. Davies, J. Teague, A. Butler, C. Stevens, S. Edkins, S. O'Meara, I. Vastrik, E. E. Schmidt, T. Avis, S. Barthorpe, G. Bhamra, G. Buck, B. Choudhury, J. Clements, J. Cole, E. Dicks, S. Forbes, K. Gray, K. Halliday, R. Harrison, K. Hills, J. Hinton, A. Jenkinson, D. Jones, A. Menzies, T. Mironenko, J. Perry, K. Raine, D. Richardson, R. Shepherd, A. Small, C. Tofts, J. Varian, T. Webb, S. West, S. Widaa, A. Yates, D. P. Cahill, D. N. Louis, P. Goldstraw, A. G. Nicholson, F. Brasseur, L. Looijenga, B. L. Weber, Y. E. Chiew, A. DeFazio, M. F. Greaves, A. R. Green, P. Campbell, E. Birney, D. F. Easton, G. Chenevix-Trench, M. H. Tan, S. K. Khoo, B. T. Teh, S. T. Yuen, S. Y. Leung, R. Wooster, P. A. Futreal and M. R. Stratton (2007). "Patterns of somatic mutation in human cancer genomes." Nature **446**(7132): 153-158.

Gros, A., P. F. Robbins, X. Yao, Y. F. Li, S. Turcotte, E. Tran, J. R. Wunderlich, A. Mixon, S. Farid, M. E. Dudley, K. Hanada, J. R. Almeida, S. Darko, D. C. Douek, J. C. Yang and S. A. Rosenberg (2014). "PD-1 identifies the patient-specific CD8(+) tumor-reactive repertoire infiltrating human tumors." J Clin Invest **124**(5): 2246-2259.

Grosso, J. F., M. V. Goldberg, D. Getnet, T. C. Bruno, H. R. Yen, K. J. Pyle, E. Hipkiss, D. A. Vignali, D. M. Pardoll and C. G. Drake (2009). "Functionally distinct LAG-3 and PD-1 subsets on activated and chronically stimulated CD8 T cells." J Immunol **182**(11): 6659-6669.

Gubin, M. M., X. Zhang, H. Schuster, E. Caron, J. P. Ward, T. Noguchi, Y. Ivanova, J. Hundal, C. D. Arthur, W. J. Kribber, G. E. Mulder, M. Toebes, M. D. Vesely, S. S. Lam, A. J. Korman, J. P. Allison, G. J. Freeman, A. H. Sharpe, E. L. Pearce, T. N. Schumacher, R. Aebbersold, H. G. Rammensee, C. J. Melief, E. R. Mardis, W. E. Gillanders, M. N. Artyomov and R. D. Schreiber (2014). "Checkpoint blockade cancer immunotherapy targets tumour-specific mutant antigens." Nature **515**(7528): 577-581.

Gupta, A., H. C. Probst, V. Vuong, A. Landshammer, S. Muth, H. Yagita, R. Schwendener, M. Pruschy, A. Knuth and M. van den Broek (2012). "Radiotherapy promotes tumor-specific effector CD8+ T cells via dendritic cell activation." J Immunol **189**(2): 558-566.

Haahr, P., S. Hoffmann, M. A. Tollenaere, T. Ho, L. I. Toledo, M. Mann, S. Bekker-Jensen, M. Raschle and N. Mailand (2016). "Activation of the ATR kinase by the RPA-binding protein ETAA1." Nat Cell Biol **18**(11): 1196-1207.

Halazonetis, T. D., V. G. Gorgoulis and J. Bartek (2008). "An oncogene-induced DNA damage model for cancer development." Science **319**(5868): 1352-1355.

Hall, A. B., D. Newsome, Y. Wang, D. M. Boucher, B. Eustace, Y. Gu, B. Hare, M. A. Johnson, S. Milton, C. E. Murphy, D. Takemoto, C. Tolman, M. Wood, P. Charlton, J. D. Charrier, B. Furey, J. Golec, P. M. Reaper and J. R. Pollard (2014). "Potentiation of tumor responses to DNA damaging therapy by the selective ATR inhibitor VX-970." Oncotarget **5**(14): 5674-5685.

Hallahan, D., J. Kuchibhotla and C. Wyble (1996). "Cell adhesion molecules mediate radiation-induced leukocyte adhesion to the vascular endothelium." Cancer Res **56**(22): 5150-5155.

Hallahan, D. E., D. R. Spriggs, M. A. Beckett, D. W. Kufe and R. R. Weichselbaum (1989). "Increased tumor necrosis factor alpha mRNA after cellular exposure to ionizing radiation." Proc Natl Acad Sci U S A **86**(24): 10104-10107.

Hanahan, D. and R. A. Weinberg (2011). "Hallmarks of cancer: the next generation." *Cell* **144**(5): 646-674.

Harbeck, N., F. Penault-Llorca, J. Cortes, M. Gnant, N. Houssami, P. Poortmans, K. Ruddy, J. Tsang and F. Cardoso (2019). "Breast cancer." *Nat Rev Dis Primers* **5**(1): 66.

Harbour, J. W., R. X. Luo, A. Dei Santi, A. A. Postigo and D. C. Dean (1999). "Cdk phosphorylation triggers sequential intramolecular interactions that progressively block Rb functions as cells move through G1." *Cell* **98**(6): 859-869.

Harris, P. S., S. Venkataraman, I. Alimova, D. K. Birks, I. Balakrishnan, B. Cristiano, A. M. Donson, A. M. Dubuc, M. D. Taylor, N. K. Foreman, P. Reigan and R. Vibhakar (2014). "Integrated genomic analysis identifies the mitotic checkpoint kinase WEE1 as a novel therapeutic target in medulloblastoma." *Mol Cancer* **13**: 72.

Hartwell, L. H. and T. A. Weinert (1989). "Checkpoints: controls that ensure the order of cell cycle events." *Science* **246**(4930): 629-634.

Hauge, S., C. Naucke, G. Hasvold, M. Joel, G. E. Rodland, P. Juzenas, T. Stokke and R. G. Syljuasen (2017). "Combined inhibition of Wee1 and Chk1 gives synergistic DNA damage in S-phase due to distinct regulation of CDK activity and CDC45 loading." *Oncotarget* **8**(7): 10966-10979.

Heald, R., M. McLoughlin and F. McKeon (1993). "Human wee1 maintains mitotic timing by protecting the nucleus from cytoplasmically activated Cdc2 kinase." *Cell* **74**(3): 463-474.

Heil, J., H. M. Kuerer, A. Pfob, G. Rauch, H. P. Sinn, M. Golatta, G. J. Liefers and M. J. Vrancken Peeters (2020). "Eliminating the breast cancer surgery paradigm after neoadjuvant systemic therapy: current evidence and future challenges." *Ann Oncol* **31**(1): 61-71.

Heitz, F., P. Harter, H. J. Lueck, A. Fissler-Eckhoff, F. Lorenz-Salehi, S. Scheil-Bertram, A. Traut and A. du Bois (2009). "Triple-negative and HER2-overexpressing breast cancers exhibit an elevated risk and an earlier occurrence of cerebral metastases." *Eur J Cancer* **45**(16): 2792-2798.

Heller, R. C., S. Kang, W. M. Lam, S. Chen, C. S. Chan and S. P. Bell (2011). "Eukaryotic origin-dependent DNA replication in vitro reveals sequential action of DDK and S-CDK kinases." *Cell* **146**(1): 80-91.

Hernandez, C., P. Huebener and R. F. Schwabe (2016). "Damage-associated molecular patterns in cancer: a double-edged sword." *Oncogene* **35**(46): 5931-5941.

Hirai, H., T. Arai, M. Okada, T. Nishibata, M. Kobayashi, N. Sakai, K. Imagaki, J. Ohtani, T. Sakai, T. Yoshizumi, S. Mizuarai, Y. Iwasawa and H. Kotani (2010). "MK-1775, a small molecule Wee1 inhibitor, enhances anti-tumor efficacy of various DNA-damaging agents, including 5-fluorouracil." *Cancer Biol Ther* **9**(7): 514-522.

Hirai, H., Y. Iwasawa, M. Okada, T. Arai, T. Nishibata, M. Kobayashi, T. Kimura, N. Kaneko, J. Ohtani, K. Yamanaka, H. Itadani, I. Takahashi-Suzuki, K. Fukasawa, H. Oki, T. Nambu, J. Jiang, T. Sakai, H. Arakawa, T. Sakamoto, T. Sagara, T. Yoshizumi, S. Mizuarai and H. Kotani (2009). "Small-molecule inhibition of Wee1 kinase by MK-1775 selectively sensitizes p53-deficient tumor cells to DNA-damaging agents." *Mol Cancer Ther* **8**(11): 2992-3000.

- Hochegger, H., S. Takeda and T. Hunt (2008). "Cyclin-dependent kinases and cell-cycle transitions: does one fit all?" Nat Rev Mol Cell Biol **9**(11): 910-916.
- Hooley, R. J., L. M. Scoutt and L. E. Philpotts (2013). "Breast ultrasonography: state of the art." Radiology **268**(3): 642-659.
- Hori, S., T. Nomura and S. Sakaguchi (2003). "Control of regulatory T cell development by the transcription factor Foxp3." Science **299**(5609): 1057-1061.
- Hosseini, H., M. M. S. Obradovic, M. Hoffmann, K. L. Harper, M. S. Sosa, M. Werner-Klein, L. K. Nanduri, C. Werno, C. Ehrl, M. Maneck, N. Patwary, G. Haunschild, M. Guzvic, C. Reimelt, M. Grauvogl, N. Eichner, F. Weber, A. D. Hartkopf, F. A. Taran, S. Y. Brucker, T. Fehm, B. Rack, S. Buchholz, R. Spang, G. Meister, J. A. Aguirre-Ghiso and C. A. Klein (2016). "Early dissemination seeds metastasis in breast cancer." Nature **540**(7634): 552-558.
- Hu, X. and L. B. Ivashkiv (2009). "Cross-regulation of signaling pathways by interferon-gamma: implications for immune responses and autoimmune diseases." Immunity **31**(4): 539-550.
- Hu, X. C., J. Zhang, B. H. Xu, L. Cai, J. Ragaz, Z. H. Wang, B. Y. Wang, Y. E. Teng, Z. S. Tong, Y. Y. Pan, Y. M. Yin, C. P. Wu, Z. F. Jiang, X. J. Wang, G. Y. Lou, D. G. Liu, J. F. Feng, J. F. Luo, K. Sun, Y. J. Gu, J. Wu and Z. M. Shao (2015). "Cisplatin plus gemcitabine versus paclitaxel plus gemcitabine as first-line therapy for metastatic triple-negative breast cancer (CBCSG006): a randomised, open-label, multicentre, phase 3 trial." Lancet Oncol **16**(4): 436-446.
- Huntoon, C. J., K. S. Flatten, A. E. Wahner Hendrickson, A. M. Huehls, S. L. Sutor, S. H. Kaufmann and L. M. Karnitz (2013). "ATR inhibition broadly sensitizes ovarian cancer cells to chemotherapy independent of BRCA status." Cancer Res **73**(12): 3683-3691.
- Hustedt, N., A. Alvarez-Quilon, A. McEwan, J. Y. Yuan, T. Cho, L. Koob, T. Hart and D. Durocher (2019). "A consensus set of genetic vulnerabilities to ATR inhibition." Open Biol **9**(9): 190156.
- Independent, U. K. P. o. B. C. S. (2012). "The benefits and harms of breast cancer screening: an independent review." Lancet **380**(9855): 1778-1786.
- Iorns, E., C. J. Lord, A. Grigoriadis, S. McDonald, K. Fenwick, A. Mackay, C. A. Mein, R. Natrajan, K. Savage, N. Tamber, J. S. Reis-Filho, N. C. Turner and A. Ashworth (2009). "Integrated functional, gene expression and genomic analysis for the identification of cancer targets." PLoS One **4**(4): e5120.
- Irwig, L., P. Macaskill and N. Houssami (2002). "Evidence relevant to the investigation of breast symptoms: the triple test." Breast **11**(3): 215-220.
- Isakoff, S. J., E. L. Mayer, L. He, T. A. Traina, L. A. Carey, K. J. Krag, H. S. Rugo, M. C. Liu, V. Stearns, S. E. Come, K. M. Timms, A. R. Hartman, D. R. Borger, D. M. Finkelstein, J. E. Garber, P. D. Ryan, E. P. Winer, P. E. Goss and L. W. Ellisen (2015). "TBCRC009: A Multicenter Phase II Clinical Trial of Platinum Monotherapy With Biomarker Assessment in Metastatic Triple-Negative Breast Cancer." J Clin Oncol **33**(17): 1902-1909.
- Ivashkiv, L. B. (2018). "IFN γ : signalling, epigenetics and roles in immunity, metabolism, disease and cancer immunotherapy." Nat Rev Immunol **18**(9): 545-558.

- Jaffray, D. A. (2012). "Image-guided radiotherapy: from current concept to future perspectives." Nat Rev Clin Oncol **9**(12): 688-699.
- Jagarlamudi, K. K. and M. Shaw (2018). "Thymidine kinase 1 as a tumor biomarker: technical advances offer new potential to an old biomarker." Biomark Med **12**(9): 1035-1048.
- Jatoi, I., J. R. Benson and I. Kunkler (2018). "Hypothesis: can the abscopal effect explain the impact of adjuvant radiotherapy on breast cancer mortality?" NPJ Breast Cancer **4**: 8.
- Jensen, M. M. and A. Kjaer (2015). "Monitoring of anti-cancer treatment with (18)F-FDG and (18)F-FLT PET: a comprehensive review of pre-clinical studies." American journal of nuclear medicine and molecular imaging **5**(5): 431-456.
- Jeon, Y., E. Ko, K. Y. Lee, M. J. Ko, S. Y. Park, J. Kang, C. H. Jeon, H. Lee and D. S. Hwang (2011). "TopBP1 deficiency causes an early embryonic lethality and induces cellular senescence in primary cells." J Biol Chem **286**(7): 5414-5422.
- Jiang, Y., Y. Li and B. Zhu (2015). "T-cell exhaustion in the tumor microenvironment." Cell Death Dis **6**: e1792.
- Jin, J., H. Fang, F. Yang, W. Ji, N. Guan, Z. Sun, Y. Shi, G. Zhou and X. Guan (2018). "Combined Inhibition of ATR and WEE1 as a Novel Therapeutic Strategy in Triple-Negative Breast Cancer." Neoplasia **20**(5): 478-488.
- Jiricny, J. (2006). "The multifaceted mismatch-repair system." Nat Rev Mol Cell Biol **7**(5): 335-346.
- Jones, R. L., J. Salter, R. A'Hern, A. Nerurkar, M. Parton, J. S. Reis-Filho, I. E. Smith and M. Dowsett (2009). "The prognostic significance of Ki67 before and after neoadjuvant chemotherapy in breast cancer." Breast Cancer Res Treat **116**(1): 53-68.
- Kabeche, L., H. D. Nguyen, R. Buisson and L. Zou (2018). "A mitosis-specific and R loop-driven ATR pathway promotes faithful chromosome segregation." Science **359**(6371): 108-114.
- Kachikwu, E. L., K. S. Iwamoto, Y. P. Liao, J. J. DeMarco, N. Agazaryan, J. S. Economou, W. H. McBride and D. Schaeue (2011). "Radiation enhances regulatory T cell representation." Int J Radiat Oncol Biol Phys **81**(4): 1128-1135.
- Takeji, Y., Y. Maehara, M. Ikebe and B. A. Teicher (1997). "Dynamics of tumor oxygenation, CD31 staining and transforming growth factor-beta levels after treatment with radiation or cyclophosphamide in the rat 13762 mammary carcinoma." Int J Radiat Oncol Biol Phys **37**(5): 1115-1123.
- Karnak, D., C. G. Engelke, L. A. Parsels, T. Kausar, D. Wei, J. R. Robertson, K. B. Marsh, M. A. Davis, L. Zhao, J. Maybaum, T. S. Lawrence and M. A. Morgan (2014). "Combined inhibition of Wee1 and PARP1/2 for radiosensitization in pancreatic cancer." Clin Cancer Res **20**(19): 5085-5096.
- Kenny, L. M., A. Al-Nahhas and E. O. Aboagye (2011). "Novel PET biomarkers for breast cancer imaging." Nucl Med Commun **32**(5): 333-335.

Kenny, L. M., D. M. Vigushin, A. Al-Nahhas, S. Osman, S. K. Luthra, S. Shousha, R. C. Coombes and E. O. Aboagye (2005). "Quantification of cellular proliferation in tumor and normal tissues of patients with breast cancer by [18F]fluorothymidine-positron emission tomography imaging: evaluation of analytical methods." Cancer Res **65**(21): 10104-10112.

Kepp, O., A. Tesniere, F. Schlemmer, M. Michaud, L. Senovilla, L. Zitvogel and G. Kroemer (2009). "Immunogenic cell death modalities and their impact on cancer treatment." Apoptosis **14**(4): 364-375.

Kibe, T., M. Zimmermann and T. de Lange (2016). "TPP1 Blocks an ATR-Mediated Resection Mechanism at Telomeres." Mol Cell **61**(2): 236-246.

Kim, H., E. George, R. Ragland, S. Rafail, R. Zhang, C. Krepler, M. Morgan, M. Herlyn, E. Brown and F. Simpkins (2017). "Targeting the ATR/CHK1 Axis with PARP Inhibition Results in Tumor Regression in BRCA-Mutant Ovarian Cancer Models." Clin Cancer Res **23**(12): 3097-3108.

Klemm, F. and J. A. Joyce (2015). "Microenvironmental regulation of therapeutic response in cancer." Trends Cell Biol **25**(4): 198-213.

Klingemann, H., L. Boissel and F. Toneguzzo (2016). "Natural Killer Cells for Immunotherapy - Advantages of the NK-92 Cell Line over Blood NK Cells." Front Immunol **7**: 91.

Koebel, C. M., W. Vermi, J. B. Swann, N. Zerafa, S. J. Rodig, L. J. Old, M. J. Smyth and R. D. Schreiber (2007). "Adaptive immunity maintains occult cancer in an equilibrium state." Nature **450**(7171): 903-907.

Kondo, M., I. L. Weissman and K. Akashi (1997). "Identification of clonogenic common lymphoid progenitors in mouse bone marrow." Cell **91**(5): 661-672.

Kostakoglu, L., F. Duan, M. O. Idowu, P. R. Jolles, H. D. Bear, M. Muzi, J. Cormack, J. P. Muzi, D. A. Pryma, J. M. Specht, L. Hovanessian-Larsen, J. Miliziano, S. Mallett, A. F. Shields, D. A. Mankoff and A. I. Team (2015). "A Phase II Study of 3'-Deoxy-3'-18F-Fluorothymidine PET in the Assessment of Early Response of Breast Cancer to Neoadjuvant Chemotherapy: Results from ACRIN 6688." J Nucl Med **56**(11): 1681-1689.

Kotsantis, P., E. Petermann and S. J. Boulton (2018). "Mechanisms of Oncogene-Induced Replication Stress: Jigsaw Falling into Place." Cancer Discov.

Krajewska, M., A. M. Heijink, Y. J. Bisselink, R. I. Seinstra, H. H. Sillje, E. G. de Vries and M. A. van Vugt (2013). "Forced activation of Cdk1 via wee1 inhibition impairs homologous recombination." Oncogene **32**(24): 3001-3008.

Kreahling, J. M., J. Y. Gemmer, D. Reed, D. Letson, M. Bui and S. Altiok (2012). "MK1775, a selective Wee1 inhibitor, shows single-agent antitumor activity against sarcoma cells." Mol Cancer Ther **11**(1): 174-182.

Krebs, M. G., J. Lopez, A. El-Khoueiry, Y.-J. Bang, S. Postel-Vinay, W. Abida, L. Carter, W. Xu, S.-A. Im, A. Pierce, P. Frewer, A. Berges, S. Y. A. Cheung, C. Stephens, B. Felicetti, E. Dean and S. J. Hollingsworth (2018). "Abstract CT026: Phase I study of AZD6738, an inhibitor of ataxia telangiectasia Rad3-related (ATR), in combination with olaparib or durvalumab in patients (pts) with advanced solid cancers." Cancer Research **78**(13 Supplement): CT026.

Kubota, K., R. Furumoto S Fau - Iwata, H. Iwata R Fau - Fukuda, K. Fukuda H Fau - Kawamura, K. Kawamura K Fau - Ishiwata and K. Ishiwata (2006). "Comparison of 18F-fluoromethylcholine and 2-deoxy-D-glucose in the distribution of tumor and inflammation." Ann Nucl Med **20**(8): 527-533.

Kuchenbaecker, K. B., J. L. Hopper, D. R. Barnes, K. A. Phillips, T. M. Mooij, M. J. Roos-Blom, S. Jervis, F. E. van Leeuwen, R. L. Milne, N. Andrieu, D. E. Goldgar, M. B. Terry, M. A. Rookus, D. F. Easton, A. C. Antoniou, Brca, B. C. Consortium, L. McGuffog, D. G. Evans, D. Barrowdale, D. Frost, J. Adlard, K. R. Ong, L. Izatt, M. Tischkowitz, R. Eeles, R. Davidson, S. Hodgson, S. Ellis, C. Nogues, C. Lasset, D. Stoppa-Lyonnet, J. P. Fricker, L. Faivre, P. Berthet, M. J. Hooning, L. E. van der Kolk, C. M. Kets, M. A. Adank, E. M. John, W. K. Chung, I. L. Andrulis, M. Southey, M. B. Daly, S. S. Buys, A. Osorio, C. Engel, K. Kast, R. K. Schmutzler, T. Caldes, A. Jakubowska, J. Simard, M. L. Friedlander, S. A. McLachlan, E. Machackova, L. Foretova, Y. Y. Tan, C. F. Singer, E. Olah, A. M. Gerdes, B. Arver and H. Olsson (2017). "Risks of Breast, Ovarian, and Contralateral Breast Cancer for BRCA1 and BRCA2 Mutation Carriers." JAMA **317**(23): 2402-2416.

Kumagai, A., J. Lee, H. Y. Yoo and W. G. Dunphy (2006). "TopBP1 activates the ATR-ATRIP complex." Cell **124**(5): 943-955.

Kupelian, P. A., V. V. Thakkar, D. Khuntia, C. A. Reddy, E. A. Klein and A. Mahadevan (2005). "Hypofractionated intensity-modulated radiotherapy (70 Gy at 2.5 Gy per fraction) for localized prostate cancer: long-term outcomes." Int J Radiat Oncol Biol Phys **63**(5): 1463-1468.

Labib, K. (2010). "How do Cdc7 and cyclin-dependent kinases trigger the initiation of chromosome replication in eukaryotic cells?" Genes Dev **24**(12): 1208-1219.

Lagadec, C., E. Vlashi, L. Della Donna, C. Dekmezian and F. Pajonk (2012). "Radiation-induced reprogramming of breast cancer cells." Stem Cells **30**(5): 833-844.

Lakhani, S. R., I. O. Ellis, S. Schnitt, P. H. Tan and M. van de Vijver (2012). "WHO Classification of Tumours of the Breast."

Lauby-Secretan, B., C. Scoccianti, D. Loomis, L. Benbrahim-Tallaa, V. Bouvard, F. Bianchini, K. Straif and G. International Agency for Research on Cancer Handbook Working (2015). "Breast-cancer screening--viewpoint of the IARC Working Group." N Engl J Med **372**(24): 2353-2358.

Lecona, E. and O. Fernandez-Capetillo (2014). "Replication stress and cancer: it takes two to tango." Exp Cell Res **329**(1): 26-34.

Lee, J., A. Kumagai and W. G. Dunphy (2007). "The Rad9-Hus1-Rad1 checkpoint clamp regulates interaction of TopBP1 with ATR." J Biol Chem **282**(38): 28036-28044.

Lee, Y. Y., Y. J. Cho, S. W. Shin, C. Choi, J. Y. Ryu, H. K. Jeon, J. J. Choi, J. R. Hwang, C. H. Choi, T. J. Kim, B. G. Kim, D. S. Bae, W. Park and J. W. Lee (2019). "Anti-Tumor Effects of Wee1 Kinase Inhibitor with Radiotherapy in Human Cervical Cancer." Sci Rep **9**(1): 15394.

Leijen, S., R. M. van Geel, A. C. Pavlick, R. Tibes, L. Rosen, A. R. Razak, R. Lam, T. Demuth, S. Rose, M. A. Lee, T. Freshwater, S. Shumway, L. W. Liang, A. M. Oza, J. H. Schellens and G. I. Shapiro (2016). "Phase I Study Evaluating WEE1 Inhibitor AZD1775 As Monotherapy and in

Combination With Gemcitabine, Cisplatin, or Carboplatin in Patients With Advanced Solid Tumors." J Clin Oncol **34**(36): 4371-4380.

Leijen, S., R. M. van Geel, G. S. Sonke, D. de Jong, E. H. Rosenberg, S. Marchetti, D. Pluim, E. van Werkhoven, S. Rose, M. A. Lee, T. Freshwater, J. H. Beijnen and J. H. Schellens (2016). "Phase II Study of WEE1 Inhibitor AZD1775 Plus Carboplatin in Patients With TP53-Mutated Ovarian Cancer Refractory or Resistant to First-Line Therapy Within 3 Months." J Clin Oncol **34**(36): 4354-4361.

Lempiainen, H. and T. D. Halazonetis (2009). "Emerging common themes in regulation of PIKKs and PI3Ks." EMBO J **28**(20): 3067-3073.

Leonard, B. C., E. D. Lee, N. E. Bhola, H. Li, K. K. Sogaard, C. J. Bakkenist, J. R. Grandis and D. E. Johnson (2019). "ATR inhibition sensitizes HPV(-) and HPV(+) head and neck squamous cell carcinoma to cisplatin." Oral Oncol **95**: 35-42.

Leone, P., E. C. Shin, F. Perosa, A. Vacca, F. Dammacco and V. Racanelli (2013). "MHC class I antigen processing and presenting machinery: organization, function, and defects in tumor cells." J Natl Cancer Inst **105**(16): 1172-1187.

Lewis, C. W., A. B. Bukhari, E. J. Xiao, W. S. Choi, J. D. Smith, E. Homola, J. R. Mackey, S. D. Campbell, A. M. Gamper and G. K. Chan (2019). "Upregulation of Myt1 Promotes Acquired Resistance of Cancer Cells to Wee1 Inhibition." Cancer Res **79**(23): 5971-5985.

Lewis, C. W., Z. Jin, D. Macdonald, W. Wei, X. J. Qian, W. S. Choi, R. He, X. Sun and G. Chan (2017). "Prolonged mitotic arrest induced by Wee1 inhibition sensitizes breast cancer cells to paclitaxel." Oncotarget **8**(43): 73705-73722.

Li, C., M. Andrade, R. Dunbrack and G. H. Enders (2010). "A bifunctional regulatory element in human somatic Wee1 mediates cyclin A/Cdk2 binding and Crm1-dependent nuclear export." Mol Cell Biol **30**(1): 116-130.

Lian, S., R. Xie, Y. Ye, Y. Lu, Y. Cheng, X. Xie, S. Li and L. Jia (2019). "Dual blockage of both PD-L1 and CD47 enhances immunotherapy against circulating tumor cells." Sci Rep **9**(1): 4532.

Liaw, D., D. J. Marsh, J. Li, P. L. Dahia, S. I. Wang, Z. Zheng, S. Bose, K. M. Call, H. C. Tsou, M. Peacocke, C. Eng and R. Parsons (1997). "Germline mutations of the PTEN gene in Cowden disease, an inherited breast and thyroid cancer syndrome." Nat Genet **16**(1): 64-67.

Lin, C., K. Kume, T. Mori, M. E. Martinez, H. Okazawa and Y. Kiyono (2015). "Predictive Value of Early-Stage Uptake of 3'-Deoxy-3'-18F-Fluorothymidine in Cancer Cells Treated with Charged Particle Irradiation." J Nucl Med **56**(6): 945-950.

Lindahl, T. and D. E. Barnes (2000). "Repair of endogenous DNA damage." Cold Spring Harb Symp Quant Biol **65**: 127-133.

Lindqvist, A., V. Rodriguez-Bravo and R. H. Medema (2009). "The decision to enter mitosis: feedback and redundancy in the mitotic entry network." J Cell Biol **185**(2): 193-202.

Linnemann, C., R. Mezzadra and T. N. Schumacher (2014). "TCR repertoires of intratumoral T-cell subsets." Immunol Rev **257**(1): 72-82.

Linnemann, C., M. M. van Buuren, L. Bies, E. M. Verdegaal, R. Schotte, J. J. Calis, S. Behjati, A. Velds, H. Hilkmann, D. E. Atmioui, M. Visser, M. R. Stratton, J. B. Haanen, H. Spits, S. H. van der Burg and T. N. Schumacher (2015). "High-throughput epitope discovery reveals frequent recognition of neo-antigens by CD4+ T cells in human melanoma." Nat Med **21**(1): 81-85.

Litton, J. K., H. S. Rugo, J. Ettl, S. A. Hurvitz, A. Goncalves, K. H. Lee, L. Fehrenbacher, R. Yerushalmi, L. A. Mina, M. Martin, H. Roche, Y. H. Im, R. G. W. Quek, D. Markova, I. C. Tudor, A. L. Hannah, W. Eiermann and J. L. Blum (2018). "Talazoparib in Patients with Advanced Breast Cancer and a Germline BRCA Mutation." N Engl J Med **379**(8): 753-763.

Litvak, V., R. Argov, N. Dahan, S. Ramachandran, R. Amarilio, A. Shainskaya and S. Lev (2004). "Mitotic phosphorylation of the peripheral Golgi protein Nir2 by Cdk1 provides a docking mechanism for Plk1 and affects cytokinesis completion." Mol Cell **14**(3): 319-330.

Liu, F., J. J. Stanton, Z. Wu and H. Piwnica-Worms (1997). "The human Myt1 kinase preferentially phosphorylates Cdc2 on threonine 14 and localizes to the endoplasmic reticulum and Golgi complex." Mol Cell Biol **17**(2): 571-583.

Liu, Q., S. Guntuku, X. S. Cui, S. Matsuoka, D. Cortez, K. Tamai, G. Luo, S. Carattini-Rivera, F. DeMayo, A. Bradley, L. A. Donehower and S. J. Elledge (2000). "Chk1 is an essential kinase that is regulated by Atr and required for the G(2)/M DNA damage checkpoint." Genes Dev **14**(12): 1448-1459.

Liu, S., J. Lachapelle, S. Leung, D. Gao, W. D. Foulkes and T. O. Nielsen (2012). "CD8+ lymphocyte infiltration is an independent favorable prognostic indicator in basal-like breast cancer." Breast Cancer Res **14**(2): R48.

Liu, S., B. Shiotani, M. Lahiri, A. Marechal, A. Tse, C. C. Leung, J. N. Glover, X. H. Yang and L. Zou (2011). "ATR autophosphorylation as a molecular switch for checkpoint activation." Mol Cell **43**(2): 192-202.

Liu, Y., Y. Yu, S. Yang, B. Zeng, Z. Zhang, G. Jiao, Y. Zhang, L. Cai and R. Yang (2009). "Regulation of arginase I activity and expression by both PD-1 and CTLA-4 on the myeloid-derived suppressor cells." Cancer Immunol Immunother **58**(5): 687-697.

LoConte, N. K., A. M. Brewster, J. S. Kaur, J. K. Merrill and A. J. Alberg (2018). "Alcohol and Cancer: A Statement of the American Society of Clinical Oncology." J Clin Oncol **36**(1): 83-93.

Lowe, M., C. Rabouille, N. Nakamura, R. Watson, M. Jackman, E. Jamsa, D. Rahman, D. J. Pappin and G. Warren (1998). "Cdc2 kinase directly phosphorylates the cis-Golgi matrix protein GM130 and is required for Golgi fragmentation in mitosis." Cell **94**(6): 783-793.

Lundberg, A. S. and R. A. Weinberg (1998). "Functional inactivation of the retinoblastoma protein requires sequential modification by at least two distinct cyclin-cdk complexes." Mol Cell Biol **18**(2): 753-761.

Luo, J., N. L. Solimini and S. J. Elledge (2009). "Principles of cancer therapy: oncogene and non-oncogene addiction." Cell **136**(5): 823-837.

Machulla, H., A. Blocher, M. Kuntzsch, M. Piert, R. Wei and J. Grierson (2000). "Simplified Labeling Approach for Synthesizing 32-Deoxy-32-[18F]fluorothymidine ([18F]FLT)." Journal of Radioanalytical and Nuclear Chemistry **243**: 843-846.

Mackey, J. R., T. Pienkowski, J. Crown, S. Sadeghi, M. Martin, A. Chan, M. Saleh, S. Sehdev, L. Provencher, V. Semiglazov, M. F. Press, G. Sauter, M. Lindsay, V. Houe, M. Buyse, P. Drevot, S. Hitier, S. Bensfia and W. Eiermann (2016). "Long-term outcomes after adjuvant treatment of sequential versus combination docetaxel with doxorubicin and cyclophosphamide in node-positive breast cancer: BCIRG-005 randomized trial." Ann Oncol **27**(6): 1041-1047.

Magnussen, G. I., E. Hellesylt, J. M. Nesland, C. G. Trope, V. A. Florenes and R. Holm (2013). "High expression of weel is associated with malignancy in vulvar squamous cell carcinoma patients." BMC Cancer **13**: 288.

Magnussen, G. I., R. Holm, E. Emilsen, A. K. Rosnes, A. Slipicevic and V. A. Florenes (2012). "High expression of Wee1 is associated with poor disease-free survival in malignant melanoma: potential for targeted therapy." PLoS One **7**(6): e38254.

Malkin, D., F. P. Li, L. C. Strong, J. F. Fraumeni, Jr., C. E. Nelson, D. H. Kim, J. Kassel, M. A. Gryka, F. Z. Bischoff, M. A. Tainsky and et al. (1990). "Germ line p53 mutations in a familial syndrome of breast cancer, sarcomas, and other neoplasms." Science **250**(4985): 1233-1238.

Malumbres, M. and M. Barbacid (2005). "Mammalian cyclin-dependent kinases." Trends Biochem Sci **30**(11): 630-641.

Malumbres, M. and M. Barbacid (2005). "Mammalian cyclin-dependent kinases." Trends Biochem Sci **30**(11): 630-641.

Malumbres, M. and M. Barbacid (2009). "Cell cycle, CDKs and cancer: a changing paradigm." Nat Rev Cancer **9**(3): 153-166.

Margenthaler, J. A. and D. W. Ollila (2016). "Breast Conservation Therapy Versus Mastectomy: Shared Decision-Making Strategies and Overcoming Decisional Conflicts in Your Patients." Ann Surg Oncol **23**(10): 3133-3137.

Marinovich, M. L., K. E. Hunter, P. Macaskill and N. Houssami (2018). "Breast Cancer Screening Using Tomosynthesis or Mammography: A Meta-analysis of Cancer Detection and Recall." J Natl Cancer Inst **110**(9): 942-949.

Matheson, C. J., D. S. Backos and P. Reigan (2016). "Targeting WEE1 Kinase in Cancer." Trends Pharmacol Sci **37**(10): 872-881.

Matsumura, S., B. Wang, N. Kawashima, S. Braunstein, M. Badura, T. O. Cameron, J. S. Babb, R. J. Schneider, S. C. Formenti, M. L. Dustin and S. Demaria (2008). "Radiation-induced CXCL16 release by breast cancer cells attracts effector T cells." J Immunol **181**(5): 3099-3107.

McGowan, C. H. and P. Russell (1995). "Cell cycle regulation of human WEE1." EMBO J **14**(10): 2166-2175.

McLaughlin, S. A. (2013). "Surgical management of the breast: breast conservation therapy and mastectomy." Surg Clin North Am **93**(2): 411-428.

McNally, J. P., S. H. Millen, V. Chaturvedi, N. Lakes, C. E. Terrell, E. E. Elfers, K. R. Carroll, S. P. Hogan, P. R. Andreassen, J. Kanter, C. E. Allen, M. M. Henry, J. N. Greenberg, S. Ladisch, M. L. Hermiston, M. Joyce, D. A. Hildeman, J. D. Katz and M. B. Jordan (2017). "Manipulating DNA

damage-response signaling for the treatment of immune-mediated diseases." Proc Natl Acad Sci U S A **114**(24): E4782-E4791.

Melnikow, J., J. J. Fenton, E. P. Whitlock, D. L. Miglioretti, M. S. Weyrich, J. H. Thompson and K. Shah (2016). "Supplemental Screening for Breast Cancer in Women With Dense Breasts: A Systematic Review for the U.S. Preventive Services Task Force." Ann Intern Med **164**(4): 268-278.

Mendez, E., C. P. Rodriguez, M. C. Kao, S. Raju, A. Diab, R. A. Harbison, E. Q. Konnick, G. M. Mugundu, R. Santana-Davila, R. Martins, N. D. Futran and L. Q. M. Chow (2018). "A Phase I Clinical Trial of AZD1775 in Combination with Neoadjuvant Weekly Docetaxel and Cisplatin before Definitive Therapy in Head and Neck Squamous Cell Carcinoma." Clin Cancer Res **24**(12): 2740-2748.

Metcalf, K. A., A. Poll, R. Royer, M. Llacuachaqui, A. Tulman, P. Sun and S. A. Narod (2010). "Screening for founder mutations in BRCA1 and BRCA2 in unselected Jewish women." J Clin Oncol **28**(3): 387-391.

Mikaelsdottir, E. K., S. Valgeirsdottir, J. E. Eyfjord and T. Rafnar (2004). "The Icelandic founder mutation BRCA2 999del5: analysis of expression." Breast Cancer Res **6**(4): R284-290.

Miller, I., M. Min, C. Yang, C. Tian, S. Gookin, D. Carter and S. L. Spencer (2018). "Ki67 is a Graded Rather than a Binary Marker of Proliferation versus Quiescence." Cell Rep **24**(5): 1105-1112 e1105.

Min, A., S. A. Im, H. Jang, S. Kim, M. Lee, D. K. Kim, Y. Yang, H. J. Kim, K. H. Lee, J. W. Kim, T. Y. Kim, D. Y. Oh, J. Brown, A. Lau, M. J. O'Connor and Y. J. Bang (2017). "AZD6738, A Novel Oral Inhibitor of ATR, Induces Synthetic Lethality with ATM Deficiency in Gastric Cancer Cells." Mol Cancer Ther **16**(4): 566-577.

Mir, S. E., P. C. De Witt Hamer, P. M. Krawczyk, L. Balaj, A. Claes, J. M. Niers, A. A. Van Tilborg, A. H. Zwinderman, D. Geerts, G. J. Kaspers, W. Peter Vandertop, J. Cloos, B. A. Tannous, P. Wesseling, J. A. Aten, D. P. Noske, C. J. Van Noorden and T. Wurdinger (2010). "In silico analysis of kinase expression identifies WEE1 as a gatekeeper against mitotic catastrophe in glioblastoma." Cancer Cell **18**(3): 244-257.

Mittendorf, E. A., A. V. Philips, F. Meric-Bernstam, N. Qiao, Y. Wu, S. Harrington, X. Su, Y. Wang, A. M. Gonzalez-Angulo, A. Akcakanat, A. Chawla, M. Curran, P. Hwu, P. Sharma, J. K. Litton, J. J. Mollndrem and G. Alatrash (2014). "PD-L1 expression in triple-negative breast cancer." Cancer Immunol Res **2**(4): 361-370.

Mohrin, M., E. Bourke, D. Alexander, M. R. Warr, K. Barry-Holson, M. M. Le Beau, C. G. Morrison and E. Passegue (2010). "Hematopoietic stem cell quiescence promotes error-prone DNA repair and mutagenesis." Cell Stem Cell **7**(2): 174-185.

Mokrani-Benhelli, H., L. Gaillard, P. Biasutto, T. Le Guen, F. Touzot, N. Vasquez, J. Komatsu, E. Conseiller, C. Picard, E. Gluckman, C. Francannet, A. Fischer, A. Durandy, J. Soulier, J. P. de Villartay, M. Cavazzana-Calvo and P. Revy (2013). "Primary microcephaly, impaired DNA replication, and genomic instability caused by compound heterozygous ATR mutations." Hum Mutat **34**(2): 374-384.

Moore, K., N. Colombo, G. Scambia, B. G. Kim, A. Oaknin, M. Friedlander, A. Lisyanskaya, A. Floquet, A. Leary, G. S. Sonke, C. Gourley, S. Banerjee, A. Oza, A. Gonzalez-Martin, C. Aghajanian, W. Bradley, C. Mathews, J. Liu, E. S. Lowe, R. Bloomfield and P. DiSilvestro (2018). "Maintenance Olaparib in Patients with Newly Diagnosed Advanced Ovarian Cancer." N Engl J Med **379**(26): 2495-2505.

Mordes, D. A., G. G. Glick, R. Zhao and D. Cortez (2008). "TopBP1 activates ATR through ATRIP and a PIKK regulatory domain." Genes Dev **22**(11): 1478-1489.

Morrow, M., J. Waters and E. Morris (2011). "MRI for breast cancer screening, diagnosis, and treatment." Lancet **378**(9805): 1804-1811.

Moudgil, D. K., N. Westcott, J. K. Famulski, K. Patel, D. Macdonald, H. Hang and G. K. Chan (2015). "A novel role of farnesylation in targeting a mitotic checkpoint protein, human Spindly, to kinetochores." J Cell Biol **208**(7): 881-896.

Mouw, K. W., M. S. Goldberg, P. A. Konstantinopoulos and A. D. D'Andrea (2017). "DNA Damage and Repair Biomarkers of Immunotherapy Response." Cancer Discov **7**(7): 675-693.

Mukesh, M. B., G. C. Barnett, J. S. Wilkinson, A. M. Moody, C. Wilson, L. Dorling, C. Chan Wah Hak, W. Qian, N. Twyman, N. G. Burnet, G. C. Wishart and C. E. Coles (2013). "Randomized controlled trial of intensity-modulated radiotherapy for early breast cancer: 5-year results confirm superior overall cosmesis." J Clin Oncol **31**(36): 4488-4495.

Munch-Petersen, B., L. Cloos, H. K. Jensen and G. Tyrsted (1995). "Human thymidine kinase 1. Regulation in normal and malignant cells." Adv Enzyme Regul **35**: 69-89.

Munsell, M. F., B. L. Sprague, D. A. Berry, G. Chisholm and A. Trentham-Dietz (2014). "Body mass index and breast cancer risk according to postmenopausal estrogen-progestin use and hormone receptor status." Epidemiol Rev **36**: 114-136.

Murrow, L. M., S. V. Garimella, T. L. Jones, N. J. Caplen and S. Lipkowitz (2010). "Identification of WEE1 as a potential molecular target in cancer cells by RNAi screening of the human tyrosine kinome." Breast Cancer Res Treat **122**(2): 347-357.

Nam, E. A., R. Zhao, G. G. Glick, C. E. Bansbach, D. B. Friedman and D. Cortez (2011). "Thr-1989 phosphorylation is a marker of active ataxia telangiectasia-mutated and Rad3-related (ATR) kinase." J Biol Chem **286**(33): 28707-28714.

NCCN. (2021). "NCCN Clinical Practice Guidelines in Oncology: Breast Cancer." 2.2021. Retrieved March 12, 2021, from https://www.nccn.org/professionals/physician_gls/pdf/breast.pdf.

NCI, N. "Cancer Stat Facts: Female Breast Cancer Subtypes." Retrieved 31 Jan, 2021, from <https://seer.cancer.gov/statfacts/html/breast-subtypes.html>.

Nelson, H. D., R. Fu, A. Cantor, M. Pappas, M. Daeges and L. Humphrey (2016). "Effectiveness of Breast Cancer Screening: Systematic Review and Meta-analysis to Update the 2009 U.S. Preventive Services Task Force Recommendation." Ann Intern Med **164**(4): 244-255.

Nghiem, P., P. K. Park, Y. Kim, C. Vaziri and S. L. Schreiber (2001). "ATR inhibition selectively sensitizes G1 checkpoint-deficient cells to lethal premature chromatin condensation." Proc Natl Acad Sci U S A **98**(16): 9092-9097.

- Nirschl, C. J., M. Suarez-Farinas, B. Izar, S. Prakadan, R. Dannenfelser, I. Tirosh, Y. Liu, Q. Zhu, K. S. P. Devi, S. L. Carroll, D. Chau, M. Rezaee, T. G. Kim, R. Huang, J. Fuentes-Duculan, G. X. Song-Zhao, N. Gulati, M. A. Lowes, S. L. King, F. J. Quintana, Y. S. Lee, J. G. Krueger, K. Y. Sarin, C. H. Yoon, L. Garraway, A. Regev, A. K. Shalek, O. Troyanskaya and N. Anandasabapathy (2017). "IFN γ -Dependent Tissue-Immune Homeostasis Is Co-opted in the Tumor Microenvironment." Cell **170**(1): 127-141 e115.
- Nissen, M. S., T. A. Langan and R. Reeves (1991). "Phosphorylation by cdc2 kinase modulates DNA binding activity of high mobility group I nonhistone chromatin protein." J Biol Chem **266**(30): 19945-19952.
- Nitz, U., O. Gluz, M. Clemens, W. Malter, T. Reimer, B. Nuding, B. Aktas, A. Stefek, A. Pollmanns, F. Lorenz-Salehi, C. Uleer, P. Krabisch, S. Kuemmel, C. Liedtke, S. Shak, R. Wuerstlein, M. Christgen, R. E. Kates, H. H. Kreipe, N. Harbeck and B. I. West German Study Group Plan (2019). "West German Study PlanB Trial: Adjuvant Four Cycles of Epirubicin and Cyclophosphamide Plus Docetaxel Versus Six Cycles of Docetaxel and Cyclophosphamide in HER2-Negative Early Breast Cancer." J Clin Oncol **37**(10): 799-808.
- Nurse, P. (1990). "Universal control mechanism regulating onset of M-phase." Nature **344**(6266): 503-508.
- O'Driscoll, M., V. L. Ruiz-Perez, C. G. Woods, P. A. Jeggo and J. A. Goodship (2003). "A splicing mutation affecting expression of ataxia-telangiectasia and Rad3-related protein (ATR) results in Seckel syndrome." Nat Genet **33**(4): 497-501.
- O'Neil, N. J., M. L. Bailey and P. Hieter (2017). "Synthetic lethality and cancer." Nat Rev Genet **18**(10): 613-623.
- Oh, J. S., A. Susor and M. Conti (2011). "Protein tyrosine kinase Wee1B is essential for metaphase II exit in mouse oocytes." Science **332**(6028): 462-465.
- Pan, H., R. Gray, J. Braybrooke, C. Davies, C. Taylor, P. McGale, R. Peto, K. I. Pritchard, J. Bergh, M. Dowsett, D. F. Hayes and Ebcctg (2017). "20-Year Risks of Breast-Cancer Recurrence after Stopping Endocrine Therapy at 5 Years." N Engl J Med **377**(19): 1836-1846.
- Paproski, R. J., M. Wuest, H. S. Jans, K. Graham, W. P. Gati, S. McQuarrie, A. McEwan, J. Mercer, J. D. Young and C. E. Cass (2010). "Biodistribution and uptake of 3'-deoxy-3'-fluorothymidine in ENT1-knockout mice and in an ENT1-knockdown tumor model." J Nucl Med **51**(9): 1447-1455.
- Pardoll, D. M. (2012). "The blockade of immune checkpoints in cancer immunotherapy." Nat Rev Cancer **12**(4): 252-264.
- Parikh, R. A., L. J. Appleman, J. E. Bauman, M. Sankunny, D. W. Lewis, A. Vlad and S. M. Gollin (2014). "Upregulation of the ATR-CHEK1 pathway in oral squamous cell carcinomas." Genes Chromosomes Cancer **53**(1): 25-37.
- Park, S. S., H. Dong, X. Liu, S. M. Harrington, C. J. Krco, M. P. Grams, A. S. Mansfield, K. M. Furutani, K. R. Olivier and E. D. Kwon (2015). "PD-1 Restrains Radiotherapy-Induced Abscopal Effect." Cancer Immunol Res **3**(6): 610-619.

- Parsels, L. A., D. Karnak, J. D. Parsels, Q. Zhang, J. Velez-Padilla, Z. R. Reichert, D. R. Wahl, J. Maybaum, M. J. O'Connor, T. S. Lawrence and M. A. Morgan (2018). "PARP1 Trapping and DNA Replication Stress Enhance Radiosensitization with Combined WEE1 and PARP Inhibitors." Mol Cancer Res **16**(2): 222-232.
- Patel, P., L. Sun, Y. Robbins, P. E. Clavijo, J. Friedman, C. Silvin, C. Van Waes, J. Cook, J. Mitchell and C. Allen (2019). "Enhancing direct cytotoxicity and response to immune checkpoint blockade following ionizing radiation with Wee1 kinase inhibition." Oncoimmunology **8**(11): e1638207.
- Peasland, A., L. Z. Wang, E. Rowling, S. Kyle, T. Chen, A. Hopkins, W. A. Cliby, J. Sarkaria, G. Beale, R. J. Edmondson and N. J. Curtin (2011). "Identification and evaluation of a potent novel ATR inhibitor, NU6027, in breast and ovarian cancer cell lines." Br J Cancer **105**(3): 372-381.
- Perou, C. M., T. Sorlie, M. B. Eisen, M. van de Rijn, S. S. Jeffrey, C. A. Rees, J. R. Pollack, D. T. Ross, H. Johnsen, L. A. Akslen, O. Fluge, A. Pergamenschikov, C. Williams, S. X. Zhu, P. E. Lonning, A. L. Borresen-Dale, P. O. Brown and D. Botstein (2000). "Molecular portraits of human breast tumours." Nature **406**(6797): 747-752.
- Perry, J. and N. Kleckner (2003). "The ATRs, ATMs, and TORs are giant HEAT repeat proteins." Cell **112**(2): 151-155.
- Peter, M., J. Nakagawa, M. Doree, J. C. Labbe and E. A. Nigg (1990). "In vitro disassembly of the nuclear lamina and M phase-specific phosphorylation of lamins by cdc2 kinase." Cell **61**(4): 591-602.
- Petrovas, C., J. P. Casazza, J. M. Brenchley, D. A. Price, E. Gostick, W. C. Adams, M. L. Precopio, T. Schacker, M. Roederer, D. C. Douek and R. A. Koup (2006). "PD-1 is a regulator of virus-specific CD8+ T cell survival in HIV infection." J Exp Med **203**(10): 2281-2292.
- Phillips, C., R. Jeffree and M. Khasraw (2017). "Management of breast cancer brain metastases: A practical review." Breast **31**: 90-98.
- Pilie, P. G., C. Tang, G. B. Mills and T. A. Yap (2019). "State-of-the-art strategies for targeting the DNA damage response in cancer." Nat Rev Clin Oncol **16**(2): 81-104.
- Pio, B. S., C. K. Park, R. Pietras, W. A. Hsueh, N. Satyamurthy, M. D. Pegram, J. Czernin, M. E. Phelps and D. H. Silverman (2006). "Usefulness of 3'-[F-18]fluoro-3'-deoxythymidine with positron emission tomography in predicting breast cancer response to therapy." Mol Imaging Biol **8**(1): 36-42.
- Piranlioglu, R., E. Lee, M. Ouzounova, R. J. Bollag, A. H. Vinyard, A. S. Arbab, D. Marasco, M. Guzel, J. K. Cowell, M. Thangaraju, A. Chadli, K. A. Hassan, M. S. Wicha, E. Celis and H. Korkaya (2019). "Primary tumor-induced immunity eradicates disseminated tumor cells in syngeneic mouse model." Nat Commun **10**(1): 1430.
- Pires, I. M., M. M. Olcina, S. Anbalagan, J. R. Pollard, P. M. Reaper, P. A. Charlton, W. G. McKenna and E. M. Hammond (2012). "Targeting radiation-resistant hypoxic tumour cells through ATR inhibition." Br J Cancer **107**(2): 291-299.

Planes-Laine, G., P. Rochigneux, F. Bertucci, A. S. Chretien, P. Viens, R. Sabatier and A. Goncalves (2019). "PD-1/PD-L1 Targeting in Breast Cancer: The First Clinical Evidences Are Emerging. A Literature Review." Cancers (Basel) **11**(7).

Plummer, E. R., E. J. Dean, T. R. J. Evans, A. Greystoke, K. Herbschleb, M. Ranson, J. Brown, Y. Zhang, S. Karan, J. Pollard, M. S. Penney, M. Asmal, S. Z. Fields and M. R. Middleton (2016). "Phase I trial of first-in-class ATR inhibitor VX-970 in combination with gemcitabine (Gem) in advanced solid tumors (NCT02157792)." Journal of Clinical Oncology **34**(15_suppl): 2513-2513.

Porter, C. C., J. Kim, S. Fosmire, C. M. Gearheart, A. van Linden, D. Baturin, V. Zaberezhnyy, P. R. Patel, D. Gao, A. C. Tan and J. DeGregori (2012). "Integrated genomic analyses identify WEE1 as a critical mediator of cell fate and a novel therapeutic target in acute myeloid leukemia." Leukemia **26**(6): 1266-1276.

PosthumaDeBoer, J., T. Wurdinger, H. C. Graat, V. W. van Beusechem, M. N. Helder, B. J. van Royen and G. J. Kaspers (2011). "WEE1 inhibition sensitizes osteosarcoma to radiotherapy." BMC Cancer **11**: 156.

Prevo, R., E. Fokas, P. M. Reaper, P. A. Charlton, J. R. Pollard, W. G. McKenna, R. J. Muschel and T. B. Brunner (2012). "The novel ATR inhibitor VE-821 increases sensitivity of pancreatic cancer cells to radiation and chemotherapy." Cancer Biol Ther **13**(11): 1072-1081.

Prevo, R., G. Pirovano, R. Puliyadi, K. J. Herbert, G. Rodriguez-Berriguete, A. O'Docherty, W. Greaves, W. G. McKenna and G. S. Higgins (2018). "CDK1 inhibition sensitizes normal cells to DNA damage in a cell cycle dependent manner." Cell Cycle **17**(12): 1513-1523.

Raccagni, I., S. Belloli, S. Valtorta, A. Stefano, L. Presotto, C. Pascali, A. Bogni, M. Tortoreto, N. Zaffaroni, M. G. Daidone, G. Russo, E. Bombardieri and R. M. Moresco (2018). "[¹⁸F]FDG and [¹⁸F]FLT PET for the evaluation of response to neo-adjuvant chemotherapy in a model of triple negative breast cancer." PLoS One **13**(5): e0197754.

Rajeshkumar, N. V., E. De Oliveira, N. Ottenhof, J. Watters, D. Brooks, T. Demuth, S. D. Shumway, S. Mizuarai, H. Hirai, A. Maitra and M. Hidalgo (2011). "MK-1775, a potent Wee1 inhibitor, synergizes with gemcitabine to achieve tumor regressions, selectively in p53-deficient pancreatic cancer xenografts." Clin Cancer Res **17**(9): 2799-2806.

Rasey, J. S., J. R. Grierson, L. W. Wiens, P. D. Kolb and J. L. Schwartz (2002). "Validation of FLT uptake as a measure of thymidine kinase-1 activity in A549 carcinoma cells." J Nucl Med **43**(9): 1210-1217.

Reaper, P. M., M. R. Griffiths, J. M. Long, J. D. Charrier, S. McCormick, P. A. Charlton, J. M. Golec and J. R. Pollard (2011). "Selective killing of ATM- or p53-deficient cancer cells through inhibition of ATR." Nat Chem Biol **7**(7): 428-430.

Reck, M., D. Rodriguez-Abreu, A. G. Robinson, R. Hui, T. Csozi, A. Fulop, M. Gottfried, N. Peled, A. Tafreshi, S. Cuffe, M. O'Brien, S. Rao, K. Hotta, M. A. Leiby, G. M. Lubiniecki, Y. Shentu, R. Rangwala, J. R. Brahmer and K.-. Investigators (2016). "Pembrolizumab versus Chemotherapy for PD-L1-Positive Non-Small-Cell Lung Cancer." N Engl J Med **375**(19): 1823-1833.

- Reits, E. A., J. W. Hodge, C. A. Herberts, T. A. Groothuis, M. Chakraborty, E. K. Wansley, K. Camphausen, R. M. Luiten, A. H. de Ru, J. Neijssen, A. Griekspoor, E. Mesman, F. A. Verreck, H. Spits, J. Schlom, P. van Veelen and J. J. Neefjes (2006). "Radiation modulates the peptide repertoire, enhances MHC class I expression, and induces successful antitumor immunotherapy." J Exp Med **203**(5): 1259-1271.
- Ren, L., L. Chen, W. Wu, L. Garribba, H. Tian, Z. Liu, I. Vogel, C. Li, I. D. Hickson and Y. Liu (2017). "Potential biomarkers of DNA replication stress in cancer." Oncotarget **8**(23): 36996-37008.
- Rehman, A. G., M. Tyson, M. Egger, R. F. Heller and M. Zwahlen (2008). "Body-mass index and incidence of cancer: a systematic review and meta-analysis of prospective observational studies." Lancet **371**(9612): 569-578.
- Rengan, A. K., A. B. Bukhari, A. Pradhan, R. Malhotra, R. Banerjee, R. Srivastava and A. De (2015). "In vivo analysis of biodegradable liposome gold nanoparticles as efficient agents for photothermal therapy of cancer." Nano Lett **15**(2): 842-848.
- Richard, S. D., B. Bencherif, R. P. Edwards, E. Elishaev, T. C. Krivak, J. M. Mountz and J. A. DeLoia (2011). "Noninvasive assessment of cell proliferation in ovarian cancer using [18F] 3'deoxy-3-fluorothymidine positron emission tomography/computed tomography imaging." Nucl Med Biol **38**(4): 485-491.
- Robert, C., G. V. Long, B. Brady, C. Dutriaux, M. Maio, L. Mortier, J. C. Hassel, P. Rutkowski, C. McNeil, E. Kalinka-Warzocho, K. J. Savage, M. M. Hernberg, C. Lebbe, J. Charles, C. Mihalciou, V. Chiarion-Sileni, C. Mauch, F. Cognetti, A. Arance, H. Schmidt, D. Schadendorf, H. Gogas, L. Lundgren-Eriksson, C. Horak, B. Sharkey, I. M. Waxman, V. Atkinson and P. A. Ascierto (2015). "Nivolumab in previously untreated melanoma without BRAF mutation." N Engl J Med **372**(4): 320-330.
- Robert, C., J. Schachter, G. V. Long, A. Arance, J. J. Grob, L. Mortier, A. Daud, M. S. Carlino, C. McNeil, M. Lotem, J. Larkin, P. Lorigan, B. Neyns, C. U. Blank, O. Hamid, C. Mateus, R. Shapira-Frommer, M. Kosh, H. Zhou, N. Ibrahim, S. Ebbinghaus, A. Ribas and K.-. investigators (2015). "Pembrolizumab versus Ipilimumab in Advanced Melanoma." N Engl J Med **372**(26): 2521-2532.
- Robson, M., S. A. Im, E. Senkus, B. Xu, S. M. Domchek, N. Masuda, S. Delalogue, W. Li, N. Tung, A. Armstrong, W. Wu, C. Goessl, S. Runswick and P. Conte (2017). "Olaparib for Metastatic Breast Cancer in Patients with a Germline BRCA Mutation." N Engl J Med **377**(6): 523-533.
- Rodriguez, C., H. Valles, A. Causse, V. Johannsdottir, J. F. Eliaou and C. Theillet (2002). "Involvement of ATM missense variants and mutations in a series of unselected breast cancer cases." Genes Chromosomes Cancer **33**(2): 141-149.
- Romond, E. H., E. A. Perez, J. Bryant, V. J. Suman, C. E. Geyer, Jr., N. E. Davidson, E. Tan-Chiu, S. Martino, S. Paik, P. A. Kaufman, S. M. Swain, T. M. Pisansky, L. Fehrenbacher, L. A. Kutteh, V. G. Vogel, D. W. Visscher, G. Yothers, R. B. Jenkins, A. M. Brown, S. R. Dakhil, E. P. Mamounas, W. L. Lingle, P. M. Klein, J. N. Ingle and N. Wolmark (2005). "Trastuzumab plus adjuvant chemotherapy for operable HER2-positive breast cancer." N Engl J Med **353**(16): 1673-1684.

- Ross, S. H. and D. A. Cantrell (2018). "Signaling and Function of Interleukin-2 in T Lymphocytes." Annu Rev Immunol **36**: 411-433.
- Ruffell, B. and L. M. Coussens (2015). "Macrophages and therapeutic resistance in cancer." Cancer Cell **27**(4): 462-472.
- Rugo, H. S., R. B. Rumble, E. Macrae, D. L. Barton, H. K. Connolly, M. N. Dickler, L. Fallowfield, B. Fowble, J. N. Ingle, M. Jahanzeb, S. R. Johnston, L. A. Korde, J. L. Khatcheressian, R. S. Mehta, H. B. Muss and H. J. Burstein (2016). "Endocrine Therapy for Hormone Receptor-Positive Metastatic Breast Cancer: American Society of Clinical Oncology Guideline." J Clin Oncol **34**(25): 3069-3103.
- Saldivar, J. C., S. Hamperl, M. J. Bocek, M. Chung, T. E. Bass, F. Cisneros-Soberanis, K. Samejima, L. Xie, J. R. Paulson, W. C. Earnshaw, D. Cortez, T. Meyer and K. A. Cimprich (2018). "An intrinsic S/G2 checkpoint enforced by ATR." Science **361**(6404): 806-810.
- Sanai, N., J. Li, J. Boerner, K. Stark, J. Wu, S. Kim, A. Derogatis, S. Mehta, H. D. Dhruv, L. K. Heilbrun, M. E. Berens and P. M. LoRusso (2018). "Phase 0 Trial of AZD1775 in First-Recurrence Glioblastoma Patients." Clin Cancer Res **24**(16): 3820-3828.
- Sanjiv, K., A. Hagenkort, J. M. Calderon-Montano, T. Koolmeister, P. M. Reaper, O. Mortusewicz, S. A. Jacques, R. V. Kuiper, N. Schultz, M. Scobie, P. A. Charlton, J. R. Pollard, U. W. Berglund, M. Altun and T. Helleday (2016). "Cancer-Specific Synthetic Lethality between ATR and CHK1 Kinase Activities." Cell Rep **14**(2): 298-309.
- Santamaria, D., C. Barriere, A. Cerqueira, S. Hunt, C. Tardy, K. Newton, J. F. Caceres, P. Dubus, M. Malumbres and M. Barbacid (2007). "Cdk1 is sufficient to drive the mammalian cell cycle." Nature **448**(7155): 811-815.
- Saraiva, M. and A. O'Garra (2010). "The regulation of IL-10 production by immune cells." Nat Rev Immunol **10**(3): 170-181.
- Sarkaria, J. N., E. C. Busby, R. S. Tibbetts, P. Roos, Y. Taya, L. M. Karnitz and R. T. Abraham (1999). "Inhibition of ATM and ATR kinase activities by the radiosensitizing agent, caffeine." Cancer Res **59**(17): 4375-4382.
- Sato, H., A. Niimi, T. Yasuhara, T. B. M. Permata, Y. Hagiwara, M. Isono, E. Nuryadi, R. Sekine, T. Oike, S. Kakoti, Y. Yoshimoto, K. D. Held, Y. Suzuki, K. Kono, K. Miyagawa, T. Nakano and A. Shibata (2017). "DNA double-strand break repair pathway regulates PD-L1 expression in cancer cells." Nat Commun **8**(1): 1751.
- Satyanarayana, A., C. Berthet, J. Lopez-Molina, V. Coppola, L. Tessarollo and P. Kaldis (2008). "Genetic substitution of Cdk1 by Cdk2 leads to embryonic lethality and loss of meiotic function of Cdk2." Development **135**(20): 3389-3400.
- Satyanarayana, A., M. B. Hilton and P. Kaldis (2008). "p21 Inhibits Cdk1 in the absence of Cdk2 to maintain the G1/S phase DNA damage checkpoint." Mol Biol Cell **19**(1): 65-77.
- Sausville, E., P. Lorusso, M. Carducci, J. Carter, M. F. Quinn, L. Malburg, N. Azad, D. Cosgrove, R. Knight, P. Barker, S. Zabludoff, F. Agbo, P. Oakes and A. Senderowicz (2014). "Phase I dose-escalation study of AZD7762, a checkpoint kinase inhibitor, in combination with gemcitabine in US patients with advanced solid tumors." Cancer Chemother Pharmacol **73**(3): 539-549.

Savitsky, K., A. Bar-Shira, S. Gilad, G. Rotman, Y. Ziv, L. Vanagaite, D. A. Tagle, S. Smith, T. Uziel, S. Sfez, M. Ashkenazi, I. Pecker, M. Frydman, R. Harnik, S. R. Patanjali, A. Simmons, G. A. Clines, A. Sartiel, R. A. Gatti, L. Chessa, O. Sanal, M. F. Lavin, N. G. Jaspers, A. M. Taylor, C. F. Arlett, T. Miki, S. M. Weissman, M. Lovett, F. S. Collins and Y. Shiloh (1995). "A single ataxia telangiectasia gene with a product similar to PI-3 kinase." *Science* **268**(5218): 1749-1753.

Schelhaas, S., K. Heinzmann, V. R. Bollineni, G. M. Kramer, Y. Liu, J. C. Waterton, E. O. Aboagye, A. F. Shields, D. Soloviev and A. H. Jacobs (2017). "Preclinical Applications of 3'-Deoxy-3'-[(18)F]Fluorothymidine in Oncology - A Systematic Review." *Theranostics* **7**(1): 40-50.

Schindelin, J., I. Arganda-Carreras, E. Frise, V. Kaynig, M. Longair, T. Pietzsch, S. Preibisch, C. Rueden, S. Saalfeld, B. Schmid, J. Y. Tinevez, D. J. White, V. Hartenstein, K. Eliceiri, P. Tomancak and A. Cardona (2012). "Fiji: an open-source platform for biological-image analysis." *Nat Methods* **9**(7): 676-682.

Schleicher, E. M., A. Dhoonmoon, L. M. Jackson, K. E. Clements, C. L. Stump, C. M. Nicolae and G. L. Moldovan (2020). "Dual genome-wide CRISPR knockout and CRISPR activation screens identify mechanisms that regulate the resistance to multiple ATR inhibitors." *PLoS Genet* **16**(11): e1009176.

Schmidt, M., A. Rohe, C. Platzer, A. Najjar, F. Erdmann and W. Sippl (2017). "Regulation of G2/M Transition by Inhibition of WEE1 and PKMYT1 Kinases." *Molecules* **22**(12).

Schrors, B., S. Boegel, C. Albrecht, T. Bukur, V. Bukur, C. Holtstrater, C. Ritzel, K. Manninen, A. D. Tadmor, M. Vormehr, U. Sahin and M. Lower (2020). "Multi-Omics Characterization of the 4T1 Murine Mammary Gland Tumor Model." *Front Oncol* **10**: 1195.

Schwartz, L. H., S. Litiere, E. de Vries, R. Ford, S. Gwyther, S. Mandrekar, L. Shankar, J. Bogaerts, A. Chen, J. Dancey, W. Hayes, F. S. Hodi, O. S. Hoekstra, E. P. Huang, N. Lin, Y. Liu, P. Therasse, J. D. Wolchok and L. Seymour (2016). "RECIST 1.1-Update and clarification: From the RECIST committee." *Eur J Cancer* **62**: 132-137.

Schwartz, M., E. Zlotorynski, M. Goldberg, E. Ozeri, A. Rahat, C. le Sage, B. P. Chen, D. J. Chen, R. Agami and B. Kerem (2005). "Homologous recombination and nonhomologous end-joining repair pathways regulate fragile site stability." *Genes Dev* **19**(22): 2715-2726.

Senkus, E., S. Kyriakides, S. Ohno, F. Penault-Llorca, P. Poortmans, E. Rutgers, S. Zackrisson, F. Cardoso and E. G. Committee (2015). "Primary breast cancer: ESMO Clinical Practice Guidelines for diagnosis, treatment and follow-up." *Ann Oncol* **26 Suppl 5**: v8-30.

Seto, T., T. Esaki, F. Hirai, S. Arita, K. Nosaki, A. Makiyama, T. Kometani, C. Fujimoto, M. Hamatake, H. Takeoka, F. Agbo and X. Shi (2013). "Phase I, dose-escalation study of AZD7762 alone and in combination with gemcitabine in Japanese patients with advanced solid tumours." *Cancer Chemother Pharmacol* **72**(3): 619-627.

Seung, S. J., A. N. Traore, B. Pourmirza, K. E. Fathers, M. Coombes and K. J. Jerzak (2020). "A population-based analysis of breast cancer incidence and survival by subtype in Ontario women." *Curr Oncol* **27**(2): e191-e198.

- Shaner, N. C., R. E. Campbell, P. A. Steinbach, B. N. Giepmans, A. E. Palmer and R. Y. Tsien (2004). "Improved monomeric red, orange and yellow fluorescent proteins derived from *Discosoma* sp. red fluorescent protein." Nat Biotechnol **22**(12): 1567-1572.
- Sharabi, A. B., C. J. Nirschl, C. M. Kochel, T. R. Nirschl, B. J. Francica, E. Velarde, T. L. Deweese and C. G. Drake (2015). "Stereotactic Radiation Therapy Augments Antigen-Specific PD-1-Mediated Antitumor Immune Responses via Cross-Presentation of Tumor Antigen." Cancer Immunol Res **3**(4): 345-355.
- Shen, R., Q. Yang, Z. Liu, Y. Wang, X. Fan, L. Li, B. Hu, W. Xiao, M. Ma, W. Chen, X. Liu, W. Shi and A. Liu (2020). "The landscape of predictive biomarkers for ATR inhibition in Chinese solid-tumor patients." Journal of Clinical Oncology **38**(15_suppl): 3626-3626.
- Sheng, H., Y. Huang, Y. Xiao, Z. Zhu, M. Shen, P. Zhou, Z. Guo, J. Wang, H. Wang, W. Dai, W. Zhang, J. Sun and C. Cao (2020). "ATR inhibitor AZD6738 enhances the antitumor activity of radiotherapy and immune checkpoint inhibitors by potentiating the tumor immune microenvironment in hepatocellular carcinoma." J Immunother Cancer **8**(1).
- Sherley, J. L. and T. J. Kelly (1988). "Regulation of human thymidine kinase during the cell cycle." J Biol Chem **263**(17): 8350-8358.
- Sherr, C. J. (1994). "G1 phase progression: cycling on cue." Cell **79**(4): 551-555.
- Shields, A. F., J. R. Grierson, B. M. Dohmen, H. J. Machulla, J. C. Stayanoff, J. M. Lawhorn-Crews, J. E. Obradovich, O. Muzik and T. J. Mangner (1998). "Imaging proliferation in vivo with [F-18]FLT and positron emission tomography." Nature Medicine **4**(11): 1334-1336.
- Shiovitz, S. and L. A. Korde (2015). "Genetics of breast cancer: a topic in evolution." Ann Oncol **26**(7): 1291-1299.
- Shrivastav, M., L. P. De Haro and J. A. Nickoloff (2008). "Regulation of DNA double-strand break repair pathway choice." Cell Res **18**(1): 134-147.
- Silver, D. P., A. L. Richardson, A. C. Eklund, Z. C. Wang, Z. Szallasi, Q. Li, N. Juul, C. O. Leong, D. Calogrias, A. Buraimoh, A. Fatima, R. S. Gelman, P. D. Ryan, N. M. Tung, A. De Nicolo, S. Ganesan, A. Miron, C. Colin, D. C. Sgroi, L. W. Ellisen, E. P. Winer and J. E. Garber (2010). "Efficacy of neoadjuvant Cisplatin in triple-negative breast cancer." J Clin Oncol **28**(7): 1145-1153.
- Singletary, K. W. and S. M. Gapstur (2001). "Alcohol and breast cancer: review of epidemiologic and experimental evidence and potential mechanisms." JAMA **286**(17): 2143-2151.
- Slamon, D., W. Eiermann, N. Robert, T. Pienkowski, M. Martin, M. Press, J. Mackey, J. Glaspy, A. Chan, M. Pawlicki, T. Pinter, V. Valero, M. C. Liu, G. Sauter, G. von Minckwitz, F. Visco, V. Bee, M. Buyse, B. Bendahmane, I. Tabah-Fisch, M. A. Lindsay, A. Riva, J. Crown and G. Breast Cancer International Research (2011). "Adjuvant trastuzumab in HER2-positive breast cancer." N Engl J Med **365**(14): 1273-1283.
- Smyczek-Gargya, B., N. Fersis, H. Dittmann, U. Vogel, G. Reischl, H. J. Machulla, D. Wallwiener, R. Bares and B. M. Dohmen (2004). "PET with [18F]fluorothymidine for imaging of primary breast cancer: a pilot study." Eur J Nucl Med Mol Imaging **31**(5): 720-724.

Spranger, S., R. M. Spaapen, Y. Zha, J. Williams, Y. Meng, T. T. Ha and T. F. Gajewski (2013). "Up-regulation of PD-L1, IDO, and T(regs) in the melanoma tumor microenvironment is driven by CD8(+) T cells." Sci Transl Med **5**(200): 200ra116.

Squire, C. J., J. M. Dickson, I. Ivanovic and E. N. Baker (2005). "Structure and inhibition of the human cell cycle checkpoint kinase, Wee1A kinase: an atypical tyrosine kinase with a key role in CDK1 regulation." Structure **13**(4): 541-550.

Sridharan, V., D. N. Margalit, S. A. Lynch, M. Severgnini, J. Zhou, N. G. Chau, G. Rabinowits, J. H. Lorch, P. S. Hammerman, F. S. Hodi, R. I. Haddad, R. B. Tishler and J. D. Schoenfeld (2016). "Definitive chemoradiation alters the immunologic landscape and immune checkpoints in head and neck cancer." Br J Cancer **115**(2): 252-260.

Steel, G. G., T. J. McMillan and J. H. Peacock (1989). "The 5Rs of radiobiology." Int J Radiat Biol **56**(6): 1045-1048.

Stewart, E., S. M. Federico, X. Chen, A. A. Shelat, C. Bradley, B. Gordon, A. Karlstrom, N. R. Twarog, M. R. Clay, A. Bahrami, B. B. Freeman, 3rd, B. Xu, X. Zhou, J. Wu, V. Honnell, M. Ocarz, K. Blankenship, J. Dapper, E. R. Mardis, R. K. Wilson, J. Downing, J. Zhang, J. Easton, A. Pappo and M. A. Dyer (2017). "Orthotopic patient-derived xenografts of paediatric solid tumours." Nature **549**(7670): 96-100.

Sun, L., E. Moore, R. Berman, P. E. Clavijo, A. Saleh, Z. Chen, C. Van Waes, J. Davies, J. Friedman and C. T. Allen (2018). "WEE1 kinase inhibition reverses G2/M cell cycle checkpoint activation to sensitize cancer cells to immunotherapy." Oncoimmunology **7**(10): e1488359.

Sun, L. L., R. Y. Yang, C. W. Li, M. K. Chen, B. Shao, J. M. Hsu, L. C. Chan, Y. Yang, J. L. Hsu, Y. J. Lai and M. C. Hung (2018). "Inhibition of ATR downregulates PD-L1 and sensitizes tumor cells to T cell-mediated killing." Am J Cancer Res **8**(7): 1307-1316.

Sung, H., J. Ferlay, R. L. Siegel, M. Laversanne, I. Soerjomataram, A. Jemal and F. Bray (2021). "Global cancer statistics 2020: GLOBOCAN estimates of incidence and mortality worldwide for 36 cancers in 185 countries." CA Cancer J Clin.

Surova, O. and B. Zhivotovsky (2013). "Various modes of cell death induced by DNA damage." Oncogene **32**(33): 3789-3797.

Swann, J. B. and M. J. Smyth (2007). "Immune surveillance of tumors." J Clin Invest **117**(5): 1137-1146.

Tan, P. H., I. Ellis, K. Allison, E. Brogi, S. B. Fox, S. Lakhani, A. J. Lazar, E. A. Morris, A. Sahin, R. Salgado, A. Sapino, H. Sasano, S. Schnitt, C. Sotiriou, P. van Diest, V. A. White, D. Lokuhetty, I. A. Cree and W. H. O. C. o. T. E. Board (2020). "The 2019 World Health Organization classification of tumours of the breast." Histopathology **77**(2): 181-185.

Tao, L., R. B. Schwab, Y. San Miguel, S. L. Gomez, A. J. Canchola, M. Gago-Dominguez, I. K. Komenaka, J. D. Murphy, A. A. Molinolo and M. E. Martinez (2019). "Breast Cancer Mortality in Older and Younger Patients in California." Cancer Epidemiol Biomarkers Prev **28**(2): 303-310.

Taylor, A. and M. E. Powell (2004). "Intensity-modulated radiotherapy--what is it?" Cancer Imaging **4**(2): 68-73.

Techer, H., S. Koundrioukoff, S. Carignon, T. Wilhelm, G. A. Millot, B. S. Lopez, O. Brison and M. Debatisse (2016). "Signaling from Mus81-Eme2-Dependent DNA Damage Elicited by Chk1 Deficiency Modulates Replication Fork Speed and Origin Usage." Cell Rep **14**(5): 1114-1127.

Tehrani, O. S. and A. F. Shields (2013). "PET imaging of proliferation with pyrimidines." J Nucl Med **54**(6): 903-912.

Teicher, B. A., Y. Maehara, Y. Kakeji, G. Ara, S. R. Keyes, J. Wong and R. Herbst (1997). "Reversal of in vivo drug resistance by the transforming growth factor-beta inhibitor decorin." Int J Cancer **71**(1): 49-58.

Telford, W. G., J. Bradford, W. Godfrey, R. W. Robey and S. E. Bates (2007). "Side population analysis using a violet-excited cell-permeable DNA binding dye." Stem Cells **25**(4): 1029-1036.

Thuriaux, P., P. Nurse and B. Carter (1978). "Mutants altered in the control co-ordinating cell division with cell growth in the fission yeast *Schizosaccharomyces pombe*." Mol Gen Genet **161**(2): 215-220.

Tibes, R., J. M. Bogenberger, L. Chaudhuri, R. T. Hagelstrom, D. Chow, M. E. Buechel, I. M. Gonzales, T. Demuth, J. Slack, R. A. Mesa, E. Braggio, H. H. Yin, S. Arora and D. O. Azorsa (2012). "RNAi screening of the kinome with cytarabine in leukemias." Blood **119**(12): 2863-2872.

Togashi, Y., K. Shitara and H. Nishikawa (2019). "Regulatory T cells in cancer immunosuppression - implications for anticancer therapy." Nat Rev Clin Oncol **16**(6): 356-371.

Toledo, C. M., Y. Ding, P. Hoellerbauer, R. J. Davis, R. Basom, E. J. Girard, E. Lee, P. Corrin, T. Hart, H. Bolouri, J. Davison, Q. Zhang, J. Hardcastle, B. J. Aronow, C. L. Plaisier, N. S. Baliga, J. Moffat, Q. Lin, X. N. Li, D. H. Nam, J. Lee, S. M. Pollard, J. Zhu, J. J. Delrow, B. E. Clurman, J. M. Olson and P. J. Paddison (2015). "Genome-wide CRISPR-Cas9 Screens Reveal Loss of Redundancy between PKMYT1 and WEE1 in Glioblastoma Stem-like Cells." Cell Rep **13**(11): 2425-2439.

Toledo, L. I., M. Altmeyer, M. B. Rask, C. Lukas, D. H. Larsen, L. K. Povlsen, S. Bekker-Jensen, N. Mailand, J. Bartek and J. Lukas (2013). "ATR prohibits replication catastrophe by preventing global exhaustion of RPA." Cell **155**(5): 1088-1103.

Toledo, L. I., M. Murga and O. Fernandez-Capetillo (2011). "Targeting ATR and Chk1 kinases for cancer treatment: a new model for new (and old) drugs." Mol Oncol **5**(4): 368-373.

Toledo, L. I., M. Murga, R. Zur, R. Soria, A. Rodriguez, S. Martinez, J. Oyarzabal, J. Pastor, J. R. Bischoff and O. Fernandez-Capetillo (2011). "A cell-based screen identifies ATR inhibitors with synthetic lethal properties for cancer-associated mutations." Nat Struct Mol Biol **18**(6): 721-727.

Tonin, P. N., A. M. Mes-Masson, P. A. Futreal, K. Morgan, M. Mahon, W. D. Foulkes, D. E. Cole, D. Provencher, P. Ghadirian and S. A. Narod (1998). "Founder BRCA1 and BRCA2 mutations in French Canadian breast and ovarian cancer families." Am J Hum Genet **63**(5): 1341-1351.

Tran, E., S. Turcotte, A. Gros, P. F. Robbins, Y. C. Lu, M. E. Dudley, J. R. Wunderlich, R. P. Somerville, K. Hogan, C. S. Hinrichs, M. R. Parkhurst, J. C. Yang and S. A. Rosenberg (2014). "Cancer immunotherapy based on mutation-specific CD4+ T cells in a patient with epithelial cancer." Science **344**(6184): 641-645.

- Troost, E. G., J. Bussink, A. L. Hoffmann, O. C. Boerman, W. J. Oyen and J. H. Kaanders (2010). "18F-FLT PET/CT for early response monitoring and dose escalation in oropharyngeal tumors." J Nucl Med **51**(6): 866-874.
- Tsutsui, S., S. Ohno, S. Murakami, A. Kataoka, J. Kinoshita and Y. Hachitanda (2003). "Prognostic significance of the coexpression of p53 protein and c-erbB2 in breast cancer." Am J Surg **185**(2): 165-167.
- Tu, X., M. M. Kahila, Q. Zhou, J. Yu, K. R. Kalari, L. Wang, W. S. Harmsen, J. Yuan, J. C. Boughey, M. P. Goetz, J. N. Sarkaria, Z. Lou and R. W. Mutter (2018). "ATR Inhibition Is a Promising Radiosensitizing Strategy for Triple-Negative Breast Cancer." Mol Cancer Ther **17**(11): 2462-2472.
- Tung, N., C. Battelli, B. Allen, R. Kaldate, S. Bhatnagar, K. Bowles, K. Timms, J. E. Garber, C. Herold, L. Ellisen, J. Krejdosky, K. DeLeonardis, K. Sedgwick, K. Soltis, B. Roa, R. J. Wenstrup and A. R. Hartman (2015). "Frequency of mutations in individuals with breast cancer referred for BRCA1 and BRCA2 testing using next-generation sequencing with a 25-gene panel." Cancer **121**(1): 25-33.
- Tutt, A., H. Tovey, M. C. U. Cheang, S. Kernaghan, L. Kilburn, P. Gazinska, J. Owen, J. Abraham, S. Barrett, P. Barrett-Lee, R. Brown, S. Chan, M. Dowsett, J. M. Flanagan, L. Fox, A. Grigoriadis, A. Gutin, C. Harper-Wynne, M. Q. Hatton, K. A. Hoadley, J. Parikh, P. Parker, C. M. Perou, R. Roylance, V. Shah, A. Shaw, I. E. Smith, K. M. Timms, A. M. Wardley, G. Wilson, C. Gillett, J. S. Lanchbury, A. Ashworth, N. Rahman, M. Harries, P. Ellis, S. E. Pinder and J. M. Bliss (2018). "Carboplatin in BRCA1/2-mutated and triple-negative breast cancer BRCAness subgroups: the TNT Trial." Nat Med **24**(5): 628-637.
- Twyman-Saint Victor, C., A. J. Rech, A. Maity, R. Rengan, K. E. Pauken, E. Stelekati, J. L. Benci, B. Xu, H. Dada, P. M. Odorizzi, R. S. Herati, K. D. Mansfield, D. Patsch, R. K. Amaravadi, L. M. Schuchter, H. Ishwaran, R. Mick, D. A. Pryma, X. Xu, M. D. Feldman, T. C. Gangadhar, S. M. Hahn, E. J. Wherry, R. H. Vonderheide and A. J. Minn (2015). "Radiation and dual checkpoint blockade activate non-redundant immune mechanisms in cancer." Nature **520**(7547): 373-377.
- Ubersax, J. A., E. L. Woodbury, P. N. Quang, M. Paraz, J. D. Blethrow, K. Shah, K. M. Shokat and D. O. Morgan (2003). "Targets of the cyclin-dependent kinase Cdk1." Nature **425**(6960): 859-864.
- Uchiyama, K., E. Jokitalo, M. Lindman, M. Jackman, F. Kano, M. Murata, X. Zhang and H. Kondo (2003). "The localization and phosphorylation of p47 are important for Golgi disassembly-assembly during the cell cycle." J Cell Biol **161**(6): 1067-1079.
- Ueberroth, B. E., J. M. Lawhorn-Crews, L. K. Heilbrun, D. W. Smith, J. Akoury, R. Ali-Fehmi, N. T. Eiseler and A. F. Shields (2019). "The use of 3'-deoxy-3'-(18)F-fluorothymidine (FLT) PET in the assessment of long-term survival in breast cancer patients treated with neoadjuvant chemotherapy." Ann Nucl Med **33**(6): 383-393.
- van der Burg, M., H. Ijspeert, N. S. Verkaik, T. Turul, W. W. Wiegant, K. Morotomi-Yano, P. O. Mari, I. Tezcan, D. J. Chen, M. Z. Zdzienicka, J. J. van Dongen and D. C. van Gent (2009). "A DNA-PKcs mutation in a radiosensitive T-B- SCID patient inhibits Artemis activation and nonhomologous end-joining." J Clin Invest **119**(1): 91-98.

- Van Linden, A. A., D. Baturin, J. B. Ford, S. P. Fosmire, L. Gardner, C. Korch, P. Reigan and C. C. Porter (2013). "Inhibition of Wee1 sensitizes cancer cells to antimetabolite chemotherapeutics in vitro and in vivo, independent of p53 functionality." Mol Cancer Ther **12**(12): 2675-2684.
- van Waarde, A., D. C. Cobben, A. J. Suurmeijer, B. Maas, W. Vaalburg, E. F. de Vries, P. L. Jager, H. J. Hoekstra and P. H. Elsinga (2004). "Selectivity of 18F-FLT and 18F-FDG for differentiating tumor from inflammation in a rodent model." J Nucl Med **45**(4): 695-700.
- Varghese, F., A. B. Bukhari, R. Malhotra and A. De (2014). "IHC Profiler: an open source plugin for the quantitative evaluation and automated scoring of immunohistochemistry images of human tissue samples." PLoS One **9**(5): e96801.
- Vassilopoulos, A., Y. Tominaga, H. S. Kim, T. Lahusen, B. Li, H. Yu, D. Gius and C. X. Deng (2015). "WEE1 murine deficiency induces hyper-activation of APC/C and results in genomic instability and carcinogenesis." Oncogene **34**(23): 3023-3035.
- Vendetti, F. P., P. Karukonda, D. A. Clump, T. Teo, R. Lalonde, K. Nugent, M. Ballew, B. F. Kiesel, J. H. Beumer, S. N. Sarkar, T. P. Conrads, M. J. O'Connor, R. L. Ferris, P. T. Tran, G. M. Delgoffe and C. J. Bakkenist (2018). "ATR kinase inhibitor AZD6738 potentiates CD8+ T cell-dependent antitumor activity following radiation." J Clin Invest **128**(9): 3926-3940.
- Vendetti, F. P., A. Lau, S. Schamus, T. P. Conrads, M. J. O'Connor and C. J. Bakkenist (2015). "The orally active and bioavailable ATR kinase inhibitor AZD6738 potentiates the anti-tumor effects of cisplatin to resolve ATM-deficient non-small cell lung cancer in vivo." Oncotarget **6**(42): 44289-44305.
- Villeneuve, J., M. Scarpa, M. Ortega-Bellido and V. Malhotra (2013). "MEK1 inactivates Myt1 to regulate Golgi membrane fragmentation and mitotic entry in mammalian cells." EMBO J **32**(1): 72-85.
- Visconti, R., R. Della Monica, L. Palazzo, F. D'Alessio, M. Raia, S. Improta, M. R. Villa, L. Del Vecchio and D. Grieco (2015). "The Fcp1-Wee1-Cdk1 axis affects spindle assembly checkpoint robustness and sensitivity to antimicrotubule cancer drugs." Cell Death Differ **22**(9): 1551-1560.
- Visconti, R., L. Palazzo, R. Della Monica and D. Grieco (2012). "Fcp1-dependent dephosphorylation is required for M-phase-promoting factor inactivation at mitosis exit." Nat Commun **3**: 894.
- Vitale, I., G. Manic, R. De Maria, G. Kroemer and L. Galluzzi (2017). "DNA Damage in Stem Cells." Mol Cell **66**(3): 306-319.
- Vollebergh, M. A., E. H. Lips, P. M. Nederlof, L. F. A. Wessels, M. K. Schmidt, E. H. van Beers, S. Cornelissen, M. Holtkamp, F. E. Froklage, E. G. E. de Vries, J. G. Schrama, J. Wesseling, M. J. van de Vijver, H. van Tinteren, M. de Bruin, M. Hauptmann, S. Rodenhuis and S. C. Linn (2011). "An aCGH classifier derived from BRCA1-mutated breast cancer and benefit of high-dose platinum-based chemotherapy in HER2-negative breast cancer patients." Ann Oncol **22**(7): 1561-1570.
- Waks, A. G. and E. P. Winer (2019). "Breast Cancer Treatment: A Review." JAMA **321**(3): 288-300.

- Walsh, T., J. B. Mandell, B. M. Norquist, S. Casadei, S. Gulsuner, M. K. Lee and M. C. King (2017). "Genetic Predisposition to Breast Cancer Due to Mutations Other Than BRCA1 and BRCA2 Founder Alleles Among Ashkenazi Jewish Women." JAMA Oncol **3**(12): 1647-1653.
- Wang, B., L. Sun, Z. Yuan and Z. Tao (2020). "Wee1 kinase inhibitor AZD1775 potentiates CD8+ T cell-dependent antitumour activity via dendritic cell activation following a single high dose of irradiation." Med Oncol **37**(8): 66.
- Wang, C., G. Wang, X. Feng, P. Shepherd, J. Zhang, M. Tang, Z. Chen, M. Srivastava, M. E. McLaughlin, N. M. Navone, G. T. Hart and J. Chen (2019). "Genome-wide CRISPR screens reveal synthetic lethality of RNASEH2 deficiency and ATR inhibition." Oncogene **38**(14): 2451-2463.
- Wang, Y., J. Seemann, M. Pypaert, J. Shorter and G. Warren (2003). "A direct role for GRASP65 as a mitotically regulated Golgi stacking factor." EMBO J **22**(13): 3279-3290.
- Wardman, P. (2007). "Chemical radiosensitizers for use in radiotherapy." Clin Oncol (R Coll Radiol) **19**(6): 397-417.
- Weichselbaum, R. R., H. Liang, L. Deng and Y. X. Fu (2017). "Radiotherapy and immunotherapy: a beneficial liaison?" Nat Rev Clin Oncol **14**(6): 365-379.
- Weigel, M. T. and M. Dowsett (2010). "Current and emerging biomarkers in breast cancer: prognosis and prediction." Endocr Relat Cancer **17**(4): R245-262.
- West, S. C. (2003). "Molecular views of recombination proteins and their control." Nat Rev Mol Cell Biol **4**(6): 435-445.
- Whelan, T. J., J. P. Pignol, M. N. Levine, J. A. Julian, R. MacKenzie, S. Parpia, W. Shelley, L. Grimard, J. Bowen, H. Lukka, F. Perera, A. Fyles, K. Schneider, S. Gulavita and C. Freeman (2010). "Long-term results of hypofractionated radiation therapy for breast cancer." N Engl J Med **362**(6): 513-520.
- Williamson, C. T., R. Miller, H. N. Pemberton, S. E. Jones, J. Campbell, A. Konde, N. Badham, R. Rafiq, R. Brough, A. Gulati, C. J. Ryan, J. Francis, P. B. Vermulen, A. R. Reynolds, P. M. Reaper, J. R. Pollard, A. Ashworth and C. J. Lord (2016). "ATR inhibitors as a synthetic lethal therapy for tumours deficient in ARID1A." Nat Commun **7**: 13837.
- Wimberly, H., J. R. Brown, K. Schalper, H. Haack, M. R. Silver, C. Nixon, V. Bossuyt, L. Pusztai, D. R. Lannin and D. L. Rimm (2015). "PD-L1 Expression Correlates with Tumor-Infiltrating Lymphocytes and Response to Neoadjuvant Chemotherapy in Breast Cancer." Cancer Immunol Res **3**(4): 326-332.
- Withers, H. R. (1971). "Regeneration of intestinal mucosa after irradiation." Cancer **28**(1): 75-81.
- Wolff, A. C., M. E. Hammond, D. G. Hicks, M. Dowsett, L. M. McShane, K. H. Allison, D. C. Allred, J. M. Bartlett, M. Bilous, P. Fitzgibbons, W. Hanna, R. B. Jenkins, P. B. Mangu, S. Paik, E. A. Perez, M. F. Press, P. A. Spears, G. H. Vance, G. Viale, D. F. Hayes, O. American Society of Clinical and P. College of American (2013). "Recommendations for human epidermal growth factor receptor 2 testing in breast cancer: American Society of Clinical Oncology/College of American Pathologists clinical practice guideline update." J Clin Oncol **31**(31): 3997-4013.

- Woo, R. A. and R. Y. Poon (2003). "Cyclin-dependent kinases and S phase control in mammalian cells." *Cell Cycle* **2**(4): 316-324.
- Woolf, D. K., M. Beresford, S. P. Li, M. Dowsett, B. Sanghera, W. L. Wong, L. Sonoda, S. Detre, V. Amin, M. L. Ah-See, D. Miles and A. Makris (2014). "Evaluation of FLT-PET-CT as an imaging biomarker of proliferation in primary breast cancer." *Br J Cancer* **110**(12): 2847-2854.
- Yang, L., C. Shen, C. J. Pettit, T. Li, A. J. Hu, E. D. Miller, J. Zhang, S. H. Lin and T. M. Williams (2020). "Wee1 Kinase Inhibitor AZD1775 Effectively Sensitizes Esophageal Cancer to Radiotherapy." *Clin Cancer Res* **26**(14): 3740-3750.
- Yap, T. A., B. O'Carrigan, M. S. Penney, J. S. Lim, J. S. Brown, M. J. de Miguel Luken, N. Tunariu, R. Perez-Lopez, D. N. Rodrigues, R. Riisnaes, I. Figueiredo, S. Carreira, B. Hare, K. McDermott, S. Khalique, C. T. Williamson, R. Natrajan, S. J. Pettitt, C. J. Lord, U. Banerji, J. Pollard, J. Lopez and J. S. de Bono (2020). "Phase I Trial of First-in-Class ATR Inhibitor M6620 (VX-970) as Monotherapy or in Combination With Carboplatin in Patients With Advanced Solid Tumors." *J Clin Oncol* **38**(27): 3195-3204.
- Yap, T. A., D. S. P. Tan, A. Terbuch, R. Caldwell, C. Guo, B. C. Goh, V. Heong, N. R. M. Haris, S. Bashir, Y. Drew, D. S. Hong, F. Meric-Bernstam, G. Wilkinson, J. Hreiki, A. M. Wengner, F. Blatt, A. Schlicker, M. Ludwig, Y. Zhou, L. Liu, S. Bordia, R. Plummer, E. Lagkadinou and J. S. de Bono (2021). "First-in-Human Trial of the Oral Ataxia Telangiectasia and RAD3-Related (ATR) Inhibitor BAY 1895344 in Patients with Advanced Solid Tumors." *Cancer Discov* **11**(1): 80-91.
- Yersal, O. and S. Barutca (2014). "Biological subtypes of breast cancer: Prognostic and therapeutic implications." *World J Clin Oncol* **5**(3): 412-424.
- Yiannakopoulou, E. (2014). "Etiology of familial breast cancer with undetected BRCA1 and BRCA2 mutations: clinical implications." *Cell Oncol (Dordr)* **37**(1): 1-8.
- Zelevsky, M. J., Z. Fuks, M. Hunt, H. J. Lee, D. Lombardi, C. C. Ling, V. E. Reuter, E. S. Venkatraman and S. A. Leibel (2001). "High dose radiation delivered by intensity modulated conformal radiotherapy improves the outcome of localized prostate cancer." *J Urol* **166**(3): 876-881.
- Zerjatke, T., I. A. Gak, D. Kirova, M. Fuhrmann, K. Daniel, M. Gonciarz, D. Muller, I. Glauche and J. Mansfeld (2017). "Quantitative Cell Cycle Analysis Based on an Endogenous All-in-One Reporter for Cell Tracking and Classification." *Cell Rep* **19**(9): 1953-1966.
- Zheng, H., F. Shao, S. Martin, X. Xu and C. X. Deng (2017). "WEE1 inhibition targets cell cycle checkpoints for triple negative breast cancers to overcome cisplatin resistance." *Sci Rep* **7**: 43517.
- Zhou, Z. W., C. Liu, T. L. Li, C. Bruhn, A. Krueger, W. Min, Z. Q. Wang and A. M. Carr (2013). "An essential function for the ATR-activation-domain (AAD) of TopBP1 in mouse development and cellular senescence." *PLoS Genet* **9**(8): e1003702.
- Zoete, V., M. Irving, M. Ferber, M. A. Cuendet and O. Michielin (2013). "Structure-Based, Rational Design of T Cell Receptors." *Front Immunol* **4**: 268.
- Zou, L. and S. J. Elledge (2003). "Sensing DNA damage through ATRIP recognition of RPA-ssDNA complexes." *Science* **300**(5625): 1542-1548.

Zou, W. (2005). "Immunosuppressive networks in the tumour environment and their therapeutic relevance." Nat Rev Cancer **5**(4): 263-274.